Product Distribution and Mechanistic Aspects in Pyrolytic Decomposition of Some Commodity Plastics

A Thesis

Submitted in Partial Fulfillment of the Requirements

For the Degree of

DOCTOR OF PHILOSOPHY

By

Ujwala Hujuri

DEPARTMENT OF CHEMICAL ENGINEERING

INDIAN INSTITUTE OF TECHNOLOGY, GUWAHATI

May, 2012

DEPARTMENT OF CHEMICAL ENGINEERING
INDIAN INSTITUTE OF TECHNOLOGY
GUWAHATI

CERTIFICATE

This is to certify that the work contained in the thesis entitled **"Product Distribution and Mechanistic Aspects in Pyrolytic Decomposition of Some Commodity Plastics"**, by **Ujwala Hujuri** has been carried out under our supervision and that this work has not been submitted elsewhere for a degree.

Dr. Sasidhar Gumma
(Associate Professor)

Dr. Aloke Kumar Ghoshal
(Professor)

Dedicated to

My mother (in memoriam)

With love and gratitude

ACKNOWLEDGEMENTS

As I sit here to pen down my acknowledgements, I refresh my long journey to finally arrive at this stage in my research endeavour. Really, it has been a long journey…marked with sweat and tears, smiles and cheers!

Among various names that I would like to acknowledge, firstly it would be my thesis supervisor, **Dr. Sasidhar Gumma**, who has always showed me the way to handle things on my own. I was greatly influenced by his approach towards problem-solving. It took me quite some time to model the system; finally it was possible because of his intervention. I am really thankful to him for his help during GC troubleshooting. His careful scrutiny and minute observations helped me immensely in improving the quality of my work.

I would also like to offer my sincere gratitude to my thesis supervisor, **Prof. Aloke Kr. Ghoshal**, who has showed great interest in the topic. His vast knowledge of chemistry and constant encouragement helped me dig deep into the chemistry of polymer decomposition. That area would have remained unexplored without his motivation and belief in me. His basic understanding of things and experience helped me a lot in analyzing the experimental findings.

The project was beset with difficulties and there were times when I used to break down. *"You will have to make the best use of whatever you have"*, was what I used to hear from both of my mentors. That provided me with the much needed thrust that put me back into work. It has been a great privilege to work under their guidance.

I would like to acknowledge **Dr. Ramgopal V. S. Uppaluri** (Department of Chemical Engineering), Chairman of the Doctoral Committee for his valuable suggestions during the course of my work. His queries during the progress review seminars gave me the necessary feedback to improve my work. I would also like to offer my sincere thanks to **Dr. G. Pugazhenthi** (Department of Chemical Engineering) and **Dr. Manabendra Ray** (Department of Chemistry), Doctoral Committee members, for their useful recommendations during the progress review seminars.

I would like to acknowledge **Dr. Prabirkumar Saha**, Ex. HOD (Department of Chemical Engineering) and **Dr. Anil Verma**, Ex. DPPC Chairman (Department of Chemical Engineering) for their suggestions regarding administrative and academic matters. My special

thanks go to **Dr. Bishnupada Mandal** (Department of Chemical Engineering) for allowing me to use his GC during the crucial stage of my work.

I am thankful to Mr. Prasun Bhattacharjee, Mr. Dipak Kr. Barman, Mr. Kaustavmoni Deka, Mr. Balen Chandra Mahanta, Mr. Jayanta Kr. Mout, the scientific staff of the department for helping me immensely during the course of my study. Thanks are also due to other technical and non-technical staff of the department for helping me in different ways over the years.

I express my sincere gratitude to Mr. Kishore Das, CIPET Guwahati for providing me with the MFI test report of two plastics I studied.

Life at IITG would not have been so memorable without my friends, seniors and juniors with whom I have spent some good time. The names which need special mention are Dr. Biswanath Saha, Dr. Subham Paul, Dr. Monash P., Dr. Pradip Chowdhury who have helped me in some way or the other during the course of the study. I will cherish the moments spent in the company of Simadri, Sucheta, Abhijit, Balakrushna, Kabita madam, Bandana madam and Aparajita during my days at IITG. I am grateful to my friend Mr. Kaalva Srinivasulu for all his help and encouragement.

I would like to acknowledge my family for all their sacrifice, patience and constant support throughout my research work. They have always been there along the ups and downs. I would like to express my gratitude to my father for all his love and care. It's because of his motivation that I could take up and pursue my doctoral research. I am indebted to my brothers and sister, Arindam, Jenkins and Raktima, whose love and support kept me going in the hardest of times. I would like to especially thank my husband, Rupam for his dedicated support, understanding, and for keeping the faith in me. He has helped me immensely during my thesis writing, starting from editing the figures to carefully proof-reading my thesis. This work would not have seen completion without his help and support.

Finally, my heartiest regards go to my mother, who has been in my heart in every step of the way and been a constant source of inspiration for me. I thank her for giving me the strength and courage to fight against all the odds and come out successfully at the end.

Ujwala Hujuri

ABSTRACT

Recent years have seen remarkable demand for plastic goods in varied fields of application. With the rise in the use of plastics, there is a parallel rise in the generation of waste plastics. Due to the non-biodegradable nature of most of the plastics, their presence in the waste stream has become a major concern. Pyrolysis of plastics offers a technological solution to the management of this voluminous waste which, otherwise, would end up in landfills.

Pyrolysis of plastics results in the production of liquid and gaseous hydrocarbons along with a solid carbonaceous residue. These liquid and gaseous fractions have remarkable potential to be upgraded to fuels or petrochemicals. Depending on the types of plastic and operating temperature, different types of products are obtained. A systematic study of pyrolysis behaviour of plastics and their product characterization is of significant importance for potential application of pyrolysis as a valuable feedstock recycling process.

The aim of this work is to study the decomposition behavior of mixed plastics vis-à-vis their constituent plastics, to investigate the presence of interaction between the constituent plastics, and subsequently to study the effect of interaction on their product distribution. This work also aims to correlate the product evolution from pyrolysis of plastics with the decomposition pathways.

Three types of commodity plastics, *viz.* low density polyethylene (LDPE), polypropylene (PP) and polyethylene terephthalate (PET) were chosen in this work. Thermogravimetric (TG) studies were systematically carried out; firstly for the single plastics and subsequently for their binary and ternary mixtures over a wide range of compositions. Temperature was varied from 25 to 600^{o}C at a heating rate of 10^{o}C min^{-1} and all the TG experiments were carried out in an inert atmosphere.

A non-interacting decomposition curve, calculated for the plastic mixtures showed significant deviation from experimental derivative thermogravimetric (DTG) curve, indicating interaction between the constituent plastics. An interacting model was developed to describe pyrolysis kinetics of the plastic mixtures. Interaction parameters were calculated for each of the binary pair. Good correlations of binary data were obtained using the interacting model. The ternary decomposition behavior was also predicted fairly well with the help of binary interaction parameters. Multiple peak temperature values in the DTG curve obtained for some of the plastic mixtures were also successfully mimicked by this model.

Product distribution studies were carried out by using a gas chromatograph, firstly for the single plastics, and consequently for their binary and ternary mixtures. The pyrograms were analyzed to quantify C5-C44 hydrocarbons in the evolved gases from pyrolysis of the plastics/plastic mixtures over the temperature range of 200-600^{o}C. Maximum evolution of lighter hydrocarbons (C5-C10) was observed at or around maximum decomposition temperatures of the plastics. The following reaction types were considered to explain the decomposition mechanism of LDPE and PP, both of which decompose by free radical mechanism; (a) main chain cleavage to form chain- terminus radicals; (b) intramolecular hydrogen transfer to generate internal radicals; (c) intermolecular hydrogen transfer to form both volatile products and radicals; and (d) β-scission to form both volatiles and terminally unsaturated polymer chains. PET decomposed mainly by heterolytic mechanism at low temperatures (<300^{o}C). β-hydrogen transfer reactions were responsible for the formation of oligomers with olefin and carboxyl end groups. However, the high molecular species observed at low temperature (≈300^{o}C) were possibly due to the formation of cyclic oligomers resulting from an intramolecular ester exchange reaction.

Product distribution study carried out for the mixtures showed that the mixture composition as well as selection of decomposition temperature had significant influence on product

evolution profile. At low temperature of decomposition, interaction was not evident and the plastics apparently decompose independent of one another. However, at higher temperatures (>400^{o}C), product distribution was influenced by their mutual interaction. This was explained with the help of a suitable mechanism for the mixtures.

The results presented in this work indicate that decomposition of constituent plastics is not independent of one another. Enhancement of the decomposition process was observed by lowering of maximum decomposition temperature. Product distribution from pyrolysis of mixed plastics is a function of composition of the constituent plastics and the operating temperature. Both these parameters should be carefully chosen to obtain the required range of hydrocarbon products.

Keywords: decomposition mechanism; low density polyethylene (LDPE); plastic mixtures; polyethylene terephthalate (PET); polypropylene (PP); product distribution; pyrolysis.

TABLE OF CONTENTS

LIST OF TABLES

LIST OF FIGURES

LIST OF SYMBOLS

$\frac{d\alpha}{dt}$	rate of reaction (min^{-1}),
$\frac{d\alpha}{dT}$	rate of degradation ($^oC^{-1}$)
$\left.\frac{d\alpha}{dT}\right\|_1$	rate of degradation of plastic 1 at temperature T
$\left.\frac{d\alpha}{dT}\right\|_2$	rate of degradation of plastic 2 at temperature T
$\left.\frac{d\alpha}{dT}\right\|_3$	rate of degradation of plastic 3 at temperature T
$\left.\frac{d\alpha}{dT}\right\|_{12}$	rate of degradation to account for possible interactions of constituent plastics 1 and 2 in their binary mixture, at temperature T
$\left.\frac{d\alpha}{dT}\right\|_{13}$	rate of degradation to account for possible interactions of constituent plastics 1 and 3 in their binary mixture, at temperature T
$\left.\frac{d\alpha}{dT}\right\|_{23}$	rate of degradation to account for possible interactions of constituent plastics 2 and 3 in their binary mixture, at temperature T
$\left.\frac{d\alpha}{dT}\right\|_{mix}$	rate of degradation of mixture at temperature T
E	activation energy ($kJ\ mol^{-1}$)
$f(\alpha)$	reaction model
k_0	pre-exponential factor (K^{-1})
M_n	number average molecular weight
M_w	weight-average molecular weight
n	order of the chemical reaction
R	Universal gas constant ($kJ\ mol^{-1}\ K^{-1}$).

R_p	primary radical
R_s	secondary radical
R_s'	short secondary radical
R_t	tertiary radical
t	time (minutes)
T	temperature (^oC)
T_0	temperature at which decomposition starts (^oC)
T_f	maximum degradation temperature beyond which there is no further weight loss (^oC)
T_{max}	temperature at which the maximum rate of degradation occurs (^oC)
W	sample weight at any temperature T or time t (mg)
W_0	initial weight of the sample (mg)
W_∞	final sample weight (mg)
x_1	weight fraction of the plastic 1 in the mixture
x_2	weight fraction of the plastic 2 in the mixture
x_3	weight fraction of the plastic 3 in the mixture

GREEK LETTERS

α	fractional conversion
β	heating rate ($^oC\ min^{-1}$)
β_{12}, γ_{12}	binary interaction parameter for plastic 1 and 2
β_{13}, γ_{13}	binary interaction parameter for plastic 1 and 3
β_{23}, γ_{23}	binary interaction parameter for plastic 2 and 3

LIST OF ABBREVIATIONS

ASTM	American Society for Testing Materials
DEG	diethylene glycol
DVT	divinyl terephthalate
FID	Flame Ionization Detector
GC	Gas Chromatograph/chromatography
GC/MS	Gas Chromatograph/Mass Spectrometer
HACA	Hydrogen abstraction-C_2H_2 (acetylene) addition
HDPE	high density polyethylene
HGA	Hybrid Genetic Algorithm
ICTAC	International Confederation of Thermal Analysis and Calorimetry
LDPE	low density polyethylene
MMA	monomethyl acrylate
MPW	municipal plastic waste
MSW	municipal solid waste
MVT	monovinyl terephthalate
MWD	molecular weight distribution
PAHs	polycyclic/polynuclear aromatic hydrocarbons
PAMS	poly(α-methylstyrene)
PBT	polybutylene terephthalate
PE	polyethylene
PET	polyethylene terephthalate
PMMA	poly(methylmethacrylate)
PP	polypropylene
PS	polystyrene
PSW	plastic solid waste
PTFE	polytetrafluoroethylene

PTT	poly (trimethylene terephthalate)
PVC	polyvinyl chloride
PWM	plastic waste management
RCD	random chain dissociation
RDF	refuse derived fuel
RT	retention time
RT_i	retention time at start of peak
RT_f	retention time at end of peak
SDMT	standard deviation minimization technique
SSSP	solid state shear pulverization
TGA	Thermogravimetric Analyzer/analysis
TPA	terephthalic acid
TPD	tons per day
VOCs	volatile organic compounds
WTE	waste-to-energy

CHAPTER 1

Introduction

This chapter focuses on the background based on which present research is undertaken. It presents the current solid waste generation scenario, how waste plastics have become an environmental concern, various procedures adopted for plastics waste management, and different recycling techniques. Finally, the importance of present research and its objectives are elaborated.

1.1 Solid Waste Generation Scenario

Municipal Solid Waste (MSW) "includes commercial and residential wastes generated in a municipal or notified areas in either solid or semi-solid form excluding industrial hazardous wastes but including treated bio-medical wastes" as stated in Municipal Solid Wastes (Management and Handling) Rules, 2000 [1]. MSW consists of daily used items like papers, grass clippings, plastic carry bags and pouches, packaging materials, construction and demolition debris, clothing, bottles, rubbers and tyres, metals, food scraps, paint, and batteries.

Low income countries have the lowest percentage of urban populations and the lowest waste generation rates ranging between 0.4 to 0.9 kg per capita per day. The countries with middle-income range have waste generation rates ranging from 0.5 to 1.1 kg per day. The high income countries show the greatest generation rates which vary from 1.1 to 5.07 kg per capita per day [2]. Over the last few decades, the global scenario of generation, recycling, composting, and disposal of MSW has changed substantially. In 2010, the US generated about 250 million tons of solid waste, thus increasing the waste generation rate from 1.7 to 2 kg per capita per day between 1980 and 2010 [3]. Between 1980 and 2010, disposal of waste to a landfill has decreased from 89 percent to about 54 percent of MSW. In the European Union countries, over

250 million tons of MSW are produced each year, with an annual growth of 3%. In 1990, each individual in the world produced an average of 250 kg of MSW generating in total 1300 million tons of MSW [4]. In 2010, this amount almost doubled leveling at 2300 million tons.

As far as India is concerned, with rapid population growth and economic development in the last few decades, there has been significant increase in MSW generation. This increase in MSW generation has not been confined to cities or large towns, but has also spread to small towns mainly due to the overall growth of the country [5]. The per capita waste generation rate in urban India has increased from 0.44 kg/day in 2001 to 0.5 kg/day in 2011, fuelled by changing lifestyles and increased purchasing power of urban Indians [4]. Urban population growth and increase in per capita waste generation has resulted in a 13.6% increase in the waste generated by Indian cities within only a decade since 2001. The total MSW generated in urban India is estimated to be 68.8 million tons per year [5].

As is the case with almost every developing country, India, too, is facing difficulties in disposing off the enormous amounts of MSW that the country produces every day. The pertinent challenges that require immediate action are MSW collection from every household, factory and institution, and developing efficient, environmentally safe means for its transport and disposal. The use of sanitary landfills, which refers to a managed, controlled site equipped with systems to reduce leachate and landfill gas migration into the surrounding environment, may be looked upon as an effective means towards solid waste disposal. However, scientific means should be followed in the disposal sites, which otherwise might lead to overthrowing landfills, serious emission, and ground water pollution. Thus, the problem of dumping solid waste in the localities (which, in turn, poses a threat to the environment owing to health and hygiene issues) can be solved if scientific means of disposal in sanitary landfills are widely practiced.

As part of solid waste management program, promoting and implementing reduction of solid waste at the source, recycling, and composting may also be looked upon as viable alternatives to landfill disposal. Presently, there are a total of 79 composting plants in operation in India, and about 35 new composting plants are proposed [5]. It has been reported that the calorific value of some composting rejects (up to 60% of the input MSW) is as high as 11.6 MJ/kg [5]. This value is much higher than the minimum calorific value of 7.5 MJ/kg recommended for economically feasible energy generation through grate combustion waste-to-energy (WTE) plant [5]. Therefore, the residues of mixed MSW composting operations can be used for producing refuse derived fuel (RDF) or can be combusted in a WTE plant directly.

1. 2 Plastic Wastes

Plastics have become an inseparable and integral part of our daily lives. Annual consumption of plastics has seen a tremendous growth in the last few decades. This can be attributed to their unique properties like light-weight, easy processability, user-friendly designs, durability, strength, energy efficiency, and cost effectiveness. Plastics have penetrated into virtually all areas that one can think of. Packaging, agricultural applications, automotives and industrial applications, drug delivery systems, artificial implants, other healthcare applications, water desalination, soil conservation, flood prevention, preservation and distribution of food, housing, communication materials, security systems are some of the areas to name a few. With so large and varied applications, plastics contribute to an ever increasing volume in the solid waste stream. Global annual consumption of plastic materials has increased from 5 million tons in 1950 to nearly 100 million tons in 2001 [6]. In the United States, plastic solid waste (PSW) found in MSW has increased from 11% (by weight) in 2002 [7], to 12.4% (by weight) in 2010 [3]. It is estimated that plastic waste constitutes approximately 8-9 % (by weight) of total MSW in India [1].

The plastic waste comprises two major categories of plastics, *viz*. thermoplastics and thermoset plastics. Of the total 10,000 tons per day (TPD) of post-consumer plastic waste generated in India, thermoplastics have a major share of 80% and thermoset type make up the rest 20% [8]. The thermoplastics are recyclable plastics which include polyethylene terephthalate (PET), low density polyethylene (LDPE), poly vinyl chloride (PVC), high density polyethylene (HDPE), polypropylene (PP), polystyrene (PS), etc. However, thermoset plastics are alkyd, epoxy, ester, melamine formaldehyde, phenol formaldehyde, silicone, urea formaldehyde, polyurethane resins, metalized and multilayered plastics etc. Polyolefins account for a major share in the total plastics consumption in India. Packaging is the major plastics consuming sector in India, with 52% of the total consumption [9], followed by consumer products and the construction industry. Considering the global scenario, packaging accounts for 37.2% of all plastics consumed in Europe, 44% in US and 35% worldwide [3,10]. Among different commodity plastics, LDPE, PP and PET are mainly used in the packaging industry, the various applications being packaging films and carrier bags (LDPE), food and confectionaries packaging (PP), and packaging beverages and water bottles (PET). Thus, LDPE, PP and PET share a major portion of waste plastics in the MSW stream. The plastics found in MSW stream are non-biodegradable in nature. Moreover, plastic wastes are very visible as they contribute to a large volume of total solid waste [11]. Precisely because of their high visibility, waste plastics have been viewed as a serious solid waste problem. Most of the plastics cannot be easily returned to the natural carbon cycle because of their non-biodegradability. Therefore their presence in the waste stream poses a serious problem where there is a lack of efficient end of life management of plastic waste. The following measures are commonly practiced for management of plastic wastes.

1.3 Plastic Waste Management

The fundamental objective of plastic waste management (PWM) is two-fold; first, to minimize waste, and second, to efficiently manage the waste still produced. This is generally accomplished by following the hierarchy, commonly known as the '3R approach' (Reduce, Reuse, Recycle) as stated below.

1.3.1 Reduce

Reduce refers to source reduction, which is a means of waste prevention. Source reduction is the practice of designing, manufacturing, purchasing, or using materials (such as products and packaging) in ways that reduce the amount or toxicity of trash created [12]. Source reduction, including reuse, can help reduce waste disposal and handling costs, because it avoids the costs of recycling, municipal composting, land filling, and combustion. Source reduction also conserves resources and reduces pollution, including greenhouse gases that contribute to global warming. As such, source reduction is the most effective way to minimize waste, and therefore is the objective of utmost importance to be achieved in waste management hierarchy. There can be different strategies to achieve source reduction, *viz.* toxic chemical substitution, production process modification, finished product reformulation, production modernization, improvements in operations and maintenance etc.

1.3.2 Reuse

Reusing items is another way to stop waste at the source because it delays or avoids that item's entry in the waste collection and disposal system. Some of the plastics, particularly those used in packaging applications, end up their life in the waste stream shortly after their single use. Considering the short life-span of those plastics, reusing should be practiced after the intended purpose for their use has been fulfilled. Reusing is always preferred over recycling as it is less

energy intensive, conserves fossil fuels since plastic production uses 4–8% of global oil production, *i.e.* 4% as feedstock and 4% during conversion [13,14] and reduces carbon-dioxide (CO_2), nitrogen-oxides (NO_x) and sulphur-dioxide (SO_2) emissions [15]. The practice of the habit of reusing materials should be inculcated in individuals from childhood which would help them to keep away from the 'throw away' culture.

1.3.3 Recycle

Recycling processes can be divided into material recycling or energy recovery techniques. Material recycling involves segregation and sorting of waste materials; cleaning and preparation of these separated fractions for reprocessing and remanufacture. After waste prevention, recycling has shown to result in the highest climate benefit compared to other waste management approaches. This is the most important approach which needs to be focused in developing countries like India. This is because waste prevention techniques like source reduction only reduce the volume of waste; it does not tackle the volume of waste that still remains to be disposed. Again, any article cannot be reused for an infinite period of time, as after a certain period, it would become unsuitable to be used any further due to issues related to health and hygiene. Thus, after a certain period of time, the waste must be recycled so as to prevent them from going into landfills.

Primary recycling

The conversion of scrap plastics by standard processing methods into products having performance characteristics equivalent to the original products made of virgin plastics is termed as primary recycling [16]. It is also known as re-extrusion, as it involves re-introduction of the scrap material from plastics to the extrusion cycle. Primary recycling is only feasible with clean scrap; therefore it is limited to in-house recycling of process scraps those are

obtained from the faulty products, or from edges and parts of molded products, which are pelletized and re-introduced into the processing machinery. Therefore, it is not a good choice for post-consumer waste plastics which pose challenges for their segregation, collection and cleaning.

Secondary recycling

Secondary recycling, also known as mechanical recycling is the process of recovering plastic solid waste (PSW) for the reuse in manufacturing plastic products having less demanding performance by one or a combination of processes like melting, shredding or granulation. Only single component plastics can be used. Therefore, sorting and cleaning are two very important steps in mechanical recycling. Thus, commingled plastics in MSW pose a greater challenge to the recyclers to make the single plastic components from them suitable for mechanical recycling to make good quality homogeneous end products. Efforts were made by polymer technologists in the 1970s to recover materials from waste plastics suitable for material recycling, but practical experience has shown that reprocessing of mixed contaminated plastics produces polymer polyblends those have inferior mechanical properties and less durability compared with those produced from virgin polymers. At present, plastics can be sorted automatically, using various techniques such as X-ray fluorescence, infrared and near infrared spectroscopy, electrostatics and floatation [17]. However, economic viability of such an operation in commercial application is a matter of concern.

Again, degradation of plastics caused by various means, *viz*. photo-oxidation or mechanical stress, is one of the major problems faced by mechanical recyclers [15, 17]. Moreover, conditions existing at waste bins and dumping sites of MSW make the situation aggravated due to mixing of soil, dirt, etc. with the waste plastics. Therefore if cleaning and washing processes are not practiced properly, quality of the products obtained by mechanical recycling is

questionable. Nonetheless, mechanical recycling presents an economic and practical route for PSW recovery for the case of rigid and foam plastics [15, 18]. The plastic industry is raw-material-intensive and raw material accounts for about 70% of the total production cost,; thus, a wide scope exists for mechanical recycling to develop and expand, saving scarce and valuable petro-based virgin raw material reserves of the country [9]. Recycling industry has emerged parallel to the virgin plastic industry in India. There are more than 2500 recycling units with an average output of 350 tons per annum. These 2500 recycling units recycle 60% of the total plastic waste generated in the country, which is the highest in the world.

Tertiary recycling

Also known as chemical or feedstock recycling, tertiary recycling refers to advanced technology processes which convert plastic materials into smaller molecules, usually liquids or gases, suitable for use as a feedstock for the production of new petrochemicals and plastics [15, 19]. These products are similar in properties to petroleum derived fuels, and therefore can be used as fuels. Examples of chemical recycling are pyrolysis or thermal cracking, gasification, liquid-gas hydrogenation, visbreaking, steam or catalytic cracking and the use of PSW as a reducing agent in blast furnaces [15]. The main advantage of chemical recycling lies in its possibility of handling heterogeneous and contaminated polymers with limited pre-treatment procedures. In recent times, pyrolysis and catalytic cracking processes have drawn considerable attention as a method for obtaining various fuel fractions from PSW.

Quaternary recycling

Also known as incineration with energy recovery, it is another option which involves combustion of the waste to recover their thermal content, providing an alternative source of energy. Basically, incineration is a waste treatment process, wherein the waste plastics are

combusted to convert the waste into ash, flue gas and heat. This heat can in turn be used to generate electrical power or generate process steam. Plastic materials possess a very high calorific value (when burned) since they are derived from crude oil [18]. However, incineration can be considered as a convenient energy source only when the heating values of plastics are considerably high and material recycling rate is low. Table 1.1 compares the calorific values of some plastics with some fuels [20, 21]. Since these plastics possess high heating values, they could make a convenient energy source. However, it is not regarded as an economical process in case of those plastics that do not have a high calorific value (>7.5 MJ/kg). Waste plastics with lower heating value can be burned, but it will not maintain adequate temperature without the addition of auxiliary fuel.

Table 1.1 Calorific values of some major plastics compared with common fuels [20, 21]

Material	Calorific value (MJ/kg)
PE	43.3-46.5
PP	46.5
PS	41.9
Kerosene	46.5
Gas oil	45.2
Heavy oil	42.5
Petroleum	42.3
Household PSW mixture	31.8

Moreover, reduction of solid waste in incinerators through combustion leads to the formation of by-products which exit the incinerator in the form of fly ash and bottom ash. Thus an incinerator actually transforms the original waste materials (or resources) into several new forms of wastes: air emissions, ash, and liquid discharge. This raises environmental concerns mainly due to emission of certain air pollutants such as CO_2, NO_x and SO_x, volatile organic compounds (VOCs), and polycyclic aromatic hydrocarbons (PAHs). Further, there are huge

costs associated with incineration, if it is to be profitable and carried out in an environmentally friendly manner [16]. This has to be taken up only when other material recovery processes fail due to economical constraints. However, if stringent conditions are maintained in the design of incinerators, and material recycling is not energy efficient, quaternary recycling is preferred over landfill disposal and incineration without energy recovery.

1.4 Importance of the Study

The quality of products obtained from recycling is of paramount importance so as to validate recycling in terms of safety and hygiene issues. Regulations and legislations are being enforced in India to keep a check in recycling activities and quality of products obtained from recycling. However, it will need proper planning and an efficient work-force to make it an organized activity. As state-of-art technologies are not properly followed in the unorganized sector, quality of the recycled products becomes questionable. Incineration and landfill are the other two most widely used methods for combating plastics disposal problem. But, the increased environmental concern due to the high rate of pollution from incinerators and decreasing landfill sites prompted researchers to look for alternative methods such as tertiary recycling. Pyrolysis or thermal cracking of plastics is one such potential chemical recycling technique, wherein the plastics are heated, either in absence or in limited supply of oxygen, to yield solid, liquid or gaseous hydrocarbons.

Pyrolysis can be conducted at various temperature levels, reaction times, pressures, and in the presence or absence of reactive gases or liquids, and catalysts. Plastics pyrolysis proceeds at low (<400°C), medium (400–600°C) or high temperature (>600°C). In this process, waste plastics break down to yield gas, distillates and char in widely variable relative amounts. But, the principal output products are gaseous and liquid hydrocarbon fractions that are remarkably similar to the refinery cracking products. These have tremendous potential to be used as fuels,

petrochemicals, and monomers. Depending on the polymers or polymer mixtures fed and the operating conditions used, yields also vary. Both gaseous and liquid products are mixtures of numerous different compounds. The residue obtained from pyrolysis is known as char, which incorporate fillers, pigments, and ash. The char can be upgraded to produce activated carbon, which is an important adsorbent. However, in case of catalytic process, catalyst particles get contained in the residue, and thus their separation becomes another concern. Moreover, the presence of hetero-elements, such as chlorine and bromine is undesirable, as these elements distribute over the three product phases-gas, liquid, and solids, reducing their market potential and value. The problem of fractionating the products and upgrading to commercial specifications, while separating undesirable impurities, must be investigated on a case-by-case basis. There has been a renewed interest among the researchers in exploring the application of pyrolysis of waste plastics, with or without the aid of a catalyst, as a means for feedstock recycling, preferably for producing gasoline range fuels (C6-C12). Although a viable option, this method can be quite expensive considering the fact that waste plastics are actually mixtures of several plastics with different compositions and thus require different processing conditions. The tertiary recycling (or cracking) of plastics has to be combined with other technologies, such as MSW collection, categorization and pre-treatment at the upstream end, as well as various separations and product recovery processes on the downstream end. Another issue with this method is the high energy input requirement, as some post consumer plastic waste requires temperatures as high as 700°C [13]. Even if one leaves out the upstream and the downstream processes involved, pyrolysis of mixed plastics itself is a very complicated phenomenon to deal with.

Thus, one of the main issues that need to be addressed is the pyrolysis behaviour of mixed plastics vis-á-vis single plastics to study the usefulness of pyrolysis to be applied economically. For example, if pyrolysis behaviour of HDPE, PET, and PP are studied separately for

optimization of process parameters like temperature, residence time in the reactor, one would have three sets of data. If pyrolysis studies are carried out for their binary or ternary mixtures, the optimization parameters might not match with any of those data sets, or these might have some proximity to one or two of them. This aspect cannot be approximated if a qualitative or quantitative assessment is not made about their interaction. At the same time, decomposition pathways need to be focused to have an understanding of the decomposition process and product distribution.

Another concern of this process is the high temperature required for obtaining some specific products, which can be lowered down by using effective catalysts, thereby reducing costs. In addition, catalysts can also be used to control product composition. However, expensive zeolite catalysts increase the cost of the cracking process. From an economic standpoint, using an effective catalyst at lesser quantities will make feedstock recycling an attractive option.

Thermogravimetric analysis using a Thermogravimetric Analyzer (TGA) coupled with evolved gas analysis by using a Gas Chromatograph (GC) is a common approach for such studies to elucidate the plastics decomposition mechanism, as well as product distribution and optimization of reaction conditions. The broad objective of the present work is to study the thermal decomposition kinetics of mixed plastics with emphasis on finding out possible interaction between them, analyze the product distribution and to understand the effect of reaction temperature and plastic composition on the product distribution.

1.5 Objectives of the Study

A vast amount of work in the relevant area has been reported in the literature and research in this area is continuously growing in search of innovative ways to narrow down the product distribution to the desired range by appropriate selection of plastics operating temperature, catalyst, proper design of reactor and mixing techniques. But, there is a dearth of literature

aimed at studying the interaction between the plastic components in pyrolysis of plastic mixtures and correlating the same with the mechanistic aspects and product distribution. This is crucial if one needs to design a commercial process for pyrolysis of plastic mixtures. The idea behind the present investigation is to understand the interaction between the constituent plastics in terms of product evolution from their pyrolysis. LDPE, PP and PET are selected as the target plastics in our study, since they share a major portion of waste plastics in India, as discussed earlier in *Section 1.2*.

Thus the aim of the present research is two-fold; first, to study the pyrolysis kinetics of binary and ternary mixtures of plastics in a TGA and development of a model to represent their pyrolysis behaviour, which can also quantify the interaction (if present) between the constituent plastics; and second, to investigate the possible effect of interaction on their product distribution at different stages of degradation by analysis of evolved products from pyrolysis of the plastic mixtures. Temperature dependency of product evolution is studied and an attempt is made to correlate the same with the decomposition mechanism of the plastics over a wide range of temperature (200-600^{o}C).

The novelty of the research work lies in the systematic approach adopted here to understand thermal decomposition behaviour of plastic mixtures. An interacting model has been developed which could describe thermal decomposition behavior of binary and ternary mixtures with the help of binary interaction parameters. Product distribution studies have been carried out for different compositions of binary and ternary plastic mixtures over a wide range of temperature. Decomposition pathways have been proposed for different plastic mixtures, which are in line with experimental findings. To the best of our knowledge, such studies have not been reported in literature so far. In this context, the present research project has been undertaken with the following objectives.

- Study of degradation kinetics of pure, binary and ternary plastic mixtures containing LDPE, PP and PET.

- Modeling pyrolysis kinetics of binary and ternary plastics mixtures of LDPE, PP and PET.

- Study of product distribution from pyrolysis of pure plastics (LDPE, PP and PET) over a wide range of temperature (200-600^{o}C) and to understand the corresponding reaction mechanism.
- Study of product distribution from pyrolysis of binary plastic mixtures (LDPE/PP, PP/PET and LDPE/PET over a wide range of temperature and composition of constituent plastics and understand the effect of interaction on product evolution profile. An attempt will be made to deduce possible reaction mechanism based on these ideas.
- Study of product distribution from pyrolysis of ternary mixtures of LDPE, PP and PET over a wide range of temperature and plastic mixture composition. An attempt will also be made to deduce the possible reaction mechanism.

Chapter 2 presents a literature review on kinetics, product distribution and mechanistic aspects of plastic decomposition. **Chapter 3** elaborates the theoretical work carried out to model pyrolysis behaviour of binary and ternary mixtures of plastics. **Chapter 4** explains the details of equipments and procedure followed. **Chapter 5** discusses on the experimental results involving modeling pyrolysis behaviour of mixed plastics (LDPE, PP, and PET) and product distribution from the single plastics as well as their binary and ternary mixtures, and explains the possible reaction mechanism of their decomposition. **Chapter 6** presents conclusions and gives a direction for future research.

CHAPTER 2

Literature Review

This chapter presents the state-of-the-art development in the area of pyrolysis of plastics by elaborating relevant studies. First, thermal decomposition process of solids is discussed by referring to available theories in literature. Different kinetic model functions used in kinetics analysis are elaborated. The literature pertaining to pyrolysis kinetics is discussed by incorporating significant works on both single and mixed plastics by isothermal and dynamic measurements. Different model-fitting and model-free techniques are discussed. Effects of various parameters on product distribution are also explained by referring to appropriate literature. Decomposition mechanisms of plastics are reported as proposed by different research groups at different levels of complexity. The potential area of research is thus highlighted for prospective work.

2.1. Thermal Decomposition of Solids

Solid polymeric materials undergo both physical and chemical changes when heated. Decomposition of a solid material signifies breakdown of one or more constituents of the material into simpler atomic groups. Thermal decomposition is intended to imply that such reorganization is brought about by an increase in temperature. Thus, thermal decomposition of a solid may be regarded as encompassing all processes which involve destruction of the stabilizing forces of its crystal lattice, including both chemical reactions and physical reorganizations (*e.g.,* melting and recrystallization) [22]. The chemical processes involved in decomposition are responsible for the generation of flammable volatiles, which escape into the vapour phase. The process of thermal decomposition should not be confused with thermal

degradation, wherein the action of heat or elevated temperature causes a loss of physical, mechanical, or electrical properties of a material [23].

Extent of decomposition is indicated by the fractional conversion (α) of the solid reactant into product. Thus a necessary prerequisite of any decomposition study is the unambiguous definition of α in terms of some directly measurable parameter. In principle, any parameter quantitatively related to α can be used for such studies, though, in practice, weight loss, product gas evolution and enthalpy change have found the most widespread application [24-27]. Coupling such studies with analytical techniques (*e.g.* mass spectrometry, gas chromatography, etc) provides information on the product evolution. This data could be useful to identify the stoichiometry of reaction. The weight loss data can be obtained against time (for isothermal studies) or temperature (for dynamic studies) from a Thermogravimetric Analyzer (TGA). Then α can be calculated by using the relation:

$$\alpha = \frac{(W_0 - W)}{(W_0 - W_\infty)} \qquad (2.1)$$

where, W_0 is the initial weight of the sample, W is the sample weight at any temperature, T or time, t, and W_∞ is the final sample weight.

Two alternative methods have been used in kinetic investigations of thermal decomposition of solids: in one known as isothermal measurement, weight loss measurements are made against time, while the reactant is maintained at a constant temperature, while, in the second known as dynamic measurement, the sample is subjected to a controlled rising temperature. From weight loss data, α values are calculated using *equation (2.1)* to plot α versus t. Measurements using both techniques have been widely exploited in the determination of kinetic characteristics and parameters of the decomposition process [28-33].

In the more traditional approach, *i.e*. isothermal studies, maintaining constant temperature throughout the reaction period represents an ideal condition which cannot be achieved in practice, since finite time is required to heat the material to the required temperature. Consequently, the initial segment of '*α vs. t*' plot cannot refer to isothermal conditions, though the effect of such deviation can be minimized by careful design of equipment. Characteristic features of *α* vs. *t* curves for isothermal decomposition of solids are discussed with reference to Figure 2.1, in which the abscissa denotes the elapsed time and ordinate denotes *α* [22]. Similar types of α vs. t curve can also be obtained for dynamic measurements. Section **P** is not associated with decomposition. The weight loss observed in this section could be possibly due to escape of adsorbed water or impurities on the surface. In kinetics analysis, it is sometimes convenient to use data from which the influences of any initial reaction, **P**, have been subtracted. Section **Q** is the induction period, which indicates the initial slow phase of decomposition which later accelerates. Induction period is usually terminated by the development of stable nuclei (often completed at a low value of *α*). Section **R** reflects an acceleratory period corresponding to the growth of nuclei. This process may be accompanied by further nucleation, up to the maximum rate of reaction rate at **S** (point of inflection along segment **RT**), after which the nuclei begin to overlap. The process of decomposition reaches the steady-state regime corresponding to the constant value of the absolute rate of decomposition at **S**. Thereafter, the continued expansion of nuclei is no longer possible, due to consumption of reactant and impingement and coalescence of developed nuclei and ingestion of undeveloped nucleation sites, and the rate of decomposition starts to decrease. This accounts for the onset of the deceleratory period **T** which lasts until the completion of reaction **U**. One or several sections of the curve preceding **S** point may be negligible in extent or be absent altogether. This results into a wide variety of

different types of kinetic behaviour, in which the maximum reaction rate, **S**, is achieved at different values of α.

The rate determining step in any such reactions can be either (i) the transportation of reactants to, or from, a zone of preferred reaction (diffusion), or (ii) a chemical reaction, *i.e.* one or more bond redistribution steps, generally occurring at the reactant-product interface [24, 34]. In mechanistic studies dealing with pyrolysis of plastics, kinetics analysis centers on rate processes from which the effects of diffusion are specifically excluded. These studies establish the reaction stoichiometry of the decomposition process incorporating individual rate constants (*k)* of different steps.

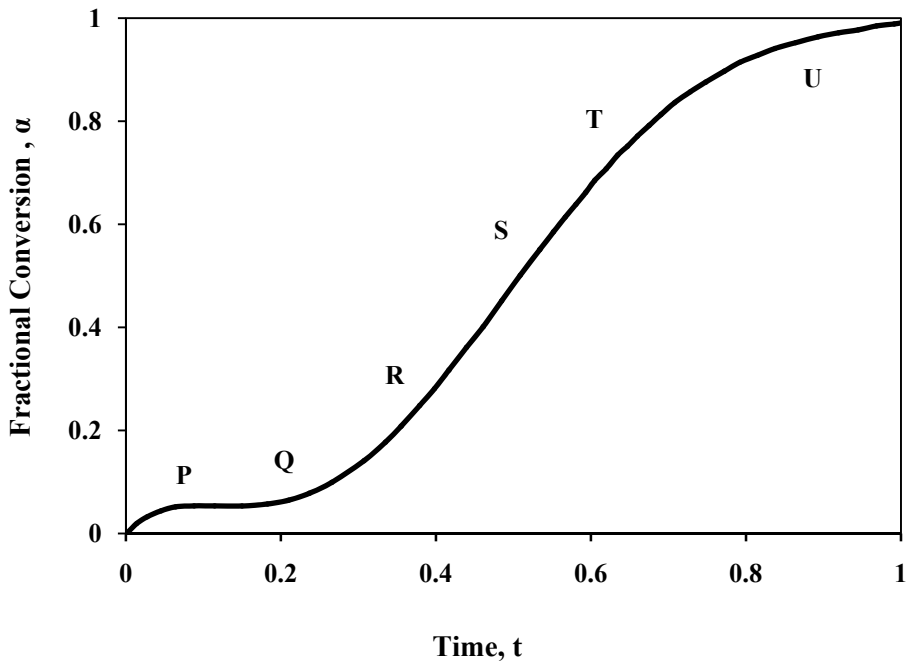

Figure 2.1 Generalized '*α-t'* plot summarizing characteristic kinetic behaviour observed for thermal decompositions of solids [22]

Increase in reaction rate with temperature are often found to obey the Arrhenius equation (*equation 2.2*), from which the apparent values of the pre-exponential factor, k_o (K^{-1}), and the activation energy, E (kJ mol^{-1}), are calculated.

$$k = k_0 \exp(-E/RT) \qquad (2.2)$$

Rate of decomposition reaction is expressed in terms of kinetics model equations combined with the Arrhenius approach of the temperature function:

$$\frac{d\alpha}{dt} = k_0 \exp(-E/RT) f(\alpha) \qquad (2.3)$$

Where, *T,* the temperature (in Kelvin), dα/d*t*, the rate of reaction (min^{-1}), and *f(α)*, the reaction model (Table 2.1). The terms k_0 and E, defined earlier, are known as the Arrhenius parameters. R is the universal gas constant (kJ mol^{-1} K^{-1}).

Integrating the above equation gives the integral form of the rate law,

$$g(\alpha) = kt \qquad (2.4)$$

where, *g(α)* is the integral reaction model.

Combining *equation 2.2* and *2.4*, we get,

$$g(\alpha) = k_0 \ exp(-E/RT)t \qquad (2.5)$$

f(α) may take various forms based on the underlying assumptions of nucleation and nucleus growth, geometrical contraction, diffusion, and chemical reaction [31,35-40]. According to the nucleation and growth models, formation and growth of nuclei are considered to be rate-limiting. The nucleation process involves conversion of a small volume of reactant into a stable particle of product and continued reaction (growth) occurs preferentially at the interfacial zone of contact between these two phases. Sites of initiation of reaction are widely

regarded as occurring exclusively at reactant surfaces, possibly at limited number of points at the reactant surface known as defects or imperfections and are frequently identified as possessing locally enhanced reactivity [24]. The initially generated germ nucleus, consisting of a few atoms is generally regarded as unstable due to the high ratio of surface strain to volume. It may, however, develop into a growth nucleus, which increases in size through advance of the reactant-product interface into the bulk of the crystallite, so reducing the relative importance of the surface strain term. Nucleation rate is different from the growth rate and the model accounts for both of them. Single-step nucleation, which is based on the assumption that the generation of a single molecule (atom, ion-pair, etc.) of product constitutes the establishment of a nucleus, gives rise to either exponential law or linear law. On the other hand, multi-step nucleation, which is based on the assumption of several distinct steps, gives rise to power law. These steps could be either successive processes in the vicinity of a particular site, or the interactions of some mobile energetic participants (excitons, interstitial ions, etc.), while the product species are apparently immobilized [24].

According to the models based on geometrical contraction, the progress of the product layer from the surface to the inner crystal is considered to be rate-limiting. It is different for various crystal morphologies (cubic, cylindrical, spherical etc). In case of diffusion models, diffusion of reactant or product is considered to be rate-limiting. For reaction order models, the rate law is based on considerations for homogeneous kinetics [40].

For isothermal Thermogravimetric (TG) experiments, *equation (2.3)* can be rewritten as:

$$\frac{d\alpha}{dt} = k(T) f_m(\alpha) \qquad (2.6)$$

$$g_m(\alpha) = \int_0^{\alpha} \frac{d\alpha}{f_m(\alpha)} = k_m(T) \int_0^{t} dt = k_m(T)t \qquad (2.7)$$

$k_m(T)$ can be expressed as:

$$\ln k_m(T_i) = \ln k_{0,m} - \frac{E_m}{RT_i} \qquad (2.8)$$

Here, the subscript '*m*' corresponds to the reaction model selected. For each reaction model, the rate constants are evaluated at several temperatures, T_i and the Arrhenius parameters are determined from *equation (2.8)*. The various forms of *f(α)* and *g(α)* are shown in Table 2.1.

Table 2.1 Solid state rate expressions for *f(α)* and *g(α)* [40]

Model	**Differential Form** $f(\alpha)=\frac{1}{k}\frac{d\alpha}{dt}$	**Integral Form** $g(\alpha)=kt$
Reaction-order Models		
nth order	$(1-\alpha)^n$	$[1/(1-\alpha)^{n-1}-1]/(n-1)$
Zero-order	1	α
First-order	$1-\alpha$	$-\ln(1-\alpha)$
Second-order	$(1-\alpha)^2$	$(1-\alpha)^{-1}-1$
Third-order	$(1-\alpha)^3$	$0.5((1-\alpha)^{-2}-1)$
Nucleation Models		
Prout-Tompkins	$\alpha(1-\alpha)$	$\ln[\alpha/1-\alpha]$
Power Law	$2\alpha^{(1/2)}$	$\alpha^{(1/2)}$
Power Law	$3\alpha^{(2/3)}$	$\alpha^{(1/3)}$
Power Law	$4\alpha^{(3/4)}$	$\alpha^{(1/4)}$
Avarami-Erofe'ev	$2(1-\alpha)[-\ln(1-\alpha)]^{1/2}$	$[-\ln(1-\alpha)]^{1/2}$
Avarami-Erofe'ev	$3(1-\alpha)[-\ln(1-\alpha)]^{2/3}$	$[-\ln(1-\alpha)]^{1/3}$
Avarami-Erofe'ev	$4(1-\alpha)[-\ln(1-\alpha)]^{3/4}$	$[-\ln(1-\alpha)]^{1/4}$
Geometrical Contraction Models		
Contracting area	$2(1-\alpha)^{1/2}$	$[1-(1-\alpha)^{1/2}]$
Contracting volume	$3(1-\alpha)^{2/3}$	$[1-(1-\alpha)^{1/3}]$
Diffusion Models		
1-D diffusion	$1/2\alpha$	α^2
2-D diffusion	$[-\ln(1-\alpha)]^{-1}$	$[(1-\alpha)\ln(1-\alpha)]+\alpha$
3-D diffusion-Jander eqn.	$3(1-\alpha)^{2/3}/2(1-(1-\alpha)^{1/3})$	$[1-(1-\alpha)^{1/3}]^2$
Ginstling-Brounshtein	$(3/2((1-\alpha)^{-1/3}-1)$	$1-(2\alpha/3)-(1-\alpha)^{2/3}$

For dynamic measurements carried out at a constant heating rate, the explicit temperature/time dependence in *equation (2.3)* is eliminated through a trivial transformation in *equation (2.9)* [33-38],

$$\beta \frac{d\alpha}{dT} = k_0 \exp(-E/RT) f(\alpha) \qquad (2.9)$$

Where, $\beta = \frac{dT}{dt}$ is heating rate (^{o}C min^{-1}) and $\frac{d\alpha}{dT}$ is rate of reaction (K^{-1}).

2.2. Kinetics Studies in Pyrolysis of Plastics

2.2.1. Kinetic models based on thermogravimetry

Single plastics

Pyrolysis of plastics is a thermal decomposition process, which involves thermal break-down of the plastic to yield various hydrocarbons. It involves complex reactions, and therefore evaluation of kinetic parameters for all possible elementary step reactions, poses a great challenge. A vast amount of work [28-30, 41-43] has been reported to estimate the thermal degradation kinetics of plastics by both empirical and fundamental theoretical techniques. The development and ready availability of reliable and accurate electronic microbalances have led to their wide application in kinetic studies of decomposition of plastics [44, 45]. TGA is a widely applied technique to study the pyrolysis kinetics of plastics. As already explained in the previous section, the weight loss data obtained from TGA can be used to calculate α. Kinetic analysis of '*α-t'* measurements usually involves curve-fitting of the experimental data to well known reaction models (*f(α) or g(α)*), which is commonly known as model-fitting approach. Most of these studies deal with determination of overall kinetic parameters such as E, k_o and *f(α)* (kinetics triplet).

Model-fitting methods involve two fits: the first determines the model that best fits the data *(equation 2.4)* while the second determines specific kinetic parameters such as the activation energy (E) and frequency factor (k_o) using the Arrhenius equation *(equation 2.2)*. On the other hand, isoconversional methods calculate E values at progressive degrees of conversion without any modelistic assumptions. The standard isoconversional method [37] is based on taking the natural logarithm of *equation 2.5* giving,

$$-\ln t = \ln\left(\frac{k_o}{g(\alpha)}\right) - \frac{E}{RT} \qquad (2.10)$$

A plot of ($-\ln t$) versus $1/T$, at each α yields E (from the slope) for that α, regardless of the model. Friedman's method [46] is based on taking the natural logarithm of *equation 2.3* giving

$$-\ln\left(\frac{d\alpha}{dt}\right) = \ln(k_o f(\alpha)) - \frac{E}{RT} \qquad (2.11)$$

A plot of $\ln(d\alpha/dt)$ versus $1/T$ at each α yields E (from the slope) for that α regardless of the model.

Thermogravimetic (TG) analysis coupled with model-fitting approach is commonly used for such studies to evaluate the apparent overall kinetic parameters [31-33, 35, 36, 42, 43, 47-52]. In most works reported in literature, model-fitting methods are applied to evaluate pyrolysis kinetics parameters using single heating rates and n^{th} order reaction model (which are estimated after minimizing deviation between experimental and simulated data). However, International Confederation of Thermal Analysis and Calorimetry (ICTAC) project, 2000 ruled out the validity of thermal kinetics analysis using single heating rate [31]. Modern model-fitting thermal kinetics analysis methods use multi-heating rates, thus taking care of

multi-step reactions which might occur during thermal decomposition and incorporate possible partial diffusion, back reaction, branch reaction, etc. in the model equations [35-36].

Polymer pyrolysis kinetics has been commonly described by n^{th} order reaction [31-33, 35, 36, 47-49] or Prout-Tompkins model [42, 43]. The 1^{st} order reaction model is most commonly used among all the n^{th} order reaction models [51, 53]. The other, more complex models have large number of fit parameters, which limits their practical usability. However, researchers have explored the applicability of different available models to characterize the kinetic behaviour of polymers.

Saha *et al.* [33] investigated the thermal pyrolysis kinetics of polyethylene terephthalate (PET) from different sources of soft drink bottles using a simple n^{th} order reaction model and ASTM E698. Thermal degradation was carried out in dynamic condition at three different heating rates of 10, 15 and 25^{o}C min^{-1} under nitrogen atmosphere. Kinetic parameters were obtained from three dynamic TGA curves at three different heating rates using ASTM E698 and from one TGA curve at the heating rate of 10^{o}C min^{-1} using n^{th} order model techniques. The n^{th} order model technique was found to be better in predicting the experimental data than ASTM E698 technique.

It has been noticed that majority of two-parameter models, including unknown rate constants and unknown activation energies in the equation, can describe the kinetic curves using single heating rates with satisfactory accuracy. However, the resultant values of activation energy may be different. The description of a series of kinetic curves measured under different heating rates by a two-parameter equation is more difficult. Only some models can satisfactorily fit the series of curves. Mamleev *et al.* [32] proposed a new algorithm for computing activation energies and rate constants by approximating TGA data obtained over a wide temperature range and with temperature-time relationships. Eighteen known kinetic

models corresponding to different physical and chemical processes were tested in order to select the most suitable model(s). They concluded that analysis using multiple heating rates gives reliable results than those employing single heating rate.

Again, differences were noticed in the dynamic methods, due to temperature gradients across the decomposing sample. The temperature gradient within the sample resulted in different reaction rates. Thus, TG analysis of thermal decomposition reactions refers more or less to sample-averaged reaction rates. To overcome this drawback, Hornung *et al.* [47] studied thermal degradation of polyamide 6 under isothermal conditions in an isothermal gradient free reactor (closed loop type reactor) with evolved gas analysis by means of on-line mass spectrometry, which aided in the determination of degree of conversion [47]. With proper design of the reactor, the heating time of the sample and the free reactor volume were minimized. With the help of the mass spectrometric data, the degree of conversion was determined which enabled determination of formal kinetic parameters of the decomposition reaction. They compared kinetic parameters evaluated therefrom with those obtained from TG by dynamic means and concluded that the measured parameters were comparable to data obtained from dynamic measurements at low heating rates.

Martin-Gullon *et al.* [48] studied thermal decomposition of PET, both under inert and oxygen environment in a TGA for a temperature range of 25-800^{o}C. Pyrolysis was carried out under dynamic conditions using three different heating rates (5, 10 and 20^{o}C min^{-1}), while combustion studies were carried out at 10^{o}C min^{-1} for different amounts of oxygen (10, 20 and 33% in helium). The decomposition kinetics of PET was satisfactorily modeled by assuming two parallel reaction schemes, where each part decomposed independently. The results showed that the reaction started at around 377-427^{o}C, which accounted for 80% weight loss of the initial material. This was attributed to the first part, with a 1^{st} order reaction. The second part started to decompose after the completion of decomposition of the

first part, which accounted for 6% weight loss. Even in the presence of oxygen, decomposition started at same temperature range, yielding 1^{st} order reaction kinetics with similar parameters to that of the first part of the pyrolysis process. However, in the second part, due to combustion of the char residue, different kinetic parameters were obtained, depending on the oxygen concentration.

Wang *et al.* [50] studied non-isothermal TG kinetics of polytrimethylene terephthalate (PTT) with various molecular weights under argon, air and nitrogen atmosphere by Freeman-Carroll, Friedman and Chang methods. The experimental data indicated that PTT exhibited similar decomposition process in argon and nitrogen, while it followed a much different mechanism in air. Both onset temperature and maximum weight-loss temperature showed an increase with an increase in molecular weight of PTT. The kinetic parameters (activation energy, order and frequency factor) increased with molecular weight of PTT under argon atmosphere. However, these kinetic parameters showed a reverse trend when the atmosphere was changed to air.

Gao *et al.* [51] established a relation for determining reaction order from experimental data of dynamic measurements to avoid direct use of 1^{st} order kinetics. The reaction order and the other two reaction parameters thus obtained were comparable to those from isothermal measurements. Gao *et al.* [54], in another work made an attempt to calculate Arrhenius parameters for the thermal degradation of polyethylene (PE) by estimating the fraction of bonds broken (instead of the use of the mass conversion or weight loss of the sample). The work found that the activation energy thus obtained is close to the values for C-C bond scissions and β C-H bond scissions of hydrocarbon radicals. In another work [55], they concluded that both dynamic and isothermal degradation of polypropylene (PP) are unlikely to be described by a 1^{st} order reaction model. The appropriate reaction order was determined according to the α value corresponding to the maximum decomposition temperature observed

in dynamic measurements. The validity of the thus determined reaction order of (n = 0.35) for the dynamic degradation was verified by similar values of activation energy in a comparison of 'α *vs.* t' plot using single heating rate with the isoconversional plot. The isothermal degradation of the PP was described by reaction order n = 0.35, while the activation energy and pre-exponential factor of the isothermal degradation were reported to be similar to those measured in the dynamic degradation.

Saha *et al.* [52] explored the possibility of applying different reaction models and six different model fitting techniques (n^{th} order, Friedman, Freeman-Carroll, Chang, ASTM E698 and a newly proposed SDMT, standard deviation minimization technique) to evaluate the kinetics triplet for the thermal decomposition of waste PET soft drink bottles by both isothermal and non-isothermal studies. Non-isothermal experiments at four different heating rates and isothermal experiments at four different temperatures were carried out in a TGA. SDMT technique was found to best predict the experimental data and hence offered the optimum kinetic triplets for PET decomposition. In another work, Saha *et al.* [56] employed Hybrid Genetic Algorithm (HGA) technique to attain the globally optimum kinetic parameters using dynamic TG analysis using multi-heating rates for waste PET, waste low density polyethylene (LDPE) and PP.

However, selection of appropriate model and initial guess of kinetics parameters are major drawback of model fitting methods [36]. Moreover, the kinetics triplet obtained by model-fitting technique from non-isothermal condition is highly uncertain and cannot be compared with the kinetics triplet obtained from isothermal condition [37]. This uncertainty mainly comes from model incorrectness, experimental error, initial value approximations and the drawbacks associated with many optimization techniques to find the global optimum. These drawbacks of model fitting can be avoided with the use of isoconversional methods, also known as Vyazovkin's model-free methods [36,37,57-59]. Vyazovkin model-free approach is

a trustworthy way of obtaining reliable and consistent kinetic information from both non-isothermal and isothermal data. It can also help to reveal the complexity of multiple reactions due to the dependencies of activation energy on the extent of conversion [60, 61].

Saha *et al.* [57] applied the Vyazovkin model-free approach to study non-isothermal decomposition of waste PE sample using various temperature integral approximations such as Coats and Redfern, Gorbachev, Agrawal and Siva Subramanian, and a new approximation with a new method for direct integration. Initial strong and increasing E dependency on α in case of non-isothermal decomposition was attributed to initiation at weak links. Again, weak but increasing E dependency on α in the later stages was attributed to dependence of distribution of size of volatile products on heating rate and random scission. Weak and decreasing followed by weak but increasing function of α in case of isothermal decomposition was said to be possibly due to existence of two opposite effects, nucleation, and distribution of size of volatile products. In another work, Saha *et al.* [62] used the same model free method for isothermal and non-isothermal decomposition kinetics analysis of PET sample. For non-isothermal studies, activation energy was found to be a weak but increasing function of conversion, whereas for isothermal studies, it was found to be a strong and decreasing function of conversion.

Westerhout *et al.* [53] studied pyrolysis kinetics of LDPE, high density polyethylene (HDPE), PP and polystyrene (PS) by isothermal TGA experiments at temperatures below 450^{o}C. They commented that the scatter in the reported kinetic parameters, obtained by different researchers in low temperature pyrolysis of these polymers is due to the use of simple first order kinetic models over a wide conversion range. They determined the kinetic parameters with the help of a simple 1^{st} order model for high conversions (70-90%), and a model developed in the study, *viz.* random chain dissociation model (RCD) for the entire conversion range (10-90%). The influence of important parameters, such as molecular

weight, extent of branching and β-scission on the pyrolysis kinetics was studied with the RCD model. The effect of the extent of branching was found to be quite significant, but the effect of the initial molecular weight and β-scission was found to be minor.

Catalysts were found to be very effective in terms of lowering of decomposition temperature and reaction time. Although a wide variety of catalysts have been employed to crack plastics, zeolites have proven particularly effective. Filho *et al.* [63] investigated the effect of ZSM-5, and ZSM-12 in lowering the activation energy of PP by applying Vyazovkin model free approach, and found ZSM-12 to be more effective. The percentage weight loss of PET by both thermal and catalytic degradation was investigated by Cheng and Chiu [64]. The extent of degradation was found to be tremendously affected by temperature between 400 and 500^{o}C. Among the twelve different catalysts used in catalytic cracking experiments, copper (II) chloride was found to be the most active in terms of decrease in carbonaceous residue and enhancement of degradation rate. Marcilla *et al.* [65] investigated catalytic pyrolysis of LDPE in a TGA in nitrogen atmosphere, at a heating rate of 5^{o}C min^{-1}, to study the effect of the type and concentration of different catalysts on the thermal decomposition of the plastic by using MCM-41, USY and ZSM-5. MCM-41 was found to be more effective in reducing the temperature of the LDPE decomposition, than the other two types. They also observed that maximum rate of decomposition was obtained at different temperatures for different samples. A kinetic model involving two pathways, one for the catalytic and the other for non-catalytic, was also developed which showed a very good correlation of data for all the runs performed using the same catalyst.

Mixed Plastics

Literature in evaluation of pyrolysis kinetics of mixed plastics is scarce (as compared to those available for single plastics). Westerhout *et al.* [53] observed that pyrolysis of polymer

mixtures behave quite similarly to pure polymers and they claimed that the additivity rule is the correct approach for this problem. Miranda *et al.* [66] studied the vacuum pyrolysis of commingled plastics containing PVC. The study involved a comparison of the experimental curve of the decomposition of the mixture with a calculated non-interacting component decomposition curve based on the behaviour of the individual polymers. The results obtained indicate that some interactions occurred at high temperatures (>375^{o}C).

Chowlu *et al.* [67] employed isoconversional technique to study the variation of activation energy (E) with conversion (α) for five different mixture compositions of LDPE and PP. They observed that for all the mixture compositions, initially E was a slow but increasing function of α and then became a very strong function of α towards the end of decomposition. Detailed kinetic models of thermal decomposition of mixtures of PS and poly(α-methylstyrene) (PAMS) have also been reported [68-71]. It was found that the decomposition rate of PS was inversely proportional to the molecular weight of the other species, *i.e.* PAMS [68]. The binary degradation of PS and PP was modeled at the mechanistic level by combining the individual component models and adding interactions between PS and PP derived species [72-74]. To increase the enhancement in the PP degradation rate, solid state shear pulverization (SSSP) and changes in the PS/PP weight ratio were used to manipulate the interfacial area between PS and PP during binary pyrolysis. PP degradation rate increased by 25% by using SSSP compared to no premixing. Stepwise pyrolysis of plastic mixtures was also reported in the literature [75, 76] which confirmed that different molecular structures of plastics resulted into different reaction mechanisms of thermal decompositions.

Faravelli *et al.* [75] investigated the effect of the mixing scale of PE and PP in the melt and found that if the mixing scale of the polymers is poor, the decomposition of each of the polymer behaves independently of the other. Conversely, when the mixing reached the molecular scale, co-pyrolysis took place with partial interactions. Marcilla *et al.* [77]

developed an elementary reaction model by assuming no interaction for evaluating catalytic effects of HZSM-5, FCC, and HUSY in the pyrolysis of a PE-PP mixture and concluded that FCC catalyst showed optimum properties. In another work, Marcilla *et al.* [78] carried out thermal and catalytic decomposition of PP and reported that the addition of MCM-41 at a loading of 16% produced a remarkable decrease of almost 110^{o}C in the temperature of maximum decomposition rate. Decomposition kinetics of PP was satisfactorily modeled assuming two independent processes with and without the catalyst action of the MCM-41. The model was capable of correlating all the details observed in a single TG curve.

The goal of the most works reported so far has been the characterization of the decomposition process in terms of overall kinetic parameters determined on the basis of α *vs.* t curves [31-33, 35, 36, 42, 43, 47- 52]. The overall kinetic parameters give an overall idea of the reaction kinetics, but mostly they ignore possible pathways of decomposition of the polymer. Some reaction models have been proposed in literature, which refer to global apparent kinetics [79] or to a few step mechanisms [30, 80]. In general, these models do not take into account the detailed chemistry of plastic degradation and describe the pyrolysis process by means of simplified reaction paths. Each individual reaction step is equivalent to and representative of a complex network of reactions. There lies the limitation of overall kinetics estimation, as it fails to address the detailed mechanistic chemistry of polymer decomposition. This approach can only adequately describe the apparent kinetics in a narrow range of heating rates and operating conditions. A single step model is not able to cover a wide range of heating rates, temperatures and conversion levels with the same kinetic parameters. Therefore, dynamic and isothermal analyses reveal different decomposition rates of reaction. Furthermore, the possible presence of mass and heat transfer limitations, which are generally neglected, spreads the range of variation of these kinetic constants.

2.2.2 Kinetic models based on mechanistic modeling

The importance of a mechanistic model capable of accounting for the differences in starting material and able to describe the reaction process over a wide range of heating rates and temperatures is apparent. The mechanistic model not only allows the prediction of the detail of product distribution (a significant step in the possible upgrading of solid wastes), but also helps in the identification of possible pollutant formation (like polycyclic aromatic hydrocarbons, PAH). Thus, mechanistic modeling has gained popularity among the researchers as a valuable tool to address the detailed kinetic scheme of decomposition of plastics.

Mechanistic models based on elementary reactions

For the models based on elementary reactions, the reaction rates are expressed in terms of concentration of the species involved in the elementary steps. Johannes *et. al.* [81] described thermal cracking using steps of individual reactions on the basis of well-known kinetic equations and experimental data obtained for the decomposition of LDPE. These kinetic models typically involve a great number of kinetic parameters and do not account for secondary reactions that take place during pyrolysis.

Peterson *et al.* [61] used isoconversional method to calculate activation energies for PS, PP, and PE degradation as a function of extent of conversion and corresponding degradation mechanism was proposed. Chan and Balke [82] developed a comprehensive kinetic model for thermal degradation of PP and fitted to molecular weight distribution (MWD) data of products (obtained by size-exclusion chromatography). Reaction temperatures of 275 to 315^{o}C were examined with reaction times of up to 48 hours. They observed that with increase in reaction time, molecular weights (both weight-average, M_w and number average, M_n) and polydispersity of the products decreased. A limiting version of the model containing only a

single variable parameter, an apparent rate constant, was found to be sufficient to provide excellent fits of all MWD data. The variations with temperature provided Arrhenius plots. They obtained a lower value of activation energy (123.8 kJ mol^{-1}) than expected, which was attributed to the temperature range examined and presence of weak links. In their successive work, Chan and Balke [83] used the same kinetic model to study time-temperature superposition for PP degradation by defining a 'reduced time'. This reduced time is the product of a temperature-dependent rate constant and reaction time. Using high temperature size-exclusion chromatography, experimental measurements of thermally degraded polypropylene showed that MWDs were superimposable at identical reduced times except when reaction times were less than 2 min. Degradation temperatures and reaction times extended from 250°C and 14 days to 375°C and 1 min. The extent of degradation was found to be similar for 2 minutes at 350°C, 12 hours at 275°C and 14 days at 250°C.

Bockhorn *et al.* [80] investigated isothermal decomposition kinetics of PE and PP using a gradient free reactor with on-line mass spectrometry. Global kinetic parameters for the overall degradation were determined. In the case of PE degradation, a change of the apparent reaction order with temperature was observed, whereas in the case of PP degradation, a constant apparent order of reaction within the investigated temperature range was found. On the basis of this data and corresponding literature, rate equations were formulated and kinetic models for PE and PP degradation, consistent with the measured rate coefficients, were discussed.

Mechanistic models based on multi-step reactions

These kinetic models incorporate multi-step reactions in the proposed kinetic scheme which account for secondary reactions that take place during pyrolysis. These models are typically

complex, consisting of a large numbers of kinetic parameters and reactions that describe and quantify the pyrolysis decomposition products [73-75, 84-86].

These models are based on predictions of a typical free radical chain mechanism (for polyolefins) involving reaction steps such as random or chain-end scissions, inter- and intra-molecular hydrogen abstractions, unzipping, backbiting, radical recombination and disproportionation reactions [73, 74].

In another study, Marongiu *et al.* [87] reported detailed kinetic modeling of thermal degradation of vinyl polymers (PS, PP and PE) with the help of a unified approach. The main feature of this approach was that the same model can be applied to all the three polymers. In fact, the thermal degradation of vinyl polymers was always kinetically based on the same reaction classes, which have only a few reference kinetic parameters and can be defined from analogous gas phase reactions. The kinetic scheme for the different polymers was then built by selecting only the proper reactions in the different classes. They observed that the three polymers behave quite similarly: one step degradation and no char formation. PS however showed higher reactivity and higher tendency to unzip to monomer.

Some of the models, reported in literature [88, 89] are developed based on population balance equations solved by method of moments. These moment equations describe the statistical distribution and evolution of different families of dead and live species in the liquid and gas phase characteristic of the MWD of the products. This approach facilitates comparatively reduces the computing times required to solve the huge number of equations. Thus, this technique is worthwhile to describe MWD of species evolved in pyrolysis of plastics or plastic mixtures, also called 'distribution kinetics' [88-90].

Kruse *et al.* [73] developed a mechanistic model to describe the thermal degradation process of PS, by developing differential equations describing the evolution of structurally distinct

polymer species. Unique polymer groups were devised which helped in capturing the decomposition chemistry. The model included over 2700 reactions and tracked 64 species. Programs were developed using the programming language Perl to assemble moment equations from input of the polymeric features to be tracked. The model predictions for the evolution of M_n and M_w and yields of styrene, dimer, and trimer compare very well with experimental data for the degradation of PS over a large temperature range and with different initial molecular weights. Evolution of low molecular weight products from experiments reported in the literature is also captured. In another work [74], they developed a mechanistic model to predict formation of low molecular weight products from pyrolytic decomposition of PP following a similar approach. The conversion among species was described using typical free radical reaction types, including inter and intramolecular hydrogen transfer, mid and end chain β-scission, radical addition, bond fission, disproportionation and radical recombination. The model predictions compared well with experimental data obtained over a temperature range of 350-420^{o}C.

Detailed kinetic models of PE, PP and PS were also reported by Richards *et al.* [70, 71]. Ranzi *et al*. [85] adopted a numerical approach to present a mechanistic model which described the radical chain pyrolysis reactions of PE and PP taking place in the liquid phase.

The mechanistic models, discussed in this section, provide a better basis for modeling and extrapolation than the alternative kinetic models aimed at determination of overall kinetics. The former takes into account molecular structure/property relationships and fundamentals of physical and organic chemistry in model formulation [91]. These advantages are offset somewhat, however, because of the large computing time often associated with mechanistic simulation. In light of this, kinetic models based on 'lumping system' have been developed, which aims at reducing the dimension of the reactant space by lumping together real compounds having similar properties into a properly selected number of compound classes

[91-94]. As an example, individual components of the pyrolysis product stream can be grouped into compound classes such as parrafins, iso-paraffins, alkylaromatics, alkylnaphthenes, alkylhydroaromatics, or olefins, long-chain-olefins, naphthenes etc. The theoretical development and application of lumping to handle complex systems has seen a growth within last four decades. Lin *et. al.* [93] improved the conventional lumping scheme to account for the catalytic degradation of HDPE and PP over fluidized acidic catalysts in a fluidized bed reactor. In a following study, Cardona and Corma [94] presented a kinetic model for the pyrolysis of PP in a stirred batch reactor and accounted for thermal and catalytic cracking as well as coke formation using decay functions, one as a function of time and the other as a function of coke concentration on catalyst.

2.3. Decomposition Mechanism of Polymers

Decomposition modes are often subdivided according to the reaction patterns, which are mainly dictated by molecular structure and the presence of catalysts. Accordingly, thermal decomposition of plastics can follow three major pathways: side-group elimination, random scission and chain-end scission or depolymerization, also known as unzipping [34, 95].

- *Side-group elimination* takes place generally in two steps. The first step is the elimination of side groups (e.g., HCl in case of polyvinylchloride, PVC) attached to the backbone of the polymer. This leaves an unstable polyene macromolecule that undergoes further reaction, including the formation of aromatic molecules, scission into smaller fragments, or the formation of char. PVC, polyvinylfluoride and polyacrylonitrile follow this decomposition pathway.
- *Random scission* involves the formation of free radicals by arbitrarily breaking the polymer chain at some point on the polymer backbone, producing small repeating series of oligomers of varying chain lengths. PE, PP, PS, polybutadiene and

polyisobutene decompose by this mechanism. The size distribution over the resulting fragments is largely Gaussian, with the average molecular weight continuously descending with rising pyrolysis temperature and time. Thus, polyolefins are converted into PE waxes and oils, often high in α-olefins. Conversely, PP products yield a much more branched product mix.

- In *chain-end scission or unzipping*, polymer is broken up from the end groups successively yielding the corresponding monomers and terminal free radicals. Several polymers decompose by this mechanism including Poly(methyl methacrylate) (PMMA), polytetrafluoroethylene (PTFE). This decomposition mode is of practical interest, since monomer is a high value product. However, monomethyl acrylate (MMA) generated is not necessarily fit as polymerization grade, and often used as a viscosity index improver of lubricating oil, in acrylic varnishes, rather than as a monomer [95].

Polymer decomposition by random or chain-end scission is a radical chain reaction which involves a number of steps, *viz*. initiation, propagation and termination. A typical radical decomposition mechanism of PE is shown in *Scheme 1* [80]. Gao *et al.* [54] proposed *β*-scission of radicals as a part of thermal decomposition mechanism of PE, which provided a detailed understanding of hydrogen transfer in the polymer melt and accounted for hydrogen gas formation in the pyrolysis of PE.

Initiation:

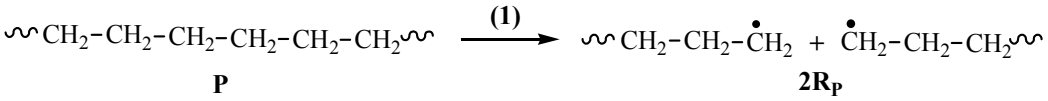

Propagation:

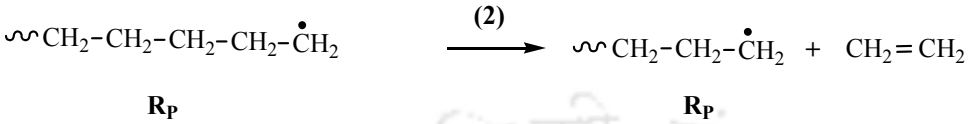

hydrogen transfer, intramolecular

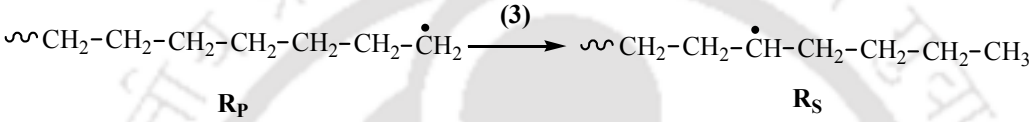

β-scission

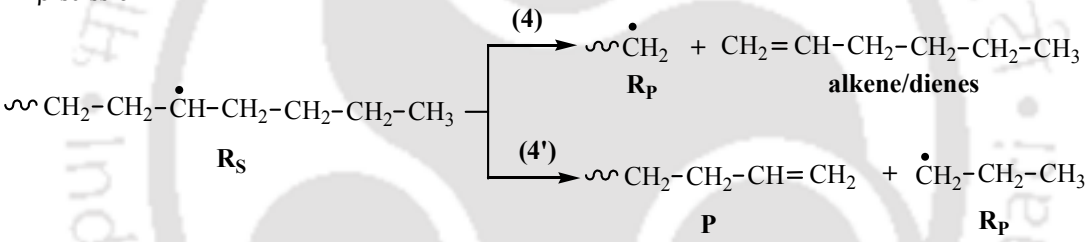

hydrogen transfer, intermolecular

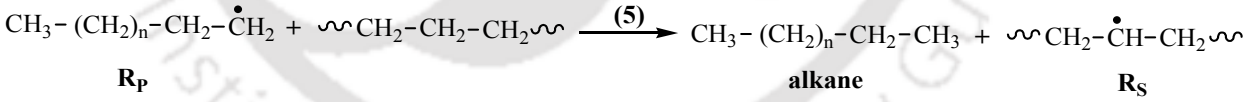

Termination (2nd order): recombination

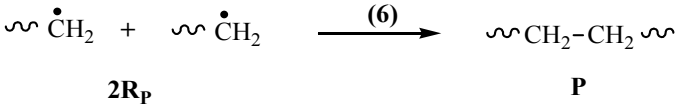

Scheme 1: A typical free radical mechanism for decomposition of PE [80]; P: PE, R_p: Primary radical, R_s: Secondary radical

It involves basically five reaction types:

- Main-chain cleavage to form chain terminus radicals, known as primary radicals (R_p) which marks the initiation step (reaction 1)
- Intramolecular radical transfer or backbiting (reaction 3) to form internal radicals, known as secondary radicals (R_s). It is worthwhile to note here that R_p is more reactive than R_s. Thus, once they are formed they have a tendency to get stabilized; hence they transform themselves to R_s.
- β-scission to form both volatile products and terminally unsaturated polymer residues, e.g., β-scission of R_p produces ethylene (reaction 2), whereas β-scission of R_s gives alkene/diene (Reaction 4) and a polymer with terminated double bond (reaction 4′).
- Intermolecular radical transfer between R_p and the polymer producing alkane. Intermolecular transfer might also occur between R_s and the polymer (reaction 5).
- Radical recombination to form a stable product, which marks the termination step (reaction 6)

Intramolecular transfer reactions are favored at lower temperature, while β-scission and intermolecular transfer reactions are favored only at higher temperature (> 400^{o}C) [80, 96]. It should be noted that the primary radical is regenerated in each step, which further attacks the main polymer chain, or transforms itself to a secondary radical. This process continues till the polymer chain length considerably reduces. Among the various intramolecular transfer reactions described in literature, 1,5-Hydrogen transfer is the most common, which proceeds via a six-membered ring intermediate [54, 80, 87, 96].

Scheme 2 presents the radical chain mechanism of thermal decomposition of PP. It is analogous to the mechanism of PE degradation (*Scheme 1*). It involves the same classes of

reactions as that of PE; *viz*. main-chain cleavage, intramolecular and intermolecular hydrogen transfer reactions, *β*-scission, radical recombination, disproportionation reactions etc. The only difference arises due to the presence of tertiary carbon centers at alternate carbon atom along the chain-backbone in PP, which renders it more reactive than PE. Due to the presence of this tertiary carbon, main products obtained from PP are mostly branched hydrocarbons. Different backbiting reactions originating from an end-chain radical shown in the scheme are 1,3-, 1,4-, 1,5- and 1,6-end hydrogen transfer (reactions 9-12 in *Scheme 2*). Here too, 1,5-end hydrogen transfer reactions are more favorable, which account for the formation of some specific products [74, 80, 87]. Different backbiting reactions originating from a mid-chain radical considered in the scheme are 1,3-, 1,4- and 1,5-mid hydrogen transfer (reactions 13-15 in *Scheme 2*). These mid-hydrogen transfer reactions are slower than the end-hydrogen transfer reaction due to entropic barriers; however they are considered important as they lead to the formation of specific unsaturated oligomers [74].

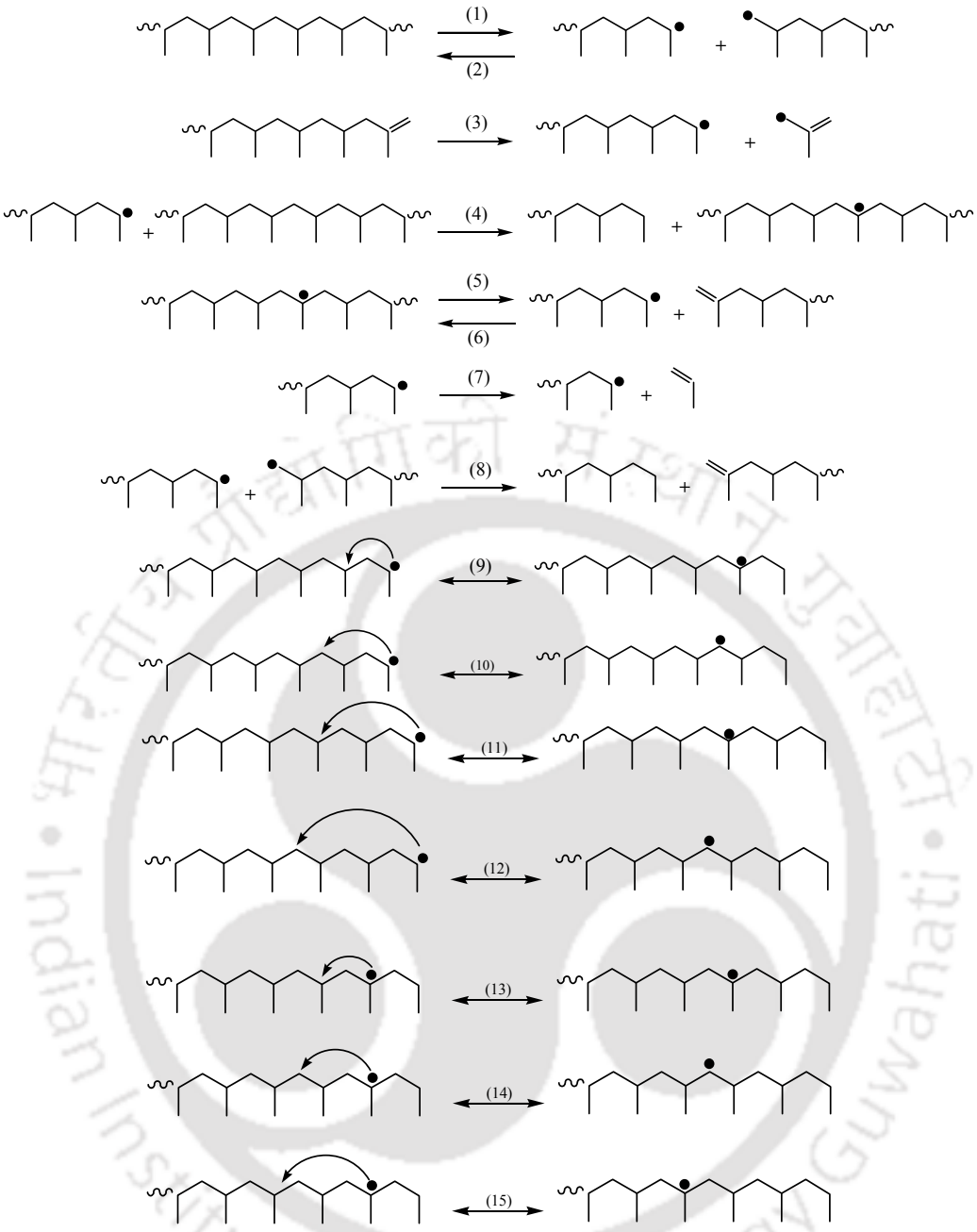

Scheme 2: A typical free radical decomposition mechanism for PP; (1) chain fission, (2) radical recombination, (3) allyl chain fission, (4) intermolecular hydrogen abstraction, (5) mid-chain β-scission, (6) radical addition, (7) end-chain β-scission, (8) disproportionation, (9) 1,3-end-hydrogen transfer, (10) 1,4-end hydrogen transfer, (11) 1,5-end hydrogen transfer, (12) 1,6-end hydrogen transfer, (13) 1,3-mid hydrogen transfer, (14) 1,4-mid hydrogen transfer, and (15) 1,5-mid hydrogen transfer.

Scheme 3 presents a simplified thermal decomposition mechanism for PS. Initiation reactions of the following two types can be identified in PS, *i.e.* either random scission of the C-C bond to form one primary radical and one secondary benzyl radical with a strong benzylic resonance (reaction 1), or chain-end scission to form one secondary benzyl and the resonantly stabilized allyl benzene radical (reaction 3). Propagation step consists of the sequence of H-abstraction and *β*-scission or unzipping reactions. There are following two types of H-abstraction reactions. One is intermolecular abstraction, in which the radicals abstract the hydrogen from a different molecule, as shown in reaction 4. Other is intramolecular abstraction, in which the radicals can easily form five-, six-, or seven-membered ring intermediates, as a result of 1,4-, 1,5- or 1,6- transfer reactions. However, just as in the case of PE or PP, 1,5-transfer reactions are the most favorable, which leads to the formation of a the tertiary benzylic radical (reaction 8). It undergoes *β*-scission to form a secondary benzylic radical and a polymer species with an unsaturated end (reaction 5). The reverse reaction (reaction 6), which is termed as radical addition, results into a tertiary radical. End chain β-scission (reaction 7) of the benzyl radical results in the formation of styrene monomer and Termination takes place by either recombination (reaction 2), or disproportionation (reaction 9).

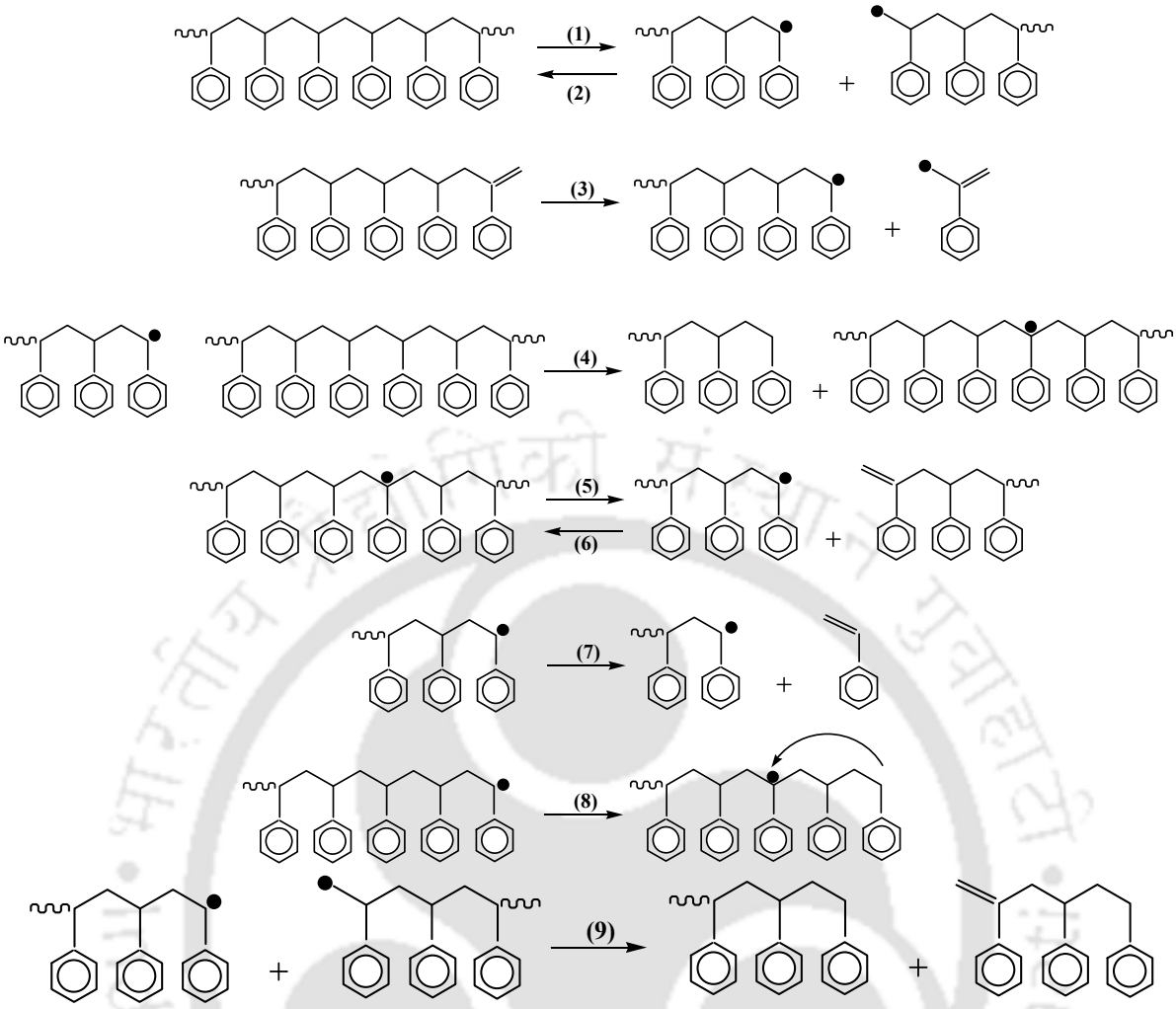

Scheme 3: A typical free radical decomposition mechanism for PS [73]; (1) chain fission, (2) radical recombination, (3) allyl chain fission, (4) hydrogen abstraction, (5) mid-chain *β*-scission, (6) radical addition, (7) end-chain *β*-scission, (8) 1,5-hydrogen transfer and (9) disproportionation.

Scheme 4 depicts a possible decomposition mechanism for PET [97]. Its repeat unit consists of a benzene ring, two ester (-COO-) groups along with two methylene (-CH_2-) groups. Generally, decomposition of PET proceeds by heterolytic (or ionic) mechanism, rather than homolytic (or radical) mechanism [98]. Decomposition starts at the ester linkage via a six-membered ring intermediate, which leads to the formation of an acid end and an unsaturated end (reaction 1) [99-101]. The reactions that followed are combination of chain-scission,

splitting off of small molecules (e.g, CO_2 or CH_3CHO etc) from such chain-ends (reaction 3-4) and a rearrangement reaction (reaction 5) . Formation of polycyclic hydrocarbons (PAHs) has also been reported in literature for which formation of benzene is vital.

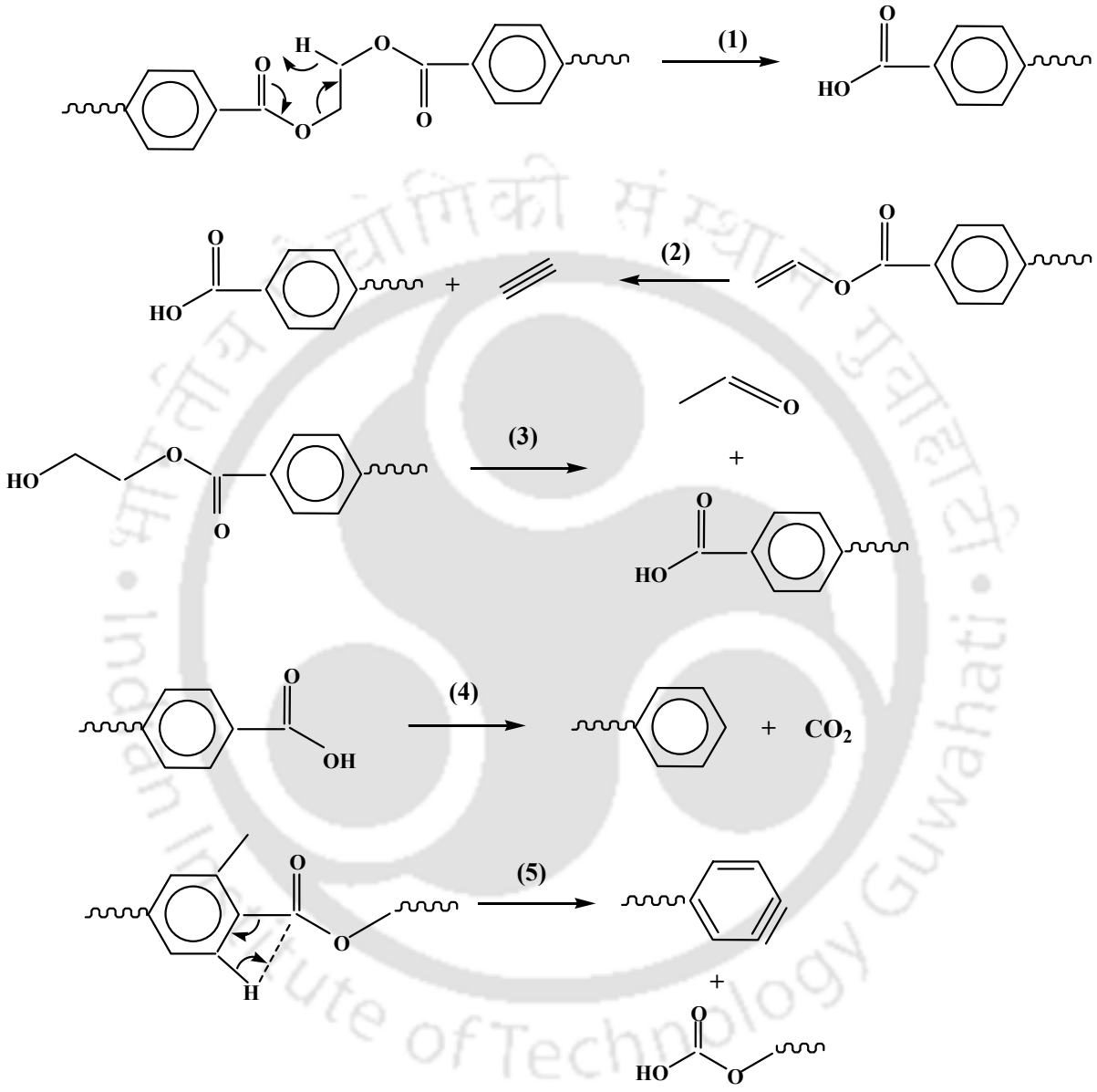

Scheme 4: Possible decomposition pathways for PET [97]

A typical route for formation of PAH by H abstraction-C_2H_2 addition (HACA) mechanism is shown in *Scheme 5,* as proposed by Frenklach *et al.* [102]. Growth of aromatic structures via

the dimerisation and coalescence of PAHs as proposed by Mukherjee *et al.* [103] is also presented.

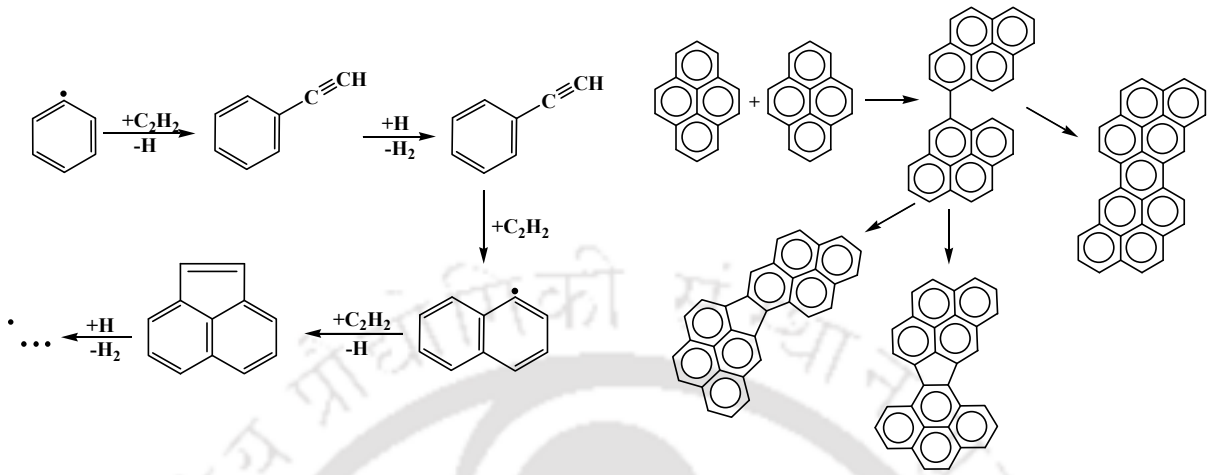

Scheme 5: Left: Growth of PAHs according to the H abstraction-C_2H_2 addition (HACA) mechanism [102]; Right: Growth of aromatic structures via the dimerisation and coalescence of PAHs [103]

2.4 Product Distribution from Pyrolysis of Plastics

The principal output products from pyrolysis of plastics are gaseous and liquid hydrocarbon fractions that are remarkably similar to the refinery cracking products [95]. However, their chemical composition and properties strongly depend on the plastic source. Due to diverse chemical composition and structure of the source plastics, considerably larger variations in compositions of the pyrolysis-derived fuels are likely vis-à-vis petroleum-derived fuels. There is a direct link between polymer structure and its primary pyrolysis products, the latter primarily resulting from the breakage of bonds followed by some molecular or free radical rearrangement. Secondary reactions gradually convert the primary products into more stable, less reactive products. Product distribution hence primarily depends on structure of the parent plastic, residence time, relative rates of bond breakage of different species. As a rule, bond

breakage becomes easier at high temperature. Product distribution study thus plays a key role in characterizing and assessing the viability of commercial plastic pyrolysis procedures. Different types of reactors coupled with GC or GC/MS have been studied for product analysis, apart from the studies carried out in TGA and GC combination. The use of a wide variety of reactor designs, operating conditions, and catalysts resulted in reported product distributions that vary significantly.

Effect of reaction time and degradation temperature on the characteristics of the liquid product from pyrolysis of a waste plastics mixture (HDPE:LDPE:PS=3:2:3:1) was investigated by Lee *et al.* [104]. Pyrolysis experiments were carried out in a stirred semi batch reactor at 350^{o}C and 400^{o}C, wherein they observed that cumulative yield of liquid products at 400^{o}C sharply increased with increase of reaction time, compared to that at 350^{o}C. The order for the main products obtained at 350^{o}C was firstly aromatic products, followed by olefin products, while at 400^{o}C paraffin products were also obtained after the olefins. Walendziewski and Steininger [105] reported thermal and catalytic degradation of PE between 370-450^{o}C. An increase in degradation temperature of PE led to a modest increase of gas and liquid products with boiling point <360^{o}C, combined with a sharp decrease in residue. Mastral *et al.* [106] carried out pyrolysis of HDPE between 640-700^{o}C with different residence times (0.8-2.6s) in the reactor. They developed a model based on a radical mechanism that could predict the product distribution. Gas product distribution for pyrolysis of PE derived from random-scission hypothesis was proposed by Faravelli *et al.* [107]. They introduced backbiting reactions into the kinetic scheme to predict the larger amounts of selected products. In order to investigate the decomposition behaviour of PP at low temperatures and very low reaction rates, fractional pyrolysis of PP is performed under dynamic conditions. PP was heated with a linear temperature program and fractions of similar sample sizes were collected in five cold traps. Sampling was carried out at temperatures,

below that of isothermal measurements, which revealed a decreasing amount of alkenes and alkanes and an increasing amount of dienes with temperature [80].

Lattimer [96] observed volatile pyrolyzates to masses well above 1000 Daltons by field ionization mass spectrometry of the products evolved during pyrolysis of PE. Decomposition process was described by a free radical mechanism in which 1-alkenes were observed as the major pyrolyzates, with only very small amount of alkanes and dialkenes being formed. Decomposition studies [108, 109] carried out on PET reported about equal quantities of gas and liquid with a proportion of solid residue around 10%. The gases mainly contain oxides of carbon (CO and CO_2) (nearly 90%) [108]. Benzene and toluene were the major components in the liquid [109]. Montaudo *et al.* [98] studied the primary thermal decomposition mechanism of PET by mass spectrometry using negative chemical ionization. They found that cyclic oligomers, formed by intramolecular exchange (ionic) reactions are the primary pyrolysis products, which further decompose by β-H transfer reactions to generate open chain oligomers with olefin and carboxylic end groups. Montaudo *et al.* [110] in another work reported structural characterization of the products obtained by isothermal degradation of PET in the temperature range of 270-370^{o}C. The results indicated the formation of cyclic oligomers which decompose at higher temperature. Anhydride containing oligomers and acetaldehyde were detected at various temperatures. They also carried out few experiments by adding p-toluene sulphonic acid to PET, which induced a strong hydrolytic reaction with consequent increase of carboxyl end groups.

In another study by Martin-Gullon *et al*. [48], different gases evolved from thermal decomposition of waste PET were analyzed by carrying out one pyrolysis run and one combustion run in a batch laboratory scale tubular reactor at 850°C at fuel-rich conditions, where an appreciable amount of PAH was detected. Holland and Hay [97] studied the thermal degradation of PET by thermal analysis-Fourier transform infrared spectroscopy, and

the effect of comonomer (*viz*. diethyelene glycol and isophthalic acid) modifications of PET on thermal stability. They observed that these comonomer units promoted thermal degradation through increased chain flexibility and more favorable bond angles, respectively. Infrared analysis indicated that the residue obtained after pyrolysis, consisted of interconnected aromatic rings.

Lee *et al.* [104] investigated the pyrolysis of a waste plastic mixture of HDPE, LDPE, PP and PS at 350^{o}C and 400^{o}C to study the effect of reaction time and degradation temperature on characteristics of the liquid product. They observed that cumulative yield of the liquid product at 400^{o}C increased sharply with reaction time compared to that at 350^{o}C. Kaminsky *et al.* [111] studied the product distribution from pyrolysis of a PVC-poor light fraction separated from mixed plastic waste (MPW) by using a fluidized bed reactor and reported that the share of the aromatic liquid hydrocarbons is around 48.4% by weight. Conesa *et al.* [112] investigated the pyrolysis of two types of PE, with different degree of branching, in a continuous fluidized bed reactor. Exit gases were collected in a Teflon bag to be analyzed with the help of a GC equipped with a Flame Ionization Detector (FID). The gases analyzed were methane, ethane, ethylene, propane, propylene, acetylene, butane, butylene, pentane, benzene, toluene, xylene and styrene. A kinetic model was applied to the data, which considered that the secondary reaction took place via the same scheme proposed for batch pyrolysis. The results indicated that the tar obtained from the pyrolysis of the two types of PE decompose in a similar way.

Williams and Williams [113] carried out pyrolysis of six thermoplastics (HDPE, LDPE, PS, PP, PET and PVC), which represent more than two-thirds of all plastic production in Western Europe, in a static batch reactor in a nitrogen atmosphere. These six plastics were then mixed together to simulate the plastic fraction of municipal solid waste found in Europe. The effect of mixing on the product yield and composition was examined. A heating rate of 25^{o}C min^{-1}

was used, to a final reaction temperature of 700°C. The results showed that the polymers studied did not react independently, but some interaction was observed between samples. The product yield for the mixture of plastics at 700°C was 9.63% gas, 75.11% oil, 2.87% char and 2.31% HCl. The gaseous products included identified H_2, CH_4, C_2H_4, C_2H_6, C_3H_6, C_3H_8, C_4H_8, C_4H_{10}, CO_2 and CO. The composition of oils was determined using Fourier transform infrared spectrometry and size exclusion chromatography. Analysis showed the presence mainly of aliphatic compounds with small amounts of aromatic compounds.

Bhaskar *et al.* [114] investigated thermal decomposition of real MPW obtained from Japan, and compared it with pyrolysis of two model mixed plastics (PE/PP/PS/PVC, and PE/PP/PS/PVC/PET) carried out at 430°C at atmospheric pressure by batch operation. The quantitative analysis of the liquid products (collected at the end of experiment) was performed by using GC with FID to obtain carbon number distribution of the liquid products. It was found that the presence of PET in model mixed plastics and MPW resulted in an increase in the formation of new chlorinated hydrocarbons in liquid products and also drastically reduced the formation of inorganic chlorine content.

Catalytic decomposition of plastics has shown the greatest potential to be developed into a commercialized process. In comparison to the purely thermal process, catalytic cracking narrows and provides better control over hydrocarbon products distribution. Ortega *et al.* [115] reported catalytic and thermal decomposition of LDPE in a fixed-bed reactor which resulted in several fuel products. Among the various catalysts used, *viz.* Ga-MCM-41, Al-MCM-41, commercial FCC Y zeolite, and natural mordenite, natural mordenite showed the highest selectivity towards liquid products. Achilias *et al.* [116] carried out both catalytic pyrolysis and chemical recycling (by dissolution/reprecipitation) of waste plastics made from HDPE, LDPE, and PP by using a fixed bed reactor. Miranda *et al.* [117] investigated vacuum

pyrolysis of commingled plastics containing PVC, where they carried out step-wise pyrolysis at 360^{o}C and 520^{o}C in a batch reactor.

Cracking efficiency of different catalysts, *viz.* ZSM-5, zeolite-Y, mordenite, and amorphous silica-alumina on HDPE was investigated by Seo *et al.* [118], where pyrolysis was carried out in a batch reactor, and product analysis was done in GC/MS. Both zeolites and silica-alumina increased olefin content in oil products, and ZSM-5, and zeolite-Y particularly enhanced the formation of aromatics and branched hydrocarbons. ZSM-5, among zeolites, showed greatest catalytic activity by producing highest amount of light hydrocarbons, whereas mordenite produced maximum amount of coke. Predel and Kaminsky [119] reported pyrolysis of mixed polyolefins in a fluidized bed reactor at 510^{o}C, and subsequently analyzed the products by GC/MS, wherein they obtained aliphatic waxes as the major product.

Williams and Slanley [120] performed pyrolysis and liquefaction of single plastics, two types of waste plastic mixtures and a simulated MSW plastic mixture in a batch autoclave reactor at 500^{o}C under both N_2 and H_2 atmosphere. The composition of the oils and gases suggested that there was significant interaction of the plastics when they were pyrolyzed as a mixture. Kaminsky *et al.* [121] studied pyrolysis of PMMA and PS in which PMMA was depolymerised to more than 98% of the monomer and PS yielded up to 75% of styrene and 10% of oligomers in an indirectly heated fluidized bed at a temperature of 450^{o}C. In another work, Yoshioka *et al.* [122] carried out pyrolysis of PET in a fluidized bed reactor between 510 and 730^{o}C, where pyrolysis gas consisted chiefly of CO_2 and CO (38-49%), the rest being liquids and a small amount of residue.

In a significant work done by Zadgaonkar [123], post-consumer waste plastics were pyrolyzed in a fluidized bed reactor in presence of coal and patented additives to convert those into solid, liquid and gaseous fuels. The author reportedly obtained 100% conversion of

the waste into value added products. GC studies carried out indicated the presence of unsaturated hydrocarbons, *i.e.* mono-olefins as well as di-olefins. These fractions also showed the presence of chlorides. Hence, in the commercial plant unsaturated fractions and chlorides would have to be removed by hydrogenation and scrubbing the gases in water respectively. PON (paraffin, olefin, naphthene) analysis also indicated the presence of aromatics in the liquid fraction. The carbon number analysis of raw liquid fraction indicated the presence of hydrocarbons with C10 to C30 carbon numbers.

From the foregoing discussions, it can be seen that there has been numerous studies aimed at characterizing plastic decomposition behaviour at different levels of complexity. Polyolefins, *viz.* PE, PP, PS and PET are the major plastics which have been studied elaborately in literature. While different existing models have been successful in simulating the experimental weight loss curve and hence estimating overall kinetic parameters, some studies address the detailed chemistry of decomposition of plastics. All these studies have contributed to the development of pyrolysis process, but are beset with some limitations.

The complex nature of polymer pyrolysis phenomena makes it difficult or virtually impossible to analyze separately each and every elementary reaction as well as to evaluate the quantitative contribution of each to the global degradation process. The kinetic models with individual reaction steps lead to a great number of kinetic parameters, which pose difficulty in simulation of industrial reactors. At the same time, the overall kinetic parameters reported in different studies are noticeably different, which raises questions upon their significance. Another major limitation of these models also lies in their ability to account for interaction of the different plastics in a mixture. Only few works have focused on thermal degradation of plastic mixtures and their mutual interactions. However, these results do not completely agree with each other and different effects were observed by different researchers. Consequently,

this approach cannot be adopted to address the effect of interaction between the constituent plastics in pyrolysis of polymer mixtures in generalized terms.

Thus, it is imperative to understand the presence of synergistic effects during the degradation of plastic mixtures. This area requires considerable attention. An engineering approach would be helpful to develop a model that can address decomposition behaviour of plastic mixtures and study their product distribution, which would streamline the process of development of an efficient pyrolysis process. Considering the complex nature of the reactions involved, it is also important to adopt a simple approach in analyzing the underlying reaction mechanism of decomposition.

CHAPTER 3

Theory

This chapter presents the theoretical work leading to development of a model that could represent the degradation behaviour of mixed plastics. The necessity of an engineering approach in kinetic modeling of pyrolysis of plastics is elaborated with a theoretical backdrop. A systematic presentation of the proposed model is made defining the model parameters. Schematics showing stepwise execution of the model function are also presented for both binary and ternary plastic mixtures.

3.1 Background

Thermal decomposition (or pyrolysis) of plastic materials brings about changes in the chemical species, resulting in formation of vapour and liquid fractions which predominantly contain hydrocarbons and solid fractions containing char. The formation of vapour of lighter hydrocarbons by pyrolysis of plastics is much more complicated than vapourization of flammable liquids. For the later, the volatiles are obtained simply by evaporation, whereas for the former, the large molecules must first be broken down into smaller molecules which are volatile at that temperature to vapourize. Plastics, being macromolecules, when heated under controlled conditions, break down into various smaller fragments, made up of a number of different hydrocarbons, oligomers of various chain lengths, and/or monomers. The volatile products will vapourize immediately upon formation, while heavier fragments will remain in the molten state, until they undergo further decomposition into lighter fragments which are volatile enough to vapourize. In the molten state, some fragments might again combine if such process is energetically favourable. Thus, pyrolysis of plastics results into a wide product distribution, which is dependent primarily on the kinetics of decomposition. This in turn, is

governed by the physical properties and chemical composition of the constituent plastics. The chemical reactions involved are so varied and complex that a complete understanding may not be possible. Moreover, due to variation in the properties of plastics, significant differences are observed in the kinetics analysis of pyrolysis of plastics; this is more apparent in case of plastic wastes which comprise of plastics from different origins. Thus, converting waste plastics to valuable chemicals is desirable, but the lack of a comprehensive understanding of the pyrolysis process (which involves high temperatures, numerous radical transformations, and a complex product distribution) presents a significant obstacle.

There is a significant number of modeling techniques available in the literature which address polymer degradation kinetics [28-30, 33, 41, 50, 52, 57, 84, 85]. These mainly comprise of the model-free and model-fitting techniques aimed at estimation of overall kinetic parameters, already explained in *Section 2.2.1*; the benefits and limitations of these techniques were also discussed earlier. On the other hand, while detailed polymer decomposition can be captured by mechanistic modeling, it has got certain disadvantages which limit its practical application, as elaborated in *Section 2.2.2*.

The necessity of a simple approach in kinetic modeling of polymer decomposition is thus apparent, which could address the decomposition behaviour of mixed plastics. Taking all these factors into account, this study was focused on decomposition behaviour of mixed plastics and development of a model that could represent their degradation behaviour. The intention of the study was to correlate and/or predict the thermal degradation kinetics of the binary and ternary mixtures of low density polyethylene (LDPE), polypropylene (PP) and polyethylene terephthalate (PET) from an engineering perspective. An interacting model was developed for studying the pyrolysis behaviour of the binary and ternary mixtures of plastics. Based on this model, the kinetics of any composition of the binary or ternary mixture could be obtained from the kinetics of the single plastics along with one additional interaction parameter for each

binary. Comparison with experimental kinetic data was made for both interacting and non-interacting models.

3.2 Model Development

The physico-chemical properties of plastics depend on the arrangement and nature of the repeat units, on the types of intramolecular forces, on molecular weight distribution, and by the degree of symmetry and uniformity in molecular structure. All these affect the melting and glass-transition temperature, miscibility with other plastics, and consequently the mutual interaction of the plastics in their melt [124]. Polymer miscibility has been extensively studied in the literature [125-127]. Though polymers are mostly immiscible, in some instances they form a partially or wholly miscible blend. This behaviour often occurs when the two materials have favourable interactions [124, 128]. Polymers undergo many radical transformation reactions during thermal degradation, and thus a pool of radicals is formed from all the components of the mixture. Consequently, interactions between the plastics cannot be completely ruled out; this should be properly taken into account during correlation and prediction of pyrolysis behaviour of plastic mixtures.

In the simplest approach to identify the interaction of the components in the mixture during pyrolysis, a calculated non-interacting component decomposition curve is drawn and compared with the experimental results. The calculated curve is generated based on the assumption that each component undergoes decomposition as if it exists as a pure plastic in the mixture and simple additivity of constituent plastics is assumed to obtain conversion of the mixture [66]. The non-interacting model is thus completely predictive in nature. The degradation rate of a plastic mixture using this model is expressed as shown in *equation (3.1)*.

$$\left.\frac{d\alpha}{dT}\right|_{mix}\{T\} = x_1 \left.\frac{d\alpha}{dT}\right|_{1}\{T\} + x_2 \left.\frac{d\alpha}{dT}\right|_{2}\{T\} \qquad (3.1)$$

where, $\left.\frac{d\alpha}{dT}\right|_{mix}$ = Rate of degradation of the mixture at temperature T, x_1= weight fraction of the plastic 1 in the mixture, x_2 = weight fraction of the plastic 2 in the mixture, $\left.\frac{d\alpha}{dT}\right|_{1}$ = Rate of degradation of plastic 1 at temperature T, $\left.\frac{d\alpha}{dT}\right|_{2}$ = Rate of degradation of plastic 2 at temperature T. In the above equation, temperature term in the parenthesis indicates the functionality.

However, such model will be unable to predict kinetic behaviour of plastic mixtures, if degradation of each plastic in the mixture is not completely independent. As will be shown later, in our case, predictions of non-interacting model deviate significantly from experimental observations. To find whether the driving force behind this behaviour is of entropic or energetic origin, one needs complete elucidation of the reaction mechanism as well as the chain architecture of the blend components. Moreover, this behaviour needs to be obtained as a function of temperature.

To overcome the limitations and still obtain/correlate the experimental data for pyrolysis of mixed plastics [129], an engineering approach is adopted for ready use in modeling; in this model, a quadratic mixing rule type expression (*equation 3.2*) is used for expressing degradation kinetics of mixed plastics. The degradation kinetics of a binary mixture is expressed as

$$\left.\frac{d\alpha}{dT}\right|_{mix}\{T\} = x_1^2\left.\frac{d\alpha}{dT}\right|_{1}\{T\} + x_2^2\left.\frac{d\alpha}{dT}\right|_{2}\{T\} + 2x_1x_2\left.\frac{d\alpha}{dT}\right|_{12}\{T\} \qquad (3.2)$$

The terms in *equation 3.2* carry same meaning as in *equation 3.1*. In addition, the $\left.\frac{d\alpha}{dT}\right|_{12}$ term represents rate of degradation at temperature T, accounting for possible interactions of the constituent plastics 1 and 2 in their binary mixture undergoing degradation.

Obviously, it will be a function of temperature. In case of binary mixtures considered, experimental data indicates that this term is also a linear function of overall weight fraction of the mixture at any given temperature.

$$\left.\frac{d\alpha}{dT}\right|_{12}\{T\} = \beta_{12}\{T\}\, x_1 + \gamma_{12}\{T\} \qquad (3.3)$$

The parameters β_{12} and γ_{12} for a mixture at a given temperature are obtained from linear regression of calculated values of $\left.\frac{d\alpha}{dT}\right|_{12}$ from *equation (3.2)*, at the same temperature, for different mixture compositions. These parameters can then be used to correlate binary mixture degradation kinetics.

An extended form of *equation (3.2)* is used for predicting the degradation kinetics of a ternary mixture.

$$\left.\frac{d\alpha}{dT}\right|_{mix}\{T\} = x_1^2\left.\frac{d\alpha}{dT}\right|_{1}\{T\} + x_2^2\left.\frac{d\alpha}{dT}\right|_{2}\{T\} + x_3^2\left.\frac{d\alpha}{dT}\right|_{3}\{T\} + 2x_1x_2\left.\frac{d\alpha}{dT}\right|_{12}\{T\} + 2x_1x_3\left.\frac{d\alpha}{dT}\right|_{13}\{T\} + 2x_2x_3\left.\frac{d\alpha}{dT}\right|_{23}\{T\} \qquad (3.4)$$

Additional terms in *equation (3.4)* carry similar meaning as they do in *equation (3.2)*. The dependency of $\left.\frac{d\alpha}{dT}\right|_{13}$ and $\left.\frac{d\alpha}{dT}\right|_{23}$ is given by *equation (3.5)* and *(3.6)*.

$$\left.\frac{d\alpha}{dT}\right|_{13}\{T\} = \beta_{13}\{T\}\, x_1 + \gamma_{13}\{T\} \qquad (3.5)$$

$$\left.\frac{d\alpha}{dT}\right|_{23}\{T\} = \beta_{23}\{T\}\ x_2 + \gamma_{23}\{T\} \qquad (3.6)$$

The schematic showing the protocol for stepwise execution of the model to find out the predicted values of rate of degradation $\left(\frac{d\alpha}{dT}\right)$ for the binary mixture of plastics *i* and *j* is shown in Figure 3.1. The same procedure is followed for the other binary mixtures and corresponding values of interaction parameters (β_{ij} and γ_{ij}) were obtained. In addition, $\left(\frac{d\alpha}{dT}\right)$ values for the ternary mixtures are calculated by using *equation (3.4)*, as shown in Figure 3.2. Thus, ternary mixture kinetics does not incorporate any additional interaction terms. Experimental binary data of various constituents of the mixture alone is sufficient to obtain all the parameters required at each temperature i.e. β_{ij} and γ_{ij} . The ternary interaction term is neglected for practical reasons; in any case it may not contribute as significantly as the binary interaction terms. Moreover, for multi-component mixture, this approach can be readily used without necessity to perform any experiments for higher order mixtures.

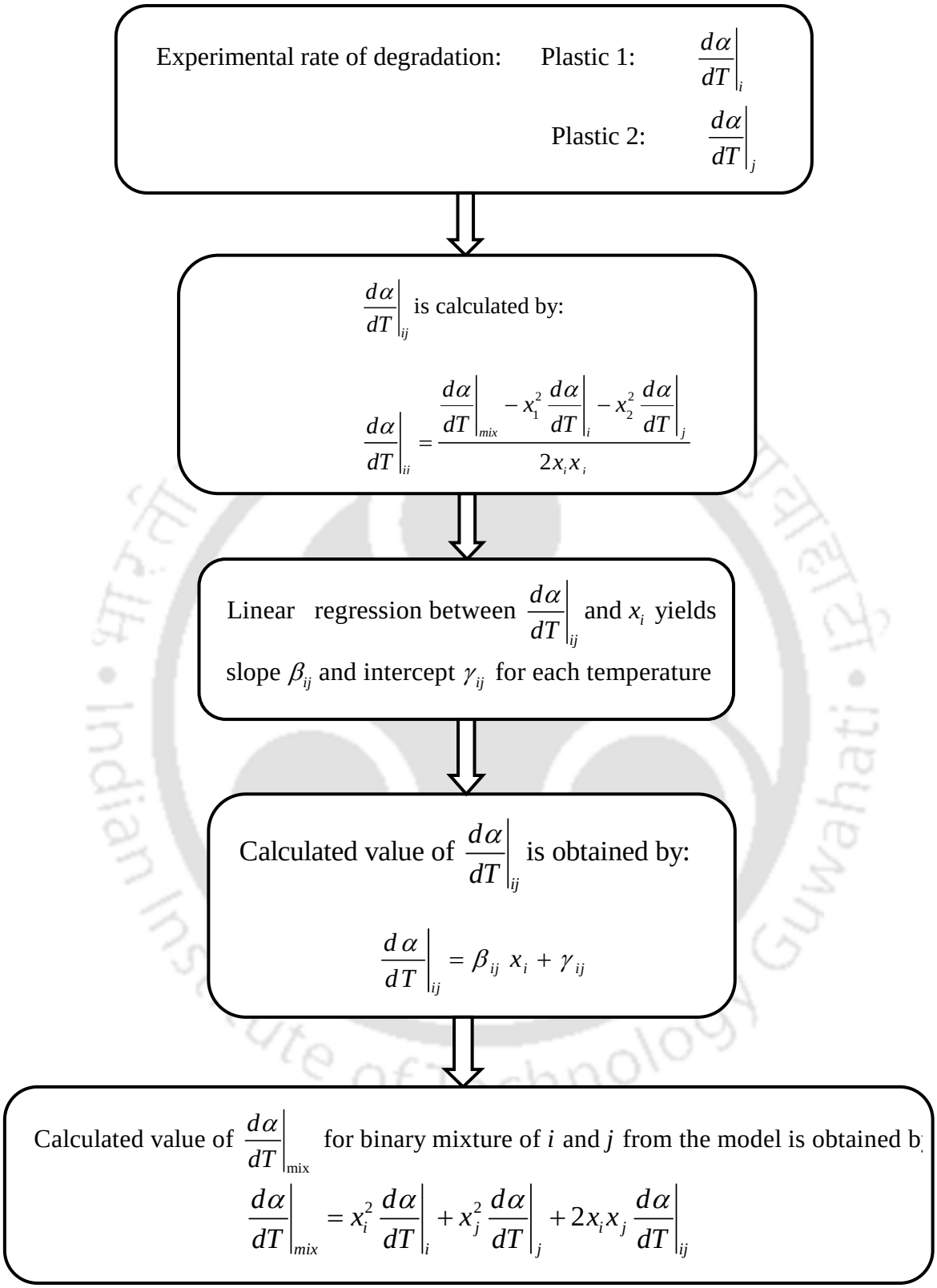

Figure 3.1 Schematic showing the stepwise execution of the model function for binary mixture

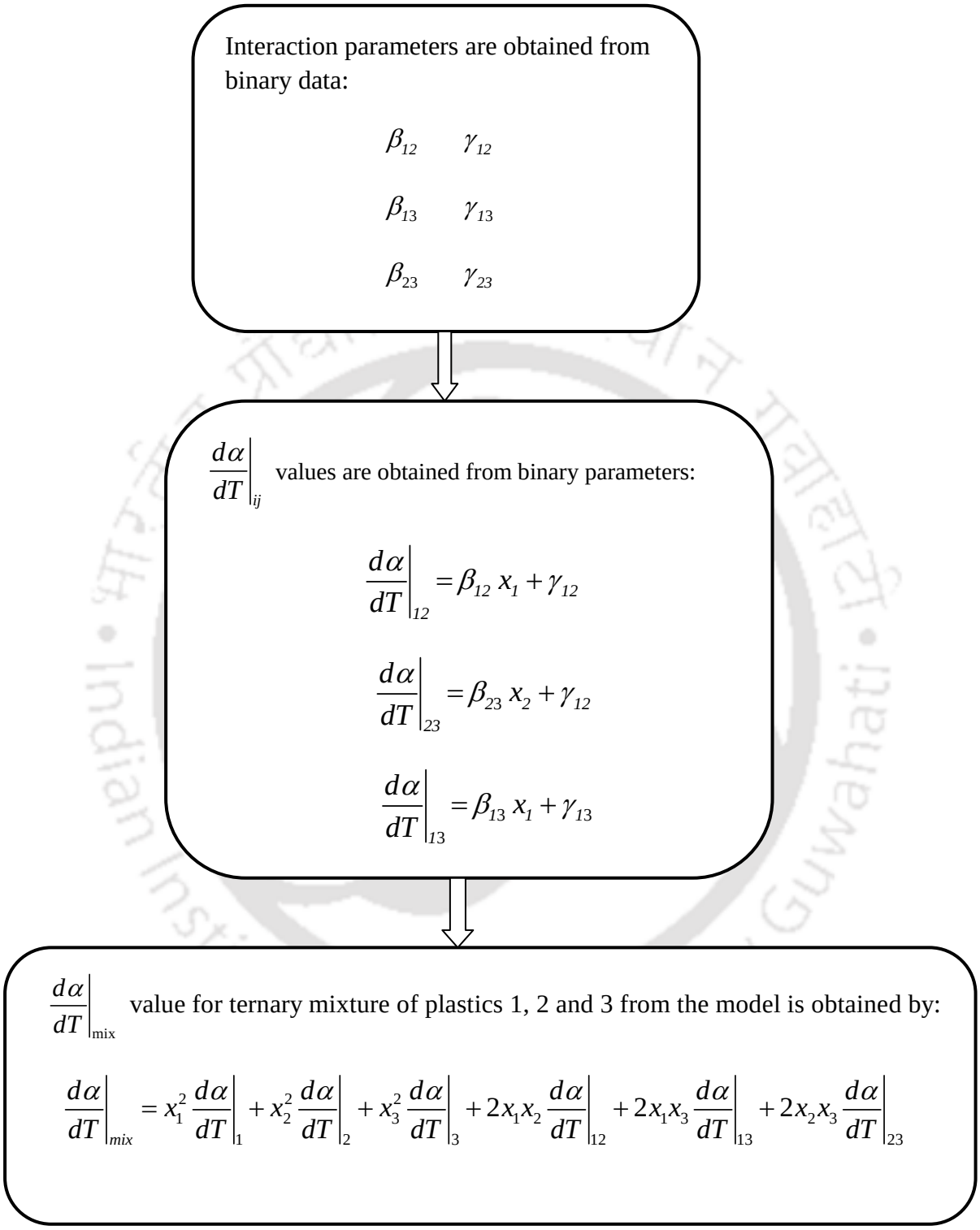

Figure 3.2 Schematic showing the stepwise execution of the model function for ternary mixture

CHAPTER 4

Experimental

This chapter provides details about the materials and equipments used and experimental protocol followed to attain the desired objectives. First, pyrolysis experiments are elaborated by providing a stepwise protocol. Different components of the equipment are shown with a schematic representation. Next, product analysis studies are explained by providing specification of the equipment and necessary parameters required for design of experiment. Standards used and calibration procedure are also detailed.

4.1 Pyrolysis Kinetics Study

4.1.1 Materials

Three types of commodity plastics, *viz.* low density polyethylene (LDPE), polypropylene (PP) and polyethylene terephthalate (PET) are used in the study. The source and physical properties of the plastics used are shown in Table 4.1 [33, 57, 59].

Table 4.1 Source and physical properties of the plastics used in pyrolysis kinetics study

Plastic type	**Source**	**Heat of fusion ($J\ g^{-1}$)**	**Melting point (^oC)**	**Melt flow index (MFI) g $(10\ min)^{-1}$**	**Percentage crystallinity**
LDPE	Waste packaging films	38.37	128.7	-	23.95
PP	IPCL, Vadodara, India (Homopolymer, PPHP, Trade name: Koylene ADL AS030N)	62.38	175.6	3	32.83
PET	Waste beverage bottle scrap M/s Coca-Cola	35.78	258.43	-	31.11

PP used was a virgin plastic, while PET and LDPE were waste plastics. Waste plastics are subjected to different thermal history during their processing, which affect their thermal behavior. Thus, to have a general view of pyrolysis behavior of plastics, both waste and pure plastics were used in the pyrolysis experiments.

4.1.2 Equipment

Thermogravimetric Analyzer

Thermogravimetric analyzer (TGA) is one of the most commonly used equipments in thermal analysis. With this equipment, changes in the sample mass, maintained in a specified atmosphere, can be monitored as a function of temperature or time. The sample mass usually decreases as a result of evaporation of the adsorbed or chemically bound water, pyrolysis of organic substances, and decomposition or evaporation of the material. However, for some samples the sample mass increases due to oxidation of metals to oxides or carbonation of oxides in some atmospheres. TGA include a high sensitivity micro-balance, a temperature-controlled furnace, a unit for evacuation and controlled environment in the furnace, and a control and data recording system.

The pyrolysis experiments were carried out in a TGA (Make: Mettler Toledo, Model: TGA/SDTA 851^{e}). Figure 4.1 shows the schematic of the TGA showing various components.

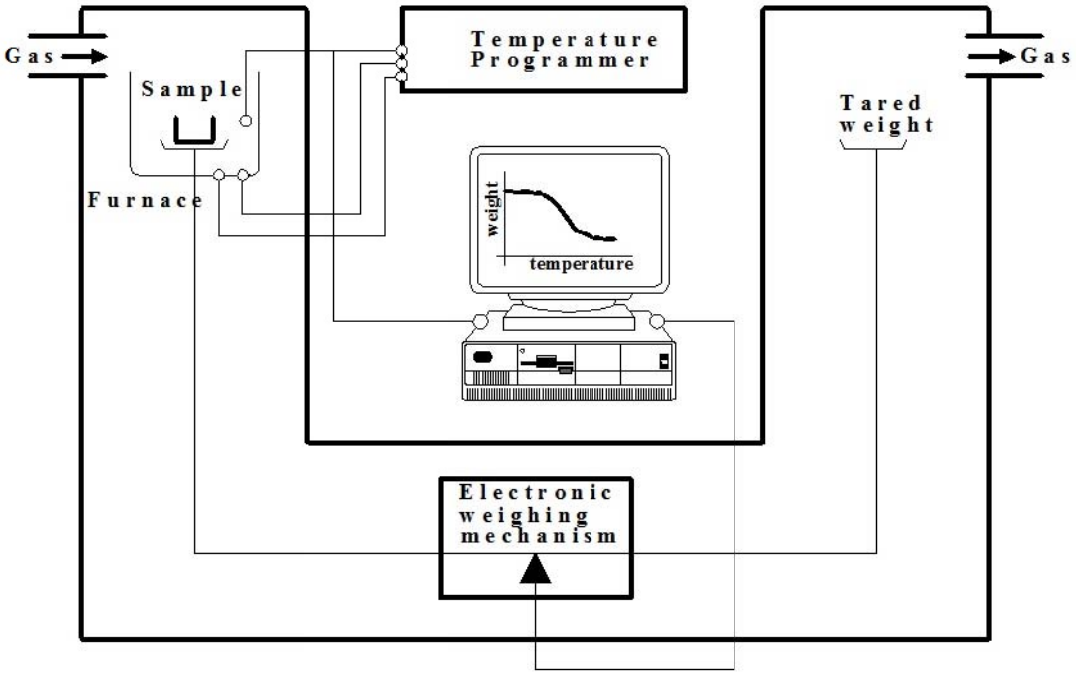

Figure 4.1 Schematic of TGA showing the micro-balance and details of gas flow

4.1.3 Procedure

The following stepwise procedure was followed for carrying out pyrolysis experiments in the TGA.

1. The plastic samples were cut into very small pieces (mesh size: -25/+35) and placed inside sample bottles.
2. Coolant water supply was started and waited till the temperature of the thermostat was stable at 22^{o}C.
3. The carrier gas (Ar/N_2) flow was started and a flow rate of 40-50 ml min^{-1} was maintained according to the specification of the equipment. The cylinder outlet pressure was not allowed to increase beyond 1 bar. Flow of the carrier gas was continued till 10-15 minutes, so as to purge any gases trapped inside TGA furnace.
4. STAR^{e} software was started.

5. The TGA module was switched on and allowed time for self calibration of the micro-balance.
6. Routine editor of the software was opened to load the analysis method by providing details of furnace heating program, carrier gas, and crucible chosen for analysis.
7. Analysis method: Temperature range 25-600^{o}C, heating rate 10^{o}C min^{-1}, inert (Ar/N_2) environment, 150 µl platinum crucible
8. The crucible was cleaned properly prior to each run. Balance was zeroed by taring the crucible before sample loading.
9. After taring, an appropriate amount of sample was transferred to the crucible and loaded on to the TGA weighing pan. In all the experiments, the total sample weight was kept within 5-10 mg to eliminate any limitation due to heat and mass transfer effects.

The following table (Table 4.2) shows the details of the mixture compositions used for kinetics analysis of different plastic mixtures. As can be seen from the table, a wide range of compositions were initially chosen for investigating pyrolysis behavior of binary mixture of LDPE and PET. However, analysis of the data (as discussed later in *Section 5.1.2*) showed that there was no drastic variation in the characteristic temperatures of decomposition of the plastic mixture with change in mixture composition within a close range. Therefore, for PP-PET combination, four different compositions were chosen for analysis. Later, it was found that three different compositions were good enough to have a general view. Thus, for binary mixture of LDPE-PP and the ternary mixture of LDPE-PP-PET, three compositions were used for analysis.

Table 4.2 Details of the mixture compositions for TGA experiments.

Mixtures	LDPE(%)	PP(%)	PET(%)
LDPE-PET	20	-	80
	25	-	75
	30	-	70
	50	-	50
	70	-	30
	75	-	25
	80		20
PP-PET	-	20	80
	-	25	75
	-	40	60
	-	80	20
LDPE-PP	20	80	-
	40	60	-
	80	20	-
LDPE-PP-PET	25	50	25
	30	10	60
	50	25	25

4.2 Product Analysis Study

4.2.1 Materials

Table 4.3 shows the plastic materials used in the product analysis experiments. Virgin plastics were used in this study, to eliminate the effects of different additives and/or impurities present in waste plastics which might affect the product distribution.

Table 4.3 Source and physical properties of the plastics used in products analysis study

Plastic type	**Source**	**Heat of fusion (J g^{-1})**	**Melting point (^{o}C)**	**Melt flow index (MFI) g (10 min)$^{-1}$**	**Percentage crystallinity**
LDPE	National Chemical Limited, Gujarat	-	126.9	5.13	-
PP	IPCL, Vadodara, India (Homopolymer, PPHP, Trade name: Koylene ADL AS030N)	62.38	175.6	3	32.83
PET	South Asian Petrochem Limited, India (AS-40 bottle grade)	44.9	248.4	-	39.05

4.2.2 Equipment

Gas Chromatograph

Gas Chromatography (GC) is a simple technique widely used to effectively determine the components present in a vapor/liquid mixture. This technique has been employed in this work to analyze the product distribution profile from pyrolysis of plastics. Product analysis experiments were performed initially using Varian 3800 GC with FID detector. Subsequently, Varian 3800 GC was replaced by Varian 450 GC with FID detector for the later part of the work. Details of experimental conditions are shown in Table 4.4.

Table 4.4 Details of experimental conditions for GC analysis

GC Parameters	Details
Column	Ultra low bleed Factor Four capillary column VF-200ms (Varian, Inc.) (30 m length, 0.25 µm film thickness, 0.25 mm ID) composed of trifluropropyl methyl stationary phase
Carrier gas	Nitrogen (N_2)
Carrier gas flow rate	1.5 ml min^{-1}
Column oven program	Isothermal segment at 30^oC with hold time 6 minutes, ramp heating from 30 to 50^oC at a rate of 0.6^oC min^{-1}, ramp heating from 50 to 300^oC at a rate of 10^oC min^{-1}
Injector temperature	200^oC
Detector temperature	280^oC
Injection mode	Splitless
Cylinder outlet pressure	80 psi (N_2), 60 psi (Air), 40 psi(H_2)

GC is an assembly of several units, which include the injector, the column and the detector, associated with a thermostatically controlled oven that enables the column to attain high temperatures. Figure 4.2 shows a typical flow path in the GC showing different units associated with it [130].

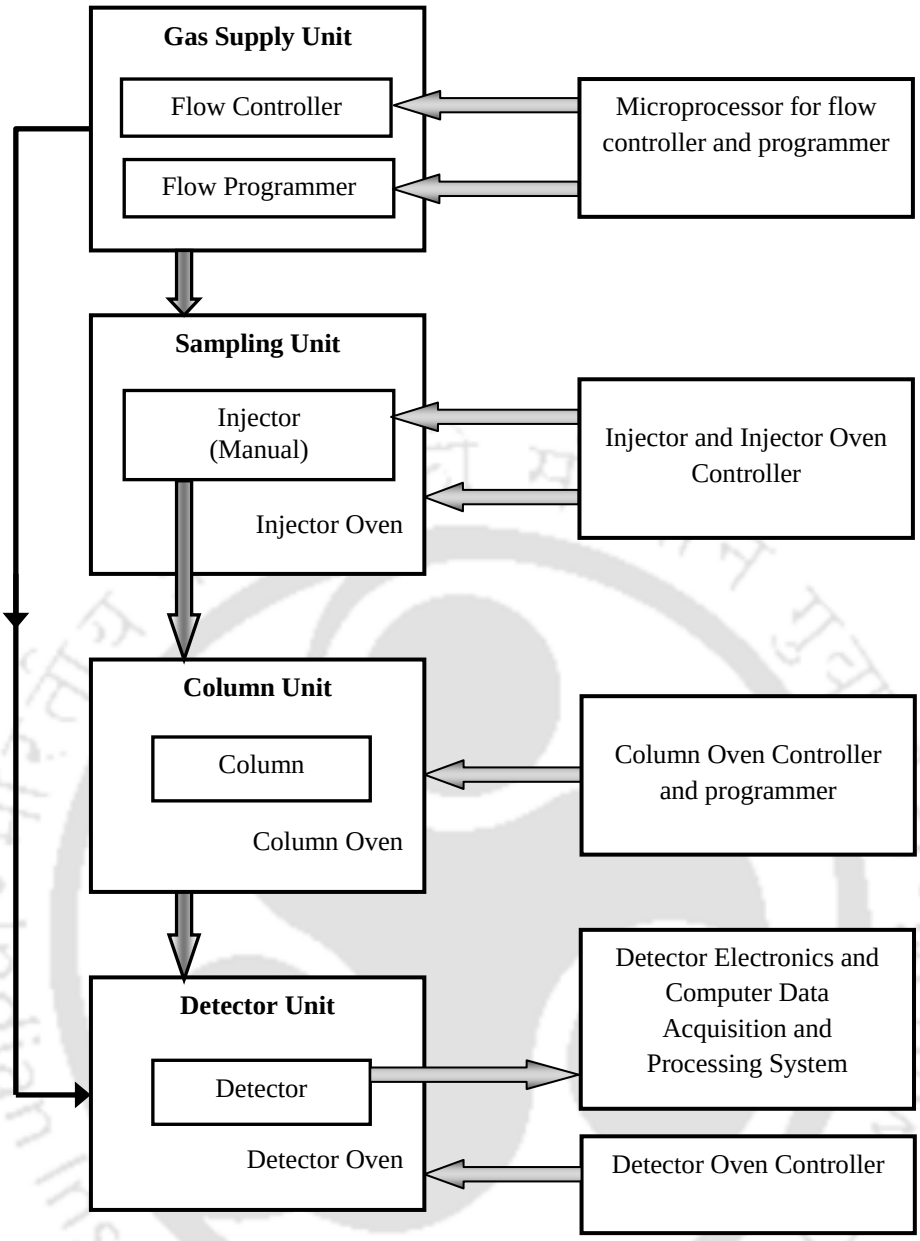

Figure 4.2 A typical flow path in the GC showing its components

The carrier gas flow, which is precisely controlled, enables reproducibility of the retention times (RT). The first unit, the gas supply unit, provides all the necessary gas supplies which may involve a number of different gases, depending on the type of detector that is chosen. Flame ionization detector (FID) will require hydrogen or some other combustible gas mixture, air or oxygen to support combustion and a mobile phase, that transports the analytes through the column, known as the carrier gas, could be nitrogen, helium or some other inert gas. The second unit is the sampling unit which contains an injector which is situated inside a

thermostatically controlled enclosure. The injector oven is serviced by its own temperature controller which both monitors and controls the temperature. The third unit is the column unit which contains the column, the essential device that actually achieves the necessary separation, and an oven to control the column temperature. The fourth unit contains the detector which is situated in its own oven. The detector oven is set at a user defined temperature and is operated isothermally, controlled by its own detector-oven temperature controller. The output from the detector is electronically modified and then acquired by the data processing computer which processes the data and prints out the report.

4.2.3 Calibration on GC

Two quantitative reference petroleum standards (ASTM D3710 Quantitative Calibration Mix containing C5-C15 hydrocarbons (Table 4.5) and ASTM D5442 Qualitative Retention Time Mix containing C16-C44 hydrocarbons (Table 4.6)) supplied by Sigma Aldrich Company, Bangalore, India, were used for calibration of the GC. For analysis of PET pyrolyzate, a Polynuclear Aromatic Hydrocarbon Mix standard (Table 4.7) supplied by Rankem Chemicals, India was used for detecting the RT range during which PAHs evolve.

Table 4.5 Standard hydrocarbons present in ASTM D3710 mix standard

Hydrocarbon	**vol. %**	**Density (g/cc)**
2-Methylbutane (C_5H_{12})	12.30	0.8646
n-Pentane (C_5H_{12})	9.39	0.7341
2-Methylpentane (C_6H_{14})	6.45	0.7526
n-Hexane (C_6H_{14})	6.39	0.6882
2,4-Dimethylpentane (C_7H_{16})	6.27	0.6640
n-Heptane (C_7H_{16})	11.17	0.7068
Toluene (C_7H_8)	9.74	0.7721
n-Octane (C_8H_{18})	6.01	0.6312
p-Xylene (C_8H_{10})	11.84	0.8666
n-Propylbenzene (C_9H_{10})	3.97	0.7667
n-Decane ($C_{10}H_{22}$)	3.49	0.7601
n-butylbenzene ($C_{10}H_{11}$)	2.96	0.8657
n-dodecane ($C_{12}H_{26}$)	3.40	0.8719
n-Tridecane ($C_{13}H_{28}$)	2.21	0.6248
n-Tetradecane ($C_{14}H_{11}$)	2.23	0.6579
n-Pentadecane ($C_{15}H_{32}$)	2.18	0.6772

Table 4.6 Standard hydrocarbons present in ASTM D5442 mix standard

Hydrocarbon name	**wt%**
n-Hexadecane ($C_{16}H_{34}$)	8.295
n-Octadecane ($C_{18}H_{38}$)	8.307
n-Eicosane ($C_{20}H_{42}$)	8.303
n-Docosane ($C_{20}H_{42}$)	8.361
n-Tetracosane ($C_{24}H_{50}$)	8.296
n-Hexacosane ($C_{26}H_{54}$)	8.314
n-Octacosane ($C_{28}H_{58}$)	8.373
n-Triacontane ($C_{30}H_{62}$)	8.298
n-dotriacontane ($C_{32}H_{66}$)	8.467
n-Hexatriacontane ($C_{36}H_{74}$)	8.291
n-Tetracontane ($C_{40}H_{82}$)	8.300
n-Tetratetracontane ($C_{44}H_{90}$)	8.397

Table 4.7 Standard hydrocarbons present in PAH mix standard*

Hydrocarbon name
Acenaphthene ($C_{12}H_{10}$)
Acenaphthylene ($C_{12}H_8$)
Anthracene ($C_{14}H_{10}$)
Benz(a)anthracene ($C_{18}H_{12}$)
Benzo(a)pyrene ($C_{20}H_{12}$)
Benzo(b)fluoranthene ($C_{20}H_{12}$)
Benzo(g,h,i)perylene ($C_{22}H_{12}$)
Benzo(k)fluoranthene ($C_{20}H_{12}$)
Chrysene ($C_{18}H_{12}$)
Dibenz(a,h)anthracene ($C_{22}H_{14}$)
Fluoranthene ($C_{16}H_{10}$)
Fluorene ($C_{13}H_{10}$)
Indeno(1,2,3-cd)pyrene ($C_{22}H_{12}$)
Naphthalene ($C_{10}H_8$)
Phenanthrene ($C_{14}H_{10}$)
Pyrene ($C_{16}H_{10}$)

*- concentration of each of the hydrocarbons is 2 mg/ml in Dichloromethane: Benzene (1:1)

Experimental procedure is outlined below.

1. *Column installation:* The capillary column was mounted onto the GC by connecting the respective ends to the injector and detector port (FID) with proper care so as not to damage the column.
2. *Measurement of carrier gas flow:* The flow rate through the column was measured using bubble flow meter before start of experiment and it was checked regularly in order to ensure accuracy of RT measurements.
3. *Column conditioning:* Before doing the calibration runs, the column was purged with normal carrier gas flow for about 20-30 minutes at ambient temperature and then conditioned thermally by heating the column oven to 320^{o}C at a rate of 4^{o}C min^{-1}. This

was done to remove any residual low-boiling species present in the column, which could otherwise produce an unsteady baseline at elevated column temperature.

4. *Sample preparation:* For ASTM D3710 quantitative standard, there was no need for any additional sample preparation technique as the standard is provided as liquid in standard 1 ml vials. For ASTM D5442, a weighed amount of standard was dissolved in required amount of hexane, and the mixture is immediately transferred to liquid vials and sealed.
5. *Method loading:* A new method was created with specific parameters as noted in Table 4.3 and loaded into GC and waited till the set temperature are reached by the column oven, detector and injector before starting the analysis. FID signal was checked after opening the hydrogen and air valves, for proper ignition. It is worth mentioning here that several trial runs were made before finally selecting the experimental parameters, which yielded the best separation of peaks for identification of different hydrocarbons based on carbon numbers present in the standards.
6. *Injection:* When the instrument was ready for analysis, the required amount of the sample was injected through a liquid syringe (Hamilton, Reno Nevada, model no. 701, 10µl) into the injector. For ASTM D3710 standard, sample injected was 0.5 µl, whereas for ASTM D5442 standard, sample injected was 1 µl.
7. *Data export:* After the run was over, test report was collected which contained the RT values against area counts of various peaks.

Details of calibration procedure and calculations are presented in *Appendix 1*.

4.2.4 Product Analysis by GC

A schematic representation of the experimental procedure for product analysis is shown in Figure 4.3. During the actual product analysis, 1 ml of the sample evolved from the TGA at temperature of interest was drawn into a gas-tight syringe (Hamilton, gas-tight, model no.

1005, 5ml) and injected into the GC by following the same protocol and experimental conditions as elaborated in *Section 4.2.3*. Initially, for analyzing the products from pyrolysis of LDPE, the temperatures were chosen as 200, 250, 300, 350, 400, 450, 500, 550, 600^{o}C and the maximum decomposition temperature (T_{max}). However, for the other two single plastics (PP and PET), temperatures of interest were chosen as 200, 300, 400, T_{max}, 500 and 600^{o}C, as there was not much observed variation in the products evolution pattern in going from 200-250^{o}C, or 300-350^{o}C etc. Again, for the mixtures temperatures of interest were limited to 300, 400, 500, and 600^{o}C. The details of the mixture compositions and temperatures for GC experiments are listed in Table 4.8.

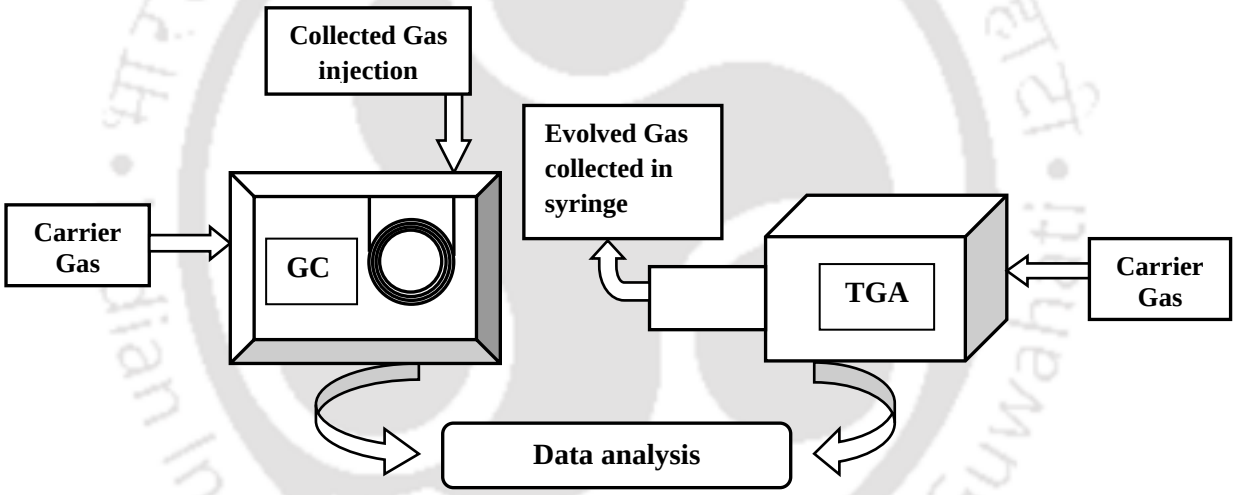

Figure 4.3 Schematic representation of the experimental procedure to carry out products analysis

Mole fractions of the eluent hydrocarbons were calculated using the correlation co-efficient obtained from the calibration procedure for both the standards as elaborated in *Appendix 1* and plotted against decomposition temperatures of the corresponding plastic/plastic mixtures. For the experiments carried out in Varian 450 GC, same protocol was followed which yielded RT data for the standard hydrocarbons, which were comparable to those obtained from Varian

3800 GC. Therefore, the same co-efficients were used for calculating the mole fractions of the hydrocarbons.

Table 4.8 Details of the mixture compositions and temperatures for GC experiments

Plastics	**LDPE(%)**	**PP(%)**	**PET(%)**	**Temperature (^{o}C)**
LDPE	100	-	-	200, 250, 300, 350, 400, 470, 500, 550, 600
PP	-	100	-	200, 300, 400, 446, 500, 600
PET	-	-	100	200, 300, 400, 435, 500, 600
LDPE-PP	20	80	-	200, 300, 400, 435, 500, 600
	50	50	-	200, 300, 400, 450, 500, 600
	80	20	-	200, 300, 400, 463, 500, 600
LDPE-PET	20	-	80	300, 400, 434, 500, 600
	50	-	50	300, 400, 439, 500, 600
	80	-	20	400, 459, 500, 600
PP-PET	-	20	80	300, 400, 432, 500, 600
	-	50	50	300, 400, 434, 500, 600
	-	80	20	300, 400, 440, 500, 600
LDPE-PP-	25	25	50	300, 400, 500, 600
PET	25	50	25	300, 400, 429, 500, 600
	50	25	25	300, 400, 436, 500, 600

CHAPTER 5

Results and Discussion

This chapter presents the systematic discussion on the results obtained from our experimental along with the modeling studies.

Section 5.1 *deals with the measurement and modeling kinetics for pyrolysis of binary and ternary plastic mixtures. The compositions of different plastic mixtures used for this study are listed in Table 4.1. The interacting model, developed in Chapter 3, is used to calculate the rate of degradation for the binary and ternary mixtures; the calculated derivative thermogravimetry (DTG) curve, thus obtained is compared with the experimental DTG curve. This part of the work has already been published in Polymer Degradation and Stability [129].*

Section 5.2, 5.3 and 5.4 *present the study of temperature dependent product evolution from pyrolysis of low density polyethylene (LDPE), polypropylene (PP) and polyethylene terephthalate (PET) respectively and subsequently explain their decomposition mechanism (as a function of temperature). The studies on LDPE and PP have been published in Waste Management [131] and Journal of Applied Polymer Science [132] respectively.*

Section 5.5, 5.6 and 5.7 *elaborate the study of temperature dependent product evolution from pyrolysis of PP-LDPE, PP-PET and LDPE-PET binary mixtures respectively, and outline their decomposition mechanism (as a function of temperature). The basic idea is to see if the interaction between the component plastics, which was observed in their thermal degradation studies, gets further manifested in their product evolution pattern.*

Section 5.8 *explains the study of temperature dependent product evolution from pyrolysis of ternary mixtures of LDPE, PP and PET, and subsequently discusses about their decomposition mechanism as a function of temperature.*

5.1 Pyrolysis Kinetics of Mixed Plastics

5.1.1 Kinetics of pyrolysis of single plastics

The plastics used in this study are LDPE, PP and PET. To model the decomposition behaviour of any plastic mixture, knowledge of decomposition kinetics of the individual components is needed. The characteristic temperatures (T_o, T_{max} and T_f) for pyrolysis of the single plastics are listed in Table 5.1. T_o is the temperature at which 0.1% of the total weight loss occurs, T_{max} is the temperature corresponding to maximum rate of decomposition, and T_f is the final decomposition temperature beyond which there is no further weight loss.

Table 5.1 Characteristic temperatures for pyrolysis of single plastics

Plastics	T_o (^oC)	T_f (^oC)	T_{max} (^oC)
PET	329	493	437
PP	337	471	446
LDPE	341	495	463

Figure 5.1 shows DTG curve for the plastics. Decomposition of PET starts earlier than the other two and its T_{max} is lowest among the three plastics. The order of thermal stability in terms of T_{max} is LDPE>PP>PET. It is evident from the figure that LDPE is the most stable among three plastics used in our study. PP decomposes essentially to completion prior to PET and LDPE as evidenced by T_f. Thermal stability of LDPE, PP and PET can be justified in terms of the structural attributes of the respective polymers. In case of PP, the presence of the

tertiary carbon atoms along the polymer backbone results in decreased degradation resistance, allowing for easier hydrogen abstraction compared to LDPE [133]. In PET**,** presence of two heterogeneous linkages between O and C in the polymer backbone possibly justifies its higher rate of degradation as compared to the other two.

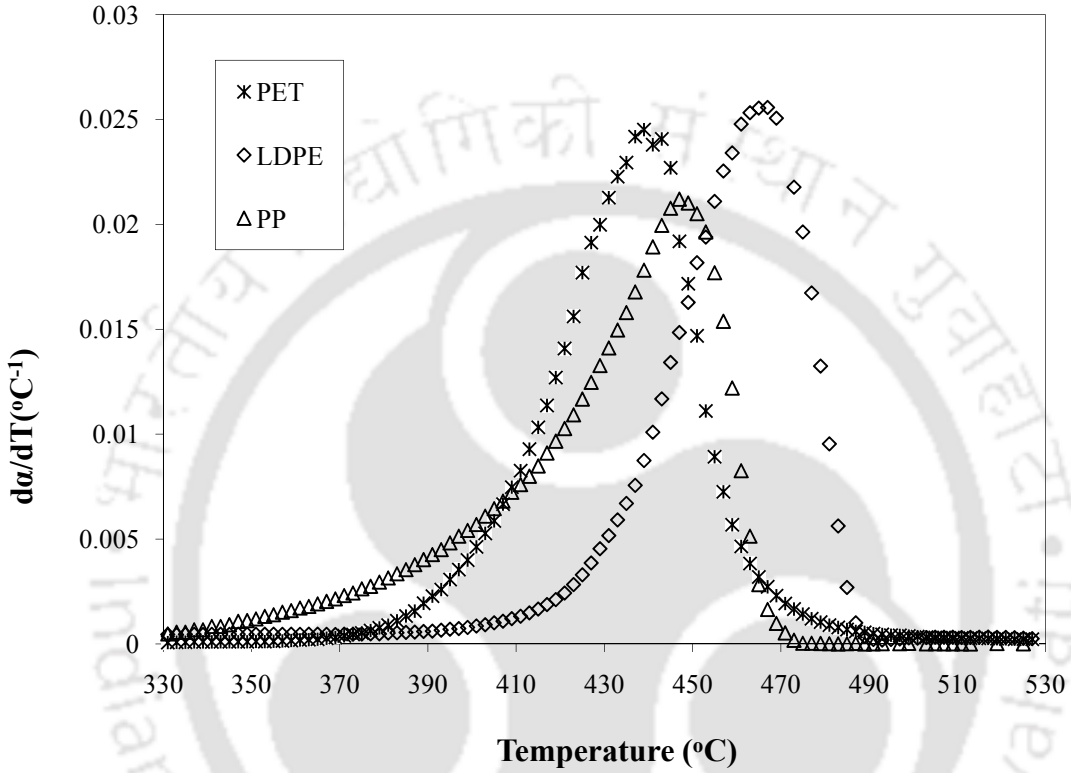

Figure 5.1 DTG curves of single plastics

5.1.2 Kinetics of pyrolysis of binary plastic mixtures

Degradation kinetics of different binary mixtures as listed in Table 4.1 (*Section 4.2.2*) were studied. Experimental DTG curves for binary mixtures of LDPE-PET, PP-PET and LDPE-PP are shown in Figures 5.2 through 5.4. For the sake of comparison and to highlight the difference between experimental and corresponding non-interacting decomposition curves, both are shown in the same plot.

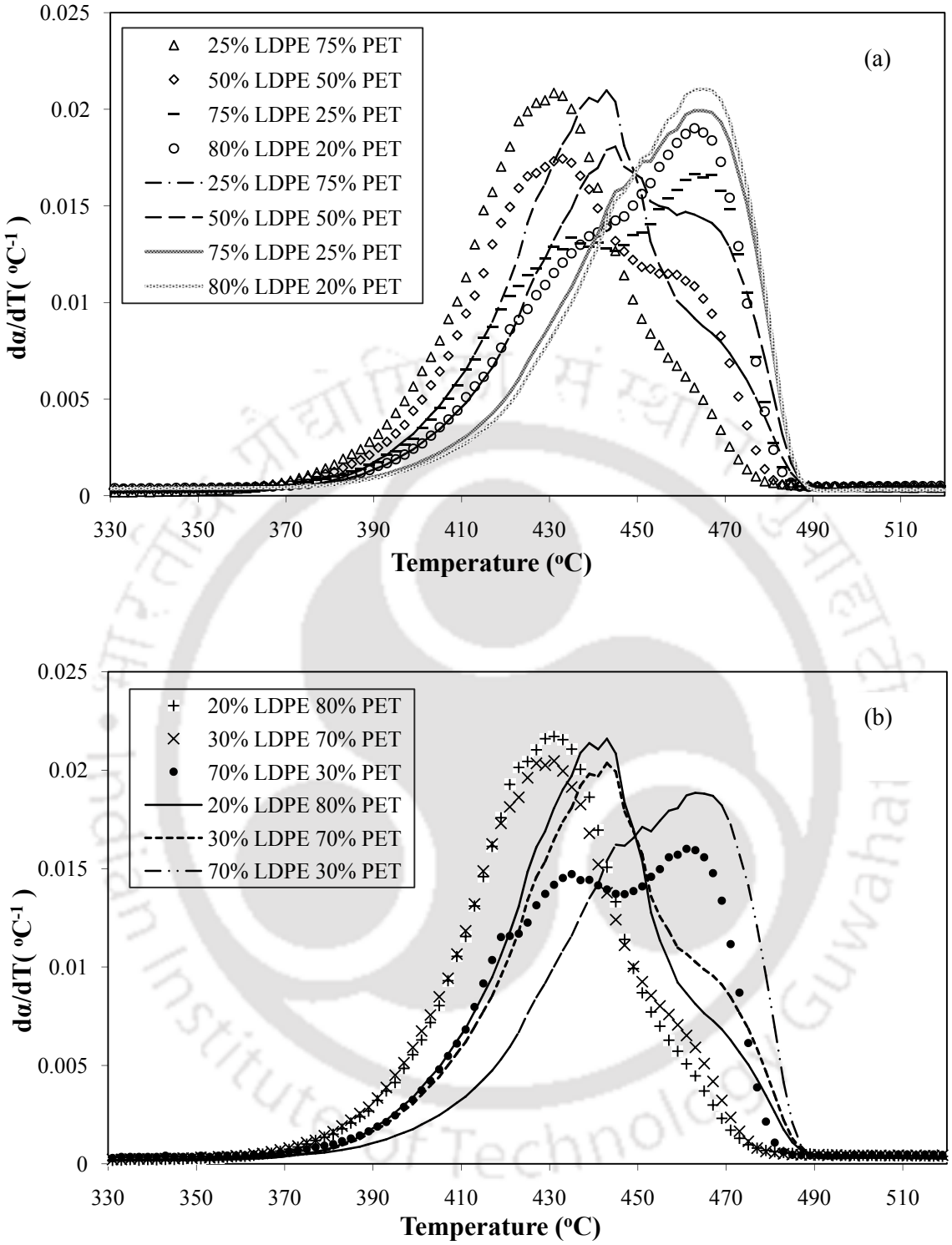

Figure 5.2 Experimental and non-interacting DTG curves of binary mixture of LDPE and PET for various compositions; (a) 25% LDPE 75% PET, 50% LDPE 50% PET, 75% LDPE 25% PET, 80% LDPE 20% PET; (b) 20% LDPE 80% PET, 30% LDPE 70% PET, 70% LDPE 30% PET (markers show experimental curve; dotted lines show non-interacting curve)

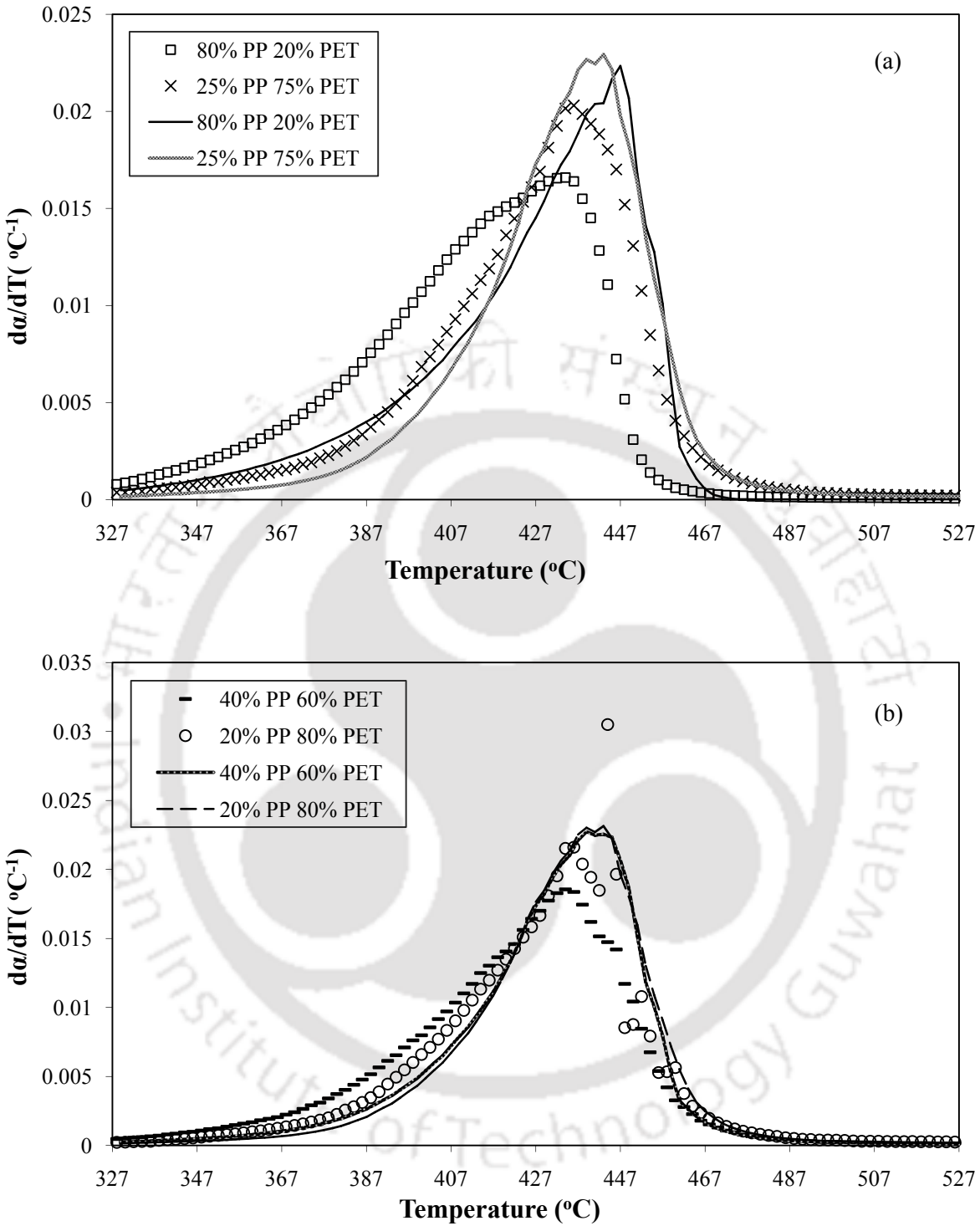

Figure 5.3 Experimental and non-interacting DTG curves of binary mixture of PP and PET for various compositions; (a) 80% PP 20% PET, 25% PP 75% PET; (b) 40% PP 60% PET, 20% PP 80% PET (markers show experimental curve; dotted lines show non-interacting curve)

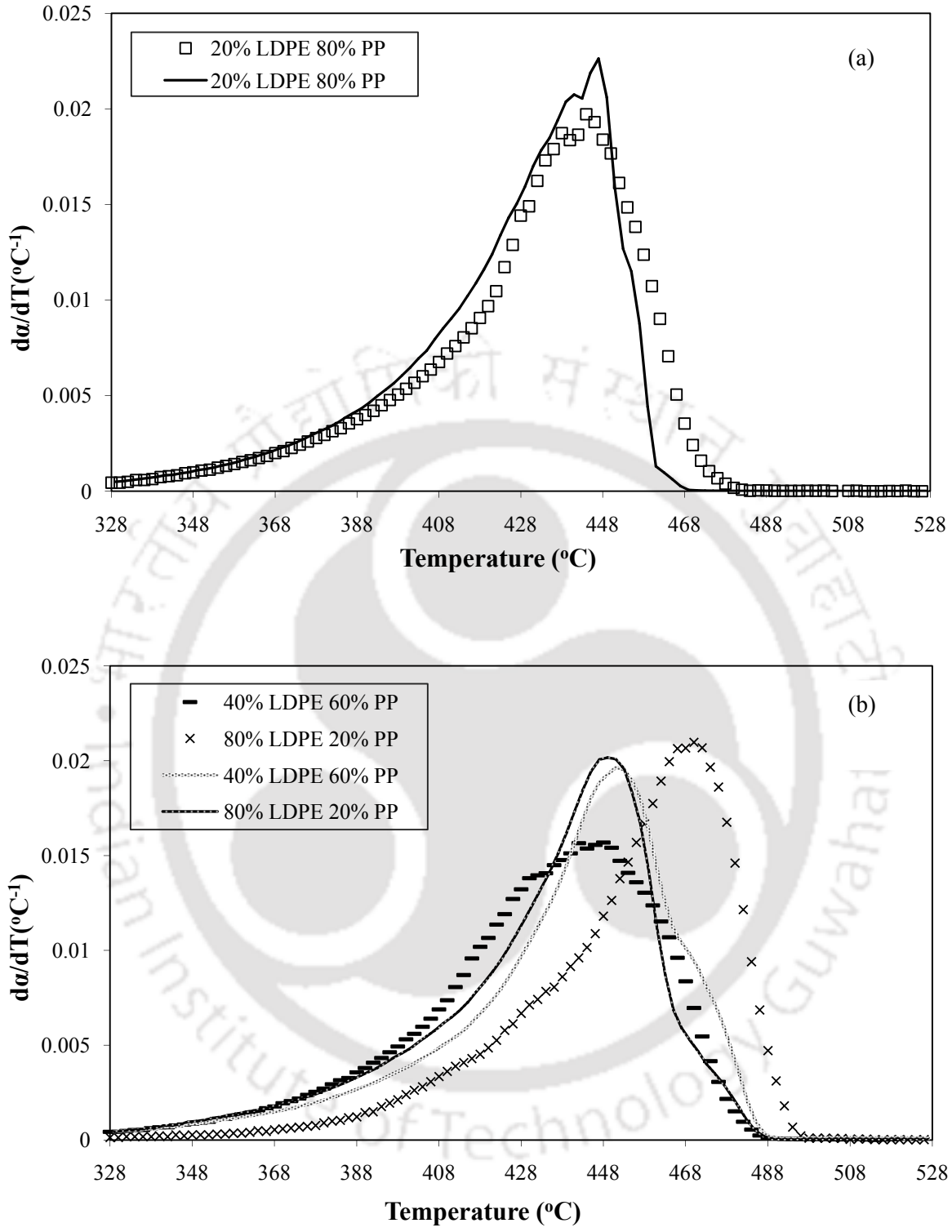

Figure 5.4 Experimental and non-interacting DTG curves of binary mixture of LDPE and PP for various compositions; (a) 20% LDPE 80% PP; (b) 40% LDPE 60% PP, 80% LDPE 20% PP (markers show experimental curve; dotted lines show non-interacting curve)

For binary mixtures of LDPE and PET, multiple peak temperatures are observed in the experimental curves (Figure 5.2) particularly for higher proportion of LDPE. It can be seen from Figure 5.2 that with increase in the percentage of PET, there is a drop in T_{max}, which is suggestive of some synergistic effect existing between them. This could possibly be explained by an intermolecular transfer of a hydrogen atom from the less stable polymer (*i.e.* PET) to a free radical depropagating chain of the second component (*i.e*. LDPE) during decomposition [66].

There is not a wide variation in the thermal stability of PET and PP. Lowering of T_{max} is observed for all the binary mixture compositions. For binary mixture of LDPE and PP, multiple peak temperatures are obtained, except for 80% PET and 20% LDPE, which shows a single T_{max}. With increase in percentage of PP, T_{max} shows a gradual decrease. Moreover, with increase in percentage of LDPE, peak height increases, and the curve becomes less dispersed. For all the mixture compositions in each binary, there was a considerable deviation between the experimental DTG and non-interacting decomposition curves. T_{max} values obtained from both the curves also differ widely, indicating the role of interaction between various plastics present in the mixture. Consequently the decomposition process of the plastics in their mixture cannot be termed to be completely independent of one another. Thus from Figures 5.2-5.4 it is obvious that non-interacting model fails to predict degradation kinetics and justifies the need for a model which can be used to correlate experimental observations.

The parameters for the proposed interacting model β_{ij} and γ_{ij} were calculated at each two degree temperature intervals in the range of interest (as already explained in *Section 3.2*). This was done by calculating $\left.\frac{d\alpha}{dT}\right|_{ij}$ for various mixtures at a specific temperature from experimental data for $\left.\frac{d\alpha}{dT}\right|_{mix}$ using *equation (3.2)* along with the experimental data for pure

component degradation kinetics (*i.e.* $\left.\frac{d\alpha}{dT}\right|_i$ and $\left.\frac{d\alpha}{dT}\right|_j$). Subsequently, these parameters β_{ij} and γ_{ij} were used to correlate the experimental data using the proposed model.

Figures 5.5, 5.6 and 5.7 illustrate the correlation of mixture degradation kinetics of binary plastic mixtures of LDPE-PET, PP-PET, and LDPE-PP using interacting model proposed in the work. It can be seen from the figures that DTG curves predicted by the interacting model closely follow the experimental curves corresponding to various mixture compositions for all the three binary mixtures. Thus it is effective in correlating the experimental observations of all the three binary mixtures over the wide range of compositions studied. Thermograms (α vs. T curves) are also drawn for all the mixture compositions, and interacting model is equally good in corroborating the experiments. Thermogravimetric curves for single plastics and different mixtures are shown in *Appendix 2*.

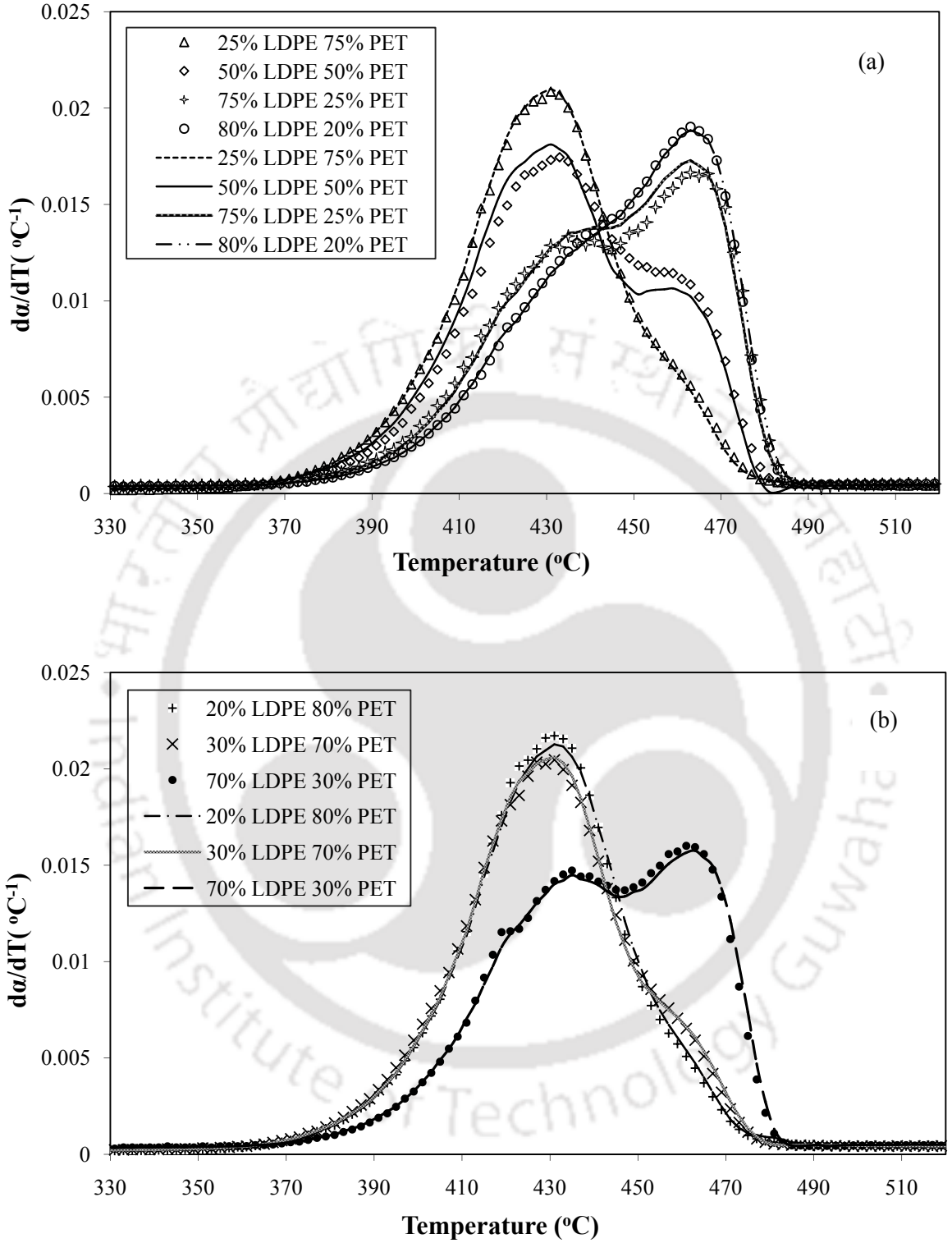

Figure 5.5 Experimental and interacting DTG curves of binary mixture of LDPE and PET for various compositions; (a) 25% LDPE 75% PET, 50% LDPE 50% PET, 75% LDPE 25% PET, 80% LDPE 20% PET; (b) 20% LDPE 80% PET, 30% LDPE 70% PET, 70% LDPE 30% PET (markers show experimental curve; dotted lines show interacting model)

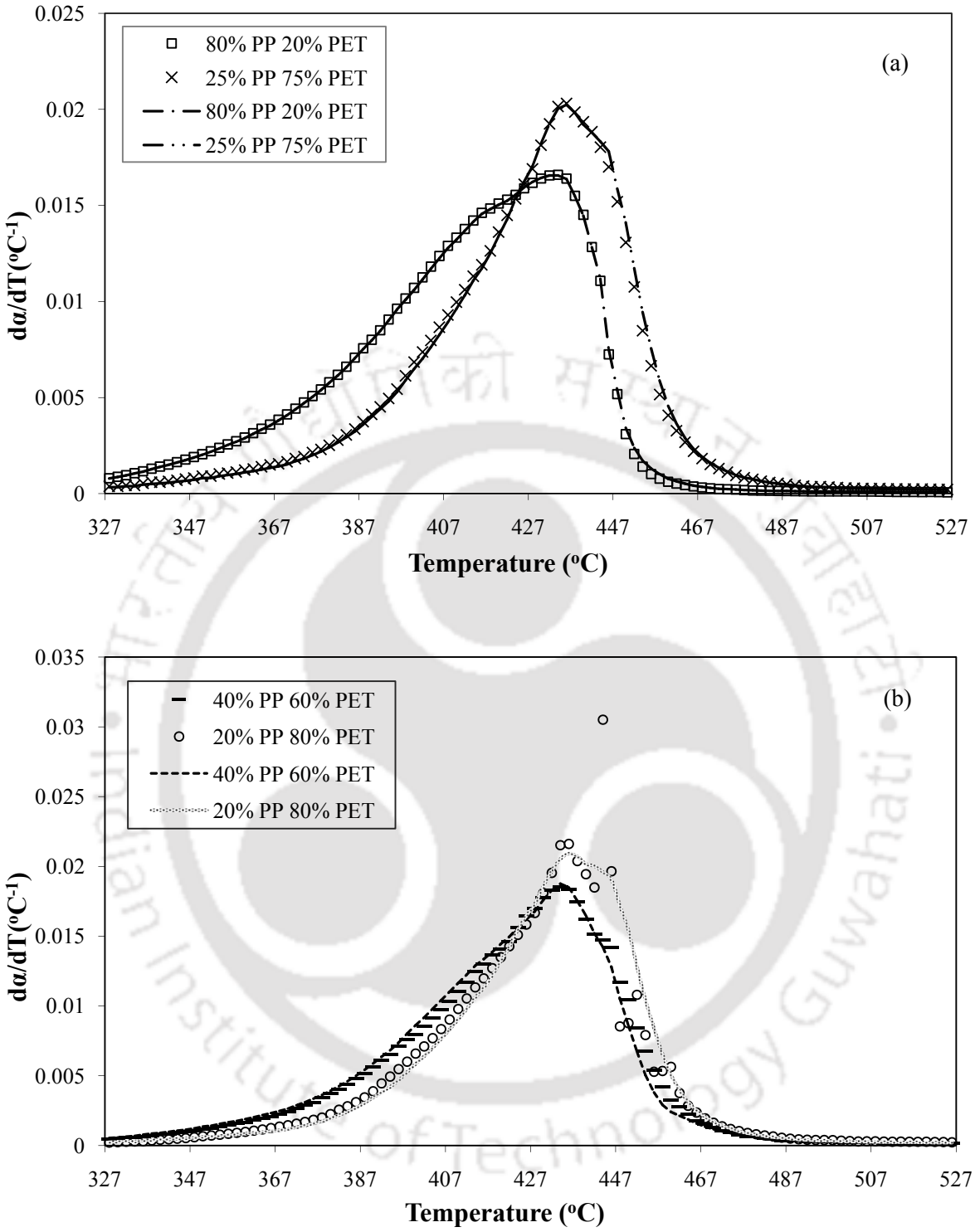

Figure 5.6 Experimental and interacting DTG curves of binary mixture of PP and PET for various compositions; (a) 80% PP 20% PET, 25% PP 75% PET; (b) 40% PP 60% PET, 20% PP 80% PET (markers show experimental curve; dotted lines show interacting curve)

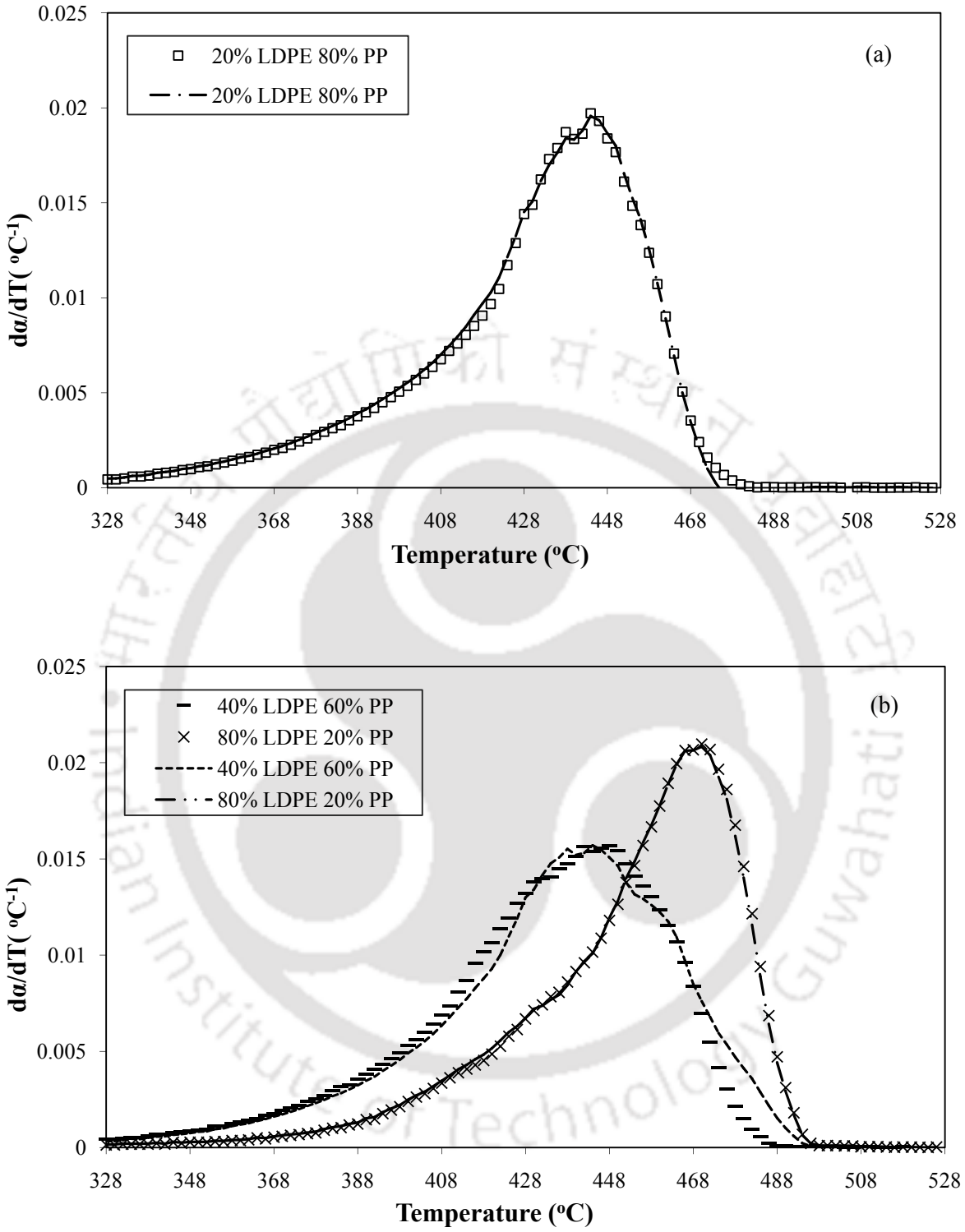

Figure 5.7 Experimental and interacting DTG curves of binary mixture of LDPE and PP for various compositions; (a) Composition – 20% LDPE 80% PP; (b) Composition – 40% LDPE 60% PP, 80% LDPE 20% PP (markers show experimental curve; dotted lines show interacting model)

A quantitative measure of effectiveness of the proposed model is readily obtained by looking at the average relative deviation (ARD) between experimental observations and the model predictions. It is defined as

$$ARD(\%) = \frac{100}{N}\sum\left|\frac{Experimental - Predicted}{Predicted}\right| \qquad (5.1)$$

where, N= Number of data points.

Table 5.2 shows the ARD (%) values of the interacting and the non-interacting models for the binary mixtures. Depending on the spread of the data points for each of the binary mixture, temperature ranges considered for this evaluation were 357-497^{o}C, 347-487^{o}C, and 337-487^{o}C for LDPE-PET, LDPE-PP and PET-PP mixtures respectively. Clearly, the ARD values for the interacting model are lower than those for the non-interacting model. Peak temperature values (both experimental and model predicted) for various mixture compositions of the binary mixtures are also listed in Table 5.2. It can be seen that the interacting model has been successful in predicting the true T_{max} for all the experiments. The two peak temperature values observed in some of the binary compositions are also replicated well by the proposed model.

Table 5.2 Peak temperature for the binary mixtures and comparison of ARD (%) values of the interacting and non-interacting model

Mixture		Peak Temperature, ^{o}C		ARD (%)	
LDPE (wt.%)	PET (wt.%)	Experimental	Interacting model	Interacting model	Non-interacting model
20	80	430	430	4.49	54.35
25	75	430	430	4.49	56.72
30	70	430	430	3.53	63.71
50	50	432	430	32.67	53.63
70	30	434, 460	434, 460	3.58	50.69
75	25	430, 462	434, 462	7.13	47.73
80	20	462	462	3.79	41.45
PET (wt.%)	PP (wt.%)				
20	80	434	434	3.17	145.64
60	40	434	434	9.3	49.55
75	25	436	436	5.83	43.44
80	20	436, 444	436	11.78	37.1
LDPE (wt.%)	PP (wt.%)				
20	80	438, 444	438, 444	20.47	494.3
40	60	442, 448	438, 444	13.72	24.83
80	20	470	470	4.06	187.45

5.1.3 Kinetics of pyrolysis of ternary plastic mixtures

Three different compositions of the ternary mixtures are studied. Figure 5.8 shows the experimental and non-interacting DTG curves for the ternary plastic mixture. As in case of the binary mixtures, significant deviations are observed between the experimental and ideal non-interacting decomposition curves. Two values of peak temperatures are observed for all the three compositions of the ternary mixtures, which cannot be predicted by the non-interacting model. Thus a simple additive non-interacting model cannot be used to predict decomposition kinetics.

Subsequently we made an attempt to model the decomposition behaviour of the ternary mixtures taking the help of the extended form of the interacting model (*equation* (*3.3*) under *Section 3.2*) proposed for ternary mixture kinetics. As it has already been explained in *Section 3.2*, binary interaction parameters (*i.e.* $\beta_{12}, \beta_{23}, \beta_{13}$ and $\gamma_{12}, \gamma_{23}, \gamma_{13}$) for each binary pair of the plastics were used to predict the ternary degradation kinetics. Figure 5.9 shows the predicted DTG curves along with the experimental curves, and although no additional exercise was done to calculate ternary interaction parameters, the ternary decomposition kinetics predictions were found to be good enough.

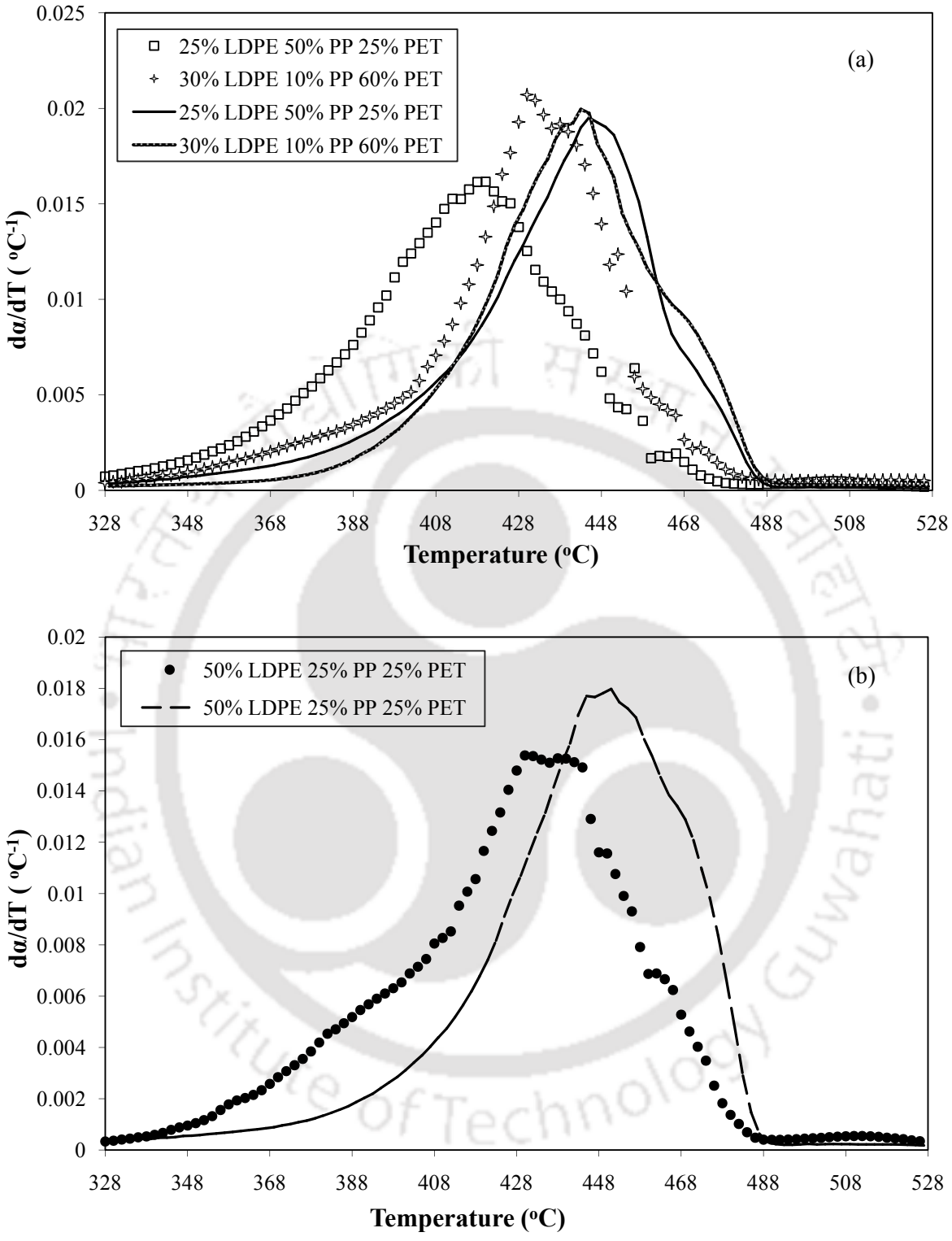

Figure 5.8 Experimental and non-interacting DTG curves of ternary mixture of LDPE, PP and PET for various compositions; (a) 25% LDPE 50% PP 25% PET, 30% LDPE 10% PP 60% PET; (b) 50% LDPE 25% PP 25% PET (markers show experimental curve; dotted lines show non-interacting curve)

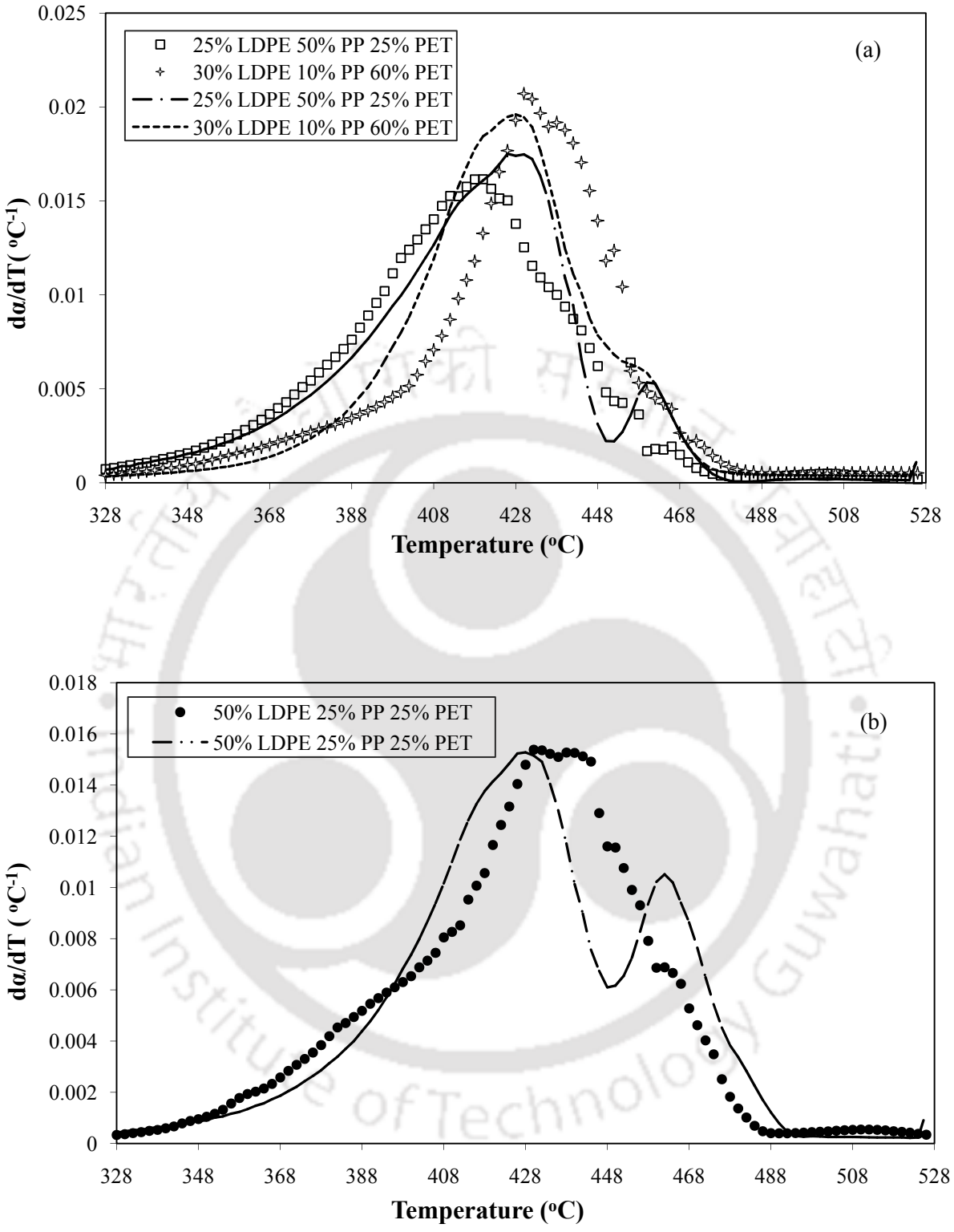

Figure 5.9 Experimental and interacting DTG curves of ternary mixture of LDPE, PP and PET for various compositions; (a) 25% LDPE 50% PP 25% PET, 30% LDPE 10% PP 60% PET; (b) 50% LDPE 25% PP 25% PET (markers show experimental curve; dotted lines show interacting model)

Table 5.3 reports the maximum degradation temperature of the ternary plastics mixtures. A comparison between the ARD (%) values of the interacting and non-interacting model for all the ternary mixture compositions is depicted in Table 5.3. Temperature range considered in case of the ternary mixtures is 337-497^{o}C, *viz*. the lowermost and the uppermost limit of the range considered for the binary mixtures. It is clear that the interacting model better predicts the behaviour of ternary plastic mixtures considered, than a non-interacting model.

Table 5.3 Peak temperature and ARD (%) values for the LDPE-PP-PET ternary mixture

Mixture			Peak temperature, ^{o}C		ARD (%)	
LDPE (wt.%)	PP (wt.%)	PET (wt.%)	Experimental	Interacting model	Interacting model	Non-interacting model
25	50	25	420, 456	426, 460	62.15	110
30	10	60	430, 438	428	36.88	93.42
50	25	25	430, 462	428, 462	32.44	87.96

In reality polymer wastes are mixture of several polymers having different thermal stability. The mixture composition and characteristics also vary from place to place. While designing and developing any reactor for thermal or catalytic decomposition of such mixture, single plastic kinetics data cannot be used straight way. Information on the kinetics for the mixture is very much essential to understand the decomposition behaviour. Such information generation is a non-trivial task as it requires numerous experiments to be performed, one each for each mixture encountered. At the same time, presence of multiple peaks in the DTG curves for the mixture does not allow us to have single data set for the kinetics triplets (activation energy, pre-exponential factor and order of reaction). The present study showed that using one additional interaction term per binary, decomposition behaviour can be successfully correlated. The ternary mixture kinetics can also be predicted fairly well using the binary interaction term.

In principle, one can extend the idea presented in this work to higher order multi-component mixtures, without requirement of any additional experiments.

5.1.4 Conclusions

A rigorous modeling of the degradation kinetics of polymer mixtures is often very difficult, since miscibility of polymers is a function of temperature along with the composition, both of which are not constant during pyrolysis. Moreover, one also needs to incorporate the interactions of the melt with products obtained during pyrolysis. Due to these reasons, modeling of pyrolysis kinetics of plastic mixtures is a complex task. On the other hand, one needs a model which can describe degradation behaviour of multi-component plastic mixtures, often encountered in pyrolysis reactors.

In this work, we used a mixing rule type approach to develop an interacting model to describe degradation kinetics of 14 different binary plastic mixtures of LDPE, PP and PET. The ternary mixture behaviour is completely predictive and only needs information obtained from the constituent binary degradation kinetics. Good correlations of binary data were obtained using the interacting model as indicated by the ARD values. Even in case of ternary mixtures, the ARD obtained using the interacting model was 50% lower than that obtained using a non-interacting model. Multiple peaks in the DTG curve obtained for both binary and ternary mixtures were also successfully mimicked by this model.

5.2 Temperature Dependent Pyrolytic Product Evolution Profile of LDPE

5.2.1 Products analysis

Figure 5.10 shows the typical thermograms (TG and DTG curves) of the pure LDPE sample used in this study. Here, $\frac{d\alpha}{dT}$ represents the rate of degradation where α is the fractional

conversion of the plastic. It is evident from this figure that T_{max} for LDPE is around 470°C. It should be noted here that the LDPE used in this work is a pure sample, and is thus different from that used in kinetics study.

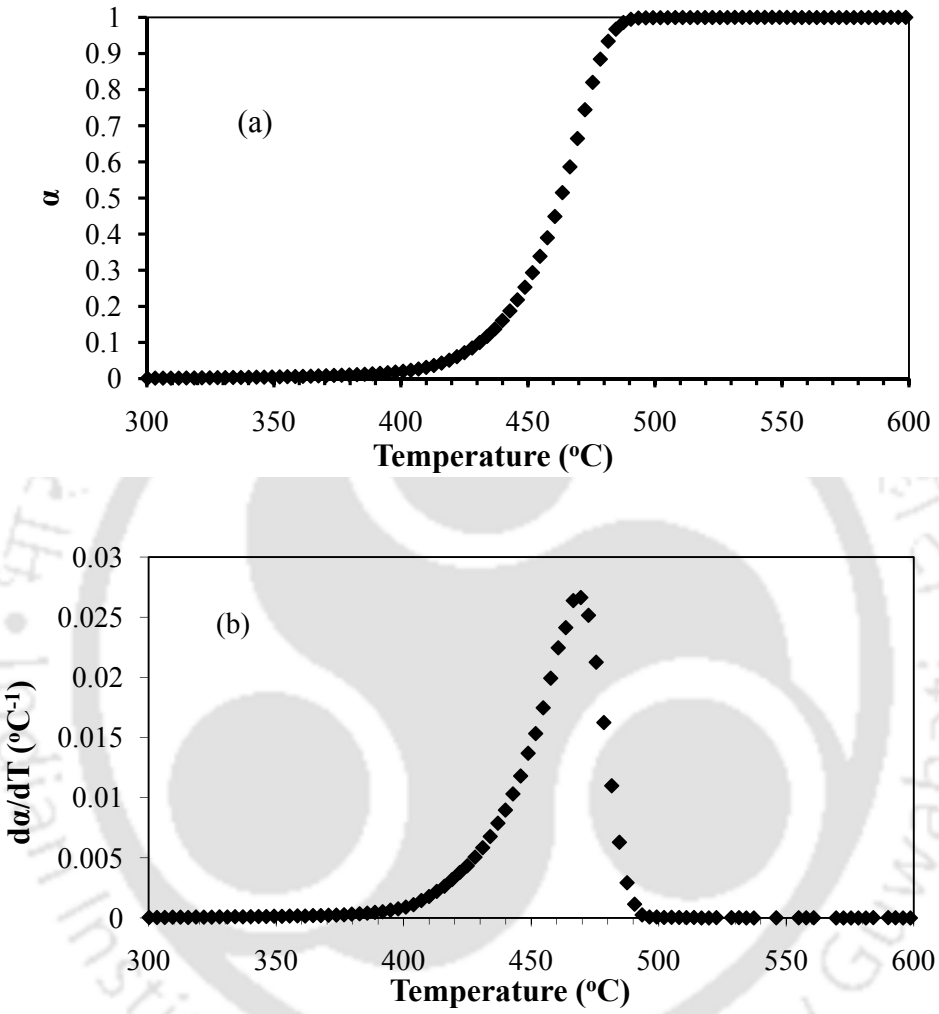

Figure 5.10 (a) TG curve of LDPE; (b) DTG curve of LDPE (heating rate: 10°C min^{-1}, Ar flow rate: 40 ml min^{-1})

The amount of residue obtained after pyrolysis of LDPE is about 0.1-2%. Pyrolysis of LDPE produces a series of hydrocarbons; the amount of straight aliphatics is usually more than their branched counterparts [80]. Figures 5.11 and 5.12 show the temperature dependency for evolution of C5-C15 and C16-C44 hydrocarbons respectively, during pyrolysis of LDPE.

They clearly show that hydrocarbon product obtained depended strongly on decomposition temperature.

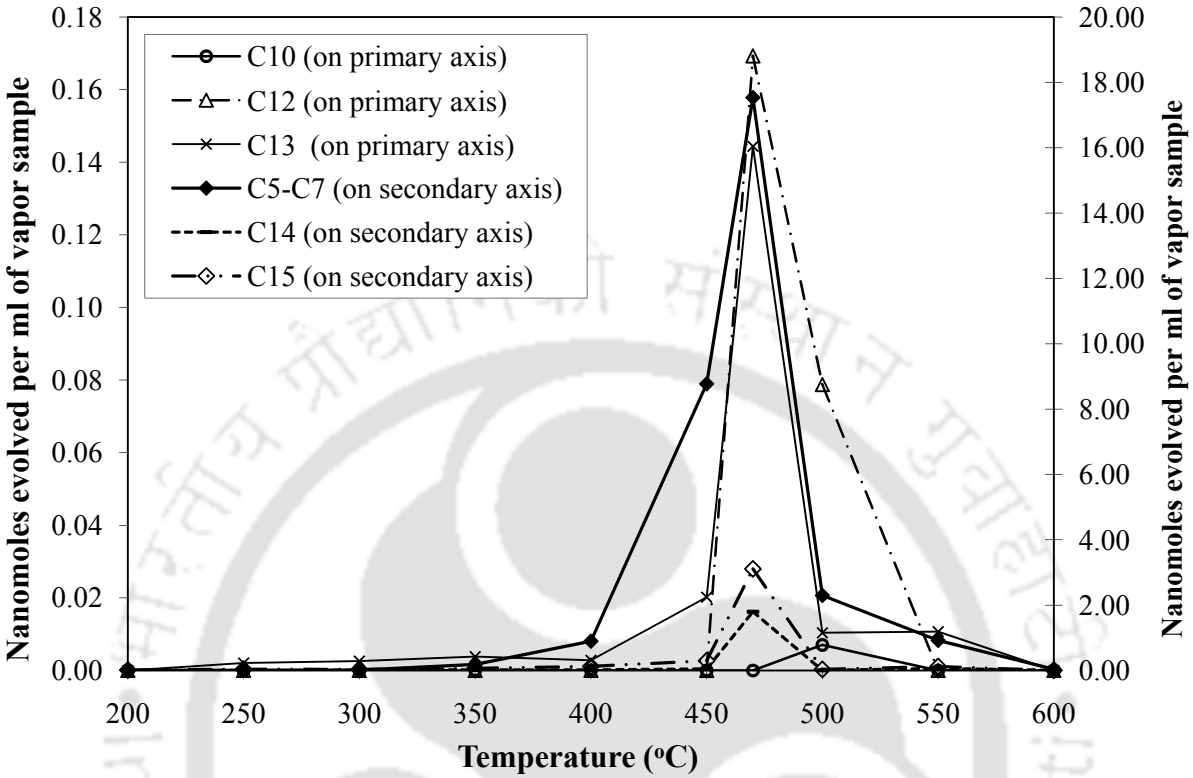

Figure 5.11 Temperature dependency of C5-C15 hydrocarbon evolution during pyrolysis of LDPE

At low temperature of decomposition (200-300°C), evolution of lighter hydrocarbons (C5-C15) essentially remains low, and as we move along the temperature scale towards 300-470°C (Figure 5.11), there is a gradual increase in the amount of lighter fractions until 470°C; these hydrocarbons attain the maximum value at this temperature. At 470°C, evolution of these lighter fractions increases by about twenty times from that at 200°C. At 500°C, it drops approximately by tenfold relative to that at T_{max}. It continues to decrease till temperature reaches 600°C, where volatile product formation decreased by more than fifty times to that at 500°C. Figure 5.11 reflects that C5-C7 hydrocarbons are the dominant species formed. C5-C7 hydrocarbons start forming near about 350°C. Beyond 400°C, substantial rise in evolution of

C5-C7 species is observed. The amount of C15, the second major fraction observed at T_{max} is about six times lower than that of C5-C7 hydrocarbons. C14 is the third largest product. There is negligible evolution of C10 hydrocarbons up to 470°C; they appear only at 500°C. Other hydrocarbons which are observed at T_{max} are C12 and C13.

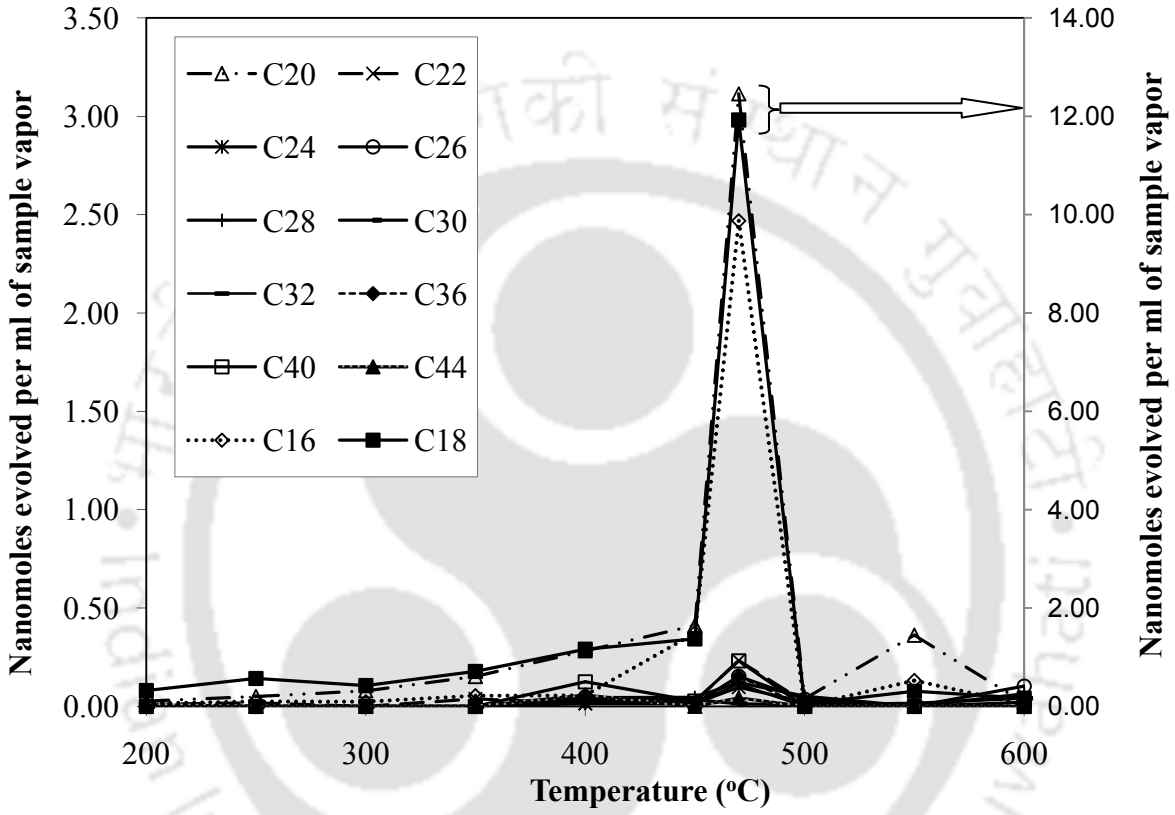

Figure 5.12 Temperature dependency of C16-C44 hydrocarbon evolution during pyrolysis of LDPE (C18 and C20 on secondary axis; all others on primary axis)

Within the low temperature regime (200-300°C), evolved species are C18, C16, C20; traces of C40 and C44 are also obtained. Again, with the rise in temperature, cracking reactions become vigorous and beyond 400°C, other hydrocarbon species (C20-C30) begin to evolve. Evolution of these fractions increased to attain a maximum at T_{max} with an increase by more than hundredfold as compared to low temperature. Beyond 470°C, production of heavier hydrocarbons continues to diminish. At 600°C, amount evolved decreased by roughly tenfold.

C16-C18 hydrocarbons are the major products amongst the heavier hydrocarbon (C16-C44) group. The amount of C16-C18 evolved is less by about 1.4 times as compared to that of C5-C7 hydrocarbons.

Variation of mole fractions of different hydrocarbon fractions is shown in Figure 5.13. It can be seen from the figure that C16-C22 fractions predominate at 200°C. C12-C15 fractions contribute to less than 10% of the total yield. Traces of C5-C10 hydrocarbons are also observed. Heavier hydrocarbons (C24 and above) are negligible at this temperature.

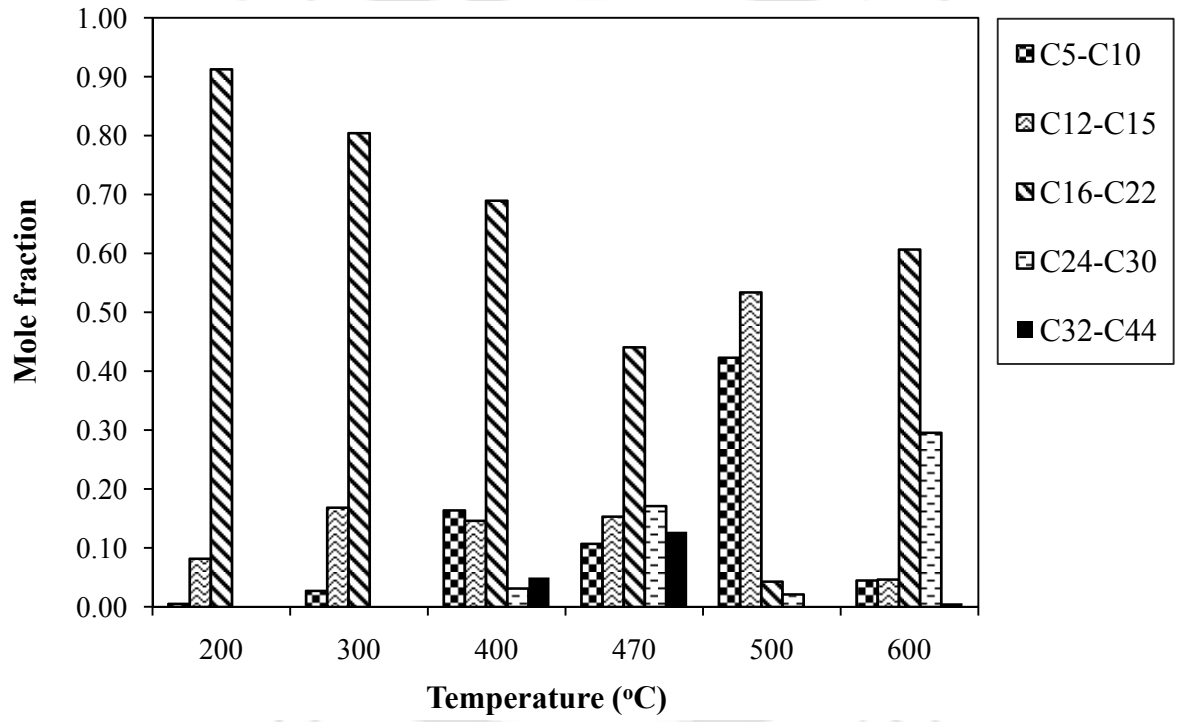

Figure 5.13 Mole fractions of C5-C44 hydrocarbons from pyrolysis of LDPE at various temperatures

As temperature increases to 300°C, relative proportion of C5-C10 and C12-C15 hydrocarbons increases, while that of C16-C22 hydrocarbons decreases; the latter however share the major portion of the total yield. At 400°C, C5-C10 hydrocarbons increases and they contribute to around 16% of the total yield, and C24-C30 and C32-C44 fractions start evolving. Howeverm

C16-C22 fraction is invariably the major product. At 470°C, relative proportion of C24-C30 and C32-C44 increases, while production of C12-C15 hydrocarbons decreases relative to that at 400°C. At 500°C, production of C5-C10 and C12-C15 significantly increases, while evolution of other hydrocarbon fractions is considerably less. Beyond 500°C, the reverse happens, with the heavier hydrocarbons sharing the major portion of the product yield.

Figures 5.14 and 5.15 show the pyrograms of LDPE at T_{max} corresponding to lighter (C5-C15) and heavier hydrocarbons (C16-C44) respectively. Pyrograms for LDPE at other temperatures are shown in *Appendix 3*. The pyrograms reveal a recurring pattern of peaks (peak triplets). Each triplet of peaks represents the diene, alkene, and alkane containing a specific number of carbons and eluting in that order [134]. As can be seen from Figure 5.14, separation of C5-C7 could not be achieved which might be due to the characteristics of the particular column used for the purpose and a broad peak represents them en masse.

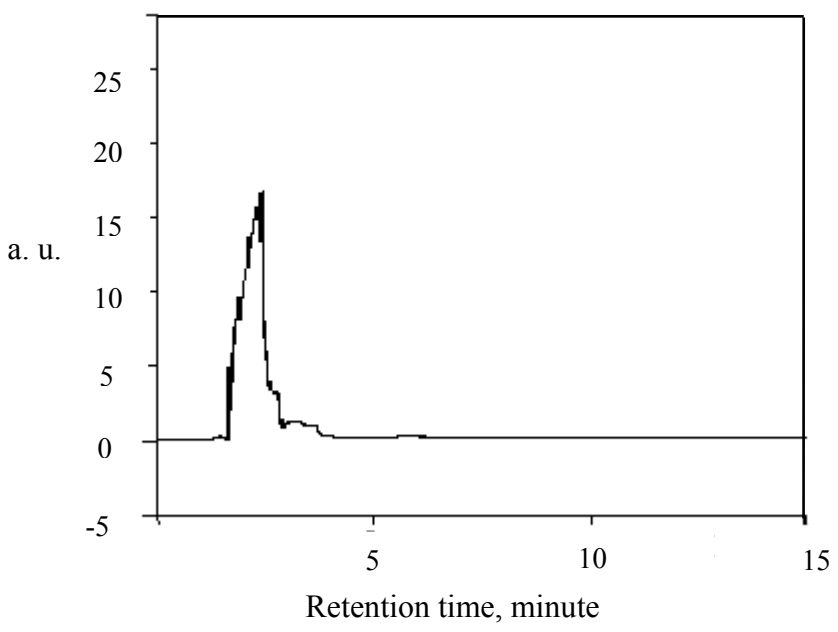

Figure 5.14 A part of the pyrogram of LDPE at T_{max} depicting C5-C7 hydrocarbons

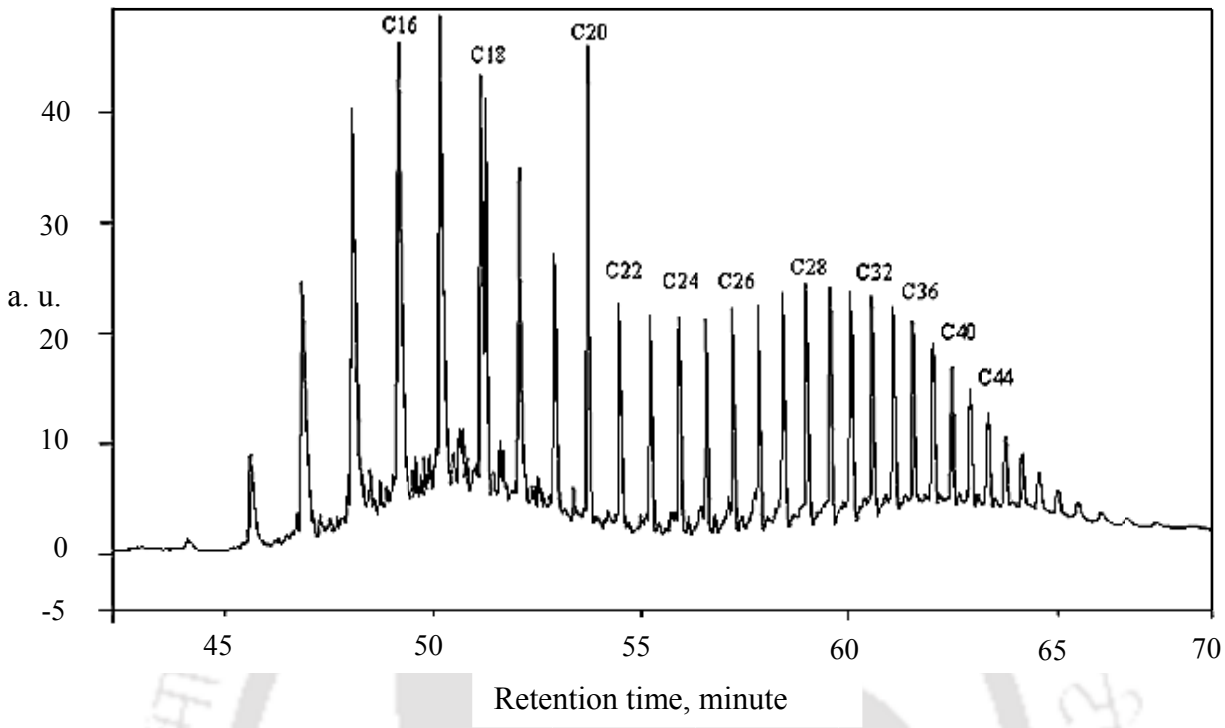

Figure 5.15 A part of the pyrogram of LDPE at T_{max} depicting C16-C44 hydrocarbons and peak triplets

After that, there are no distinct peaks until about 40 min and the chromatogram appears almost flat which is due to the fact that there are no C8 and C9 hydrocarbon products detected during this retention time. However, evolution of C8 species from LDPE has been reported in the literature [80]. Column oven program and other parameters were set so as to obtain maximum attainable separation between the different hydrocarbon species (C5-C44) in the standards used for calibration which resulted in such long times. Figure 5.15 illustrates heavier hydrocarbons eluting after 42 min of the run. A part of this chromatogram is zoomed in to show the peak triplets in Figure 5.16. Diene production is low, which has also been reported in literature [80, 96], and hence its peak is not as prominent as the other two.

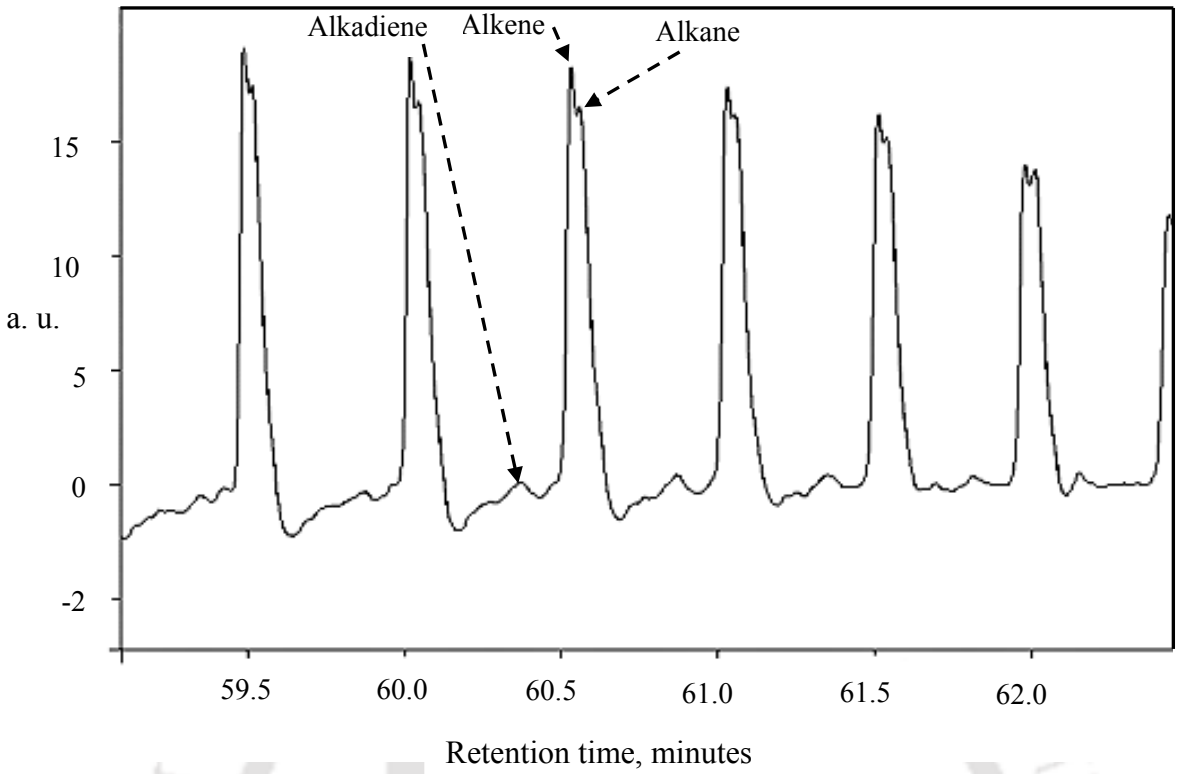

Figure 5.16 A part of the pyrogram of LDPE depicting peak triplets

5.2.2 Mechanistic analysis

Thermal decomposition of LDPE, which is an addition polymer of ethylene, proceeds essentially by random scission of the macromolecule. Different fractions thus formed by random fragmentation undergo subsequent stabilization, but they cannot be detected in the product stream until the fractions become volatile enough to migrate into the vapour phase.

The way in which a polymer molecule breaks into fragments during pyrolysis and the nature of the fragments produced depend on the types of chemical bonds involved and the stability of the resulting smaller molecules [134]. The bonds that tend to break first are the ones that form the weakest link(s) in the chain. Weak links may exist in form of side chains, peroxy, carbonyl, hydroxyl group (formed in process of radical polymerization of ethylene) or atactic portions of macromolecular chain, which could induce the degradation at an earlier stage as these are most susceptible to thermal destruction [34]. Most polymers decompose at a

temperature substantially lower than that of polymers having small chains or oligomers if there are irregularities in the chain backbone of the polymer which act as weak points [135]. Richards and Salter [69-71] in their work evaluated thermal degradation of PS by using poly(α-methylstyrene) (PMS) as a radical producing agent and confirmed the contribution of these weak links in initiating the degradation at otherwise stable temperatures. Evolution of some products at 200-300^{o}C could be justified for similar reasons in case of LDPE also.

The proposed reaction pathway shows the formation of alkanes, alkenes and diolefins, which are considered to be a part of the products evolved from pyrolysis of LDPE. Initiation reactions can involve either C-C or C-H bond cleavage. The bond dissociation energy of C-C and C-H bonds are 347 kJ mol^{-1} and 413 kJ mol^{-1} respectively. Since C-C bond is weaker of the two, its dissociation is more probable initiation step. All the C-C bonds in LDPE are theoretically of about the same strength, consequently there is no reason for one to break more easily than the other. But, in reality due to the presence of short-chain branches in LDPE, there are certain C-C bonds along the chain backbone which are more prone to degradation. Random-scission of LDPE (**P**) produces hydrocarbons with terminal (primary) free radicals (**I**), as shown in *Reaction scheme 5.2.1*.

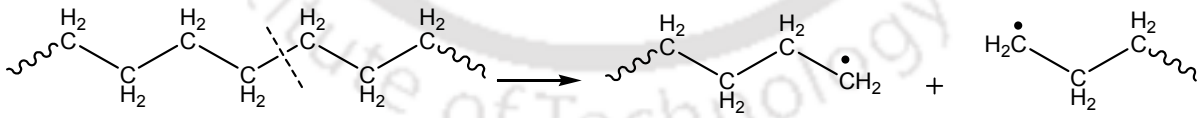

P **I**

Reaction scheme 5.2.1

The reactivity of the system is governed by the overall radical pool and consequently the competition between initiation and termination reactions has to be properly understood [86]. The primary radicals thus formed are capable of stabilizing themselves by hydrogen

abstraction reactions, *β*-scission, intermolecular and intramolecular hydrogen transfer processes, all of which aid in formation of a stable molecule. At higher temperature (>350^{o}C), C-H bond scission is followed by *β*-scission, which justifies the formation of more amount of lighter hydrocarbons beyond 350^{o}C. H-abstraction reactions propagate the reaction chain, but do not change the mean molecular weight of the system. On contrary, *β*-scission reactions are responsible for the subsequent reduction of the chain length [96, 135]. However, intramolecular reactions are extremely crucial in the radical mechanism of degradation of LDPE which justifies the preferential formation of some hydrocarbons over other species [96, 135, 136].

The GC results presented earlier indicate that the temperature plays a decisive role in product evolution profile. The reactivity of different radicals (primary or secondary) is also dictated by the C-H bond energy of the respective radicals.

Primary radicals, being less stable than the secondary, can undergo 1,5-intramolecular hydrogen transfer (*Reaction scheme 5.2.2*) transforming itself to a secondary macro-radical (**II**) and thus increasing free radical stability.

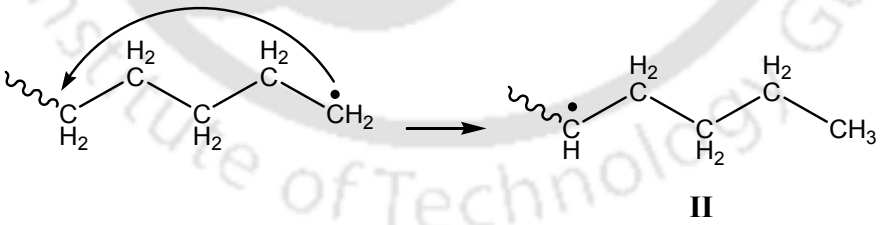

Reaction scheme 5.2.2

This new secondary radical will undergo either *β*-scission or another 1,5-H shift as shown in *Reaction scheme 5.2.3*. *β*-scission to the left of the radical (shown by route **'a'**) will produce hexene (**III**) (trimer of ethylene), and regenerate a chain-terminus radical (**I**), whereas *β*-

scission to the right (shown by route **'b'**) gives rise to a polymer with unsaturated end (**IV**) and a short chain-terminus radical (**V**), which can abstract a hydrogen atom from a neighbouring molecule to form propane.

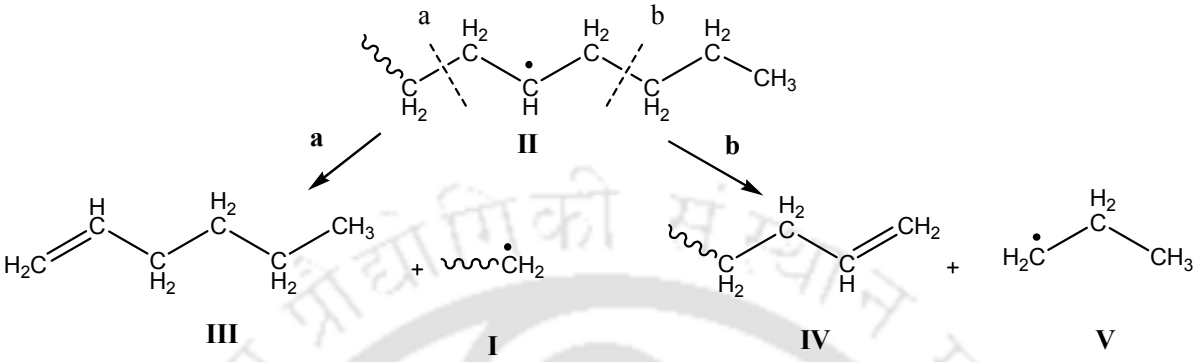

Reaction scheme 5.2.3

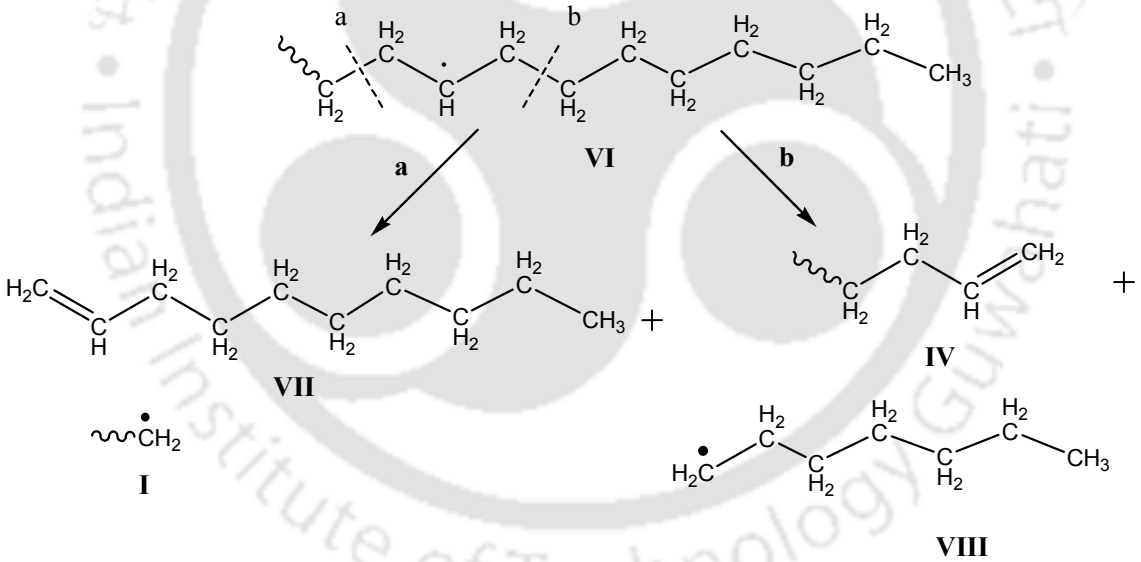

Reaction scheme 5.2.4

On the other hand, a second 1,5-H shift in **II** will move the free radical to carbon number 9 (*Reaction scheme 5.2.4*). *β*-scission of this new free radical (**VI**) would result into either a molecule of decene (**VII**), the pentamer or a heptane molecule (formed from **VIII**). This stabilization by 1,5-hydrogen transfer explains the increased yield of products in the

pyrolyzate of LDPE containing C6, C10, C14, C22 alkenes and C3,C7,C11, C15 alkanes [136]. These products are the result of performing a 1,5-H shift one, two, three and four times respectively. However, intramolecular transfer involving six-membered cyclic transition state cannot predict formation of C5, C12, C13, and C16 hydrocarbons. In our study, significant evolution of C5-C7 hydrocarbons were obtained at 400-500^{o}C. C5 (shown by structure **VI**) can possibly result following 1-4 hydrogen shift on **I** producing another secondary radical on subsequent *β*-scission as shown in *Reaction scheme 5.2.5*.

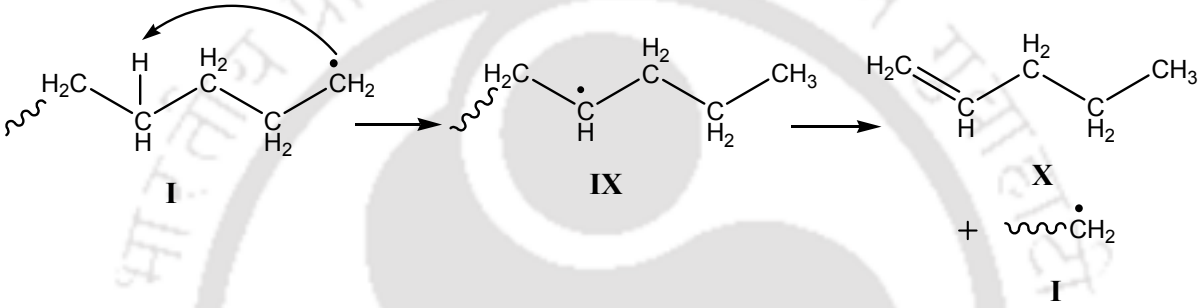

Reaction scheme 5.2.5

In addition, **I** can also undergo hydrogen abstraction reactions forming a polymer with a terminal double bond, as shown in the *Reaction scheme 5.2.6* below.

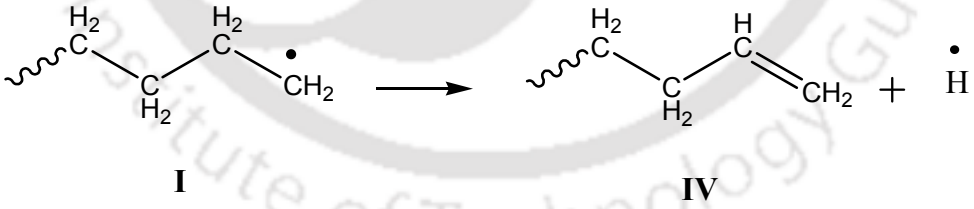

Reaction scheme 5.2.6

The formation of C12, C13, C16 hydrocarbons can be justified by introducing 1,5- and 1,6-mid-hydrogen transfer reactions into the reaction scheme. C12 hydrocarbons (**XII**) might have been formed due to two consecutive 1,5-mid-hydrogen transfer reactions of **XI** along

the chain backbone followed by *β*-scission (as shown in *Reaction scheme 5.2.7*). Similarly, C16 hydrocarbons are the product of three consecutive 1,5- mid-hydrogen transfer reactions.

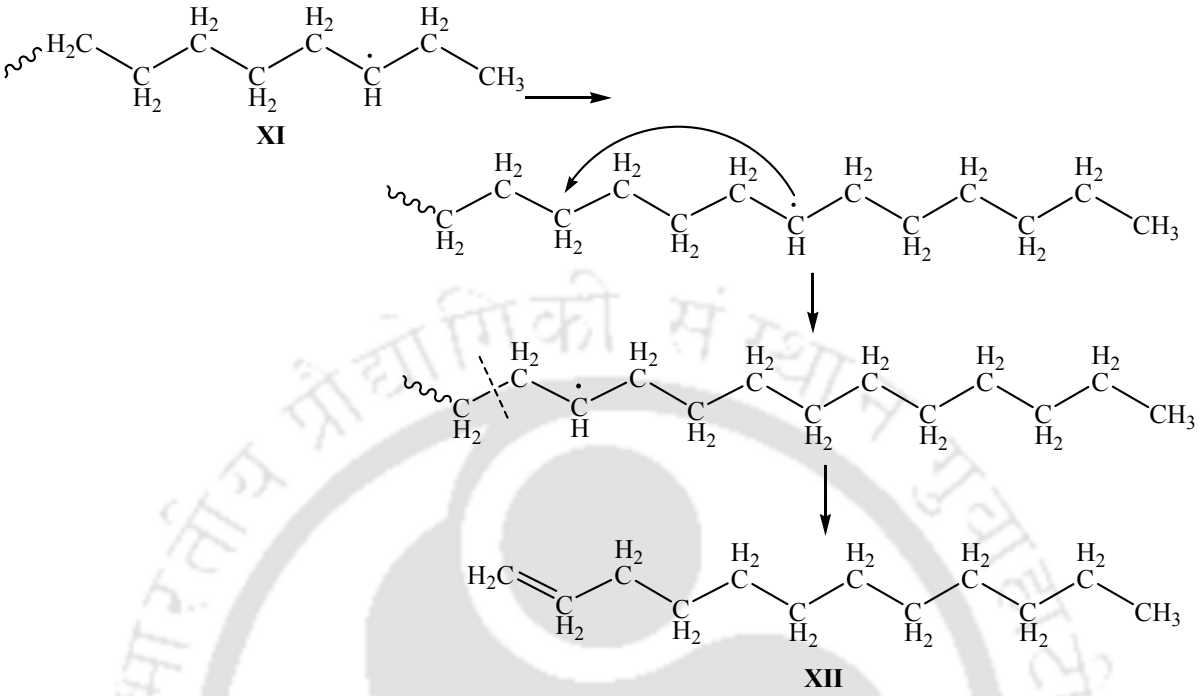

Reaction scheme 5.2.7

These mid-hydrogen transfers proposed here are similar to those included by Kruse *et al.* [74] in their mechanistic pathways to describe PP degradation to account for the formation of certain low-molecular weight hydrocarbons in the size range of C1-C15. In a similar scheme, C13 hydrocarbons may result when a free radical (**XII**) formed by 1,5-mid-hydrogen transfer undergoes a,6-mid-hydrogen transfer followed by *β*-scission.

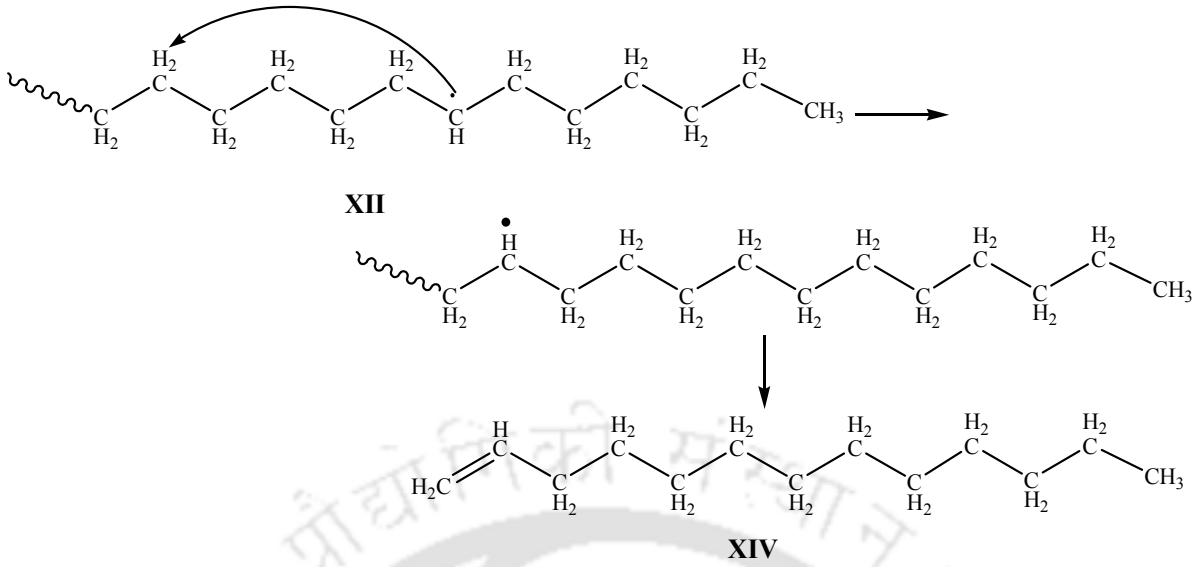

Reaction scheme 5.2.8

However, due to entropic barriers these mid-hydrogen transfer reactions are slower than the end-hydrogen transfer reactions [74] which could justify the less production of C12, C13, C16 hydrocarbons.

Table 5.4 shows the various hydrogen shifts and the corresponding products obtained from LDPE following subsequent *β*-scission of the radicals thus generated. ('=' represents the double bonded compounds, e.g. 'C6=' stands for hexene)

Table 5.4 Different hydrogen shifts and corresponding products from LDPE

Intramolecular hydrogen transfer	**Number of transfer steps**	**Products**
1, 5- end H transfer	One	C6= or C3
	Two	C10= or C7
	Three	C14= or C11
	Four	C22= or C15
1,4- end H transfer	One	C5= or C2
	Two	C5 or C8=
1,5-mid H transfer	Two	C12
	Three	C16
1,5-mid H transfer followed by 1,6-mid H transfer	One	C13=

An intermolecular hydrogen transfer from a neighbouring polymer molecule to the primary macroradical creates a saturated end (**XV**) and regenerates the secondary radical, **IX** (*Reaction scheme 5.2.9*) which may stabilize in a number of ways.

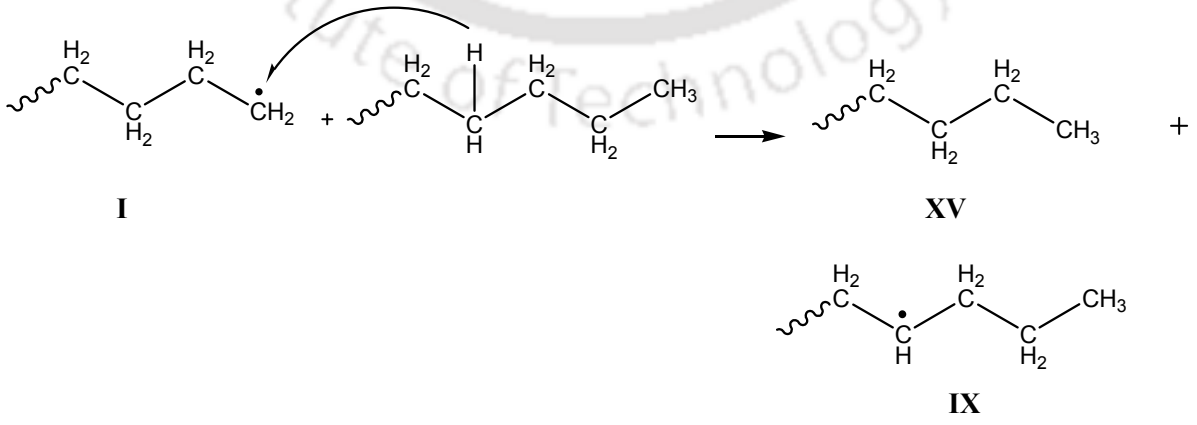

I **XV** **IX**

Reaction scheme 5.2.9

The most likely of these is *β*-scission, which produces pentene (**X**) , and a terminal free radical (as already depicted in *Reaction scheme 5.2.5*). However, intermolecular H-transfer reactions are more probable at higher temperature (>350^{o}C) [80].

At higher temperature, '**I**' might undergo depolymerization producing the monomer ethylene (**XII**). In the pyrogram (Figure 5.14) the broad peak corresponding to C5-C7 might also encompass these C2 fractions.

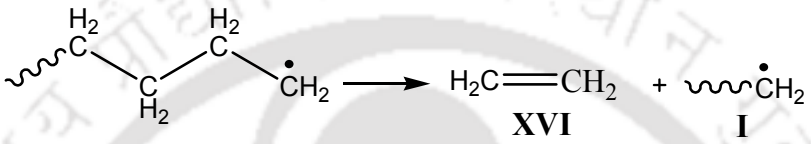

Reaction scheme 5.2.10

However unzipping to monomer is not a favourable process below 400^{o}C, when only traces of highly volatile (C1-C4) products are formed [96].

At high temperatures, a secondary radical might abstract a hydrogen atom from a polymer (**IV**) with an unsaturated end and thus transferring the radical centre to the latter. The resulting secondary radical on *β*-scission results into a diene (**XIII**) releasing one chain terminus radical (**I**).

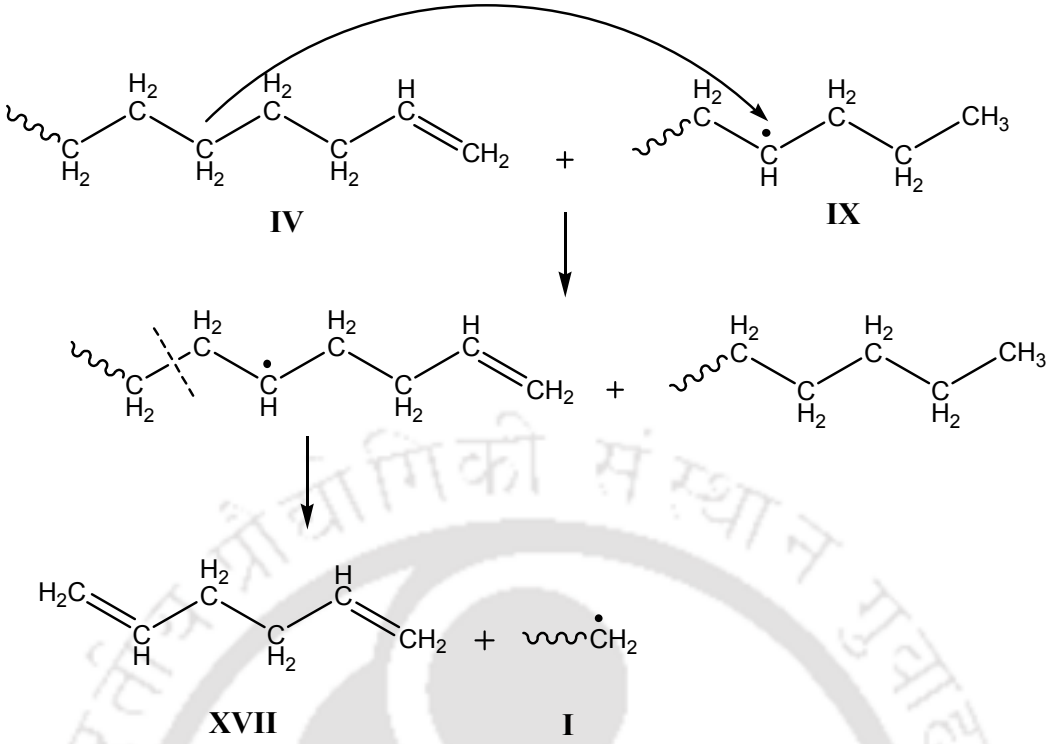

Reaction scheme 5.2.11

Higher molecular weight chain segments are more likely to produce dialkene pyrolysis product [80]. From the peak triplets as evident from Figure 16, we could expect preferential formation of alkene and dialkene species at higher temperature.

From the discussion on the reaction schemes proposed above, it is observed that alkenes are the major products of LDPE decomposition, which is also obvious from the relative areas under the peak (Figure 5.16), which also indicate that amount of alkene is substantially more than alkane, and alkadiene.

Termination reactions involve mainly two radicals present in the system, *viz*. primary, and secondary. Termination can take place via radical recombination or disproportionation reactions, which involves self-reactions of **I** and **II** and their cross-reactions as detailed below [86]. Self-reaction of **I** produces each of a polymer with unsaturated end (**IV**) and a saturated

end (**P′**), whereas self-reaction of **II** produces a polymer and a polymer with a vinyl group (**XVIII**). Cross-reaction of **I** and **II** produces **P′** and **XIV**.

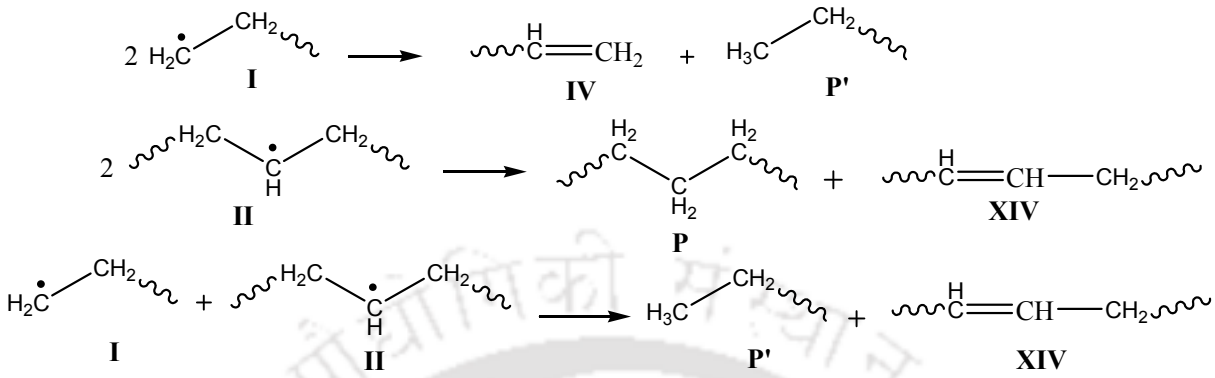

Reaction scheme 5.2.12

5.2.3 Conclusions

In this part of the study, we report species-specific evolution profiles of the volatile pyrolyzates (C5-C44) of LDPE over a broad temperature range of 200-600°C. This study shows that evolved products analysis is an important aspect of thermal decomposition study of polymers. At low temperature (200-300°C), bond fission of weak links dominates the initiation of LDPE decomposition; at temperatures above 350°C, C-C bond fission in general dominates the overall decomposition process. Maximum amount of pyrolyzates were obtained in the 470°C, which is attributed to β-scission reactions. Intra-molecular hydrogen transfer justifies preferential formation of some hydrocarbons. C5-C7 hydrocarbons were the most dominant species detected in our evaluation. Total formation of lighter hydrocarbons (C5-C15) exceeds that of heavier hydrocarbons (C16-C44) by roughly one order of magnitude. Species-specific evolution profiles at various temperatures can be readily correlated with the proposed reaction schemes.

5.3. Temperature Dependent Pyrolytic Product Evolution Profile of PP

5.3.1 Products analysis

A typical DTG curve for rate of degradation $\frac{d\alpha}{dT}$ of PP alongside of total moles of products evolved (in 1 ml of vent gas from the TGA) as a function of degradation temperature is shown in Figure 5.17. The moles evolved are calculated from GC analysis (as discussed in *Appendix 1*). It can be seen that amount of evolved product closely follows the DTG curve. The amount of residue obtained after pyrolysis of PP is about 0.1-2%.

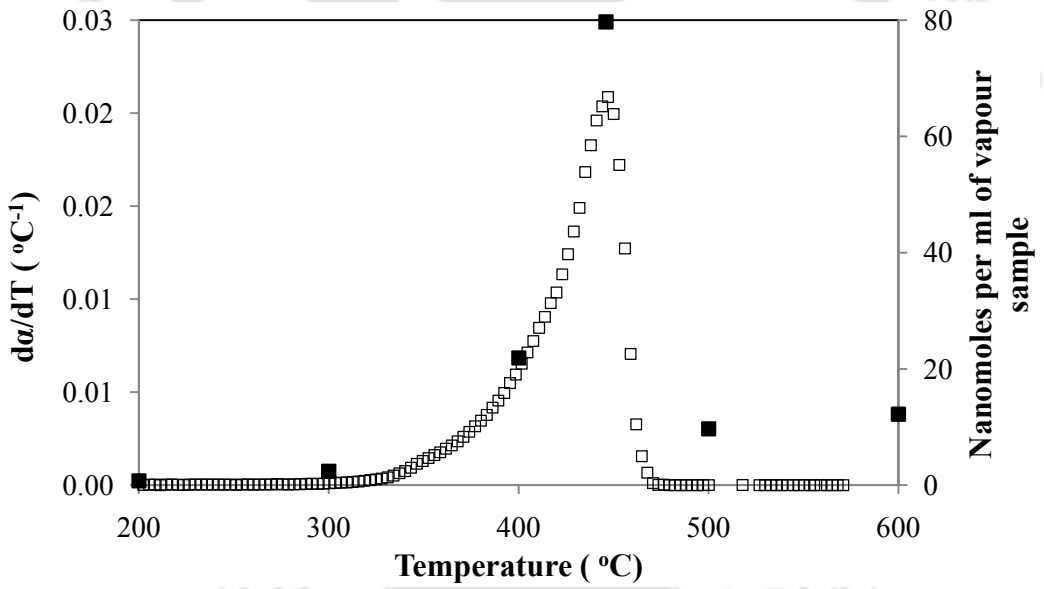

Figure 5.17 DTG curve of PP (on primary axis) and total moles evolved from pyrolysis of PP (on secondary axis); (heating rate: 10°C/ min, Ar flow rate: 40 ml/min)

It has been indicated in literature that, pyrolysis product of PP contains aliphatic hydrocarbons with methyl branches as a major portion due to the structure of the original polymer [134]; the amount of straight aliphatics is usually lower. Figure 5.18 shows partial pyrograms of PP at 200 and 300°C.

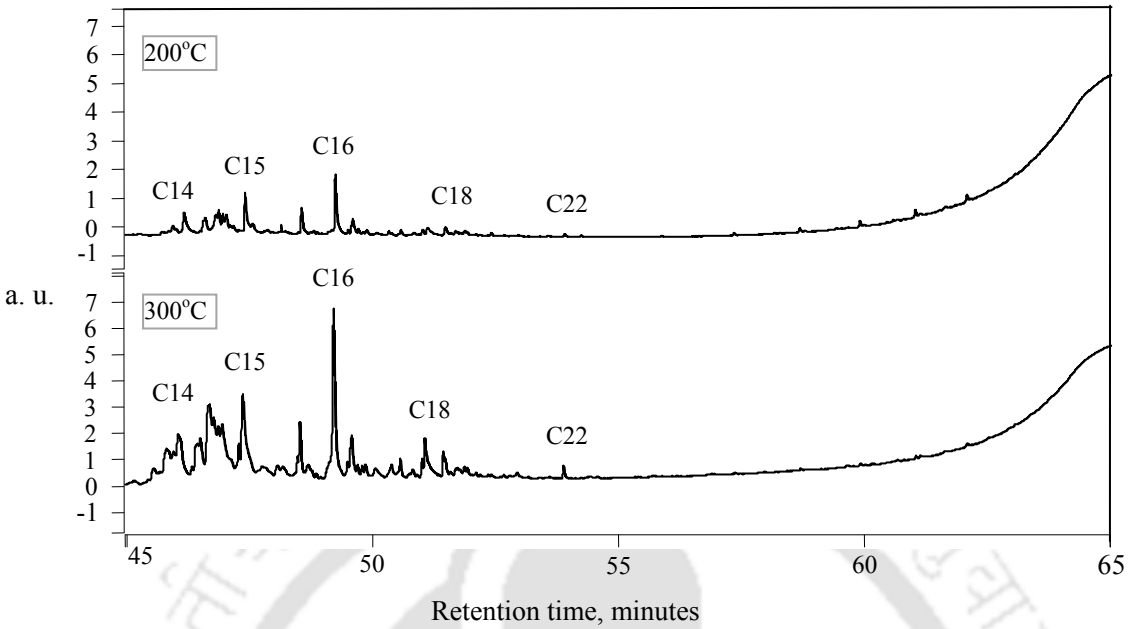

Figure 5.18 A part of the pyrogram of PP at 200 and 300°C showing hydrocarbons above C14

As can be seen in this figure, changes in molecular weight of the product is not very evident as we go from 200 to 300°C, only the amount evolved increases with temperature. Figure 5.19 depicts partial pyrograms of PP at 400 and 500°C.

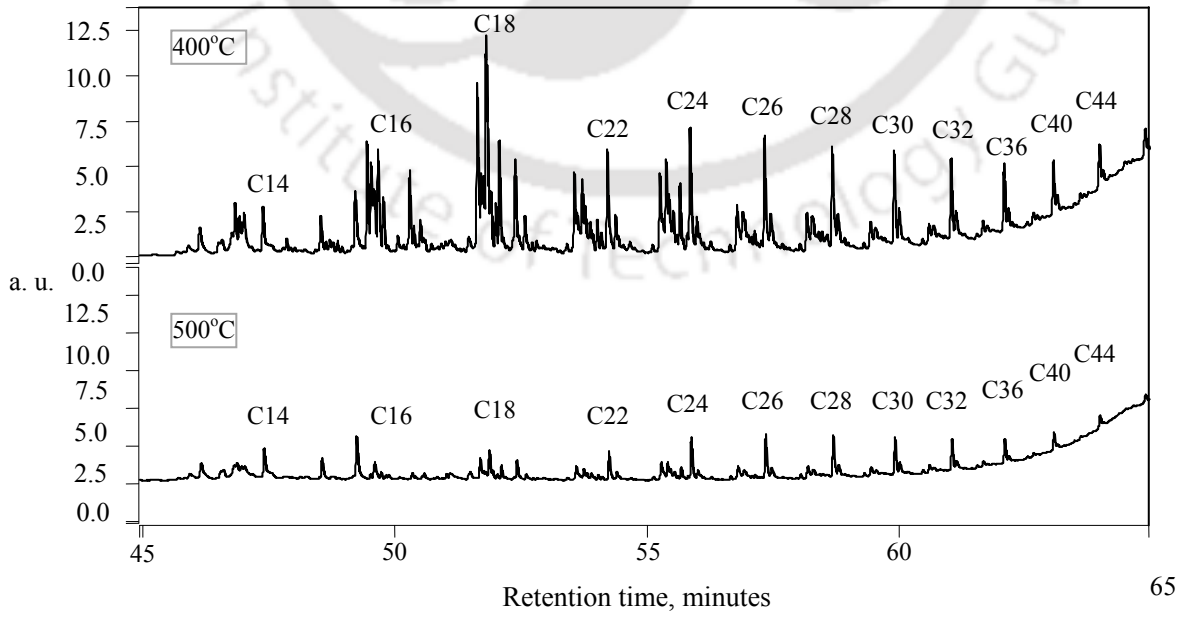

Figure 5.19 A part of the pyrogram of PP at 400 and 500°C showing hydrocarbons above C14

As temperature increases from 300 to 400°C, changes in molecular weight become quite significant. The high molecular weight species beyond C14 evolves to a great extent at 400°C and beyond, though their intensity decreases at 500°C.

Figure 5.20 represents partial pyrogram of PP at T_{max} showing lighter (C5-C15) and heavier hydrocarbons (C16-C44). Clearly, a wide range of hydrocarbons evolve from the pyrolysis. Significant evolution of C5-C6 species is observed at T_{max}. C7 and C8 species are also observed, though in a relatively very small amount.

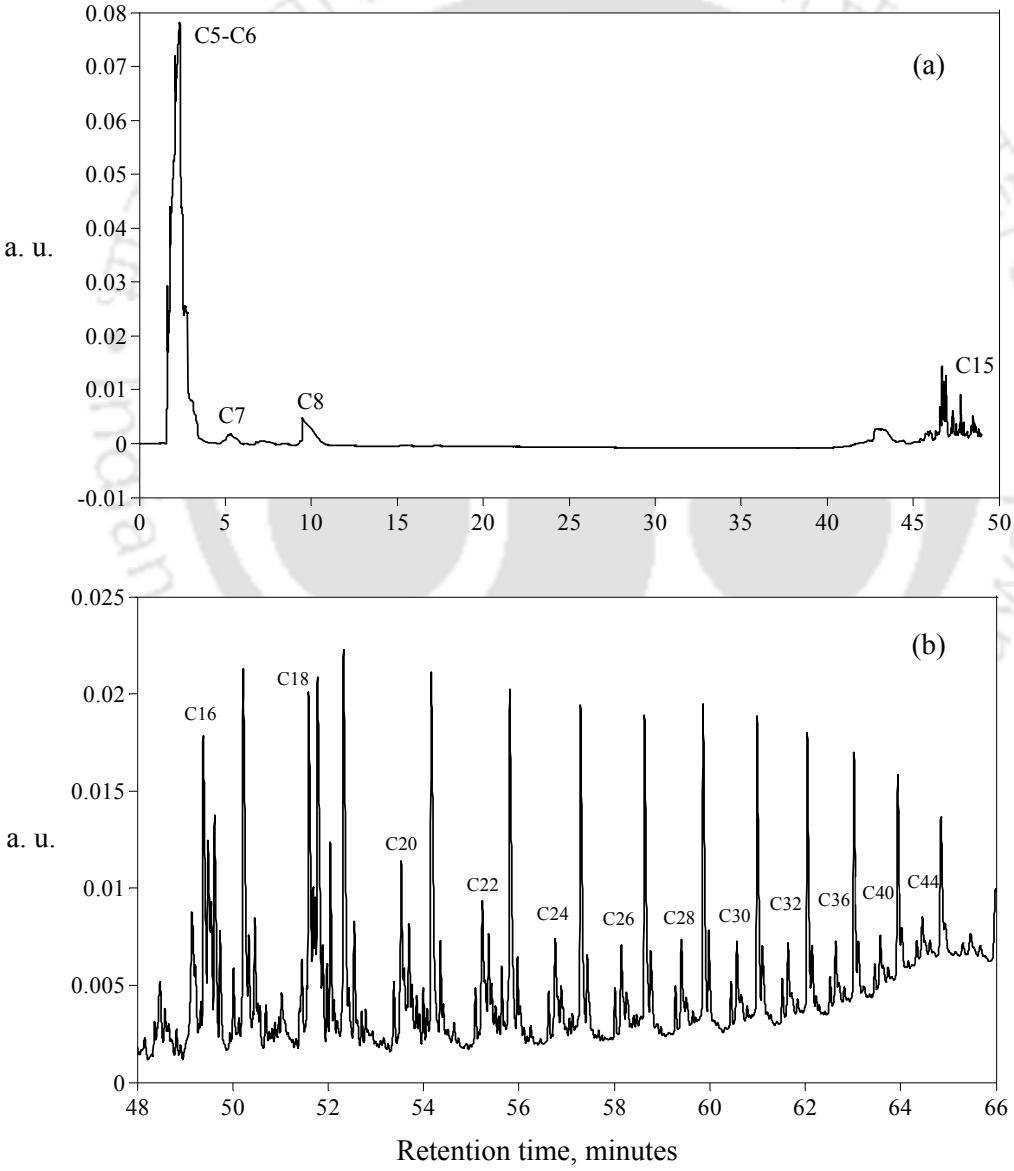

Figure 5.20 A part of the pyrogram of PP at T_{max} (446°C) (a) showing lighter hydrocarbons (C5-C15); (b) showing heavier hydrocarbons (C16-C44)

Figures 5.21 and 5.22 show the moles and mole fractions of various hydrocarbons contained in the pyrolysis product stream as a function of temperature. The change in composition of product with pyrolysis temperature is evident from these plots.

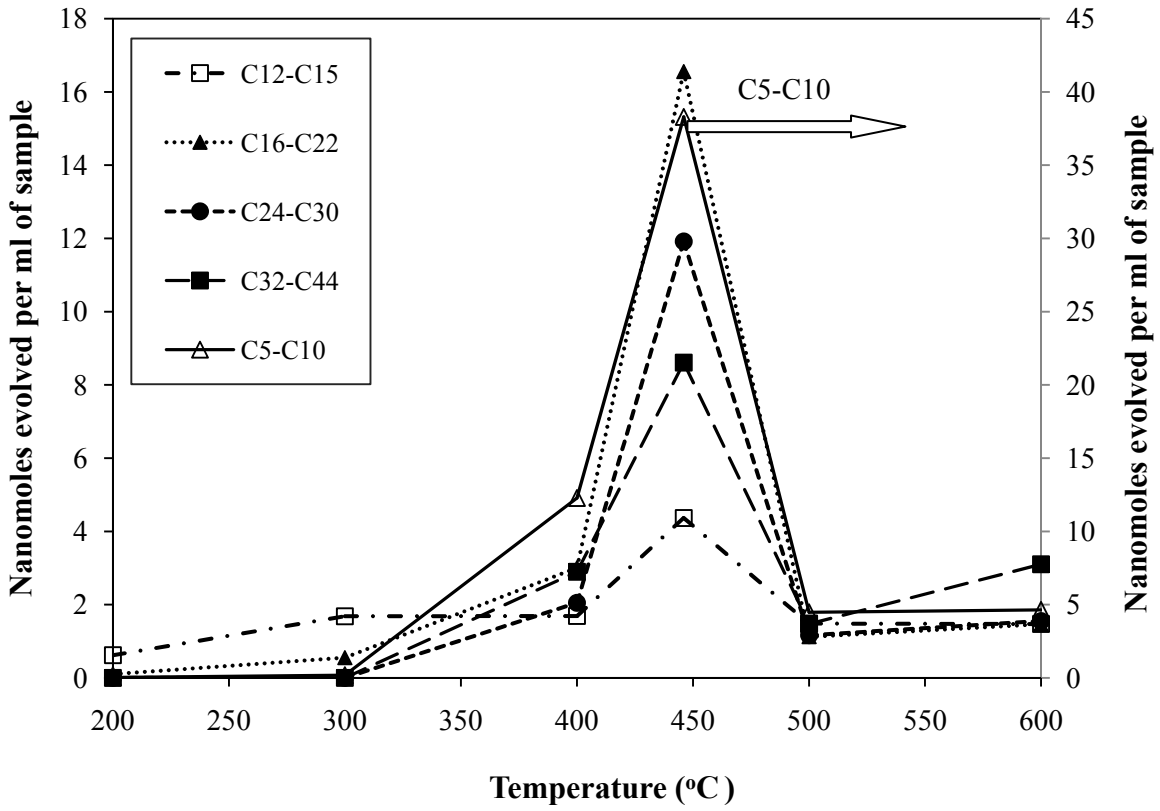

Figure 5.21 Temperature dependency of C5 to C44 hydrocarbon evolution during pyrolysis of PP

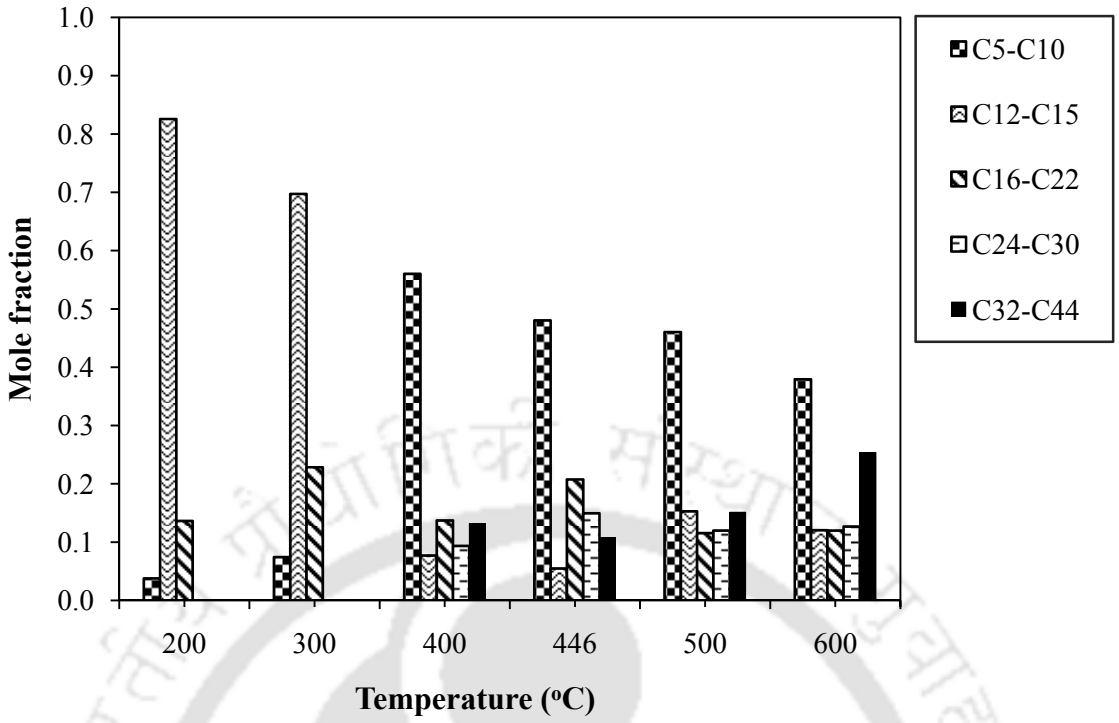

Figure 5.22 Mole fractions of C5-C44 hydrocarbons obtained from pyrolysis of PP at different temperatures

At 200°C, where less energy is available for thermal cracking, some trace quantities of C12-C15 and C16-C22 hydrocarbons are detected (Figure 5.21). This could be due to decomposition of weak bonds in the polymer molecule formed during polymerization process. The phenomenon of early decomposition of polymers is already explained for LDPE under *Section 5.2.2*. Similar scenario may exist in case of PP as well. However, we see a high proportion of C12-C15 in the product composition (Figure 5.22), due to the absence of other fractions (C24 and above). At 300°C, yield of C12-C15 and C16-C22 slightly increases and a trace amount of C5-C10 hydrocarbons is detected (Figure 5.21). Termination reactions play a vital role in characterizing product distribution. At low temperature of pyrolysis (200-300°C), radical recombination does not take place, which could be the reason behind the absence of heavy fragments in the pyrolyzate. From Figure 5.22, it is seen that as temperature increases

from 200°C to 300°C, relative yield of C5-C10 and C16-C22 increases, whereas that of C12-C15 decreases. Again, evolution of C12-C15 is more than C16-C22 within 200-300°C as compared to that at higher temperatures. At 400°C, significant production of C5-C10 is obtained (Figure 5.21) due to increase in available thermal energy for cracking. Evolution of C16-C22 increases and some amounts of heavier hydrocarbons (C24-C30 and C32-C44) are also obtained at 400°C (Figure 5.21). As we go from 300 to 400°C, there is an enormous increase in C5-C10, thereby increasing their proportion as compared to C12-C15 and C16-C22 fractions (Figure 5.22). Evolution of heavy hydrocarbons (C24-C44) probably occurs due to the recombination reactions; at higher temperature, termination by radical recombination leads to the formation of heavy hydrocarbons. Since C5-C10 hydrocarbons are volatile enough to emerge from the molten pool, they escape into the gas phase without undergoing secondary reactions to a large extent. At T_{max} (446°C), which is the maximum decomposition temperature, volatile product obtained attains a maximum as cracking reactions become vigorous. Evolution of C5-C10 increases by more than three times as compared to that at 400°C. Evolution of all other fractions increases roughly by ten times as compared to that at 400°C. At T_{max} relative production of different hydrocarbons remains more or less the same as that at 400°C, except that there are more of middle fractions (C16-C22 and C24-C30) (Figure 5.22). Beyond T_{max}, there is a decrease in the overall production of all the hydrocarbons. Yield of heavier hydrocarbons indicates that termination by radical recombination is significant.

5.3.2 Mechanistic analysis

PP is a macromolecule, which results from the addition polymerization of propylene monomer. The types of product obtained from thermal decomposition of PP depend primarily on its mode of decomposition, which in turn would depend on the structural attribute of the

polymer. The reactivity of the resultant fragments or radicals too, is an important parameter, which needs to be considered in studying the decomposition routes of polymers. This aspect has already been highlighted for LDPE, under *Section 5.2.2.*

Thermal decomposition of PP initially proceeds essentially by random scission mechanism. Here separate schemes are proposed to describe the formation of alkanes, alkenes and dienes, which are assumed to predominate the product distribution. As already mentioned under *Section 5.2.2*, initiation reactions involve C-C bond cleavage. PP undergoes random-scission reaction (*Reaction scheme 5.3.1*) at the tertiary carbon, giving rise to one primary radical (R_p) and one secondary radical (R_s) [80, 87, 137].

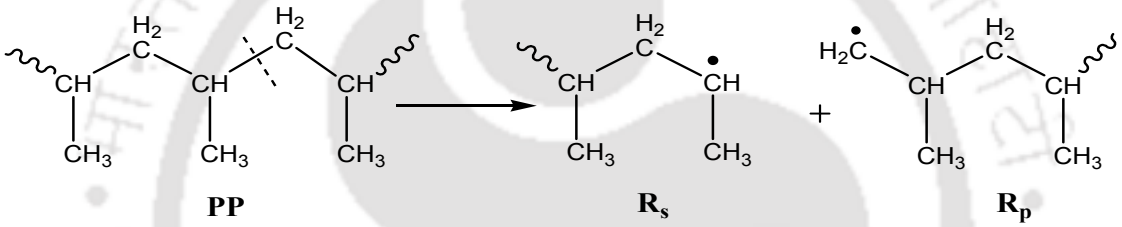

Reaction scheme 5.3.1

C-C bonds in PP are weaker than in LDPE due to the presence of tertiary carbon centres at every second carbon atom in its chain backbone, which makes it less stable than LDPE. Hence, its random scission starts at a lower temperature thereby increasing the evolution of product at 200^{o}C for PP (Figure 5.21) as compared to LDPE [131].

As in the case of LDPE, different radicals formed from random scission of PP are capable of stabilizing themselves either by hydrogen abstraction, *β*-scission, or radical recombination, all of which form a stable molecule. The reaction that would be favored for stabilization depends on temperature; for example radical recombination reactions are favored at high temperatures and accordingly production of higher hydrocarbons increases at high temperatures (Figure 5.21).

At (200-300°C), where sufficient energy is not available for termination of radicals, abstraction is the preferred route for radical stabilization. Thus, R_s (having a low degree of polymerization) undergoes abstraction (*Reaction scheme 5.3.2*) to form an alkene. Reaction 2 justifies some trace quantities of C12 and higher hydrocarbons at these low temperatures. However as temperature increases, the increase in concentration of H radicals somewhat slows down this reaction. Therefore, abstraction is possibly not favored at high temperature.

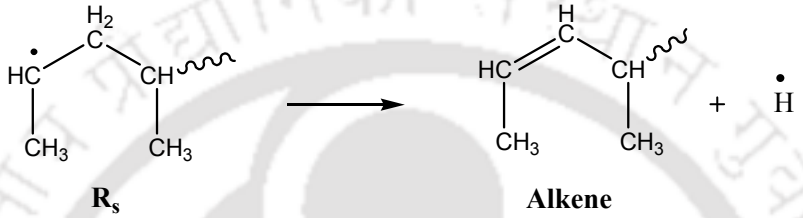

Reaction scheme 5.3.2

At high temperatures (≥300°C), other reactions *viz.* intermolecular and intramolecular H-transfer, *β*-scission, etc. come into the picture. The hydrogen transfer reactions with subsequent *β*-scission play an important role in characterizing the product distribution.

Since, R_p is less stable than either R_s or a tertiary radical (R_t), inter molecular hydrogen transfer occurs and R_p is converted to R_t (*Reaction scheme 5.3.3*).

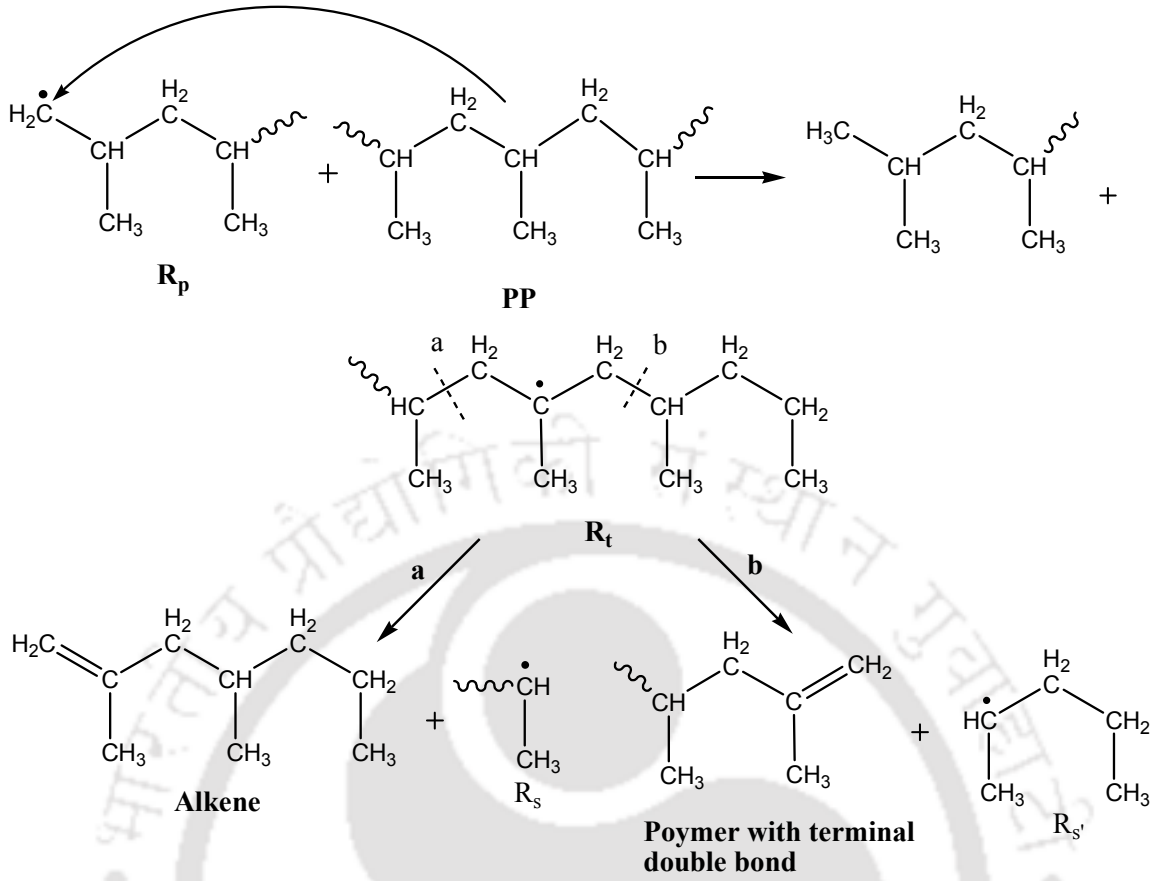

Reaction scheme 5.3.3

The H-atom attached to the tertiary C-atom is more reactive and can be easily detached (as compared to the secondary C-atom) and methyl group being small in size does not hinder migration of hydrogen atom [135]. Thus, the result of this reaction is a methyl terminal group and a more stable R_t. The latter decomposes by *β*-scission as shown in *Reaction scheme 5.3.4* (either mid-chain (route *'***a***'*) or end-chain (route *'***b***'*)) giving rise to either an alkene, and R_s, or polymer with terminal double bond, and a short secondary radical ($R_{s'}$). Thus, at higher temperature intermolecular hydrogen transfer takes place followed by *β*-scission as shown in *Reaction scheme 5.3.3*, which justifies the formation of more amounts of lighter hydrocarbons beyond 300^{o}C.

R_s (produced in *Reaction scheme 5.3.1*), on the other hand undergoes 1,5-intramolecular hydrogen transfer giving rise to a more stable R_t as shown in *Reaction scheme 5.3.4*.

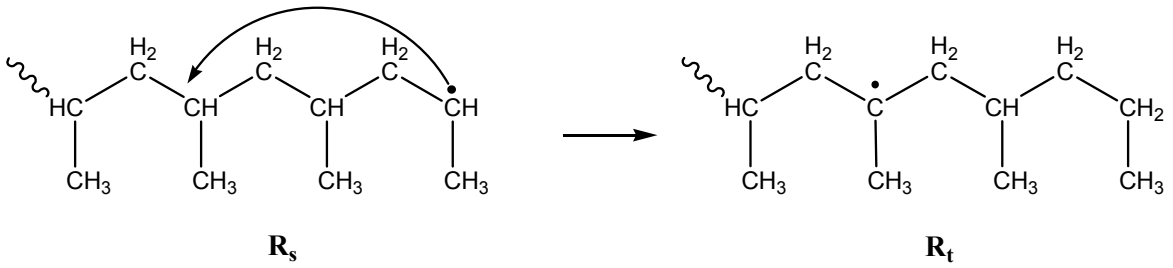

R_s **R_t**

Reaction scheme 5.3.4

This R_t, in turn decomposes by *β*-scission following route **a** or **b** as shown in *Reaction scheme 5.3.3*. Since R_s is regenerated from this reaction (following route *a*), the chain reaction will continue and produce equal number of methyl and vinyl terminal groups in the fragments of gradually decreasing molecular mass.

Intramolecular reactions such as 1,5-hydrogen transfer, as shown in *Reaction scheme 5.3.4* are crucial in the free radical decomposition of PP which justifies preferential formation of some hydrocarbons [74, 96, 136, 137]. Among all the backbiting reactions, 1,3-, 1,4-, 1,5-, and 1,6- end hydrogen transfer reactions are energetically favorable and are responsible for the formation of lighter hydrocarbons [74].

As suggested in the literature [74, 138, 139], 1,5-hydrogen transfer in R_s (*Reaction scheme 5.3.4*) is important in producing products such as dimers, trimers, tetramers, pentamers etc. In our study preferential formation of some products such as C5, C6, C9, C15 and C18 can be attributed to this mechanism. However, more of C5-C10, C12-C15 fractions are found in the product at 400-446^{o}C, indicating more of one step intramolecular hydrogen transfer, rather than higher order steps. Table 5.5 shows typical intramolecular hydrogen shifts taking place during pyrolysis of PP which results in wide distribution of products.

Table 5.5 Different Hydrogen shifts and the corresponding products from PP

Intramolecular hydrogen transfer	Number of transfer steps	Products
1,5-end H transfer	One	C5 or C9=
	Two	C11 or C15=
	Three	C17 or C21=
	Four	C23 or C27=
1,4-end H transfer	One	C3 or C8=
	Two	C8 or C12=
1,3-end H transfer	One	C2 or C6=
	Two	C5 or C9=
1,6-end H transfer	One	C6 or C11=
	Two	C14 or C18=

R_s' produced in the process (shown in *Reaction scheme 5.3.3)* undergoes inter-molecular hydrogen transfer with a macromolecule of PP producing pentane and regenerating R_t as shown in *Reaction scheme 5.3.5*.

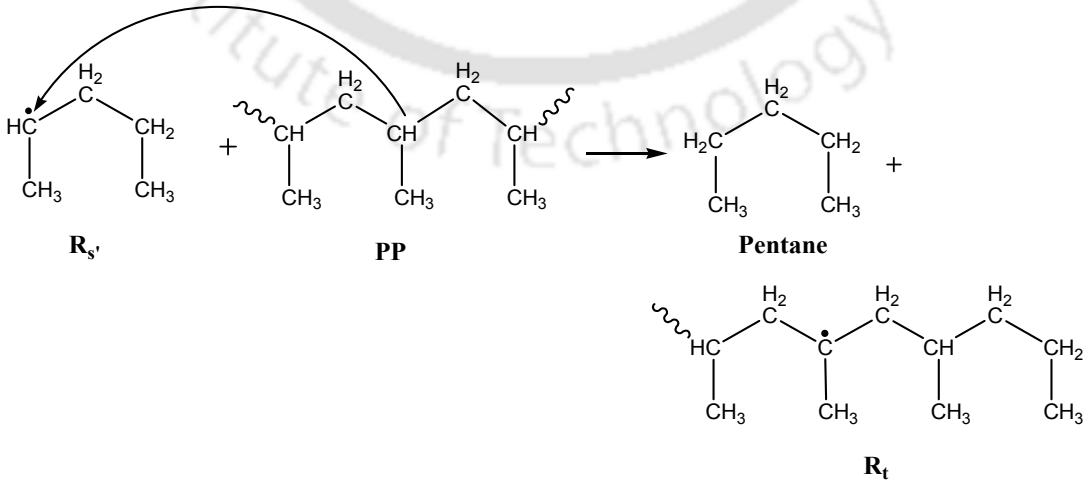

Reaction scheme 5.3.5

Propylene is reportedly one of the major products from pyrolysis of PP [74], which could possibly result following *Reaction scheme 5.3.6*. Similarly, R_p and R_s might undergo depolymerization to produce the propylene monomer.

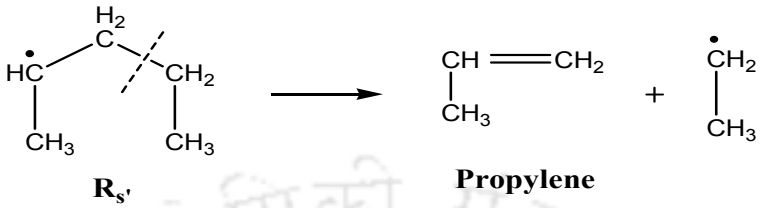

$R_{s'}$ **Propylene**

Reaction scheme 5.3.6

Just as for LDPE, the reaction shown in *Scheme 5.3.6*, being a chain-end scission, is not favorable below 400°C. But, at higher temperatures (>400°C), unzipping becomes feasible due to availability of adequate energy. In our study, the broad peak (Figure 5.20) corresponding to C5-C6 might contain C3 fractions as well.

R_t may also result by the backbiting (1,6-hydrogen transfer) of a primary macroradical [74], as shown in *Reaction scheme 5.3.7*.

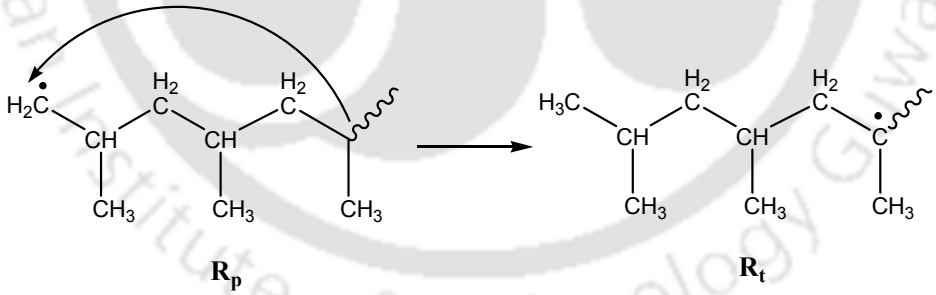

R_p **R_t**

Reaction scheme 5.3.7

R_t, on intramolecular hydrogen transfer produces an alkene (following route *a* in *Reaction scheme 5.3.3*). At higher temperature, diene formation takes place by *Reaction scheme 5.3.8*.

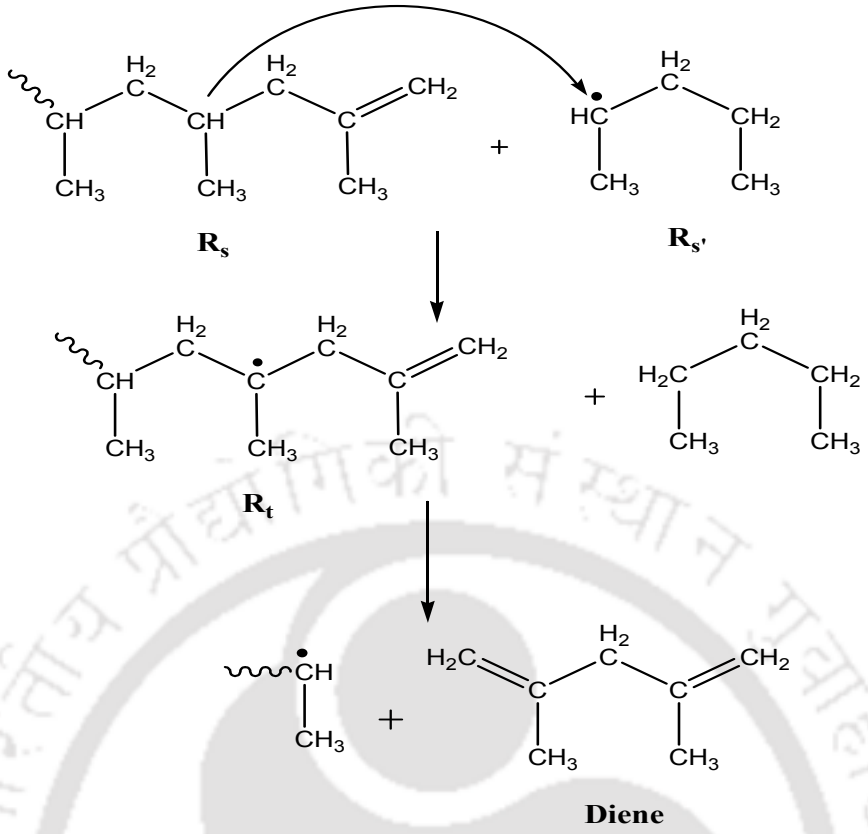

Reaction scheme 5.3.8

Higher molecular weight chain segments are more likely to produce diene [80]. As such, we could expect preferential formation of diene species at higher temperature.

Beyond 446°C, H-transfer reactions and *β*-scission reactions continue to take place, but radical recombination occurs to a greater degree, resulting in more of C24 and higher hydrocarbons.

Termination reactions involve the four families of radicals present in the system, *viz*. R_p, R_s, R_t, and $R_{s'}$. Termination via radical recombination is more likely to take place at high temperature (≥400°C), because of higher concentration of the radicals in the pool. This justifies the increased evolution of heavier hydrocarbons at temperatures above 400°C. Examples of termination via radical recombination reactions (between R_t ans R_s; and two R_s radicals) are shown in the *Reaction schemes 5.3.9* and *5.3.10.*

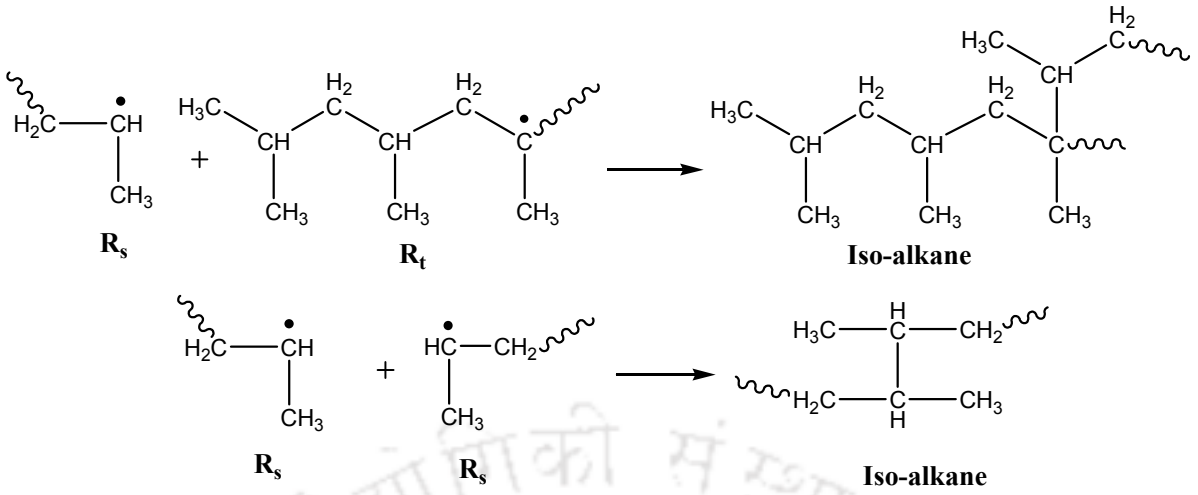

Reaction scheme 5.3.9

Again, termination by disproportionation, which is another possibility, can be represented by the Reaction scheme 5.3.10.

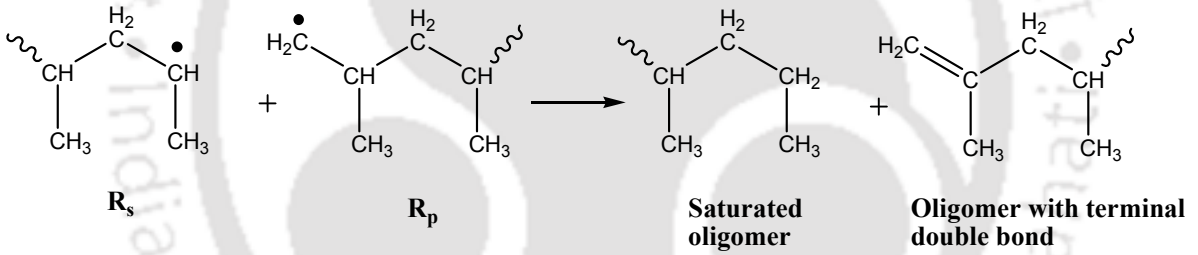

Reaction scheme 5.3.10

5.3.3 Conclusions

In this part of the work, we report product distribution of volatile hydrocarbons (C5-C44) of PP over the temperature range of 200-600^{o}C. PP, being an addition polymer, degrades primarily by random scission of the macromolecule. Its decomposition routes are similar to those described for LDPE, which also follows random scission mechanism. Difference in the mechanistic attributes of these two polymers arises due to the structural difference between them. The presence of tertiary carbon centers at alternate carbon atoms along the backbone of PP renders it more reactive than LDPE. Just was the case for LDPE, at low temperature

(200-300°C), bond fission of weak links dominates the initiation of PP decomposition; at temperatures above 300°C, C-C bond fission in general dominates the overall decomposition process. Intra-molecular hydrogen transfer justifies preferential formation of some hydrocarbons. 1,5-hydrogen transfer readily explains formation of n-pentane and trimer of propylene. As in case of LDPE, maximum amount of hydrocarbons were obtained at T_{max}. C5-C10 hydrocarbons were dominant species detected in the product mixture in our evaluation.

5.4 Temperature Dependent Pyrolytic Product Evolution Profile for PET

5.4.1 Products analysis

A typical TG curve for fractional conversion, α and DTG curve for rate of decomposition $\frac{d\alpha}{dT}$ of pure PET are shown in Figure 5.23. The maximum decomposition temperature for pure PET is about 435°C. It is notable here that PET used in this analysis is a virgin material, and is thus different from that used in *Section* 5.1. The amount of residue obtained after pyrolysis of PET is 10-12%.

Pyrolysis product of PET contains a wide array of hydrocarbons, including mostly aromatic hydrocarbons with the *p*-phenylene group (-C_6H_4-) as an inherent part, indicative of the structure of the original polymer. Figure 5.24 (a)-(c) represent pyrograms of the pyrolysis products of PET evolved at 300°C, T_{max}, and 600°C respectively. In Figure 5.24 (a), which corresponds to 300°C, only small peaks are observed, due to insufficient energy necessary for cracking. At 300°C, C5-C7 fraction produced is insignificant. Other hydrocarbons which are detected in traces are C14, C15, C16, C18, C20, C22, C24, C26, C28. C14 and higher hydrocarbons correspond to the linear and cyclic dimers (C20) and cyclic trimers (C30).

Figure 5.24 (b) depicts the pyrogram at T_{max}, marked by sharp and distinct peaks. Pyrograms of PET at other temperatures are shown in *Appendix 3*.

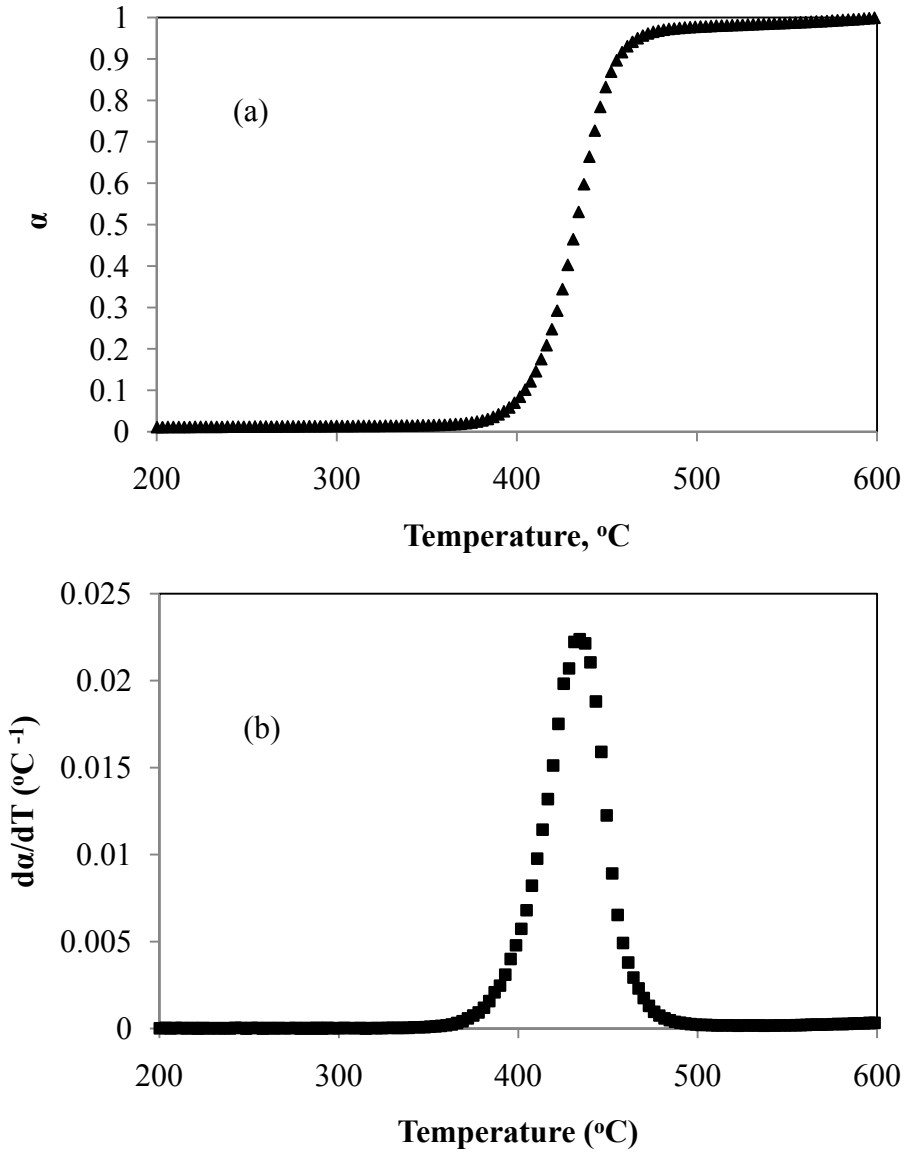

Figure 5.23 (a) DTG curve of PET; (b) TG curve of PET (heating rate: 10°C/ min, Ar flow rate: 40 ml/min)

The oligomers which were formed at lower temperatures (≤300°C) decompose further resulting in the formation of low-boiling fractions. Given the structure of PET, benzene (C6), toluene (C7), terephthalic acid (C8), monoethenyl terephthalate (C10), diethenyl terephthalate

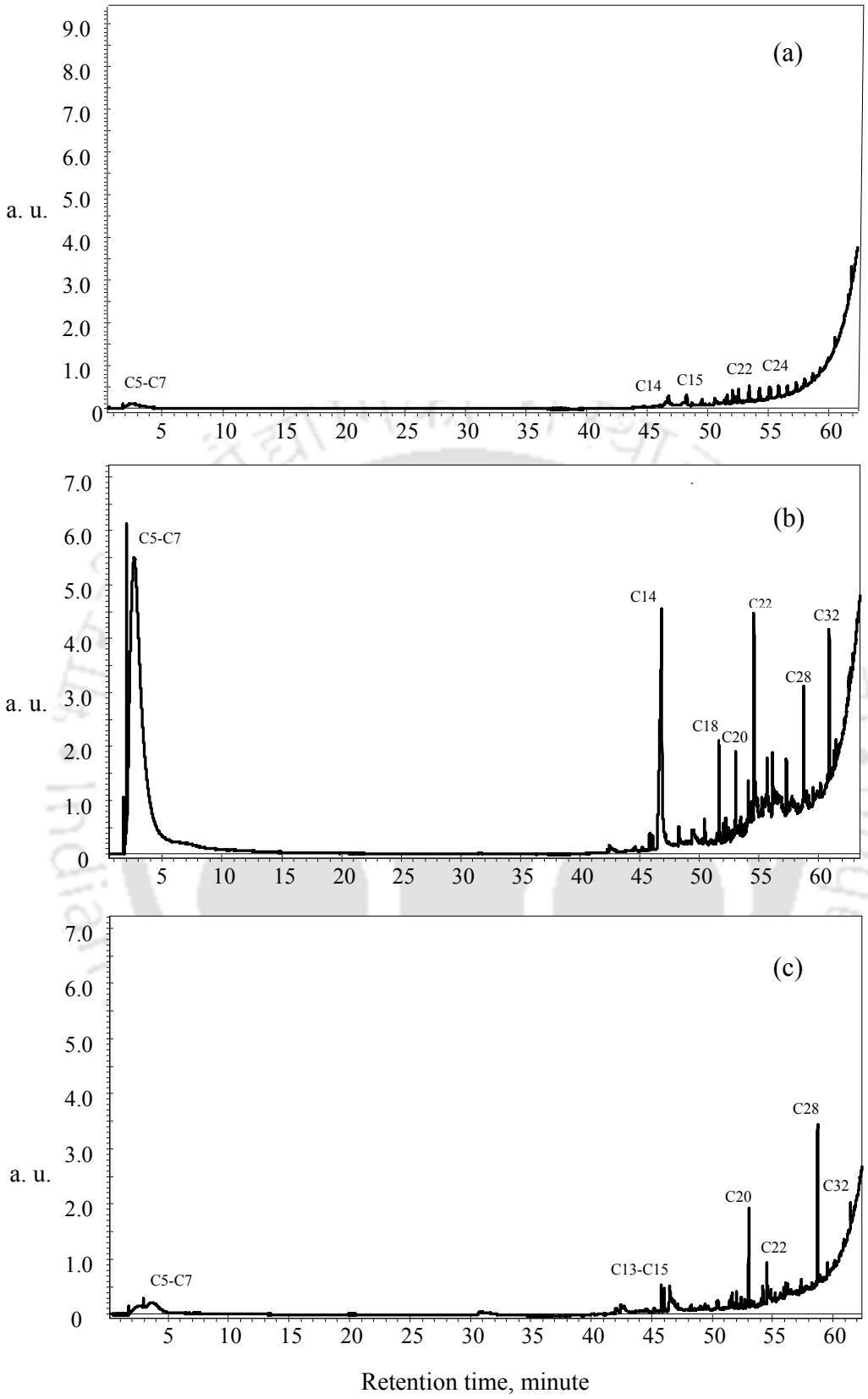

Figure 5.24 Pyrogram of PET obtained at (a) 300°C, (b) 435°C (T_{max}) and (c) 600°C

(C12) would be the major products at this temperature, while the oligomers with carboxyl and olefin ends are regenerated in these processes, which keep the degradation process alive. Here, the first broad peak represents C5-C8 en masse (Figure 5.24 (a)). Clearly, a wide range of hydrocarbons evolve from the pyrolysis. The other hydrocarbons detected in significant amounts are C12, C13, C15, C16, C18, C20, C22, C24, C28, C30, C32, C36, C40, and C44, which are mostly aromatic. Since considerable amount of benzene evolves, formation of PAHs cannot be ruled out at this temperature. Since the retention times for C12-C44 hydrocarbons are similar to PAHs in C10-C22 range (as discussed in *Appendix 1*), it is likely that pyrograms shown in Figure 5.24 also include PAHs like naphthalene (C10), acenaphthylene (C12), anthracene (C14), pyrene (C16) etc. Fig 5.24 (c) represents the chromatogram of PET at 600^{o}C. As continuous purging is done in the TGA apparatus, residence time of the products is minimal. At 600^{o}C, macromolecular chain considerably reduces in length as conversion is nearly complete at this temperature (Figure 5.23). Here C5-C8 hydrocarbons continue to evolve, but their amount decreases compared to that at T_{max}. C10 is observed in very less amount. The other aromatic/aliphatic hydrocarbons evolved are C12, C14, C22, and C24; C15, C16, C18, C26, C36, C40, and C44 are found in traces, while evolution of C20 and C28 becomes more. The products might also encompass PAHs having C12, C13, C16, C20 and C22 species.

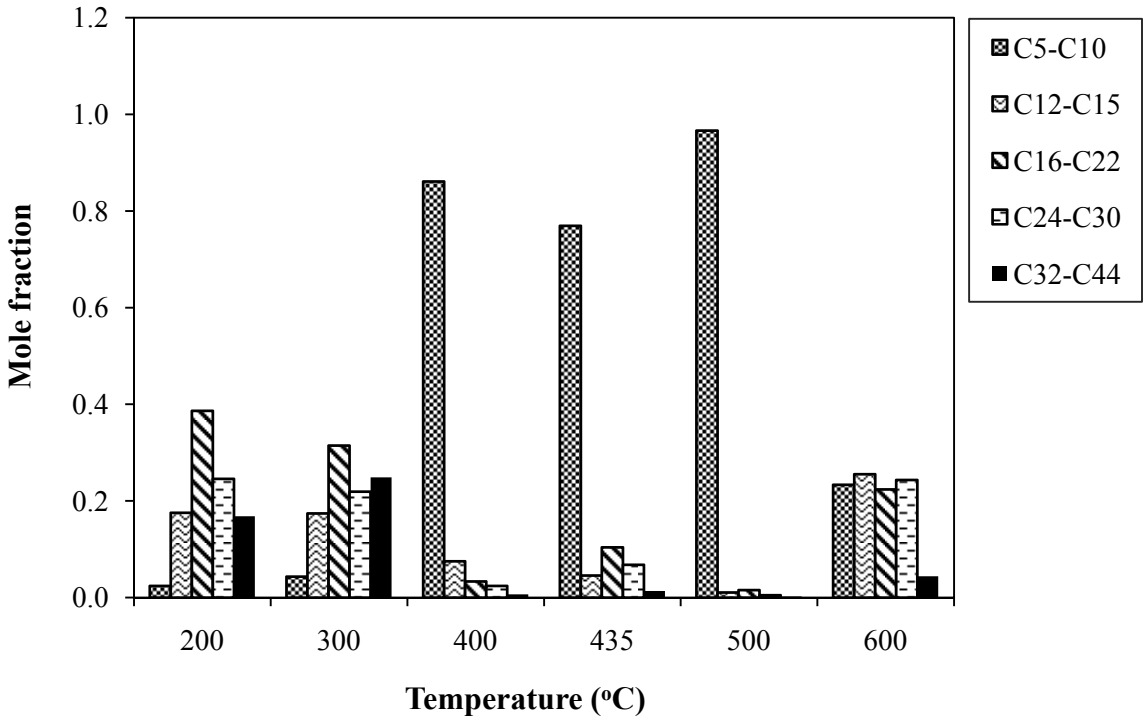

Figure 5.25 Mole fractions of different hydrocarbon fractions (C5-C44) obtained from pyrolysis of PET at different temperatures

Figure 5.25 shows the mole fractions of C5-C44 hydrocarbons contained in the pyrolysis product stream as a function of temperature. The change in composition of the products with pyrolysis temperature is evident from this plot. This quantification is done with respect to the ASTM D3710 and ASTM D5442 standards; hence it does not portray the exact amounts of PAHs in the product stream (as discussed in *Appendix 1).* The information obtained by comparing retention time of various PAHs, is however used to have a qualitative idea about their evolution at various temperatures.

At 200°C, C16-C22 and C24-C32 fractions are relatively more as compared to the lighter components. The negligible formation of C5-C10 fractions can be attributed to the extra stability of the polymer due to the resonance stabilized structures in the chain backbone, which needs higher energy to overcome the attractive forces. The detectable amounts of higher fractions are due to the cyclic oligomers (*Reaction scheme 5.4.1*) which were formed

during polymerization process and remain as weak links in the polymer molecule. Usually polymers prepared by condensation polymerization contain small amounts of small cyclic molecules along with the much higher molecular weight of linear chains. The equilibrium content of cyclic oligomers in PET is around 2% [140].

As in case of LDPE and PP, we have explained the contribution of weak links contribute to initiation of the decomposition process at otherwise stable temperatures. At 300^{o}C, C32-C44 increases and a slight increase of C5-C10 hydrocarbons is also observed, whereas C16-C22and C24-C30 diminishes in amount. As temperature proceeds, intensity of cracking reactions increase resulting in increased amount of lighter hydrocarbons. Thus, as we go from 300 to 400^{o}C, there is considerable increase in C5-C10 production, thereby increasing their proportion compared to other fractions. The relative production of different hydrocarbons decreases in the order C12-C15>C24-C30>C32-C44. At 435^{o}C, which is the maximum decomposition temperature, yield of C5-C10 hydrocarbons is still the maximum. The relative production of different hydrocarbons remains more or less the same, except that there are more of C16-C22 and C24-C30 fractions. C5-C10 continues to be the highest hydrocarbon fraction at 500^{o}C, and formation of other fractions is insignificant as compared to that of C5-C10. At 600^{o}C, relative production of the first four fractions becomes more or less the equal, while the share of the C32-C44 fraction is considerably less.

5.4.2 Mechanistic analysis

In our previous studies, we have presented mechanistic views of thermal decomposition of LDPE and PP, both of which are addition polymers which degrade by free radical mechanism. There is a great difference between the modes of decomposition of addition polymers from those of condensation polymers. Addition polymers contain aliphatic hydrogen atoms along the chain backbone, which are easily transferred following homolytic

bond cleavage in the temperature range of 200-500°C. The majority of addition polymers undergo thermal degradation through the formation of macro-radicals, which are very reactive species undergoing decomposition by bond cleavage. PET is a condensation polymer of terephthalic acid (TPA) and ethylene glycol (EG). For commercial practices, terephthalic acid is often replaced by dimethyl terephthalate (DMT), and ethylene glycol by diethylene glycol (DEG). Condensation polymers can be regarded as a sequence of monomer units containing functional groups immobilized into the polymer structure. Their decomposition pathways are often dominated by the polarity and reactivity of the functional groups within their structure, and their thermal degradation reactions are ionic and selective, rather than radical and unselective. These ionic pathways typically occur at temperatures (150-300°C), below those of typical free-radical degradation reactions. There exist considerable controversies among the researchers regarding the decomposition route of PET. Literature reports that thermal decomposition of PET does not involve radical (homolytic) pathway [98, 140, 141]. However, if the polymer is subjected to higher temperatures, radical reactions are likely to prevail. The proposed reaction pathway separately takes into account formation of cyclic oligomers, volatile hydrocarbons and polycyclic aromatic hydrocarbons (PAHs) and is considered to represent its product distribution.

The structural repeat unit of PET can be represented by the following formula.

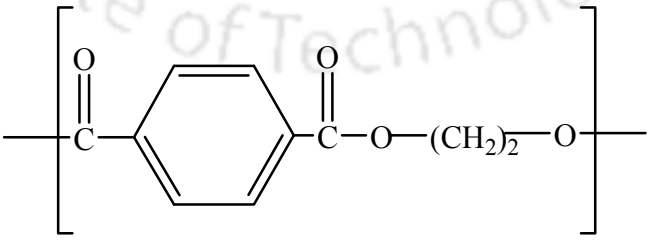

In pure PET, three general structures are present; (i) 'in chain' structures as depicted above by the structural formula, (ii) 'hydroxyl ends', and (iii) carboxyl ends [142]. The latter two

result due to nature of the polymerization reaction. The predominant structure will be the 'in chain' one, and the other two will be in a much lesser extent.

As it has already been explained that cyclic oligomers (dimers or trimers, as a weak link in the PET chain) might come out at low temperatures (200-300^{o}C). Moreover, intramolecular ester exchange reaction might also lead to the formation of cyclic as well as linear oligomers. This justifies the evolution of product fractions observed at low temperatures. As shown in *Reaction scheme 5.4.1a*, a macromolecular chain of PET might undergo intramolecular ester exchange reaction, giving rise to a cyclic trimer (C30). This involves attack of hydroxyl ends on the inner ester groups of the PET chain [98]. In a similar way, formation of a cyclic dimer (C20) and tetramer (C40) are shown in *Reaction scheme 5.4.1b* and *5.4.1c* respectively.

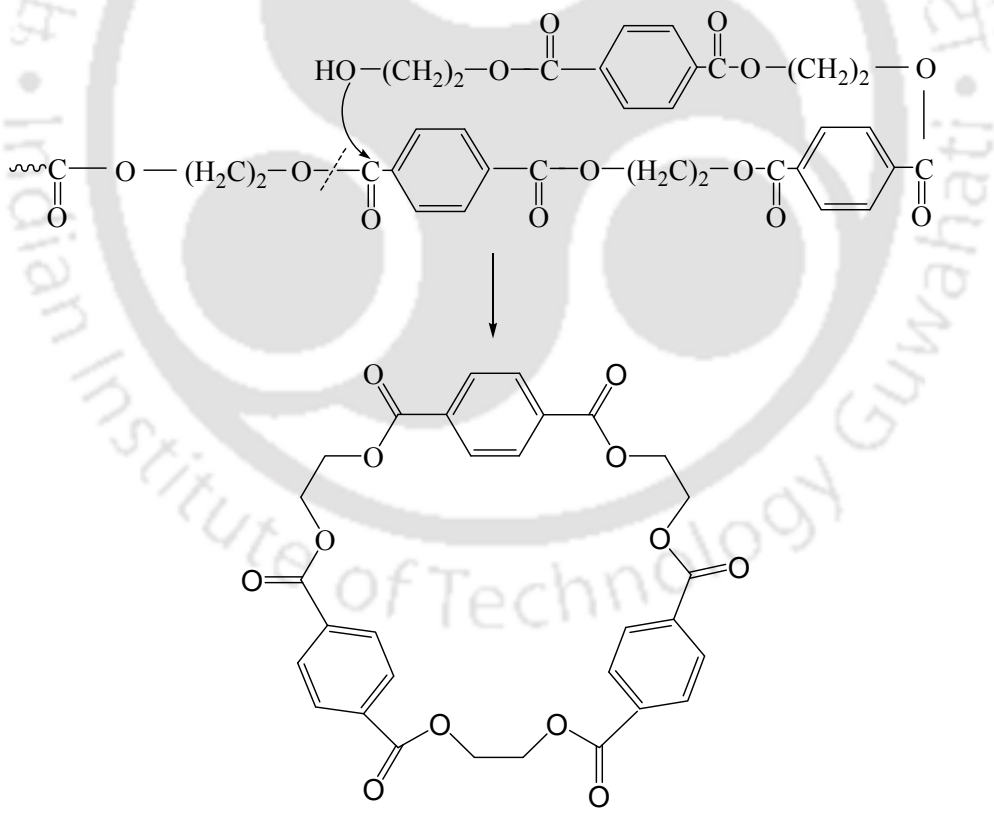

Cyclic Trimer

Reaction scheme 5.4.1a

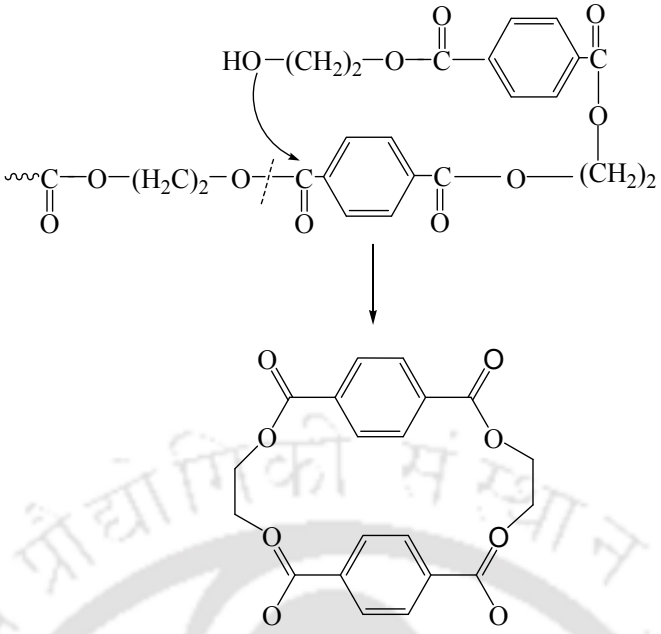

Cyclic Dimer

Reaction scheme 5.4.1b

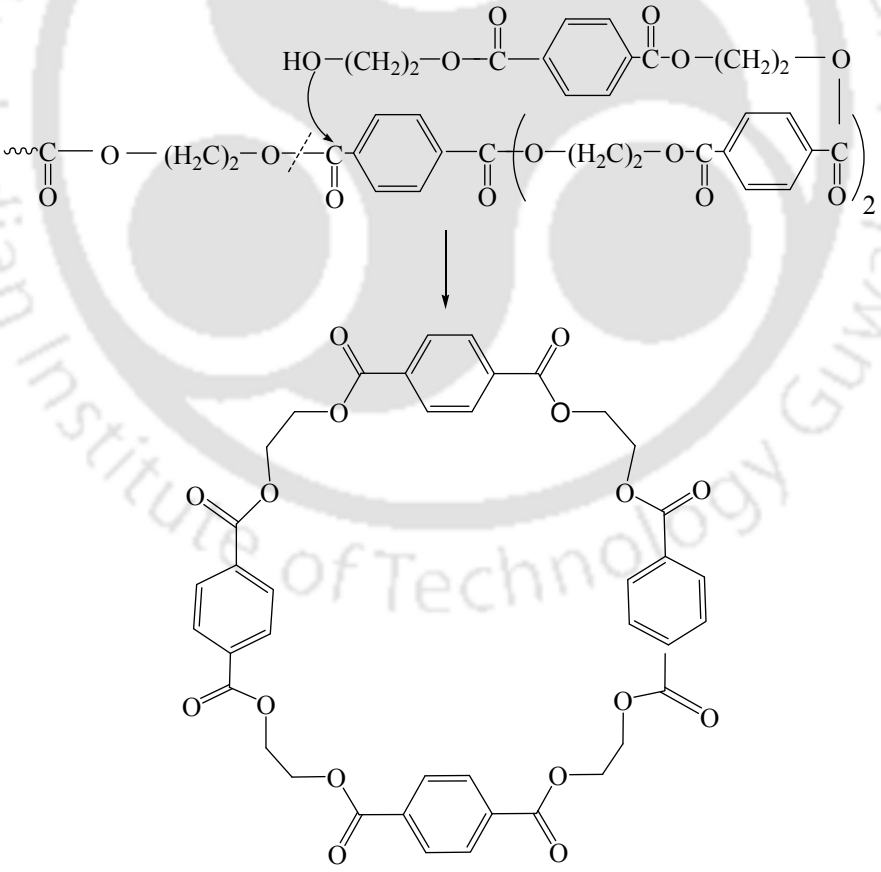

Cyclic Tetramer

Reaction scheme 5.4.1c

From here onwards, we would denote the *p*-phenylene group (-C_6H_4-) by 'Ph', and write the reaction pathways accordingly. Thus, the repeat unit of PET can be rewritten as:

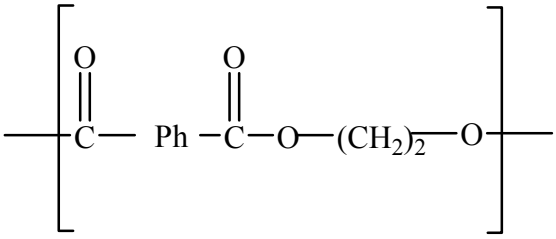

Initial decomposition of PET occurs via a six-membered ring intermediate in which hydrogen from a *β*-carbon (to ester group) is transferred to the ester carbonyl, followed by scission at the ester links, resulting in carboxylic acid end group (**I**) and vinyl end group (**II**) as depicted in the *Reaction scheme 5.4.2* [99-101].

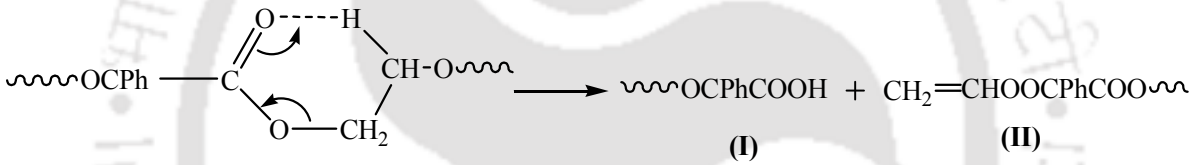

Reaction scheme 5.4.2

The carboxyl end unit (**I**) undergoes decomposition by *β*-Hydrogen transfer by two routes as shown in *Reaction scheme 5.4.3*. The route '**a**' leads to the formation of monovinyl terephthalate (**MVT**). '**I**' is regenerated in the process. The route '**b**' leads to the formation of terephthalic acid (**TPA**) (C8), and species **II**.

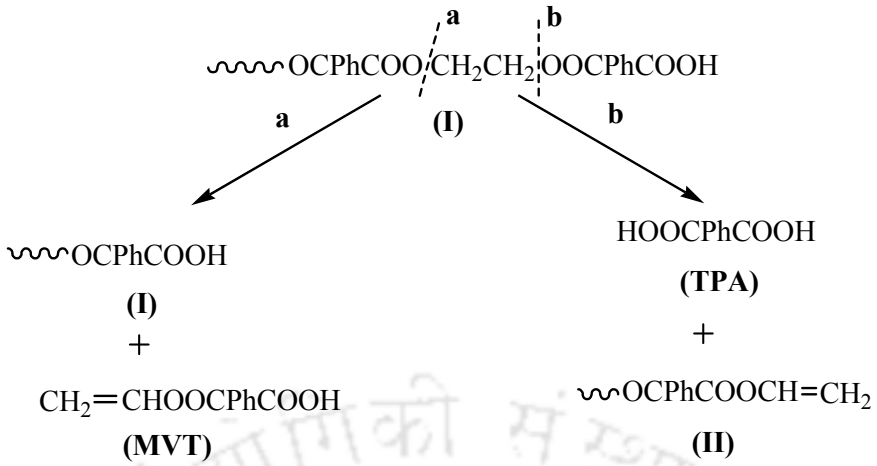

Reaction scheme 5.4.3

Similarly, the olefin end unit (**II**), thus produced in *Reaction scheme 5.4.3*, might undergo decomposition via two routes, '**a**' and '**b**' (as shown in *Reaction scheme 5.4.4*). The route '**a**' leads to the formation of monovinyl terephthalate (**MVT**) (C10), and the species '**II**', whereas route '**b**' leads to the formation of divinyl terephthalate (**DVT**) (C12), and the species '**I**'.

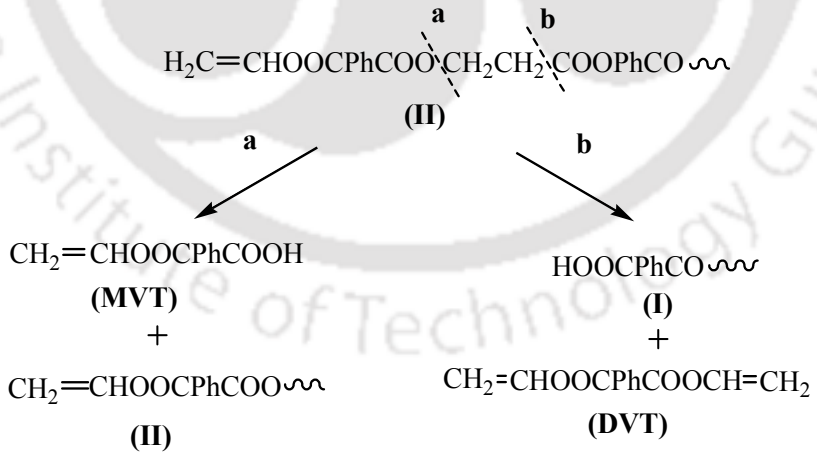

Reaction scheme 5.4.4

With increase in temperature, evolution of C5-C10 increases. As already stated, this could be due to the formation of benzene, toluene, benzoic acid, styrene, vinyl benzoate, ethyl benzene etc. The following reactions (*Reaction scheme 5.4.5-5.4.12*, discussed subsequently) explain

the formation of the aforesaid hydrocarbons. Literature reports significant production of CO_2 from pyrolysis of PET at higher temperature (beyond 300°C) [108]. This can take place from a carboxyl end group via *Reaction scheme 5.4.5*.

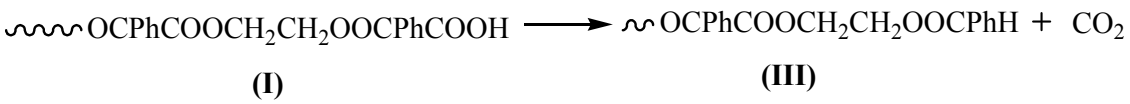

Reaction scheme 5.4.5

This path also produces a phenyl end group, which subsequently undergoes *β*-Hydrogen transfer, following a six-member rearrangement of the ester linkage, to generate vinyl benzoate and benzoic acid, following route '**a**' and '**b**' as shown in *Reaction scheme 5.4.6*. In this process, species **I** and **II** get regenerated with reduced chain length. Thus, the decomposition process of PET continues till it leaves out a carbonaceous residue.

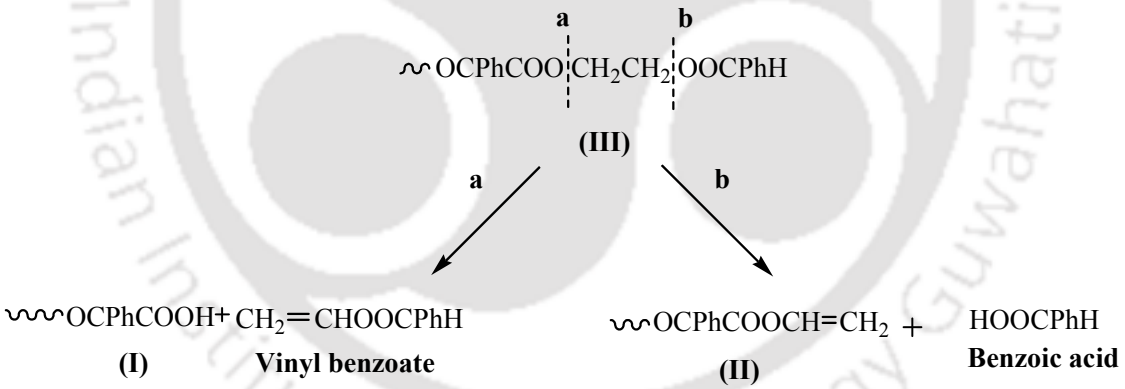

Reaction scheme 5.4.6

Vinyl benzoate produced via route '**a',** also leads to the formation of benzoic acid as shown in *Reaction scheme 5.4.7*, which is reportedly another major product of PET decomposition [99]. Benzoic acid can undergo decarboxylation to yield benzene.

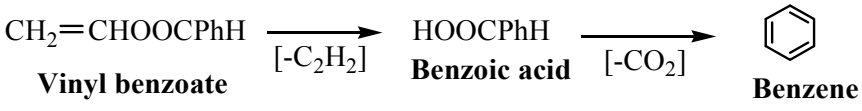

Reaction scheme 5.4.7

Again, decarboxylation of vinyl benzoate leads to the formation of styrene (*Reaction scheme 5.4.8*).

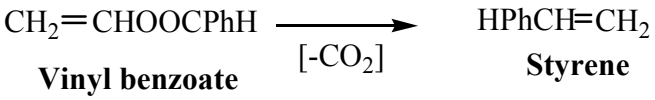

Reaction scheme 5.4.8

The olefin ends group undergoes scission at the ester link and gives rise to vinyl alcohol, which is unstable and possibly rearrange to give acetaldehyde (*Reaction scheme 5.4.9*). Our analysis, however cannot detect C2 fractions. Nonetheless, the broad peak corresponding to C5-C8 might also include these C2 fractions.

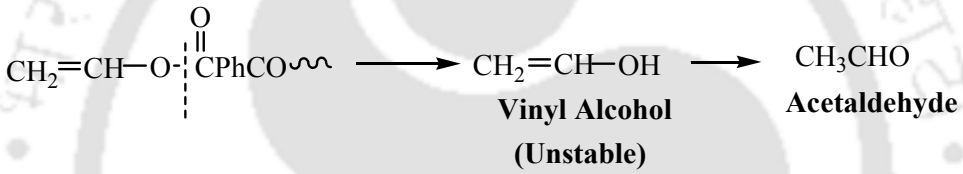

Reaction scheme 5.4.9

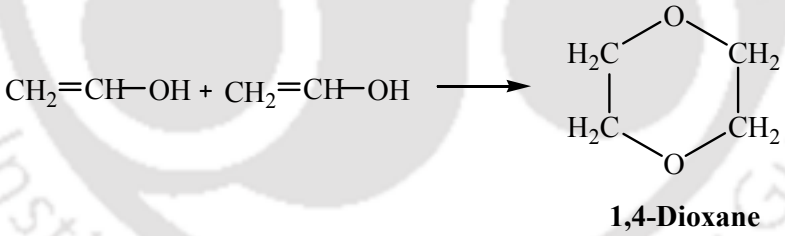

Reaction scheme 5.4.10

In the discussions so far, we have not accounted for the homolytic (free radical) scission of the PET chain. However, at high temperatures (≥400^{o}C), homolytic scission might take place [143-145]. The weakest link in the PET structure is possibly the sequence carbonyl-oxygen-methylene ($COOCH_2CH_2$), which might homolytically cleave in the following two ways (*Reaction scheme 5.4.11 and 5.4.12*):

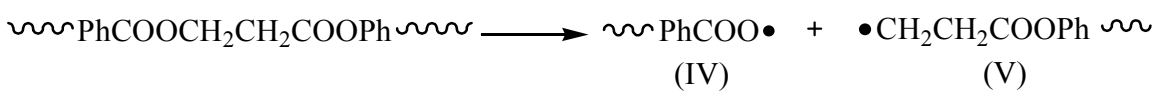

Reaction scheme 5.4.11

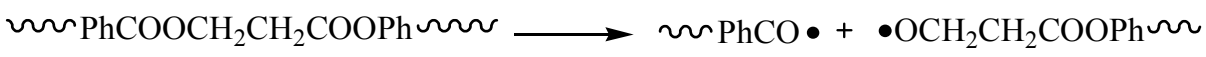

Reaction scheme 5.4.12

After the formation of these free radicals, the immediate next step will be hydrogen-abstraction, intra and intermolecular hydrogen transfer followed by *β*-scission, or recombination of the radicals, so as to generate stable molecules which can escape into the vapour phase. As an example, the free radical **IV** might abstract a hydrogen atom to form an acid end group, thus regenerating **I**, while the radical **V** might undergo intramolecular hydrogen transfer forming a vinyl end group, thus regenerating **II**.

A carbonaceous residue is obtained at the end of each degradation experiment, which constitutes approximately 10-12% of the total weight of the starting polymer. These could be due to the formation of PAHs, which are compounds with fused aromatic rings. Formation of PAHs is possible only at higher temperatures (above 400^{o}C), as discussed in the following. Formation of benzene is crucial for the inception and growth of PAHs. Literature suggests that once benzene is available, there are three possible routes by which larger PAHs may grow. The first route as suggested by Frenklach *et al.* [102], involves sequential hydrogen abstraction and C_2H_2 (Acetylene) addition (referred to as Hydrogen Abstraction C_2H_2 Addition or HACA mechanism). The second route as suggested by Mukherjee *et al.* [103] involves direct polymerization of PAHs through the initial formation of PAH dimers which further proceeds through ring-ring condensation of higher PAHs. This route leads to the formation of high molecular weight PAHs. The third route as proposed by Krestinin *et al.* [146], involves the polymerization of polyynes (a group of organic compounds with

alternating single and triple bonds) on a surface radical site and its transformation into aromatic structures leading to the breeding of radical sites and rapid growth. Polyynes are found in interstellar molecular clouds where hydrogen is scarce. In our study, however, we have considered only the first two routes to explain the formation of PAHs studied in this evaluation, as formation of polyynes is not likely under the present experimental conditions.

At low temperature (200-300^{o}C), PAHs are not formed, as at such low temperatures benzene does not evolve. After the formation of benzene (following *Reaction scheme 5.4.6 - 5.4.7* mentioned earlier), a hydrogen radical from benzene is stripped off releasing highly reactive phenyl radical [147]. This serves as the initiation step for all the subsequent reactions to follow, leading to the formation of PAH by HACA route. Following reactions (*Reaction scheme 5.4.13 – 5.4.15*) have been proposed to explain the formation of some specific PAHs like acenaphthylene ($C_{12}H_8$), benzo(a)pyrene ($C_{20}H_{12}$), and pyrene following HACA mechanism.

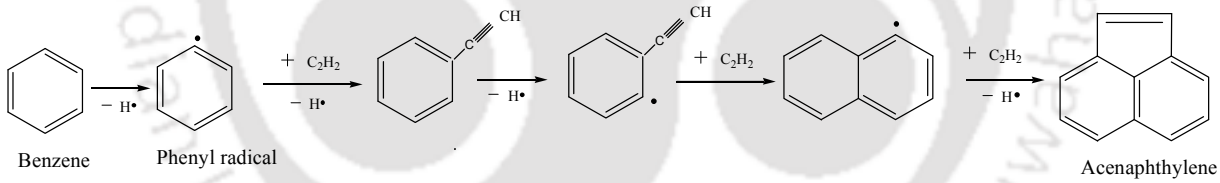

Reaction scheme 5.4.13

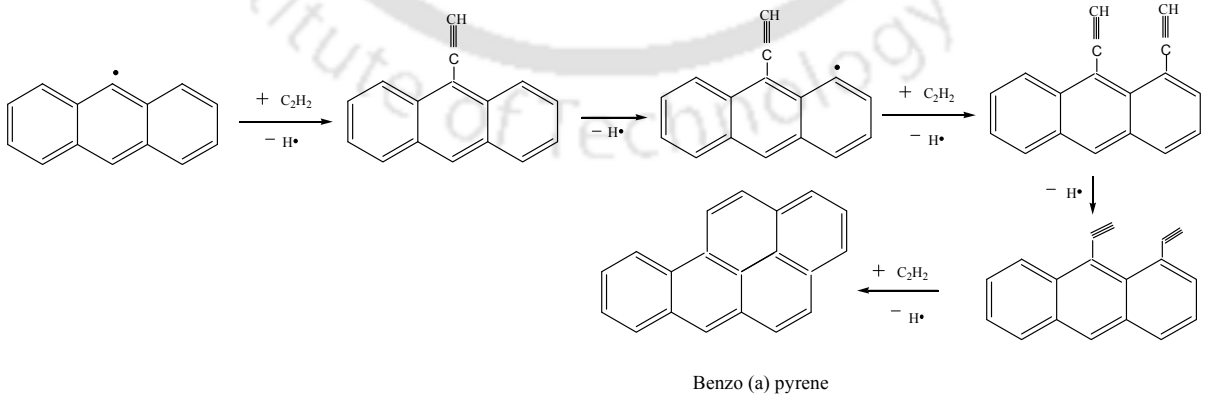

Reaction scheme 5.4.14

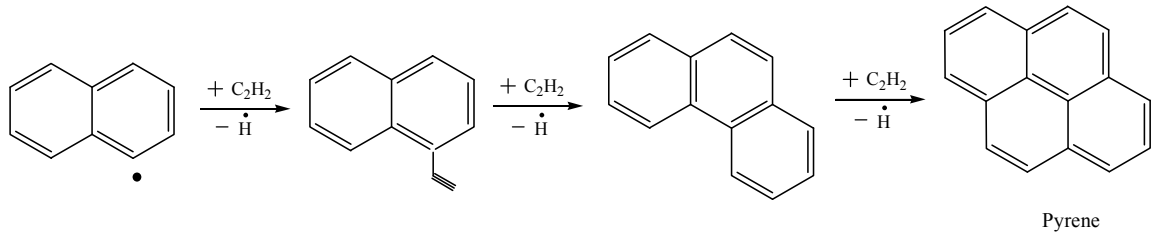

Reaction scheme 5.4.15

HACA pathways however cannot predict some of the PAHs, like benzoflouranthene. Reaction sequence 16 explains the dimerisation and coalescence of two biphenyls leading to the formation of benzofluoranthene [103].

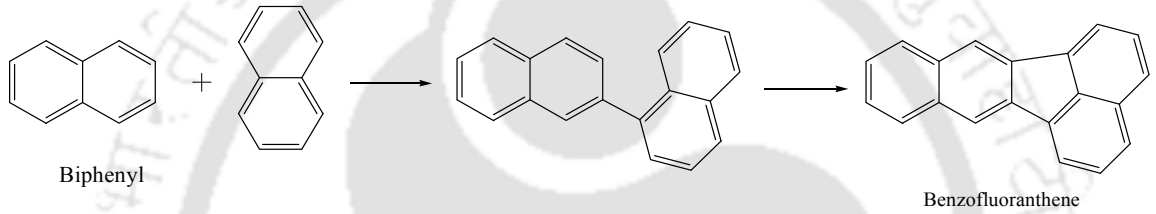

Reaction scheme 5.4.16

Cyclodehydrogenation of two toluene molecules results in the formation of anthracene (*Reaction 5.4.17*).

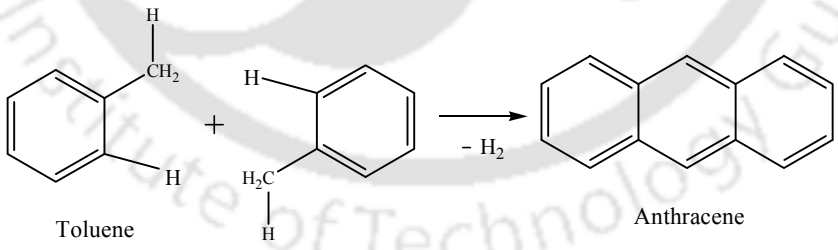

Reaction scheme 5.4.17

5.4.3 Conclusions

Pyrolysis of PET involves a network of heterolytic and homolytic chain scission reactions. Products obtained range from simple acetylene gases to complex PAHs which are solids. At low temperature (200-300^{o}C), its thermal degradation mainly occurs by heterolytic or ionic

mechanism which explains the formation of benzene, TPA, MVT, acetaldehyde, CO_2, as well as cyclic dimers and trimers. Ionic mechanism, however cannot explain the formation of most of the PAHs. Benzene is inevitable for their inception, and radical reactions could explain their formation following HACA routes. At higher temperature (at or above 400^{o}C), radical reactions come into play, which lead to the formation of PAHs along with other species. It is worth mentioning here that PAHs fall under the class of persistent organic pollutants (POP), some of which are termed as carcinogenic and hence are completely undesirable in any product stream routed to atmosphere. Thus, pyrolysis of PET should be carefully carried out so as to avoid the formation of PAHs. Again, formation of dioxin, which is due to dimerisation of vinyl alcohol, is a secondary reaction, the primary reaction being acetaldehyde formation. Thus dioxin concentration in the product stream is low enough so as not to cause any catastrophic damage to the environment. Again, carbonaceous charred product, obtained at the end can be upgraded to obtain activated carbon. Thus, pyrolysis of PET, if conducted under controlled environment, yield a host of important petrochemicals (Benzene, toluene, xylene etc.) as well as petrochemical feedstock (DVT, MVT etc.), which has got tremendous market value.

5.5 Temperature Dependent Pyrolytic Product Evolution Profile for Binary Mixtures of LDPE and PP

5.5.1 Products analysis

Figure 5.26 depicts the variation in T_{max} of the binary mixture of LDPE and PP as a function of wt.% of LDPE. The circular markers represent the calculated values of T_{max} for the binary mixture compositions using non-interacting model (where simple additivity rule is applied), whereas the square markers represent the experimental values of T_{max}. It is evident from the figure that as the percentage of LDPE increases, T_{max} for the corresponding mixture shows a

continuous increase and calculated values of T_{max} for the mixtures differ from that of the component plastics. The difference between these two values indicates the absolute degree of deviation between real values and theoretical values assuming no interaction between the plastics. Thus, it is suggestive of presence of synergistic effects between the plastics.

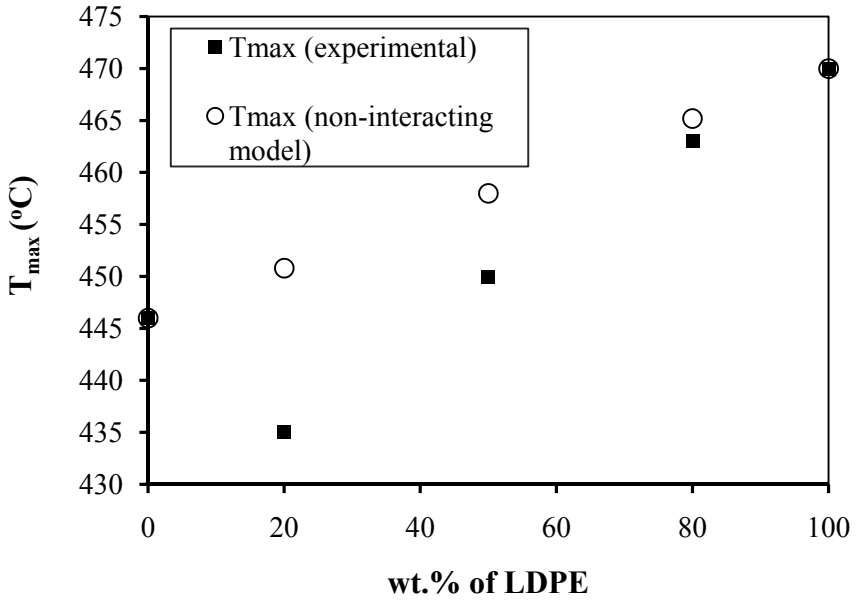

Figure 5.26 Variation in T_{max} of the binary mixture of LDPE and PP as a function of wt. % of LDPE

The synergism existing between the plastics during pyrolysis is expected to affect the overall decomposition process of their binary mixtures. To have an insight of the decomposition process, product distribution studies were carried out for the binary mixtures, and compared with those obtained for the single plastics *Section 5.2 and 5.3.*

Figures 5.27-5.29 depict the pyrograms of three binary compositions of PP and LDPE at their corresponding T_{max}. As is the case with single plastics, co-elution of C5-C7 hydrocarbons occurs and a broad peak represents them as a whole. The next peak in the chromatogram appears at about 40 min (corresponding to C12); there are insignificant amounts of C9 and

C10 hydrocarbon products. It is clear from the chromatograms that yield of C5-C7 is the maximum for all the mixture compositions. For binary mixture of 20%LDPE 80%PP, significant amount of higher hydrocarbons (above C14) has been observed. However, for binary mixture of 50%LDPE 50%PP, the intensity of peaks corresponding to higher hydrocarbons (above C22) decreases and is considerably less than the other fractions (Figure 5.28).

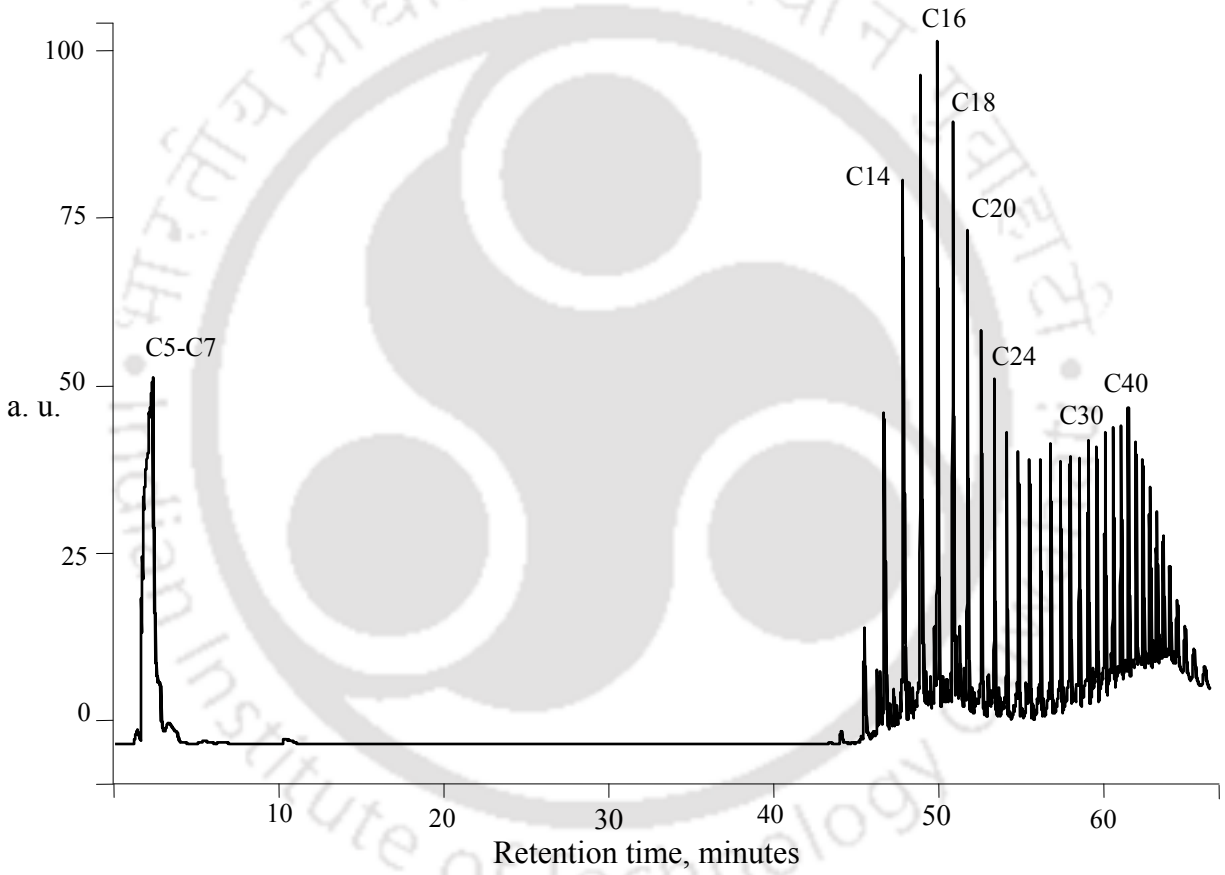

Figure 5.27 Pyrogram of binary mixture of 20% LDPE 80% PP (by wt.) at T_{max}= 435°C

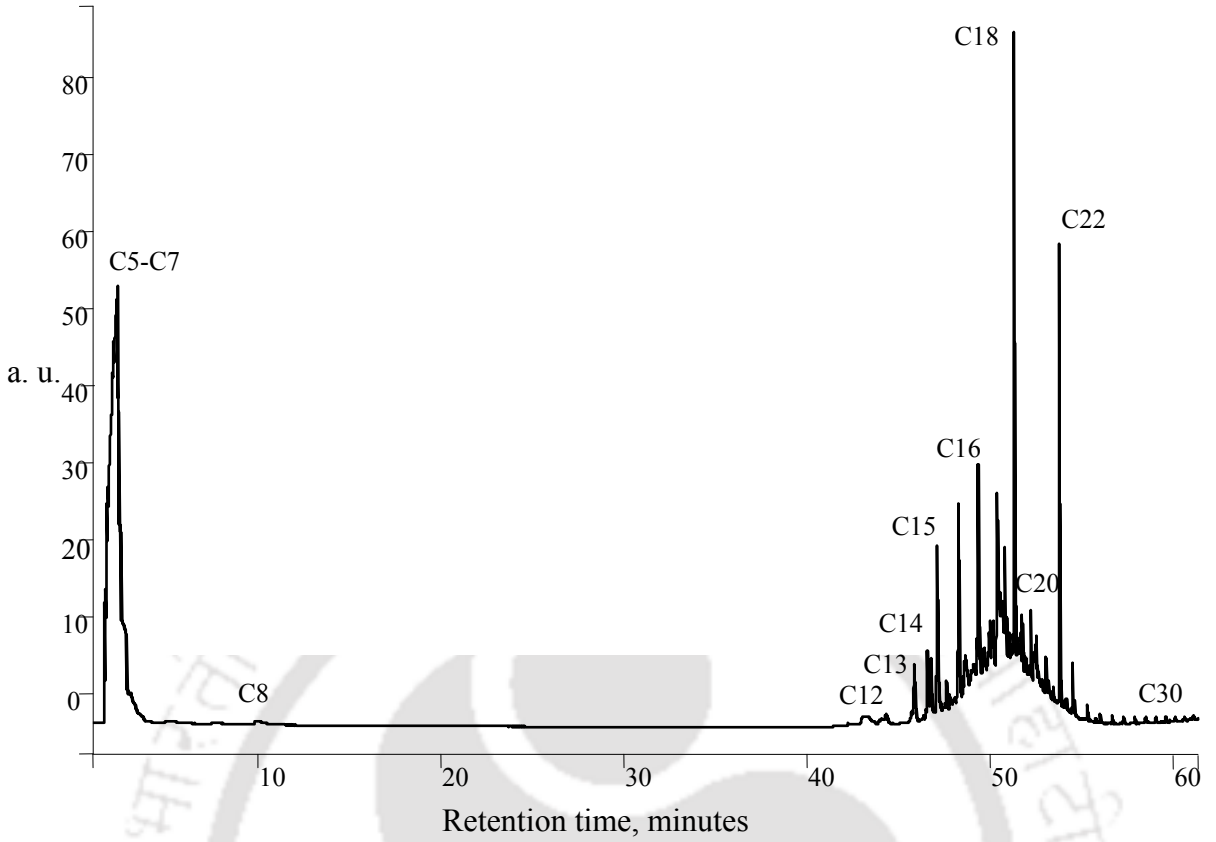

Figure 5.28 Pyrogram of binary mixture of 50% LDPE 50% PP (by wt.) at T_{max}= 450°C

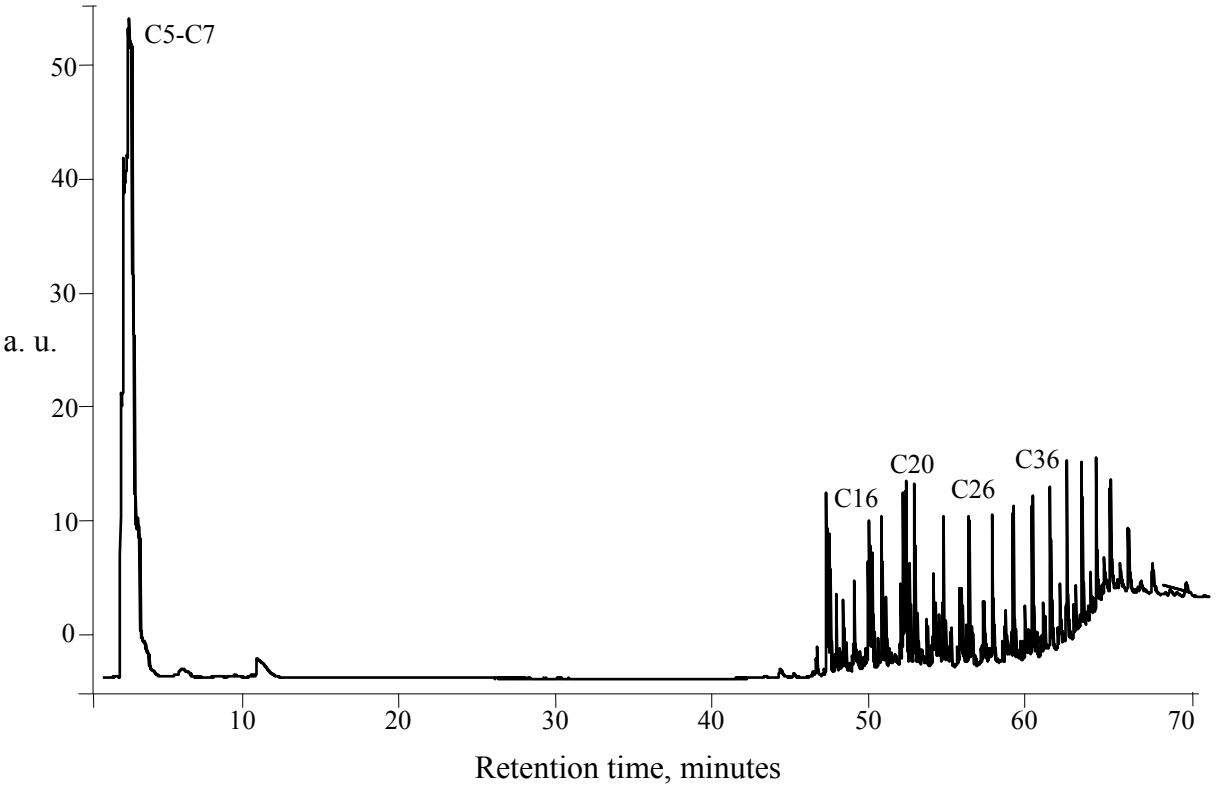

Figure 5.29 Pyrogram of binary mixture of 80% LDPE 20% PP (by wt.) at T_{max}= 463°C

Figures 5.30-5.35 depict the mole fractions of C5-C44 hydrocarbons obtained from pyrolysis of the binary mixtures as a function of percentage of PP at 200, 300, 400, T_{max} (for each of the mixtures), 500 and 600 respectively. At 200°C, products evolved are mostly due to weak-link scission. C16-C22 hydrocarbons share the major fraction of the products for pure LDPE, pure PP and also for their binary mixtures. However, for pure PP, C32-C44 fraction has an equal share as that of C16-C22 hydrocarbons. As temperature increases to 300°C, random scission of the polymer chain starts. At this temperature, C16-C22 is the major product from LDPE, whereas C12-C15 is that from PP. For the mixtures, C16-C22 are the major hydrocarbons.

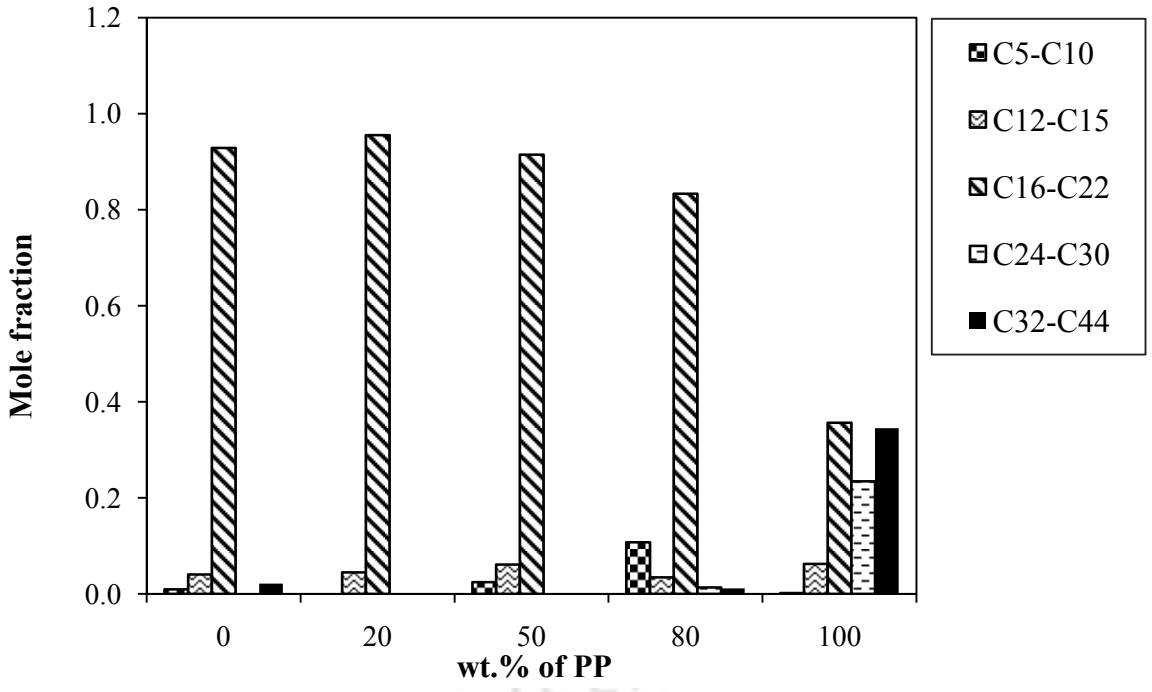

Figure 5.30 Mole fractions of C5-C44 hydrocarbons from pyrolysis of LDPE-PP mixture as a function of wt.% of PP at 200°C

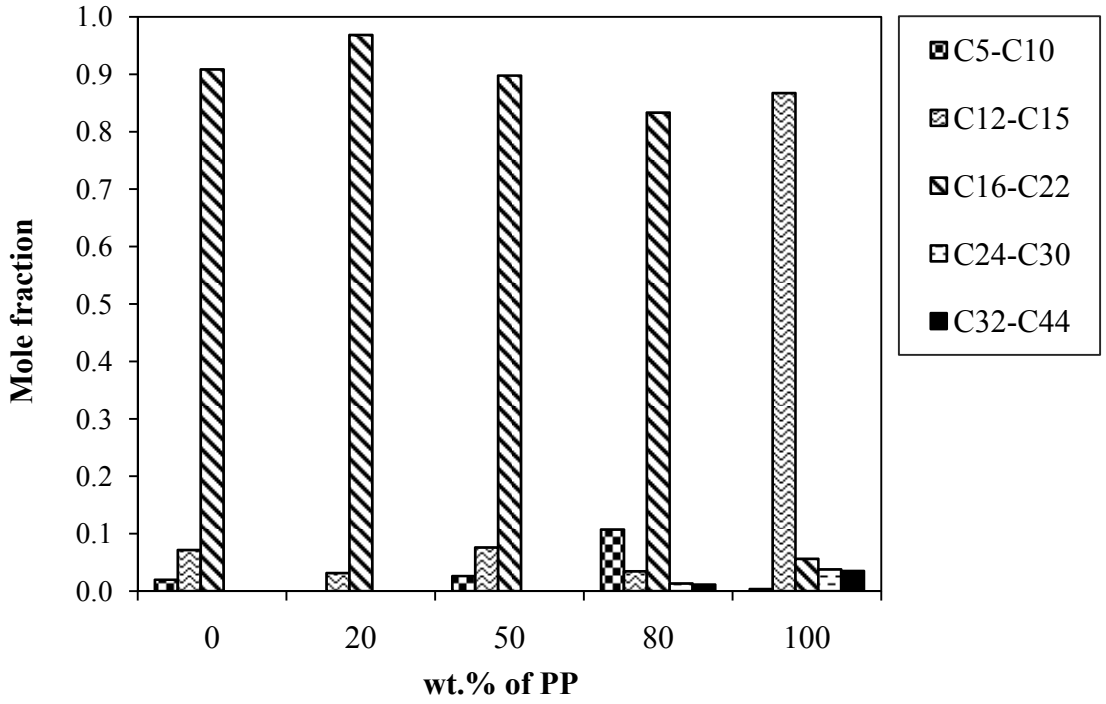

Figure 5.31 Mole fractions of C5-C44 hydrocarbons from pyrolysis of LDPE-PP mixture as a function of wt.% of PP at 300^{o}C

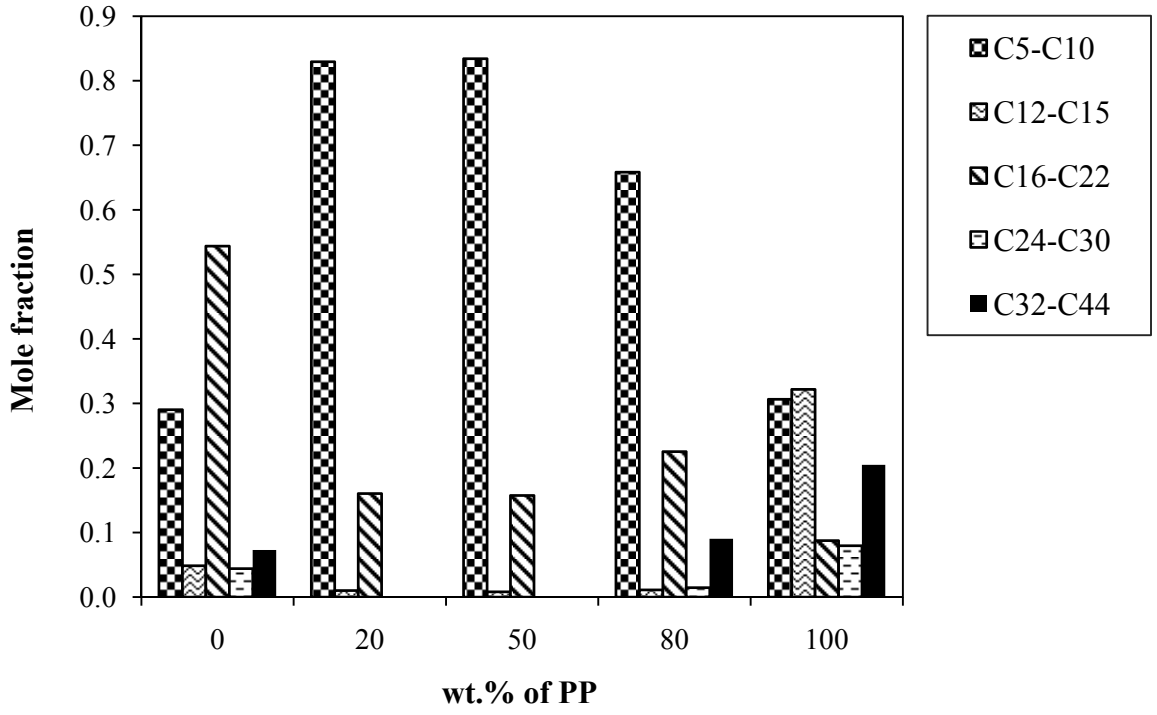

Figure 5.32 Mole fractions of C5-C44 hydrocarbons from pyrolysis of LDPE-PP mixture as a function of wt.% of PP at 400^{o}C

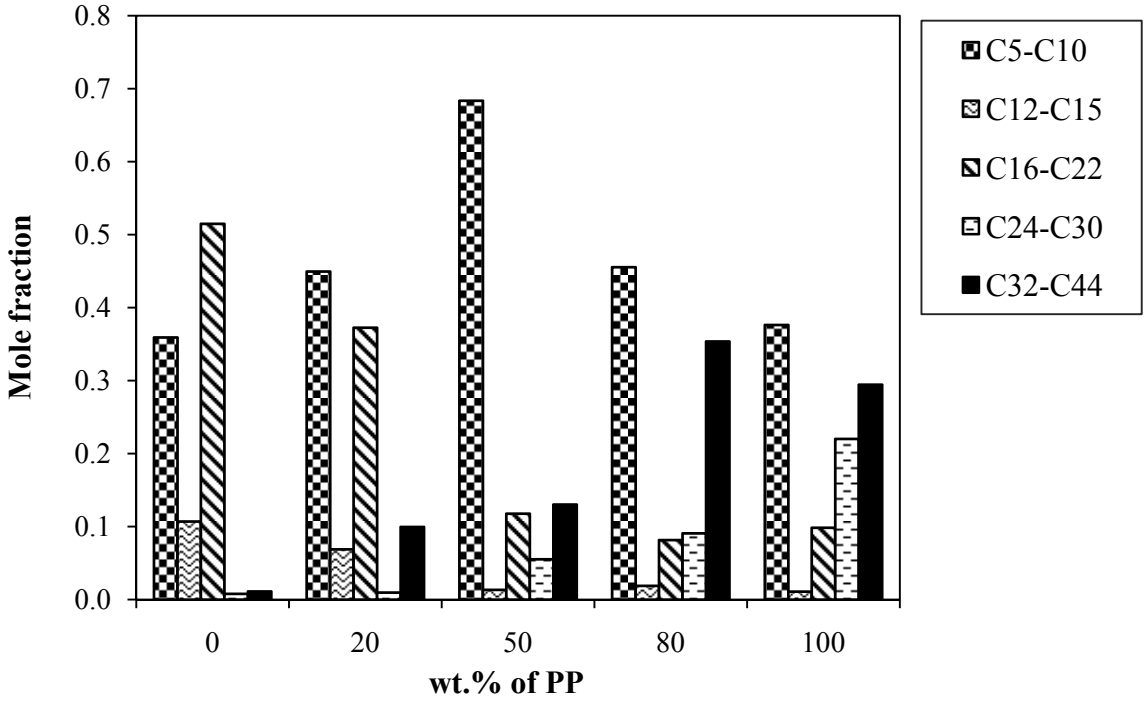

Figure 5.33 Mole fractions of C5-C44 hydrocarbons from pyrolysis of LDPE-PP mixture as a function of wt.% of PP at their respective T_{max}

At 400°C, for LDPE and PP, C5-C10 hydrocarbons form the second major product fraction; the principal hydrocarbon products being C16-C22 for LDPE, and C12-C15 for PP. In case of the mixtures, significant increase of C5-C10 is observed and C16-C22 hydrocarbons are the second major. At T_{max}, C5-C10 hydrocarbons are invariably the major product. With increase in the percentage of PP in the mixture, amount of C12-C15 and C16-C22 decreases in the mixture, while C24-C30 and C32-C44 increase in the mixture. At 500°C, C5-C10 is the chief fraction from LDPE, whereas C12-C15 is that from PP. For the mixtures, C5-C10 and C16-C22 are considerably more than other fractions. With increase in percentage of PP, C5-C10 hydrocarbons decrease, while C16-C22 hydrocarbons increase in the mixture.

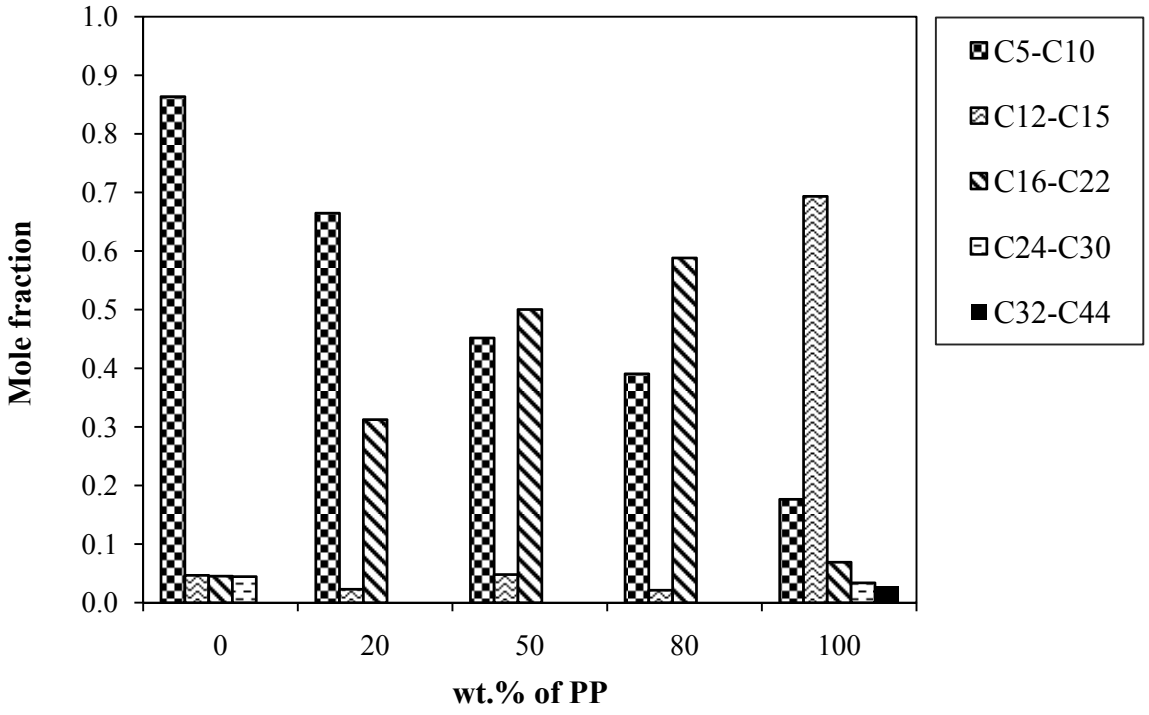

Figure 5.34 Mole fractions of C5-C44 hydrocarbons from pyrolysis of LDPE-PP mixture as a function of wt.% of PP at 500^{o}C

At 600^{o}C, C16-C22, and C5-C10 hydrocarbons are the major products, for LDPE and PP respectively. Along with those hydrocarbons, small amount of C5-C10 hydrocarbons also evolve at this temperature. For the mixtures, addition of 20% of PP to the mixture results in an increase in the yield of C5-C10 and a decrease in C16-C22 hydrocarbons. However, with further addition of PP, no further increase has been observed in evolution of C5-C10 hydrocarbons. For 50%PP 50%LDPE mixture, C16-C22 hydrocarbons are the major product, whereas for 80%PP 20%LDPE, C16-C22 and C24-C30 hydrocarbons have almost an equal share in the total yield.

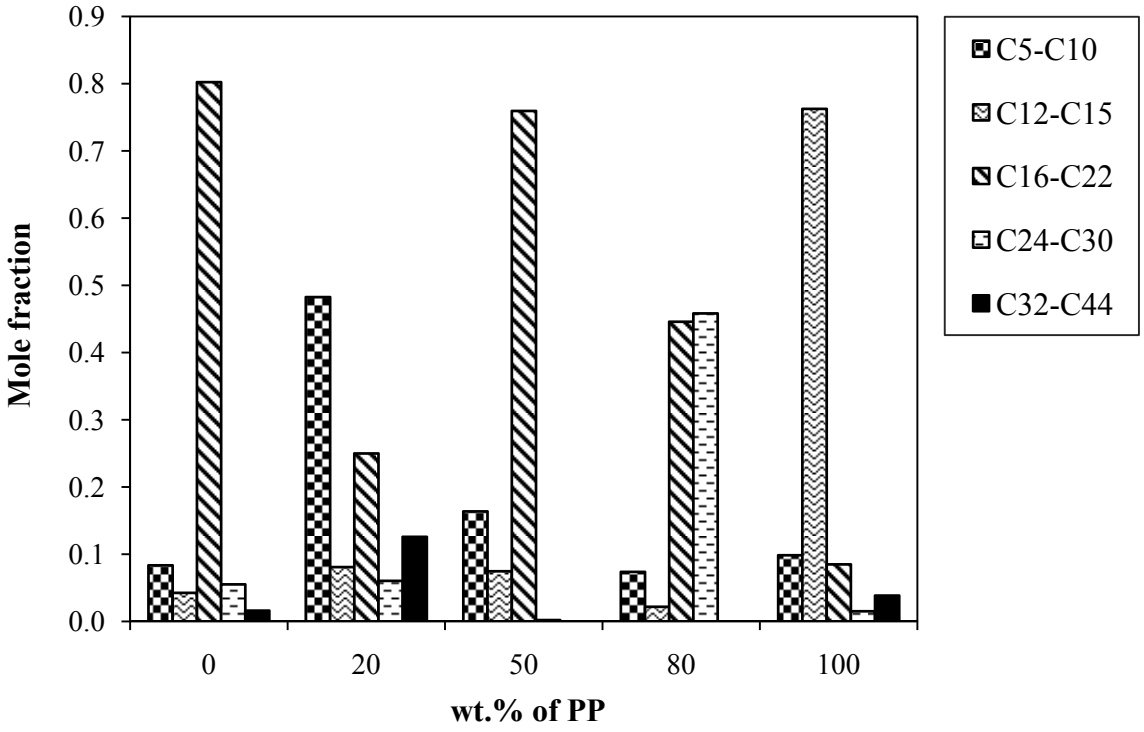

Figure 5.35 Mole fractions of C5-C44 hydrocarbons from pyrolysis of LDPE-PP mixture as a function of wt.% of PP at 600^{o}C

5.5.2 Mechanistic analysis

Thermal degradation of both PP and LDPE proceed essentially by random scission of the macromolecule, followed by intra- and intermolecular hydrogen transfer with subsequent stabilization by β-scission and hydrogen abstraction reactions. 1,3 or 1,4 or 1,5-intramolecular end/mid-hydrogen transfer reactions justify the wide range of hydrocarbons in the volatile pyrolyzate [80, 87, 96, 135,136].

At 200-300^{o}C, less energy is available for cracking. As already explained, at such low temperatures, the bonds that would break first are the ones that form the weakest link(s) in the chain. During this process, C16-C22 hydrocarbons are obtained from LDPE pyrolyzate due to intramolecular hydrogen transfer and subsequent β-scission; whereas C12-C15 are obtained from PP usually following the same route. In case of mixtures of PP and LDPE,

substantial evolution of C16-C22 has been observed between 200-300°C. The same could be explained based on mutual interaction between PP and LDPE as shown in *Reaction scheme 5.5.1*.

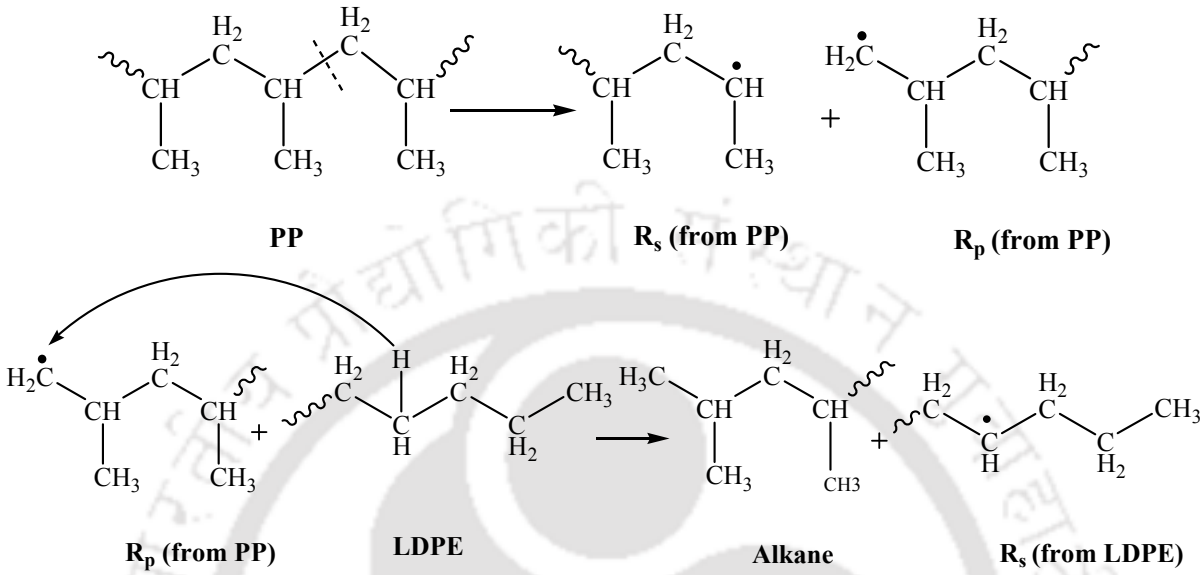

Reaction scheme 5.5.1

As PP starts degrading earlier than LDPE, we would expect free radicals to emerge from molten pool of PP, which could attack the macromolecular chain of LDPE, thus acting as an initiator to provide sufficient energy to start its dissociation at a lower level than its actual temperature of decomposition (*Reaction scheme 5.5.1*). Once the secondary radicals (from both LDPE and PP) are generated, the chain propagation and termination reactions proceed via the routes as discussed in *Section 5.2-5.3*.

As temperature reaches 400°C, considerable evolution of lighter fractions (C5-C10) has been observed, due to the availability of more energy for cracking reactions to occur. At T_{max}, C5-C10 hydrocarbons continue to evolve as cracking reactions become vigorous; heavier hydrocarbons are also observed (above C24). Formation of C5-C10 hydrocarbons might take place following different routes; however, more specifically by 1,5-intramolecular hydrogen transfer with subsequent *β*-scission, *e.g.* Pentene (C5) might have been formed following *β*-

scission on R_s. (*Reaction scheme 5.5.2*). 1,5-intramolecular hydrogen transfer reactions have already been explained under *Section 5.2.2* and *Section 5.3.2*.

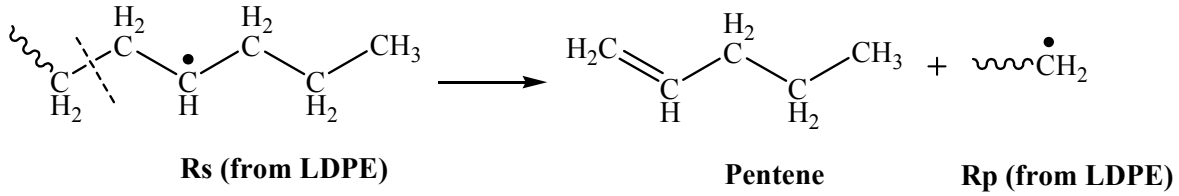

Reaction scheme 5.5.2

At T_{max}, yield of C5-C10 hydrocarbons is more in all the binary mixtures compositions than that in the pure plastics, and it is the highest for the 50% LDPE 50%PP. It has also been noticed that, at T_{max}, increase in PP content in the mixtures led to formation of heavier hydrocarbons which is also reported by Ciliz *et al.* [148]. At this high temperature, termination of the radicals is achieved by radical recombination. In LDPE, intramolecular hydrogen transfer following three or four consecutive 1,5-Hydrogen shift leads to the formation of C11, C14, C15, C22 radicals. These radicals upon combining among themselves, or with radicals generated from molten PP pool, might result in the formation of the heavy hydrocarbon species. Again, lighter hydrocarbon fragments generated from PP could combine among themselves or with those generated from LDPE and radicals from LDPE degradation might again combine among themselves resulting in heavier hydrocarbons (*Reaction scheme 5.5.3*).

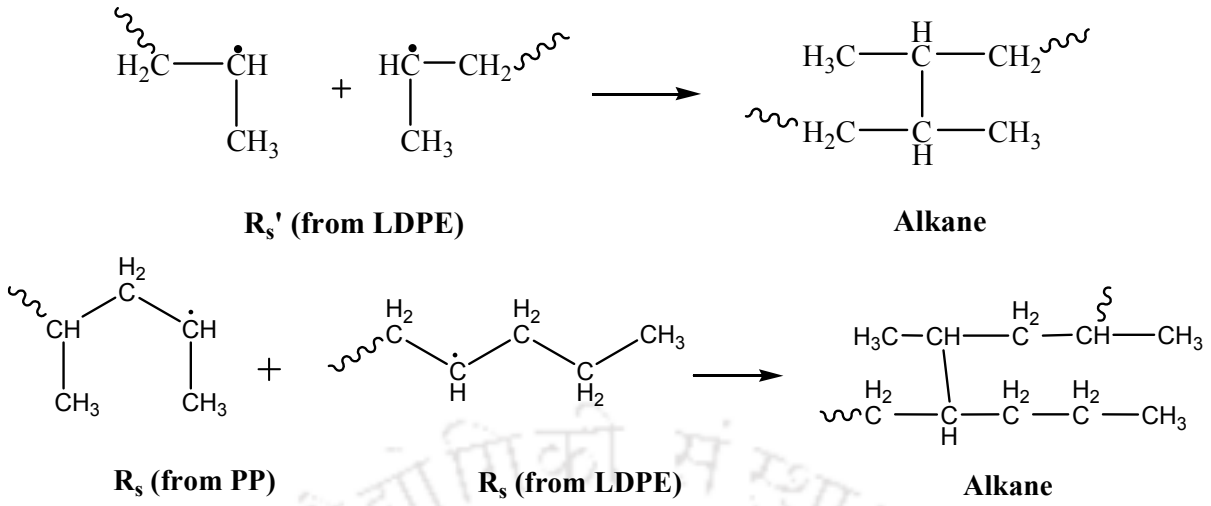

Reaction scheme 5.5.3

At 600°C, polymer chain length considerably reduces as degradation is almost complete at this temperature. C5-C10 generation is nearly constant for both LDPE and PP and is fairly low. However, with decrease in PP content in the mixture, C5-C10 production increased and highest generation was obtained for 20%PP 80%LDPE mixture. C12-C15 is again the dominant fraction in PP; similarly C16-C22 fraction predominates in LDPE. At very high temperatures such as 600°C, comparable evolution of C16-C22 and C24-C30 has been noticed for 80% PP 20% LDPE, which suggests that termination by disproportionation (shown in *Reaction scheme 5.5.4*) and radical recombination are equally important, as discussed earlier.

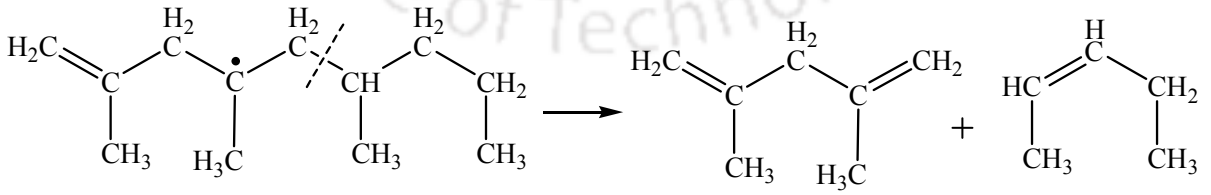

Reaction scheme 5.5.4

5.5.3 Conclusions

Analysis of the products obtained from pyrolysis of the binary mixtures of LDPE and PP has confirmed the existence of interaction between the plastics in their melt. At very low temperatures, yield of C16-C22 gets enhanced in the mixtures. An enhancement in the evolution of lighter hydrocarbons (C5-C10) in the plastic mixtures is an important observation from this study. At higher temperatures (>500^{o}C), yield of heavier fractions (above C16) also gets enhanced with increase in the percentage of PP in the mixture.

5.6. Temperature Dependent Pyrolytic Product Evolution Profile of Binary Mixture of PP and PET

5.6.1 Products analysis

Product distribution studies for pure PP and PET have been explained in *Sections 5.3* and *5.4*. Again, thermal degradation behaviour and interaction between the two plastics were discussed under *Section 5.1*, wherein the interacting model could predict their degradation profile. In this section, we have made an attempt to enumerate this interaction in terms of their product evolution profile. Thermal degradation studies carried out for the single plastics have indicated that PET is thermally less stable than PP, which is due to the presence of two heterogeneous linkages between O and C in its backbone. The variation in T_{max} for the binary mixtures is pictorially represented in Figure 5.36. The square markers represent the calculated values of T_{max} for the binary mixture compositions using non-interacting model (where simple additivity rule is applied), whereas the circular markers represent the experimental values of T_{max}. It is clear from the plot that there is an enhancement in the overall degradation process of the mixtures, which confirms synergistic effects of their binary interaction. The same has already been elaborated in *Section 5.1*.

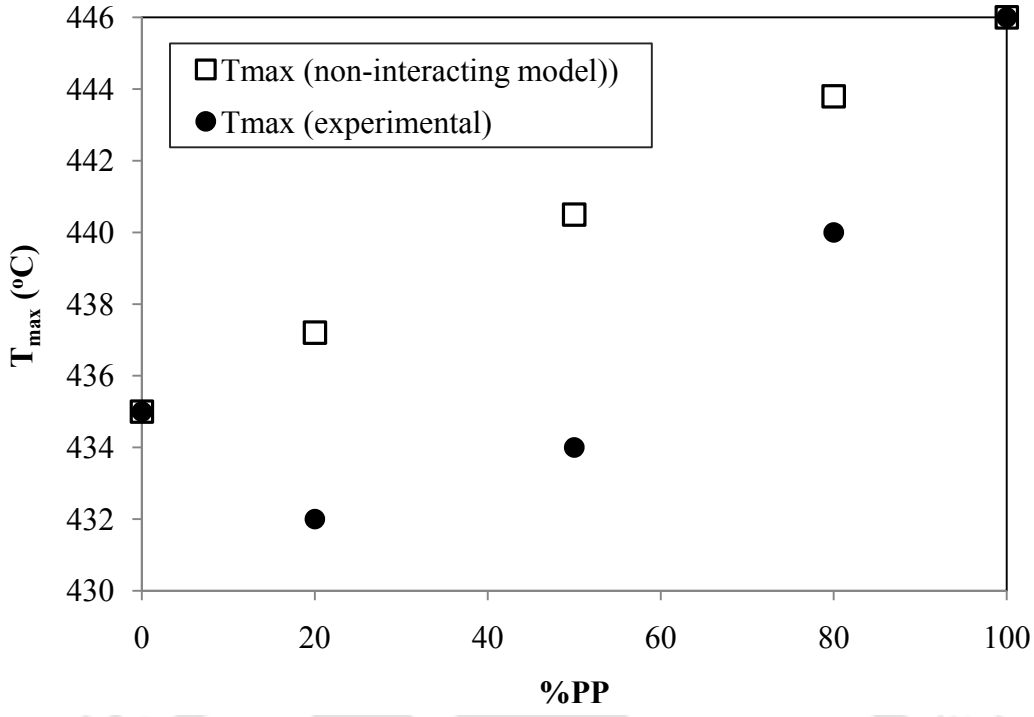

Figure 5.36 Variation in T_{max} of binary mixture of PET and PP plotted as a function of wt.% of PP

Pyrograms of the binary mixture at various temperatures are included in the Appendix 3. Figures 5.37-5.41 compare the evolution pattern of hydrocarbons obtained from the plastics, with increase in the percentage of PP as temperature is varied from 300°C to 600°C. At 300°C, energy needed for rapid disintegration of polymer molecules is not sufficient. Therefore, only small amounts of products are obtained at such low temperatures. The products which are obtained are mainly due to the breakage of weak links present across the polymer backbone. The yield of higher hydrocarbons (above C12) is more in PET as compared to C5-C10 hydrocarbons (Figure 5.38), which could be due to formation of cyclic oligomers, which has already been discussed in *Section 5.4*. On the other hand, C12-C15 is the major fraction for PP, as already discussed in *Section 5.3* and Thus at low temperatures, interactions between the two plastics are not prominent, and their decomposition mechanism is somewhat independent of each other, the same will be explained later in *Section 5.6.2*. It is evident from the Figures 5.38,

5.21 and 5.25 that for mixtures with high concentration of PP or PET, overall decomposition is dominated mostly by the product evolution pattern of the corresponding pure component; only at higher composition, the product evolution pattern deviates from that of pure species.

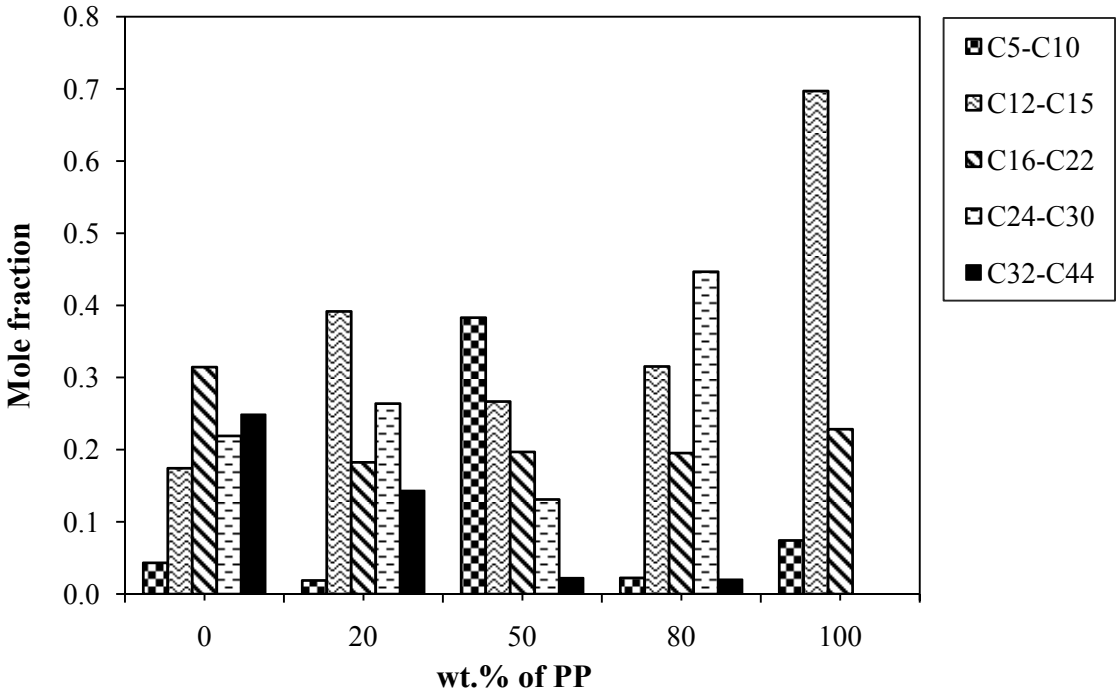

Figure 5.37 Mole fractions of C5-C44 hydrocarbons from pyrolysis of PP-PET mixture as a function of wt.% of PP at 300^{o}C

At 400^{o}C, C5-C10 hydrocarbons are the major product from both the pure plastics, PP and PET (Figure 5.38). However, as percentage of PP increases, hydrocarbons of random chain lengths start emerging in the product stream resulting into a wide product distribution. As temperature increases beyond 300^{o}C, formation of benzene from pyrolysis of PET is likely due to the more availability of radical species emerging out of PP melt, which might attack the PET fragmented chain. For 20%PP 80%PET, significant production of C24-C30 hydrocarbons are observed. These products might also include C14-C18 PAHs resulting due to the formation of benzene, which has been explained in *Section 5.4*.

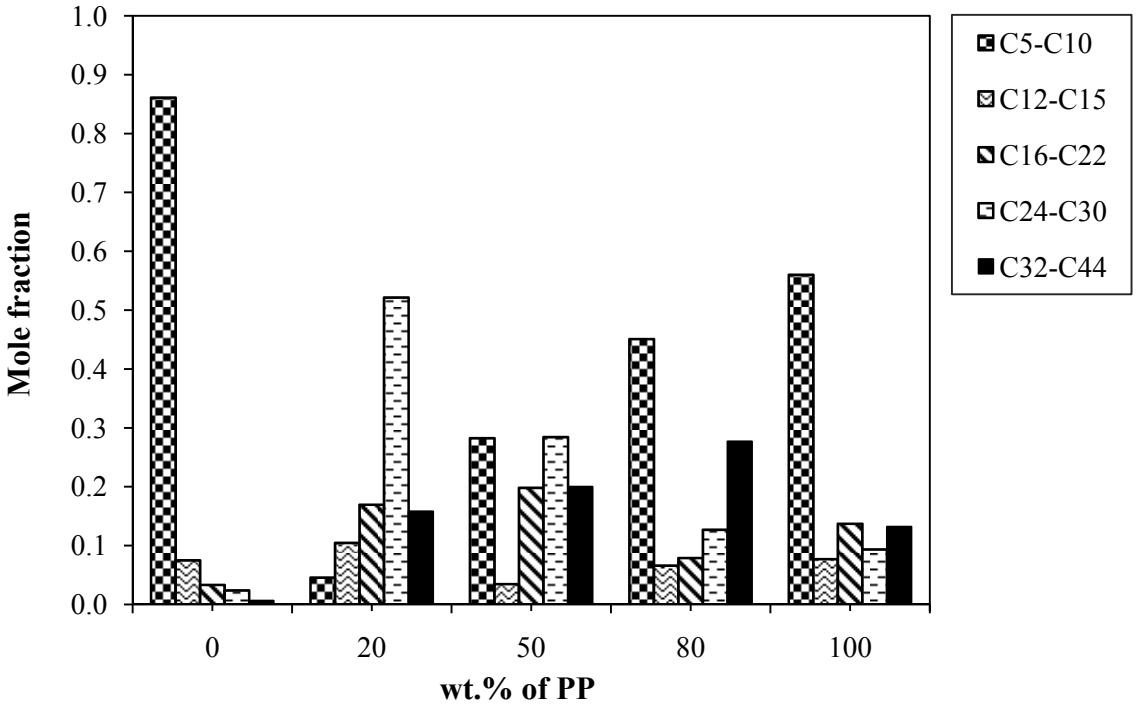

Figure 5.38 Mole fractions of C5-C44 hydrocarbons from pyrolysis of PET-PP mixture as a function of wt.% of PP at 400^{o}C

At T_{max} (Figure 5.39), evolution of C5-C10 hydrocarbons is considerably high for all the mixture compositions; specifically for 50%PP 50%PET this is highest product fraction. The major products obtained from the mixtures are likely to be isopentane, pentene, benzene and benzoic acid. The less volatile species of intermediate chain-lengths (C10 and above), however have the tendency to undergo combination reactions due to the available thermal energy which leads to the formation of heavier fractions. The heavier hydrocarbons obtained from the mixtures might also encompass PAHs, which evolve due to radical reactions of benzene. At 500^{o}C (Figure 5.40), the overall picture is more or less the same. As temperature approaches 600^{o}C, the plastics decompose nearly to completion and trace quantities of hydrocarbon products are obtained. Here, no marked difference is observed in the evolution profiles of the

products from the mixtures from that of the single plastics, except that C24-C30 fraction somewhat increases in the mixture (Figure 5.41).

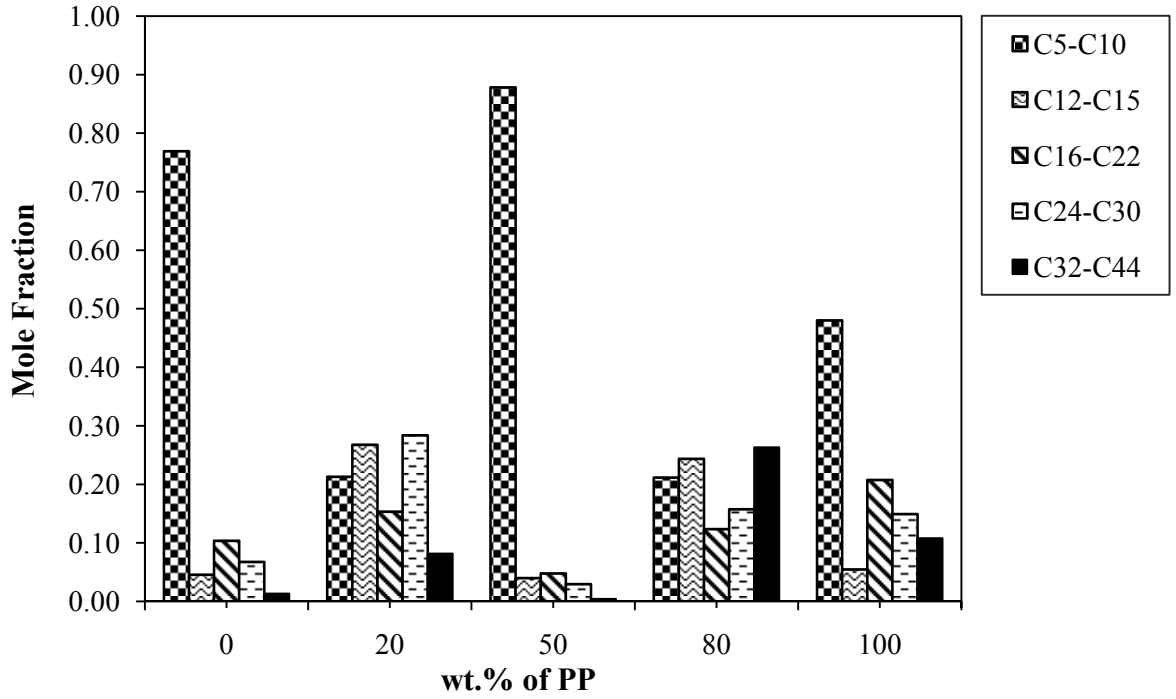

Figure 5.39 Mole fractions of C5-C44 hydrocarbons from pyrolysis of PP- PET mixture as a function of wt.% of PP at T_{max}

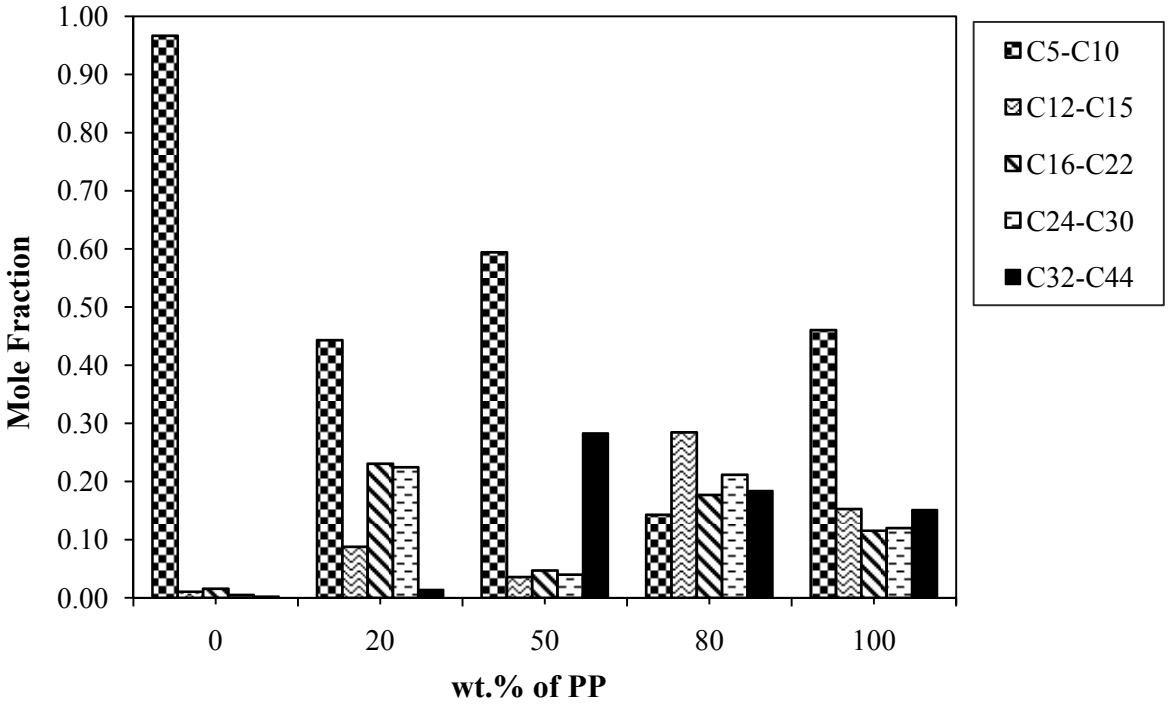

Figure 5.40 Mole fractions of C5-C44 hydrocarbons from pyrolysis of PP- PET mixture as a function of wt.% of PP at 500^{o}C

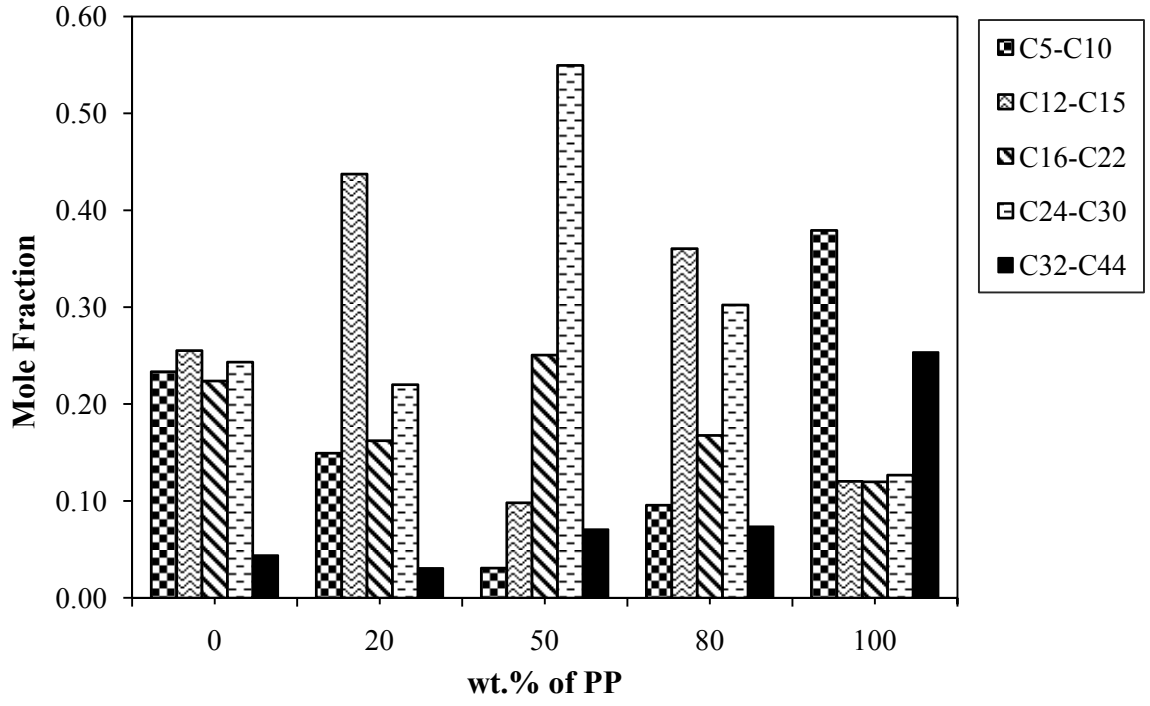

Figure 5.41 Mole fractions of C5-C44 hydrocarbons from pyrolysis of PP- PET mixture as a function of wt.% of PP at 600^{o}C

5.6.2 Mechanistic analysis

The repeat unit of PET is:

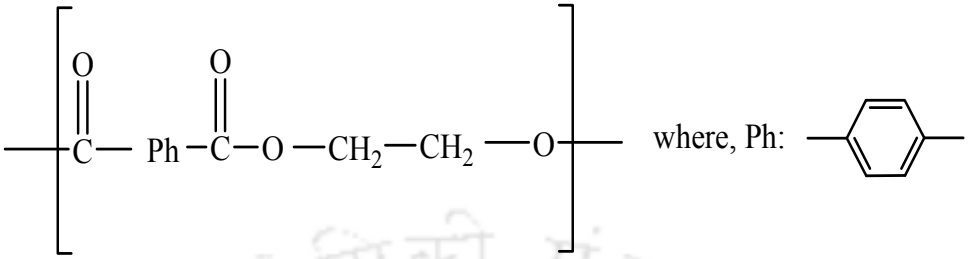

The repeat unit of PP is:

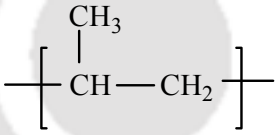

As already explained under *Section 5.3* and *Section 5.4*, PP is an addition polymer which degrade by free radical mechanism resulting into a primary radical and a secondary radical; whereas, PET is a condensation polymer which essentially degrade by ionic (heterolytic) mechanism forming acid end and olefin end. As temperature increases, PET, being thermally less stable than PP, starts to decompose earlier than PP. Hence, interaction between the two plastics is not likely at this temperature. The products that are generated from the individual plastics are due to their own characteristic decomposition behaviour. Thus, the products detected at this temperature could be cyclic oligomers (from PET), the formation of which is already elaborated under *Section 5.4.2*, and olefins (from PP) due to the elimination of the weak links (*Section 5.2.2*).

However, as temperature increases so as to induce sufficient movement of the radicals and fragments within the molten pool, there is a possibility that individual fragments from both the polymers could interact among themselves. R_p formed by random scission of PP might abstract

a hydrogen atom from methylene group of the acid end (**I**), transferring the radical center to the PET fragmented chain (*Reaction scheme 5.6.1*). Thus, PET can undergo radical reactions at a relatively lower temperature in presence of PP, which is otherwise possible only at a higher temperature (above 400^{o}C). The radical (**II**), thus generated can undergo β-H transfer giving rise to terephthalic acid (TPA). Olefin end (**I**) is regenerated in the process. Decarboxylation of TPA leads to the formation of benzoic acid, which on subsequent decarboxylation gives benzene (*Reaction scheme 5.6.2*). As already explained in *Section 5.2*, formation and growth of PAHs is mostly by homolytic routes and benzene is inevitable for their inception. Thus presence of PP might further intensify their formation as concentration of radical centers increase in the molten pool of the polymer mix in presence of PP. This, in turn, leads to the formation of benzene at a comparatively lower temperature than that in case of cracking PET alone.

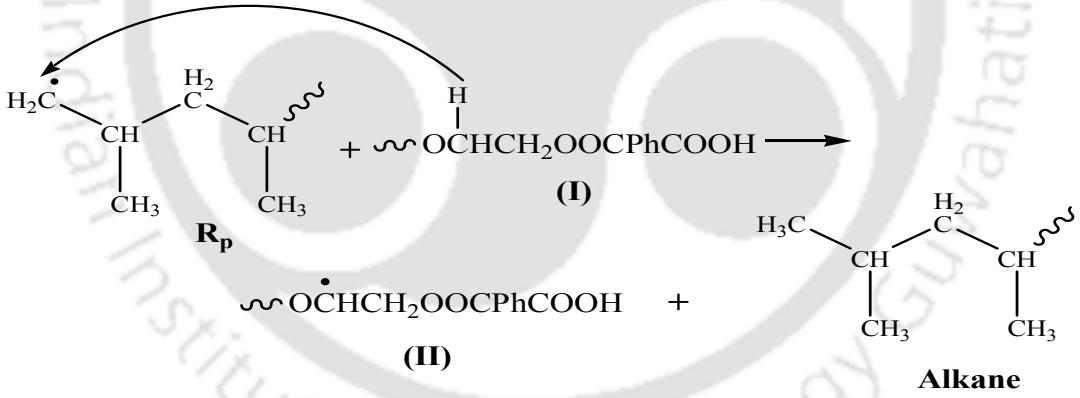

Reaction scheme 5.6.1

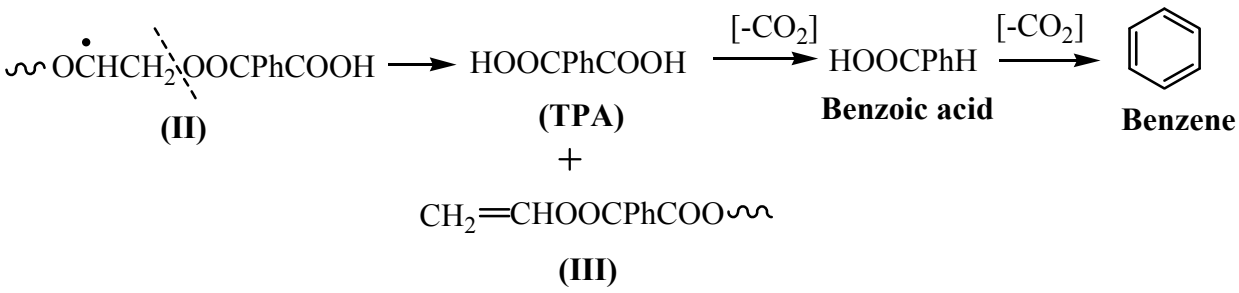

Reaction scheme 5.6.2

5.6.3 Conclusions

The present work has been aimed at exploring the possible effect of interaction in the product evolution pattern from pyrolysis of the binary mixtures of PET and PP by varying their relative ratio in the mixtures. It was observed that at low temperature (≈300^{o}C), products evolved are mostly due to characteristics of the individual polymers. This is due to the fact that PP essentially decomposes by radical mechanism, whereas PET generally decomposes by ionic mechanism at low temperature (≈300^{o}C). However, with increase in degradation temperature, radicals formed from PP start to attack the PET chain, and the radical reactions are induced to the later at a lower temperature (<400^{o}C). This results into a product distribution, which is marked by the combined effect of both the polymers. As with the other single plastics and their mixtures, maximum evolution of products takes place at T_{max}. Significant yield C5-C10 hydrocarbons are obtained from the binary mixtures. Among these, benzene, styrene, vinyl benzoate, pentene, pentane could be important products.

5.7 Temperature Dependent Pyrolytic Product Evolution Profile for Binary Mixture of LDPE and PET

5.7.1 Products analysis

Product distribution studies for pure LDPE and PET have been explained in *Sections 5.2* and *5.4* respectively. Thermal degradation behaviour of seven different compositions of their binary mixtures have already been discussed in *Section 5.1*, showing interaction between the two plastics during pyrolysis. In this section, we have made an attempt to enumerate this interaction in terms of their product evolution profile.

As already discussed, PET is thermally less stable than LDPE, due to the presence of heterogeneous linkages. There is not a huge difference in their characteristic degradation

temperatures; nonetheless, just as in the case of PET-PP binary mixtures, addition of PET has resulted in an enhancement in the overall degradation process. Figure 5.42 shows the variation in T_{max} for the binary mixtures with change in weight% of LDPE in the binary mixtures. The circular markers represent the calculated values of T_{max} for the binary mixture compositions using non-interacting model (where simple additivity rule is applied), whereas the square markers represent the experimental values of T_{max}.

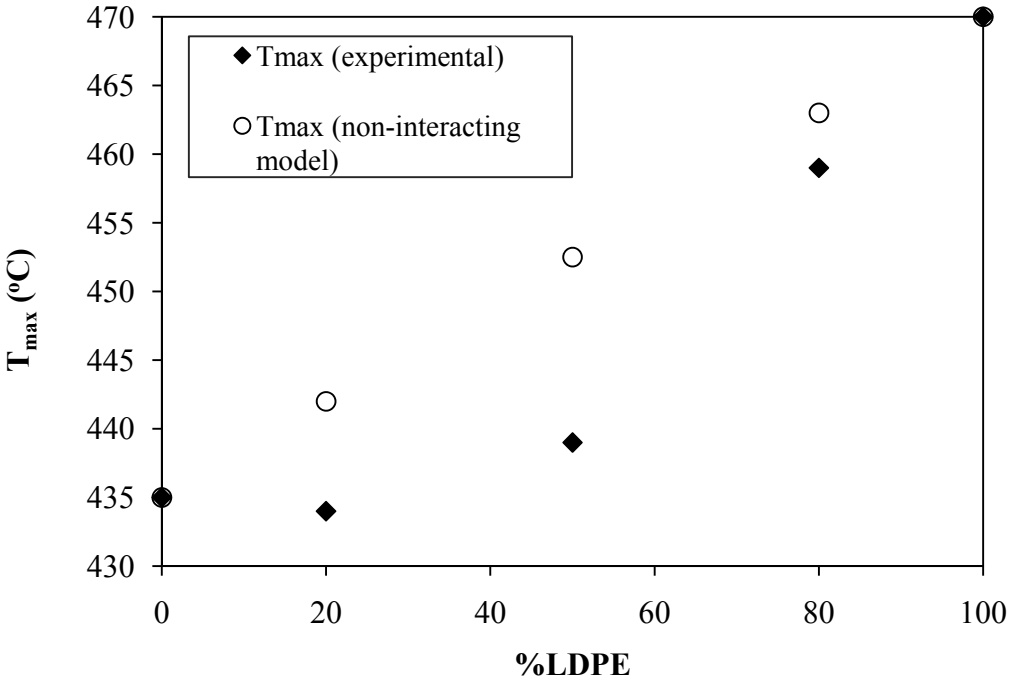

Figure 5.42 Variation in T_{max} of binary mixture of LDPE and PET plotted as a function of wt.% of LDPE

Pyrograms of the binary mixture at various temperatures are shown in Appendix 3. Figures 5.43-5.47 show the evolution pattern of the products obtained from the plastics, with increase in the percentage of LDPE, as temperature is varied from 300°C to 600°C. At low degradation temperatures, products evolved are mainly due to breakage of weak links. At 300°C, product stream mainly comprises of C16-C22 fraction for LDPE, whereas for PET, more or less equal proportions of all the fractions (above C12) are obtained. Production of C5-C10 fraction is

almost negligible. With 20% LDPE in the mixture, the amount of C24-C30 hydrocarbons produced is more. As percentage of LDPE increases to 50%, evolution of C24-C30 hydrocarbons also increases. On the other hand, C16-C22 fraction is invariably the major product in case of LDPE, though considerable amounts of C5-C10 also evolve at this temperature. However, C5-C10 is the major fraction in case of the mixtures, except for 50% LDPE 50% PET, where C24-C30 hydrocarbons are predominant.

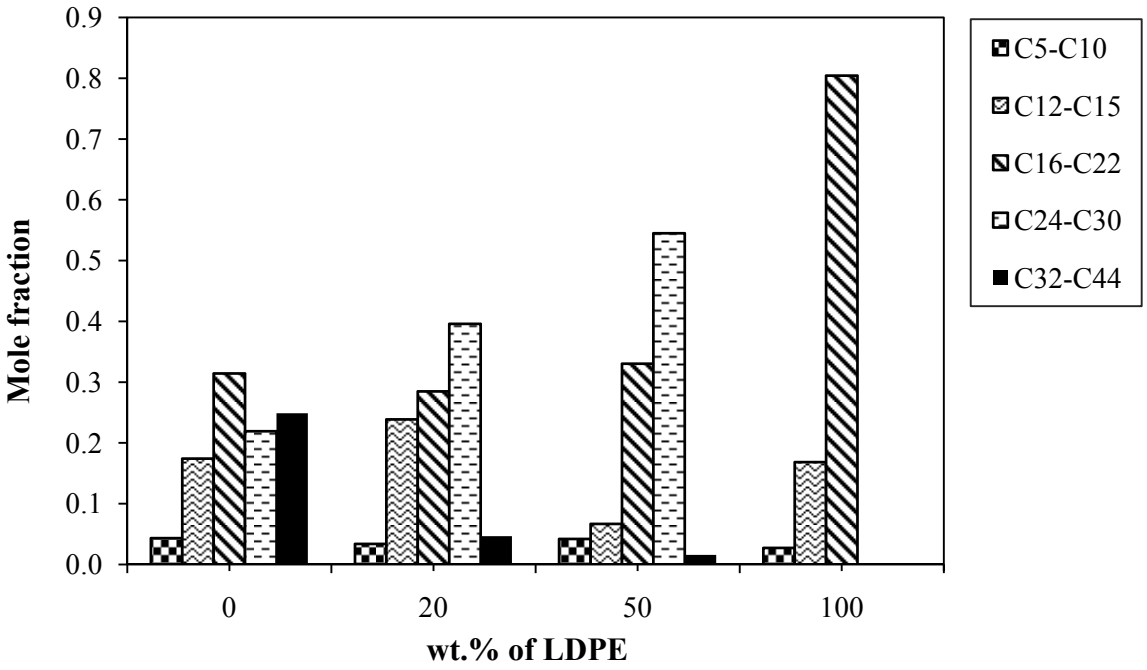

Figure 5.43 Mole fractions of C5-C44 hydrocarbons from pyrolysis of LDPE-PET mixture as a function of wt.% of LDPE at 300^{o}C

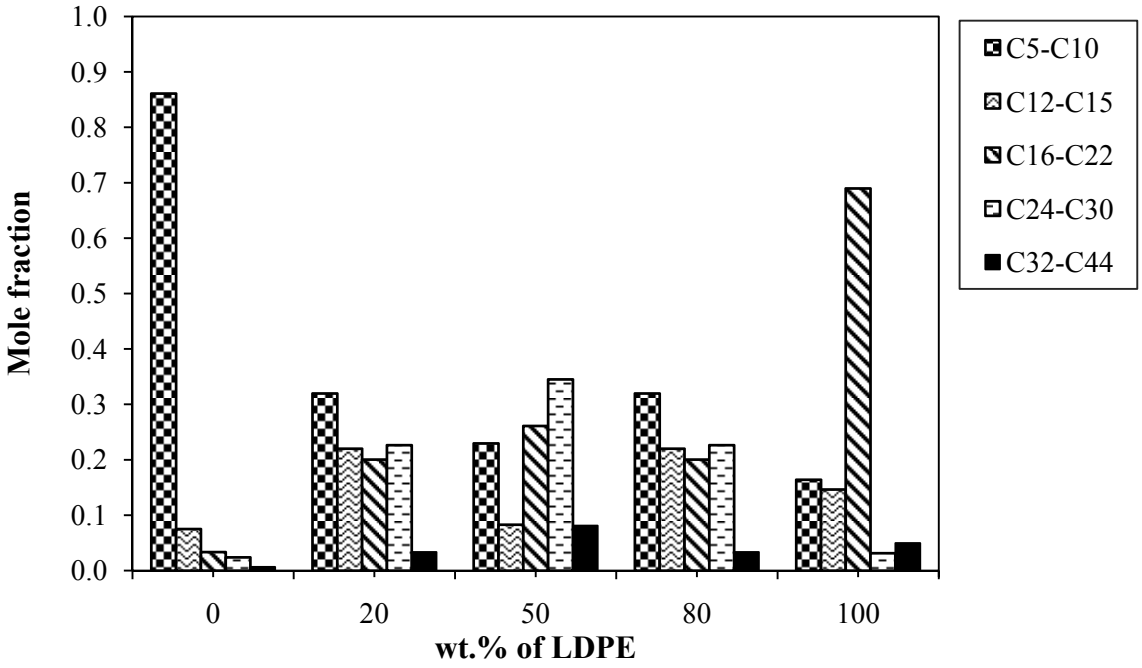

Figure 5.44 Mole fractions of C5-C44 hydrocarbons from pyrolysis of LDPE-PET mixture as a function of wt.% of LDPE at 400^{o}C

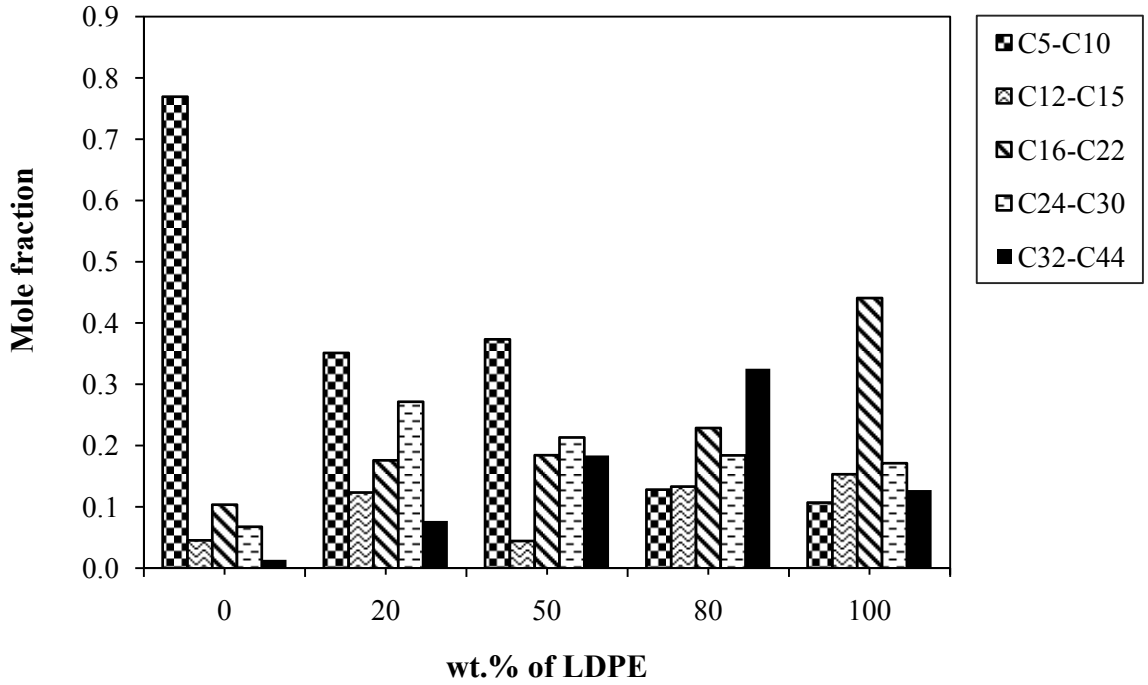

Figure 5.45 Mole fractions of C5-C44 hydrocarbons from pyrolysis of LDPE-PET mixture as a function of wt.% of LDPE at T_{max}

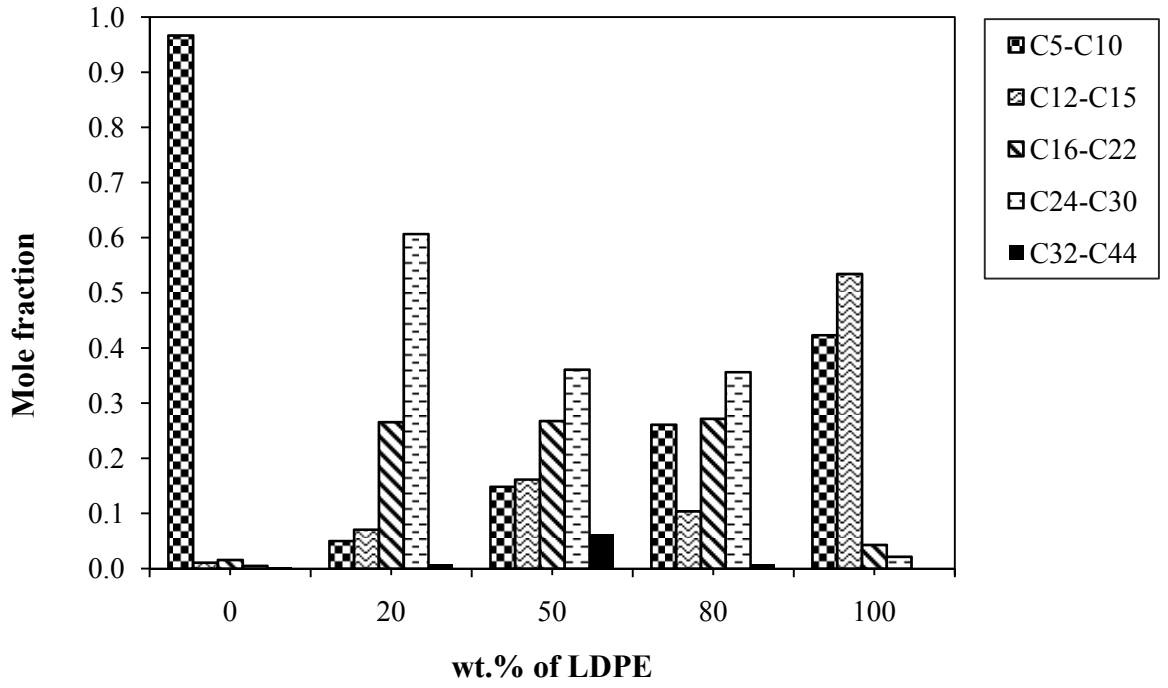

Figure 5.46 Mole fractions of C5-C44 hydrocarbons from pyrolysis of LDPE-PET mixture as a function of wt.% of LDPE at 500^{o}C

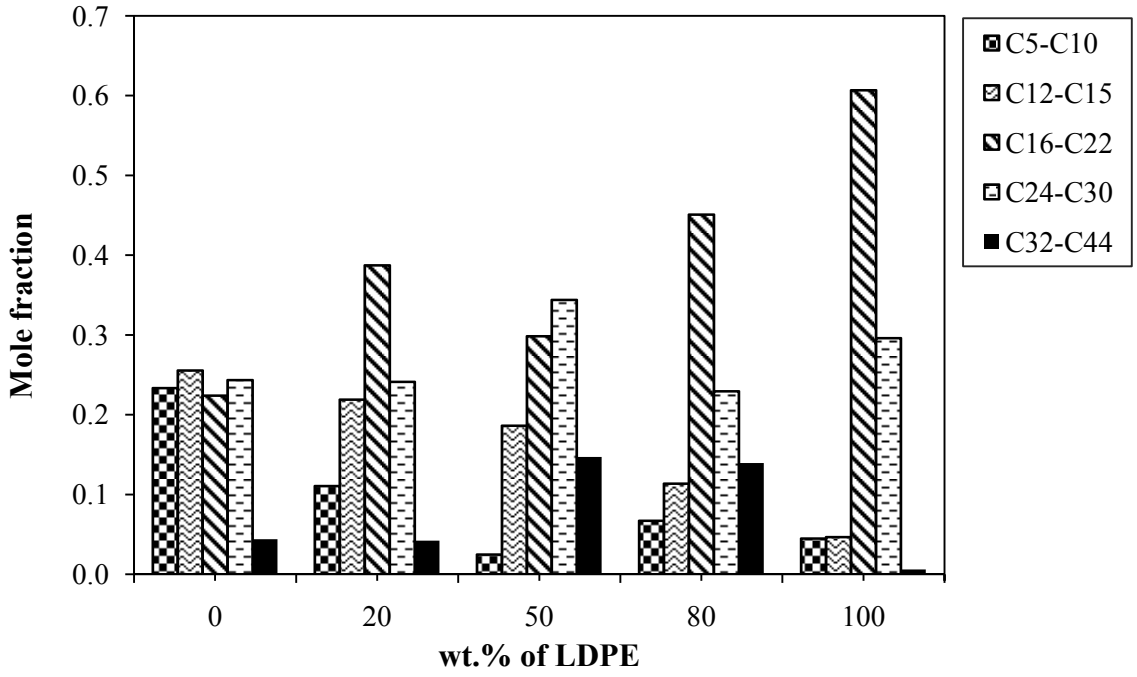

Figure 5.47 Mole fractions of C5-C44 hydrocarbons from pyrolysis of LDPE-PET mixture as a function of wt.% of LDPE at 600^{o}C

At T_{max}, where rate of degradation is maximum, evolution of lighter fractions is also maximum. Here, C5-C10 is the single largest fraction for PET, whereas C16-C22 is that corresponding to LDPE. The evolution pattern of the hydrocarbons is about the same as that at 400°C, except that C24-C30 fraction becomes more pronounced at this temperature. At 500°C, C5-C10 hydrocarbons continue to be the dominant products for PET. However, significant amount of both C12-C15 and C5-C10 is obtained from LDPE, production of the former being higher by about 10%. For the mixtures, with increase in the percentage of LDPE, relatively more amount of C12 and above hydrocarbons is obtained. As temperature is increased from 500°C, evolution of product vapours becomes less rapid, and trace amounts of products are detected at 600°C. At the end of each degradation experiment for the mixtures, a charred residue is obtained, which was also observed in case of PET alone. On the other hand, LDPE degrades to completion without much residue (0.1-2%). The charred residue could be mostly due to the formation of PAHs in case of the mixtures, which is due to the presence of PET.

5.7.2 Mechanistic analysis

As already discussed in *Section 5.4*, PET mainly decomposes by heterolytic (ionic) mechanism. However, at higher temperatures, it might also decompose by homolytic means. LDPE, on the other hand, is an addition polymer of ethylene, which essentially decomposes by homolytic (radical) mechanism. TGA experiments confirm that PET degrades earlier than LDPE. Due to the presence of four oxygen atoms in the structural unit of PET, oxides of carbon form a major group of products from its pyrolysis, which is not the case with LDPE. At the same time, phenyl group present in PET leads to the formation of a host of aromatic compounds. The negligible formation of C5-C10 fractions at low temperatures in case of pure PET, is due to the extra stability of the resonance stabilized structures in the chain backbone, which needs higher energy to overcome the attractive forces. As already discussed, detectable

amounts of higher fractions are due to the cyclic oligomers which were formed during polymerization process and remain as weak links in the polymer molecule. On the other hand, pyrolysis of LDPE produces mainly alkane, alkene and diene, wherein the amount of straight chain hydrocarbons is more as compared to the branched ones. As it has already been stated in section 5.2 that although, theoretically all the C-C bonds in LDPE should be of about same strength, short-chain branches also exist along the chain backbone, which are more prone to degradation. Products obtained at 300°C are due to those degradation reactions.

To understand the mechanistic aspects of the decomposition of the binary mixtures, we must refer to decomposition behaviour of the individual plastics. *Scheme 5.4.1* presented the heterolytic chain-scission of PET resulting in the formation of acid end and olefin end; whereas, *Scheme 5.2.1 depicted* random-scission of macromolecular chain of LDPE resulting in hydrocarbons with terminal (primary) free radicals (R_P).

The radicals, thus generated from LDPE, might attack the fragmented chain (acid end, **I**) of PET, transferring the radical center to the PET fragmented chain (*Reaction Scheme 5.7.1*). The higher fraction of C24-C30 hydrocarbons evolved in case of mixtures, indicate the possibility of such intermolecular hydrogen transfer.

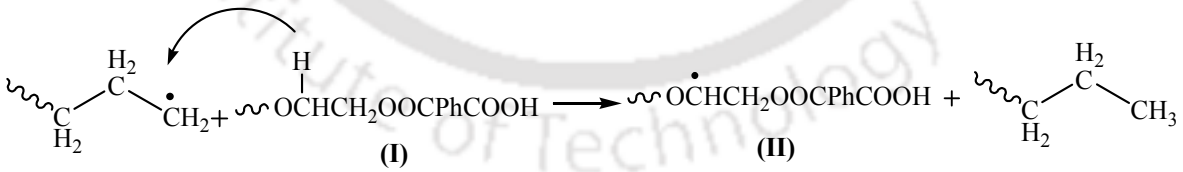

Reaction scheme 5.7.1

Thus, PET is subjected to radical reactions at a relatively lower temperature in presence of LDPE. As in case of PET-PP mixture, the radical (**II**), thus generated can undergo *β*-hydrogen transfer giving rise to terephthalic acid (TPA); and decarboxylation of TPA may yield benzoic acid/ benzene (*Reaction Scheme 5.6.2* in *Section 5.6.2*).

Thus, as in the case of binary mixtures of PET and PP, with PET and LDPE too, formation of benzene is possible at a comparatively lower temperature. Thus, formation of PAHs is more likely in case of the mixtures, than pyrolyzing PET alone. At the same time, formation of cyclic oligomers could also be favored by backbiting. Formation of cyclic trimer is already explained under *Section 5.4*.

Dienes are formed from LDPE at higher temperatures. Butadiene is formed from LDPE chain having terminal double bond by *β*-scission following intermolecular hydrogen transfer. This butadiene might combine with benzene as shown in *Reaction scheme 5.7.2*, leading to the formation of naphthalene. Another molecule of butadiene can combine with naphthalene giving rise to higher PAHs.

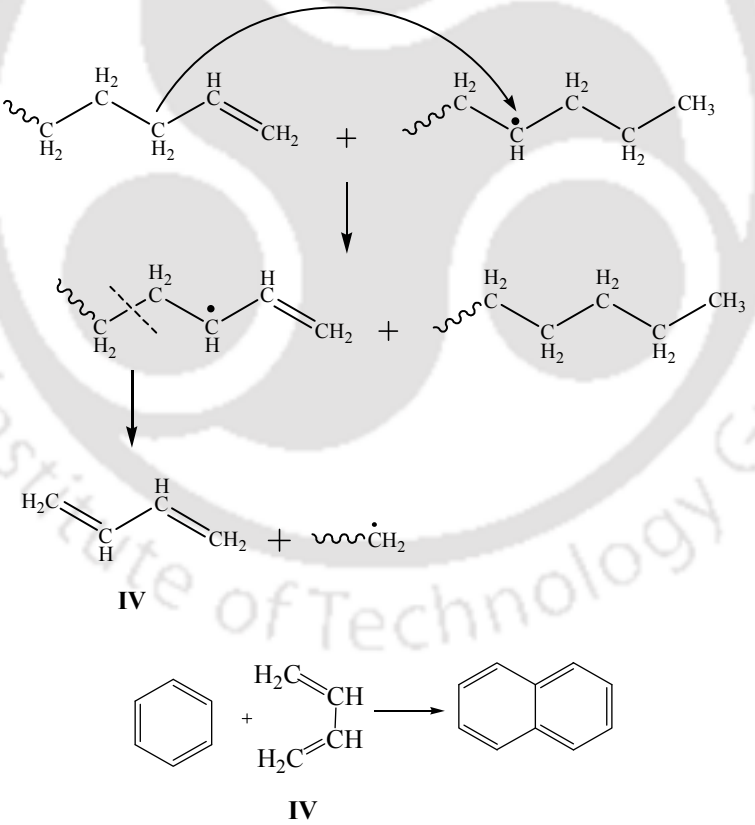

Reaction scheme 5.7.2

5.7.3 Conclusions

In this part of the work, possible effect of interaction of LDPE and PET on the product distribution in their binary mixtures was investigated. A wide distribution of products was obtained at temperatures ≥ 400°C, which could be due to the attack of the free radicals obtained from LDPE on fragmented products of PET decomposition. Production of C5-C10 was considerably high at T_{max}. Beyond T_{max}, significant yield of C16 and higher hydrocarbons was obtained. This could as well be due to increased production PAHs.

5.8 Temperature Dependent Pyrolytic Product Evolution Profile for Ternary Mixture of LDPE, PP and PET

5.8.1 Products Analysis

In an attempt to investigate the effect of the presence of a third component on product distribution, studies were performed on the ternary mixtures of the plastics following same protocol as in case of the binary mixtures. Table 5.6 reports the variation in T_{max} of the ternary mixtures with changes in percentage of LDPE in the mixtures. The experimental values of T_{max} are compared with those calculated from non-interacting model. It is evident from the table that calculated values of T_{max} are different from their experimental values and these values are greater than the latter. Thus, this difference gives a measure of absolute degree of deviation between real decomposition behaviour where, all kinds of interaction take place, and ideal decomposition behaviour, where absolutely no interaction is assumed between the plastics.

Table 5.6 T_{max} for the single and the ternary mixtures of plastics

LDPE (wt.%)	PP (wt.%)	PET (wt.%)	T_{max}, °C (experimental)	T_{max}, °C (non-interacting model)
0	0	100	435	435
0	50	50	434	440.5
25	25	50	426	446.5
25	50	25	429	449.5
50	25	25	436	455.25
0	100	0	446	446
100	0	0	470	470

Figures 5.48-5.52 show the fractional evolution of the C5-C44 hydrocarbons as a function of percentage of LDPE at 300°C, 400°C, T_{max} (for the respective mixture compositions), 500°C and 600°C respectively. Pyrograms of the ternary mixtures at different temperatures are included in *Appendix 3*.

At 300°C, C16-C22 hydrocarbons are the major products from LDPE, whereas C5-C10 is the major product for the 50%PET 50%PP binary mixture. In the ternary mixtures, as percentage of LDPE is increased to 25%, increase in the evolution of C12-C15 is observed for both the mixture compositions wherein %PP and %PET is 50% each. Evolution of C5-C10 essentially remains low for all the three ternary mixture compositions. Just as with the binary mixtures, decomposition process of individual plastics in the ternary mixtures is not much affected by the presence of other plastics at such low temperatures.

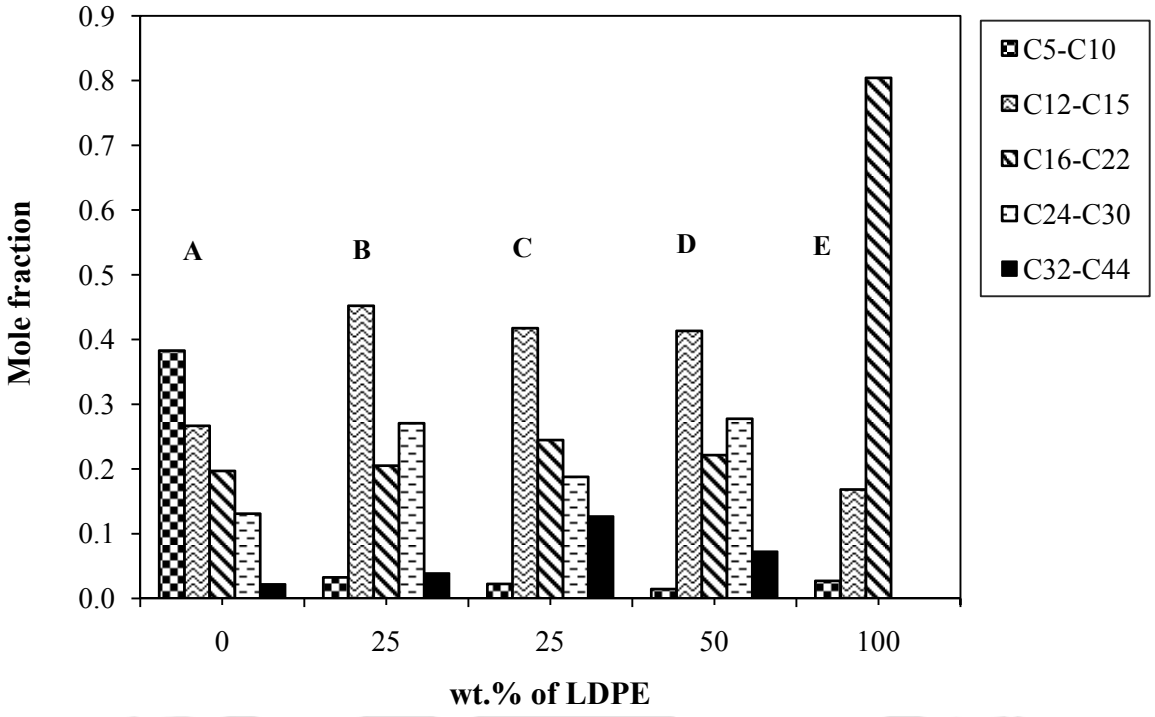

Figure 5.48 Mole fractions of C5-C44 hydrocarbons from pyrolysis of LDPE-PP-PET mixture as a function of wt.% of LDPE at 300^{o}C; (**A**-50%PP 50%PET, **B**-25%LDPE 50%PP 25%PET, **C**-25%LDPE 25%PP 50%PET, **D**-50%LDPE 25%PP 25%PET, **E**-LDPE)

As temperature is increased beyond 300^{o}C, the polymer chains start to break down at a rapid rate, and these fragmented chains of shorter chain lengths are now at a closer proximity to interact among themselves. The extent of cracking reactions and the mutual interaction between the plastics results into a greater yield of lighter hydrocarbons, which can easily escape from the melt. At 400^{o}C, C5-C10 fraction predominates in the ternary mixtures. C16-C22 is invariably the major product for LDPE. On the other hand, C16 and above hydrocarbons form a major share in the product stream obtained from 50%PET 50%PP binary mixture. Amongst the ternary mixes, 25%LDPE 50%PP 25%PET composition results into maximum production of lighter hydrocarbons.

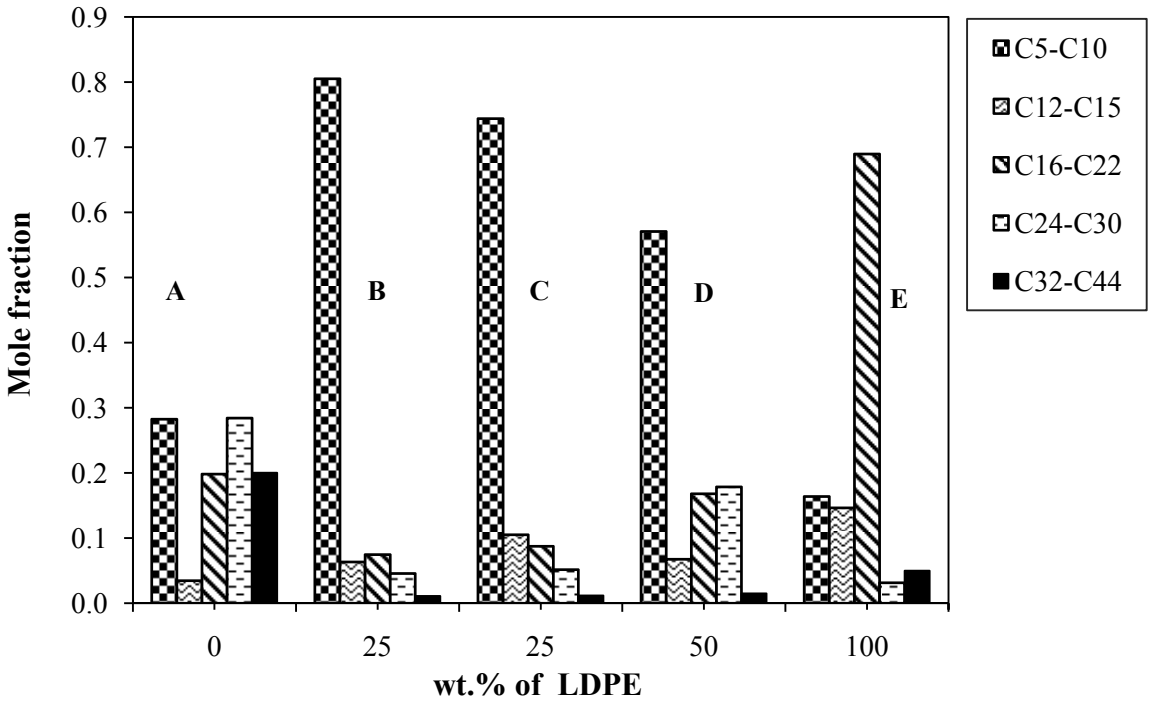

Figure 5.49 Mole fractions of C5-C44 hydrocarbons from pyrolysis of LDPE-PP-PET mixture as a function of wt.% of LDPE at 400^{o}C; (**A**-50%PP 50%PET, **B**-25%LDPE 50%PP 25%PET, **C**-25%LDPE 25%PP 50%PET, **D**-50%LDPE 25%PP 25%PET, **E**-LDPE)

At T_{max}, which is the maximum decomposition temperature for the plastics, maximum evolution of the hydrocarbons take place, due to availability of sufficient energy to undergo cracking reactions. C16-C22 is still the major product obtained from LDPE. Evolution of the other fractions remains more or less the same. For 50%PP 50%PET binary mixture, C5-C10 is the major fraction, while other fractions are obtained in traces, and C32-C44 is almost negligible. For 25%LDPE 50%PP 25%PET composition of ternary mixture, C5-C10 are the major product, while formation of C24 and above hydrocarbons is relatively more as compared with that from binary mixture of PET and PP. For 50%LDPE 25%PP 25%PET combination, yield of C5-C10 is the maximum. Evolution of C16-C22 remains more or less the same, while other fractions are rather negligible.

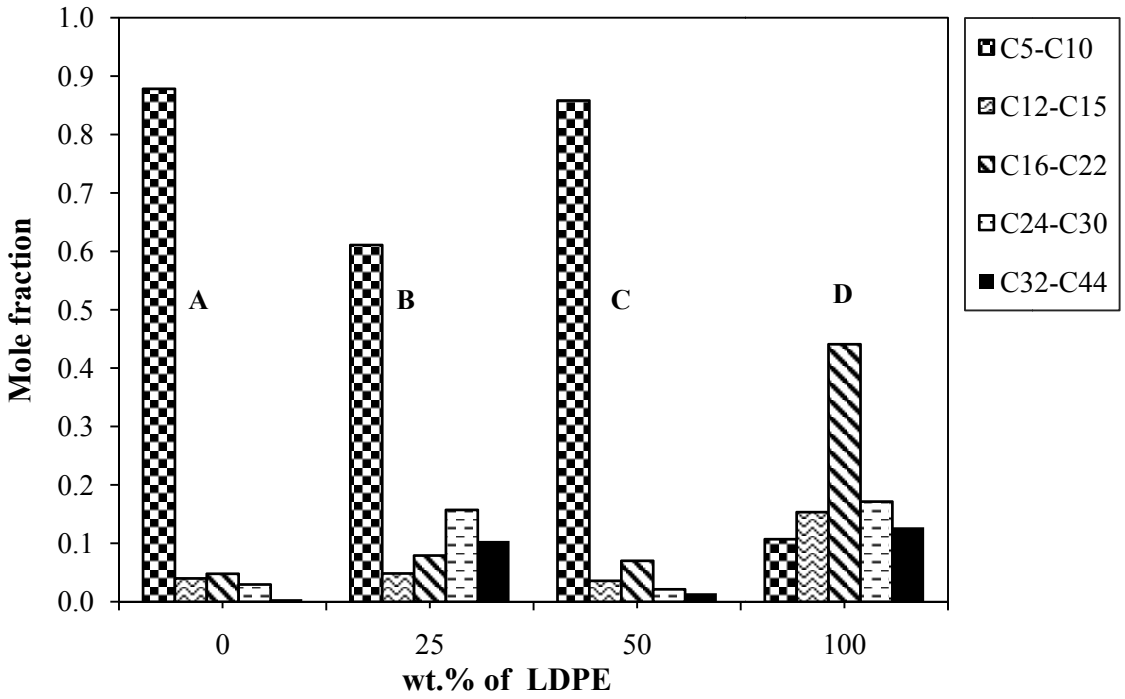

Figure 5.50 Mole fractions of C5-C44 hydrocarbons from pyrolysis of LDPE-PP-PET mixture as a function of wt.% of LDPE at T_{max}; (**A**-50%PP 50%PET, **B**-25%LDPE 50%PP 25%PET, **C**-50%LDPE 25%PP 25%PET, **D**-LDPE)

At 500°C, evolution of C5-C10 substantially decreases for PET-PP binary mixtures (50:50). Evolution of C12 and above hydrocarbons is somewhat more, and also production of C32-C44 hydrocarbons is considerable as compared to that at T_{max}. For LDPE, C12-C15 is the most dominant fraction, C5-C10 being the second largest. The other fractions remain considerably low, while C32-C44 fraction is not observed in the product stream. For 25%LDPE 50%PP 25%PET and 25%LDPE 25%PP 50%PET compositions, evolution of C12-C15 is more than C5-C10. Production of higher hydrocarbons (C16 and above) is also considerably more.

As can be seen from Fig. 5.52, more of higher hydrocarbons are obtained at 600°C. For PET-PP binary mix, formation of C24-C30 is the highest. For LDPE, C16-C22 hydrocarbons are the most dominant product, with C5-C10 being the second highest fraction. For 25%LDPE 50%PP

25%PET and 25%LDPE 25%PP 50%PET ternary mixes, C12-C15 is the dominant fraction, whereas C32-C44 is that for the 50%LDPE 25%PET 25% PP ternary mixture.

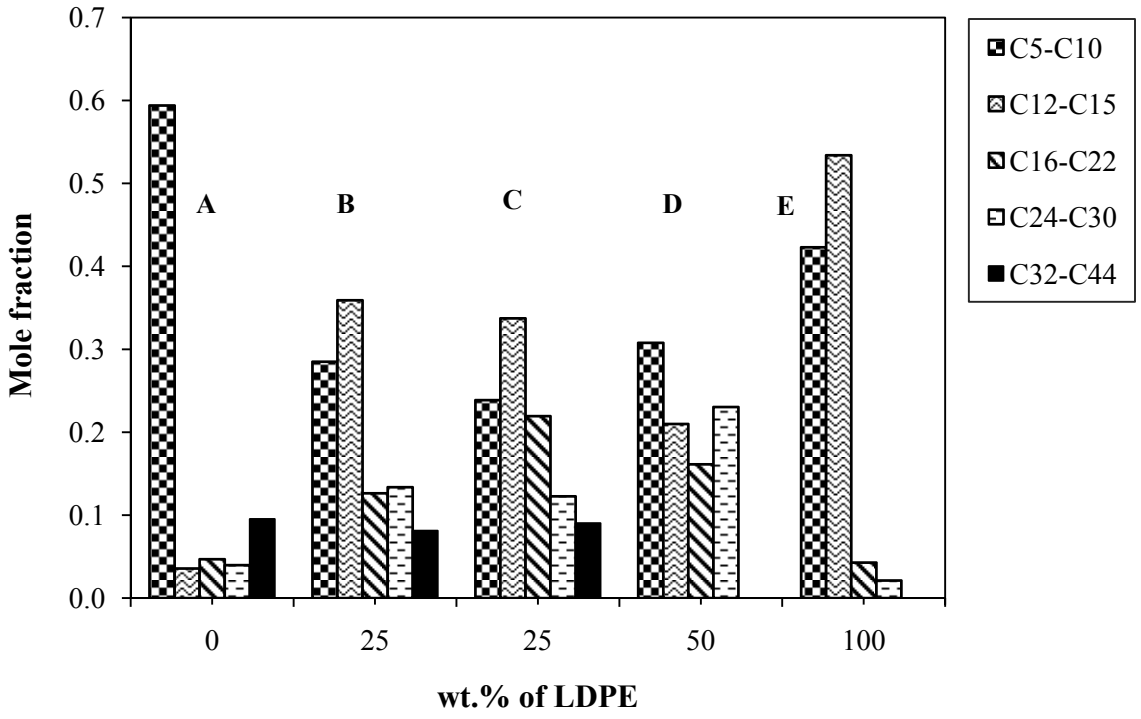

Figure 5.51 Mole fractions of C5-C44 hydrocarbons from pyrolysis of LDPE-PP-PET mixture as a function of wt.% of LDPE at 500^{o}C; (**A**-50%PP 50%PET, **B**-25%LDPE 50%PP 25%PET, **C**-25%LDPE 25%PP 50%PET, **D**-50%LDPE 25%PP 25%PET, **E**-LDPE)

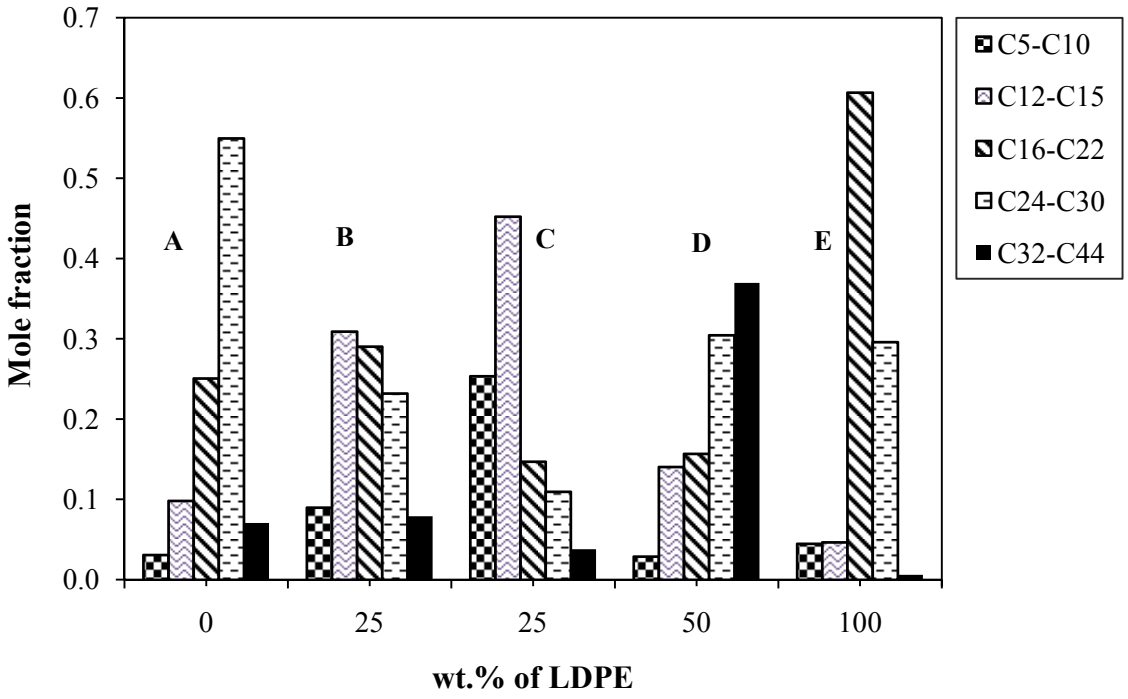

Figure 5.52 Mole fractions of C5-C44 hydrocarbons from pyrolysis of LDPE-PP-PET mixture as a function of wt.% of LDPE at 600^{o}C; (**A**-50%PP 50%PET, **B**-25%LDPE 50%PP 25%PET, **C**-25%LDPE 25%PP 50%PET, **D**-50%LDPE 25%PP 25%PET, **E**-LDPE)

5.8.2 Mechanistic Analysis

The products obtained from pyrolysis carry the fingerprints of the structure of the parent polymer, and depend on their underlying reaction mechanism of decomposition. The interaction among the radicals and the fragmented chains also have a pronounced effect on the product distribution. As stated earlier, PET decomposes mainly by ionic mechanism, whereas both LDPE and PP decomposes by free radical mechanism. Among the three polymers, both LDPE and PP are aliphatic, whereas PET has a *p*-phenylene group (-C_2H_4-) in its structure, which is aromatic. Benzene, toluene, benzoic acid, oxides of carbon, cyclic oilgomers, PAHs are the main products resulting from PET. Again, between LDPE and PP, PP is more reactive due to the presence of tertiary carbon centres at every second carbon atom in the chain backbone. On the whole, alkanes, alkenes and dienes are the main products obtained from

pyrolysis of LDPE and PP. However, branched hydrocarbons are more in the products from PP as compared to those of LDPE, which has already been explained under *Section 5.3*. Therfore, the products resulting from pyrolysis of ternary plastic mixtures will be a combination of the abovementioned products, yield of which will depend on the decomposition temperature, and their relative proportion in the mixture.

As temperature starts to increase, first the weak-links break, and thus the products which are first detected in the outlet stream are due to those weak-links. As stated earlier, PET degrades earlier than both PP and LDPE. The fractions which are detected at low temperature could be due to the linear and cyclic dimers, and trimers which has already been explained under *Section 5.4*. Thus at 300^{o}C, for the ternary mixtures too, the evolved products, which are obtained in traces, are due to the products resulting from weak link scission. Generation of C5-C10 fraction essentially remain low during the start of pyrolysis. As temperature increases further, chain-scission reactions of the macromolecular backbone start to occur. As decomposition of LDPE and PP proceeds by radical pathways, free radicals will be generated following their decomposition. The radicals, thus generated, will try to stabilize themselves, by intra or intermolecular hydrogen transfer, disproportionation, or β-scission reactions etc. It has been observed at 400^{o}C and T_{max} (for the respective mixtures) that relative production of C5-C10 fraction is significantly high in the ternary mixtures as compared with that from PET-PP binary mixture and LDPE alone. Thus, as in the case of binary mixtures of PET-PP and PET-LDPE, with the ternary mixtures too, formation of benzene is possible at a comparatively lower temperature. Thus, formation of PAHs is more likely in case of the mixtures, than pyrolyzing PET alone. At the same time, formation of cyclic oligomers could also be favored by backbiting, which has already been explained under *Section 5.7*.

As temperature increases beyond T_{max}, relative production of C5-C10 fraction comparatively decreases at the expense of C12 and higher species, which could be justified by the fact that radical recombination reactions are favored at such high temperatures. At the same time, increased production of PAHs are likely due to greater probability of radical reactions, by HACA pathways, and also by direct polymerization of PAHs, which has been explained in *Section 5.4*. Thus, mechanistic pathways for decomposition of ternary mixtures can be understood by referring to the decomposition mechanism for the corresponding binary plastic mixtures. This is analogous with our modeling study of pyrolysis behaviour of mixed plastics, in which the ternary decomposition behaviour was predicted with the help of binary interaction parameters without the necessity of doing any experiments.

5.8.3 Conclusions

This work reports product distribution studies carried out for three different compositions of the ternary mixtures of LDPE, PP, and PET. Mechanistic analysis from pyrolysis of ternary mixtures is a challenging task due to the added complexity introduced by the addition of the third component in the mixture. However, in the present work, the preceding study of the thermal decomposition behaviour of the plastics gave us some insight of the degradation process of the mixtures. Here, initially decomposition of the least stable polymer, *i.e.* PET starts. With further rise in temperatures, decomposition process starts for the other two. And once their decomposition starts, mutual interaction takes place within the molten mass of the polymers. At 400 and T_{max}, yield of C5-C10 is more pronounced due to intense cracking reactions. Beyond T_{max}, significant yield of C12 and higher hydrocarbons is obtained.

CHAPTER 6

Conclusions

This chapter presents the conclusions drawn from the present research work and provides recommendations towards future direction.

6.1 Conclusions

Thermal decomposition and corresponding product distribution of three commodity plastics, *viz.* low density polyethylene (LDPE), polypropylene (PP) and polyethylene terephthalate (PET) have been investigated in this study. A model has been developed which could address the interaction taking place between the plastics during pyrolysis. Subsequently, product distribution studies have been carried out for the pure plastics and their binary and ternary mixtures to see the effect of interaction over a wide range of temperature. An attempt has been made to identify the underlying decomposition pathways for the single plastics and their binary and ternary mixtures as a function of decomposition temperature. The overall conclusions are outlined as below:

- Thermal decomposition of constituent plastics in a mixture is not independent of each other. This has been confirmed from significant differences existing in the shape and peak temperature of the experimental DTG curve and non-interacting model in all the binary and ternary mixtures. There exists some degree of interaction between the component plastics. The interacting model proposed in this work is effective in corroborating the experimental observations of all the three binary mixtures *viz.* LDPE-PET, PET-PP and LDPE-PP over a wide range of compositions. The model has also successfully predicted the peak temperatures for all the binary compositions without

much deviation. A practical advantage of the proposed method is in prediction of degradation kinetics of any mixture with minimum experiments. The ternary mixture kinetics have also been predicted fairly well with the help of binary interaction parameters (β_{ij} and γ_{ij}) alone.

- For LDPE and PP, which are addition polymers, product formation at low temperature ($\leq 300^{o}C$) is assigned to bond fission of weak links; at high temperatures, random scission of C-C bond is responsible for the overall degradation process. Maximum amount of pyrolyzates are obtained in the T_{max}, which is due to intense cracking reactions at that temperature. 1,5-intra-molecular hydrogen transfer justifies preferential formation of some particular hydrocarbons like those containing C6, C10, C14, C22 alkenes and C3, C7, C11, C15 alkanes (in case of LDPE), and C5, C11, C17, C23 alkanes and C9, C15, C21, C27 alkenes (in case of PP) over others. C5-C7 and C5-C10 hydrocarbons were the most dominant species obtained at T_{max} for LDPE and PP respectively. On the other hand, thermal decomposition of PET, which is a condensation polymer, advances primarily by ionic mechanism. At low temperature ($200\text{-}300^{o}C$), product obtained is due to the formation or elimination of cyclic oligomers. Other hydrocarbons, (e.g., TPA, MVT, DVT) are the result of random scission of the ester linkage. At high temperatures (at or above $400^{o}C$), however, radical reactions come into play. This results in the formation of benzene, which is the precursor for PAHs. Thus, at higher temperature possibility of formation of PAH increases.
- Product distribution study carried out on binary mixtures of LDPE-PP too reveals interaction effects among the two plastics. At low temperature, evolution of C16-C22 is predominant in LDPE, whereas C12-C15 is predominant in the mixtures, which is due to mutual interaction between PP and LDPE. Evolution of C5-C10 increases in all the

mixture compositions when each of the mixture reaches T_{max}, and it is the highest for the 50%LDPE 50%PP mixture composition. With increase in the percentage of PP in the mixture, production of C12-C15 and C16-C22 hydrocarbons decrease, while C24-C30, C32-C44 fractions increase. Thus, increase in PP content in the mixtures led to formation of heavier hydrocarbons

- For binary mixtures of PP and PET, at very low temperature, interactions between the two plastics are not very prominent, and their decomposition mechanism is somewhat independent of each other. However, PET in the mixture is subjected to radical reactions at a relatively lower temperature (≈400^{o}C) than when PET is pyrolyzed alone, indicating the presence of synergistic effects at that temperature. This results in greater yield of benzene, and hence PAHs. At T_{max} yield of C5-C10 fraction is the highest for 50%PP 50%PET mixture. The major products obtained from the mixtures are likely to be benzene, styrene, vinyl benzoate, pentene, pentane.
- For the LDPE-PET mixtures too, at low temperatures, interaction between the plastics is not evident, and products that result from the plastics are due to their weak link scission. However, with increase in temperatures their mutual interaction affects the overall product distribution. At T_{max}, with increase in the percentage of LDPE, relatively more amount of C12 and above hydrocarbons is obtained. C5-C10 is the major fraction in case of the mixtures, except for 80%LDPE 20%PET, where C32-C44 is predominant.
- Just as with the binary mixtures, decomposition process of individual polymers in the ternary mixtures is not much affected by the presence of other components at such low temperatures. However, at higher temperatures (≥400^{o}C), yield of C5-C10 increases, which is suggestive of existence of favorable interaction among the plastics in their melt. In the ternary mixtures too, formation of benzene is favored at a lower

temperature (≈400^{o}C) in the mixtures than when PET is pyrolyzed alone. Thus, formation of PAHs possibly increases for the ternary mixtures too. As temperature increases beyond T_{max}, production of C5-C10 fraction comparatively decreases, while C12 and higher species increase due to greater prevalence of radical recombination reactions.

6.2 Future Work

This work has shown a direct link between the pyrolytic decomposition behavior of plastics and products obtained from their pyrolysis. However, the scope of the present research work did not permit us to explore certain areas for the present study, which could be accomplished in our future research endeavors. These areas are as outlined below:

- Plastics present in the real waste stream might also include HDPE, PS and PVC, apart from LDPE, PP and PET. The interacting model proposed in this work can be readily extended to higher order multi-component systems comprising of these plastics to simulate decomposition behavior of real plastic mixtures, which exist in waste plastic pyrolysis reactors.
- Study of product distribution from pyrolysis of these multi-component plastics can be carried out by carrying out TGA coupled with evolved gas analysis by GC or GC/MS
- Study of product distribution at a particular temperature as a function of time needs to be carried out, which would help in generation of useful information, *viz.* feed composition, degradation temperature and residence time for design of experiments for obtaining desired products from pyrolysis of mixed plastics.
- Design of a reactor system for pyrolysis of the mixed plastics to get desired range of liquid and gaseous hydrocarbons at optimum reaction conditions.

REFERENCES

[1] Ministry of Environment and Forests Notification, New Delhi, 25th September, 2000. Available at: http://envfor.nic.in/legis/hsm/mswmhr.html

[2] http://www.indiatogether.org/2004/apr/env-rethink.htm

[3] USEPA, "*Municipal Solid Waste Generation, Recycling and Disposal in the United States: 2010 Facts and Figures*", United States Environmental Protection Agency, Solid Waste Management and Emergency Response (5306P), EPA-530-F-11-005, Washington, December 2011. Available at: http://www.epa.gov/

[4] Beede, D.N. and Bloom, D.E., "Economics of the generation and management of MSW", *NBER Working Papers 5116*, National Bureau of Economic Research, Cambridge, Massachusetts, USA, May 1995.

[5] Annepu, R.K., "*Sustainable Solid Waste Management in India*", MS Thesis, Department of Earth and Environmental Engineering, The Fu Foundation School of Engineering and Applied Science, Columbia University, NY, USA, 2012.

[6] UNEP, "*Converting Waste Plastics Into a Resource. Assessment Guidelines*", United Nations Environmental Programme, Division of Technology, Industry and Economics, International Environmental Technology Centre, Osaka/Shiga, Japan, 2009.

[7] USEPA, "*Municipal Solid Waste in the United States: 2000 Facts and Figures*", United States Environmental Protection Agency, Solid Waste Management and Emergency Response (5305W), EPA530-R-02-001, June, 2002. Available at: http://www.epa.gov/

[8] The Report of the National Plastic Waste Management Task Force, Ministry of Environment and Forests, New Delhi, Government of India, 1997.

[9] Gupta S., Mohan K., Prasad R., Gupta S. and Kansal A., "Solid waste management in India: options and opportunities", *Resources Conservation and Recycling*, 24(2) (1998) 137–154.

[10] Clark, J.H. and Hardy, J.J.E., "Towards sustainable chemical manufacturing: polylactic acid – a sustainable polymer?", In: Azapagic, A., Perdon, S. and Clift, R. (Eds.), *Sustainable Development in Practice: Case Studies for Engineers and Scientists*, 1st ed., Wiley, 2004, 250–282.

[11] Siddique, R., "*Waste materials and by-products in concrete*", Springer, 2008.

[12] http://www.epa.gov/epawaste/conserve/rrr/reduce.htm

[13] JCR., "*Plastics recycling*", Final assessment report, St. Catherine's College JCR, University of Oxford (UK). Available at: http://hadriel.caths.camac.uk/jcr/html/, 2006.

[14] Perdon, S., "Introduction to sustainable development", In: Azapagic, A., Perdon, S. and Clift, R., (Eds.), *Sustainable Development in Practice: Case studies for engineers and scientists*, 1st ed., Wiley, 2004.

[15] Al-Salem S.M., Lettieri P. and Baeyens J., "The valorization of plastic solid waste (PSW) by primary to quaternary routes: From re-use to energy and chemicals", *Progress in Energy and Combustion Science*, 36 (1) (2010) 103–129.

[16] Ehrig, R.J., (Ed.), "*Plastics Recycling: Products and Services*", Hanser Publishers, 1992.

[17] Plastics recycling information sheet, http://www.wasteonline.org.uk/resources/InformationSheets/plastics.htm

[18] Al-Salem S.M., Lettieri P. and Baeyens J., "Recycling and recovery routes of plastic solid waste (PSW): A review", *Waste Management*, 29 (10) (2009) 2625–2643.

[19] Mastellone, M.L., "*Thermal treatments of plastic wastes by means of fluidized bed reactors*", Ph.D. Thesis, Department of Chemical Engineering, Second University of Naples, Italy, 1999.

[20] Williams, E.A. and Williams, P.T., "The pyrolysis of individual plastics and plastic mixture in a fixed bed reactor", *Journal of Chemical Technology and Biotechnology* 70 (1) (1997) 9–20.

[21] Mastellone, M.L., Perugini, F., Ponte, M. and Arena, U., "Fluidized bed pyrolysis of a recycled polyethylene", *Polymer Degradation and Stability*, 76 (3) (2002) 479–487.

[22] L'vov B.V., "*Thermal Decomposition of Solids and Melts: New Thermochemical Approach to the Mechanism, Kinetics and Methodology*", Springer, 2007.

[23] ASTM Standard E176, "Standard terminology of fire standards," ASTM International, West Conshohocken, PA, DOI: 10.1520/E0176-10AE01, www.astm.org.

[24] Bamford, C.H. and Tipper, C.F.H., (Eds.), "*Comprehensive Chemical Kinetics*", Volume 22, Elsevier Publishing Company, New York, 1980.

[25] Prout, E.G. and Herley, P.J., "A constant temperature reaction vessel for the thermal decomposition of solids", *Journal of Chemical Education*, 37(12) (1960) 643.

[26] Galwey, A.K., "Thermal decomposition of $KMnO_4$: A high vacuum experiment for students", *Journal of Chemical Education*, 37(2) (1960) 98-99.

[27] Goldstein, M.K. and Flanagan, T.B., "Kinetics of the thermal decomposition of silver permanganate: A solid-state chemistry experiment", *Journal of Chemical Education*, 41(5) (1964) 276-277.

[28] Heal, G.R., "A generalisation of the non-parametric, NPK (SVD) kinetic analysis method: Part 1. Isothermal experiments", *Thermochimica Acta*, 426(1-2) (2005) 15-21.

[29] Heal, G.R., "A generalisation of the non-parametric, NPK (SVD) kinetic analysis method: Part 2. Non-isothermal experiments", *Thermochimica Acta*, 426 (1-2) (2005) 23-31.

[30] Bockhorn, H., Hornung, A. and Hornung, U., "Mechanisms and kinetics of thermal decomposition of plastics from isothermal and dynamic measurements", *Journal of Analytical and Applied Pyrolysis*, 50 (2) (1999) 77-101.

[31] Brown, M.E., Maciejewski, M., Vyazovkin, S., Nomen, R., Sempere, J., Burnham, A.K., Opfermann, J., Strey, R., Anderson, H.L., Kemmler, A., Keuleers, R., Janssens, J., Desseyn, H.O., Tang, T.B., Li, C-R., Roduit, B., Malek, J. and Mitsuhashi, T., "Computational aspects of kinetic analysis: Part A: The ICTAC kinetics project-data, methods and results", *Thermochimica Acta*, 355(1-2) (2000) 125-143.

[32] Mamleev, V., Bourbigot, S., Bras, M.L, Duquesne, S. and Šesták, J., "Modeling of nonisothermal kinetics in thermogravimetry", *Physical Chemistry Chemical Physics*, 2(20) (2000) 4708-4716.

[33] Saha, B. and Ghoshal, A.K., "Thermal degradation kinetics of polyethylene terephthalate from waste soft drink bottles", *Chemical Engineering Journal* 111 (1) (2005) 39-43.

[34] Pielichowski K. and Njuguna J., "*Thermal Degradation of Polymeric Materials*," Rapra Technology Ltd., Shawbury, UK, 2005.

[35] Flammersheim H.J. and Opfermann J.R., "Formal kinetic evaluation of reactions with partial diffusion control", *Thermochimica Acta*, 337(1-2) (1999) 141-148.

[36] Opfermann J.R., Kaisersberger E. and Flammersheim H.J., "Model-free analysis of thermoanalytical data-advantages and limitations", *Thermochimica Acta*, 391 (2002) 119-127.

[37] Vyazovkin, S. and Wight, C.A., "Model-free and model-fitting approaches to kinetic analysis of isothermal and nonisothermal data", *Thermochimica Acta*, 340-341 (1999) 53-68.

[38] Khawam, A. and Flanagan, D.R., "Role of isoconversional methods in varying activation energies of solid-state kinetics: I. Isothermal kinetic studies", *Thermochimica Acta*, 429(1) (2005) 93–102.

[39] Khawam, A. and Flanagan, D.R., "Role of isoconversional methods in varying activation energies of solid-state kinetics: II. Nonisothermal kinetic studies", *Thermochimica Acta*, 436(1-2) (2005) 101–112.

[40] Galwey, A.K. and Brown, M.E., "*Thermal Decomposition of Ionic Solids: Chemical Properties and Reactivities of Ionic Crystalline Phases"*, 1st ed., Elsevier, Amsterdam, 1999.

[41] Madras, G., Chung, G.Y., Smith, J.M. and McCoy, B.J., "Molecular weight effect on the dynamics of polystyrene degradation", *Industrial and Engineering Chemistry Research*, 36 (6) (1997) 2019-2024.

[42] Burnham, A.K., "Application of the sestak-Berggren equation to organic and inorganic materials of practical interest", *Journal of Thermal Analysis and Calorimetry*, 60(3) (2000) 895-908.

[43] Burnham, A.K. and Weese, R.K., "Kinetics of thermal degradation of explosive binders Viton A, Estane, and Kel-F", *Thermochimica Acta*, 426(1-2) (2005) 85-92.

[44] Keattch, C.J. and Dollimore, D., "*An Introduction to Thermogravimetry*", Heyden, 2nd Ed., London, 1975.

[45] Widmann, G., "Quantitative isothermal DTA-studies" *Thermochimica Acta*, 11(3) (1975) 331-333.

[46] Friedman, H.L., "Kinetics of thermal degradation of char-forming plastics from thermogravimetry. Application to a phenolic plastic", *Journal of Polymer Science*, *PartC: Polymer Symposia*, 6(1) (1964) 183-195.

[47] Hornung, U., Hornung, A. and Bockhorn, H., "Investigation of thermal degradation of solids in an Isothermal, Gradient Free Reactor", *Chemical Engineering Technology*, 21(4) (1998) 332-337.

[48] Martin-Gullon, I., Esperanza, M. and Font, R., "Kinetic model for the pyrolysis and combustion of poly-(ethylene terephthalate) (PET)", *Journal of Analytical and Applied Pyrolysis*, 58-59 (2001) 635-650.

[49] Mamleev, V. and Bourbigot, S., "Modulated thermogravimetry in analysis of decomposition kinetics", *Chemical Engineering Science*, 60(3) (2005) 747-766.

[50] Wang, X-S., Li, X-G. and Yan, D., "Thermal decomposition kinetics of poly(trimethylene terephthalate)", *Polymer Degradation and Stability*, 69 (3) (2000) 361-372.

[51] Gao, Z., Amasaki, I. and Nakada, M., "A thermogravimetric study on thermal degradation of polyethylene", *Journal of Analytical and Applied Pyrolysis*, 67(1) (2003) 1-9.

[52] Saha, B. and Ghoshal, A.K., "Model-fitting methods for evaluation of the kinetics triplet during thermal decomposition of poly(ethylene terephthalate) (PET) soft drink bottles", *Industrial and Engineering Chemistry Research*, 45(23) (2006) 7752-7759.

[53] Westerhout, R.W.J., Waanders, J., Kuipers, J.A.M. and Van Swaaij, W.P.M., "Kinetics of the low-temperature pyrolysis of polyethene, polypropene, and polystyrene modeling, experimental determination, and comparison with literature models and data", *Industrial and Engineering Chemistry Research*, 36(6) (1997) 1955-1964.

[54] Gao, Z., Amasaki, I., Kaneko, T. and Nakada, M., "Calculation of activation energy from fraction of bonds broken for thermal degradation of polyethylene", *Polymer Degradation and Stability*, 81(1) (2003) 125-131.

[55] Gao, Z., Kaneko, T., Amasaki, I. and Nakada, M., "A kinetic study of thermal degradation of polypropylene", *Polymer Degradation and Stability*, 80(2) (2003), 269-274.

[56] Saha, B., Karthik Reddy, P. and Ghoshal, A.K., "Hybrid Genetic Algorithm to Find the Best Model and the Globally Optimized Overall Kinetics Parameters for Thermal Decomposition of Plastics", *Chemical Engineering Journal*, 138(1-3) (2008) 20-29.

[57] Saha, B., and Ghoshal, A.K., "Model-free kinetics analysis of waste PE sample", *Thermochimica Acta*, 451 (1-2) (2006) 27-33.

[58] Saha, B. and Ghoshal, A.K., "Model-free Kinetics Analysis of Decomposition of Polypropylene over Al-MCM-41", *Thermochimica Acta*, 460(1-2) (2007) 77-84.

[59] Saha, B., Reddy, P.K., Chowlu, A.C.K. and Ghoshal, A.K., "Model-free kinetics analysis of nanocrystalline HZSM-5 catalyzed pyrolysis of polypropylene (PP)", *Thermochimica Acta*, 468(1-2) (2008) 94-100.

[60] Vyazovkin, S. and Sbirrazzuoli, N., "Isoconversional Kinetic Analysis of Thermally Stimulated Processes in Polymers", *Macromolecular Rapid Communications*, 27(18) (2006) 1515-1532.

[61] Peterson, J.D., Vyazovkin, S. and Wight, C.A., "Kinetics of the Thermal and Thermo-Oxidative Degradation of Polystyrene, Polyethylene and Poly(propylene)", *Macromolecular Chemistry and Physics*, 202(6) (2001) 775-784.

[62] Saha, B., Maiti, A.K. and Ghoshal, A.K., "Model-free method for isothermal and non-isothermal decomposition kinetics analysis of PET sample", *Thermochimica Acta*, 444(1) (2006) 46-52.

[63] Filho, J.G.A.P., Graciliano, E.C., S. Silva A.O., Souza, M.J.B. and Araujo, A.S., "Thermo gravimetric kinetics of polypropylene degradation on ZSM-12 and ZSM-5 catalysts", *Catalysis Today*, 107-108 (2005) 507-512.

[64] Chiu, S.J. and Cheng W.H., "Thermal degradation and catalytic cracking of poly(ethylene terephthalate)", *Polymer Degradation and Stability*, 63(3) (1999) 407-412.

[65] Marcilla, A., Beltran, M. and Conesa, J.A., "Catalyst addition in polyethylene pyrolysis thermogravimetric study", *Journal of Analytical and Applied Pyrolysis*, 58–59 (2001) 117–126.

[66] Miranda, R., Yang, J., Roy, C. and Vasile C., "Vacuum pyrolysis of commingled plastics containing PVC I. Kinetic study", *Polymer Degradation and Stability*, 72(3) (2001) 469-491.

[67] Chowlu, A.C.K., Reddy, P.K. and Ghoshal, A.K., "Pyrolytic decomposition and model-free kinetics analysis of mixture of polypropylene (PP) and low-density polyethylene (LDPE)", *Thermochimica Acta*, 485(1-2) (2009) 20-25.

[68] Woo, O.S., Kruse, T.M. and Broadbelt, L.J., "Binary mixture pyrolysis of polystyrene and poly (α-methylstyrene)", *Polymer Degradration and Stability*, 70(2) (2000) 155-160.

[69] Richards, D.H. and Salter, D.A., "Thermal degradation of vinyl polymers I—Thermal degradation of polystyrene-poly(α-methylstyrene) mixtures", *Polymer*, 8 (1967) 127-138.

[70] Richards, D.H. and Salter, D.A., "Thermal degradation of vinyl polymers II—The synthesis and degradation of polystyrene containing thermally weak bonds", *Polymer*, 8 (1967) 139-152.

[71] Richards, D.H. and Salter, D.A., "Thermal degradation of vinyl polymers III-A radiochemical study of intermolecular chain transfer in the thermal degradation of polystyrene", *Polymer*, 8 (1967) 153-159.

[72] Kruse, T.M., Levine, S.E., Wong, H.W., Duoss, E., Lebovnitz, A.H., Torkelson, J.M. and Broadbelt L.J., "Binary mixture pyrolysis of polypropylene and polystyrene: A modeling and experimental study", *Journal of Analytical and Applied Pyrolysis*, 73(2) (2005) 342-354.

[73] Kruse, T.M., Woo, O.S., Wong, H.W., Khan, S.S. and Broadbelt L.J., "Mechanistic modeling of polymer degradation: A comprehensive study of polystyrene", *Macromolecules*, 35(20) (2002) 7830-7844.

[74] Kruse, T.M., Wong, H.W. and Broadbelt L.J., "Mechanistic modeling of polymer pyrolysis: Polypropylene", *Macromolecules*, 36 (25) (2003) 9594-9607.

[75] Faravelli, T., Bozzano, G., Colombo, M., Ranzi, E. and Dente, M., "Kinetic modeling of the thermal degradation of polyethylene and polystyrene mixtures", *Journal of Analytical and Applied Pyrolysis*, 70(2) (2003) 761-777.

[76] Bockhorn, H., Hentschel, J., Hornung, A. and Hornung, U., "Environmental Engineering: Stepwise pyrolysis of plastic waste", *Chemical Engineering Science*, 54(15-16) (1999) 3043-3051.

[77] Marcilla, A., García-Quesada, J.C., Sánchez, S. and Ruiz, R., "Study of the catalytic pyrolysis behaviour of polyethylene–polypropylene mixtures", *Journal of Analytical and Applied Pyrolysis*, 74(1-2) (2005), 387-392.

[78] Marcilla, A., Gómez, A., Reyes-Labarta, J.A. and Giner, A., "Catalytic pyrolysis of polypropylene using MCM-41: kinetic model", *Polymer Degradation and Stability*, 80(2) (2003) 233-240.

[79] Chan, J.H. and Balke, S.T., "The thermal degradation kinetics of polypropylene: Part III. Thermogravimetric analyses", *Polymer Degradation and Stability*, 57(2) (1997) 135-149.

[80] Bockhorn, H., Hornung, A., Hornung, U. and Schawaller D., "Kinetic study on the thermal degradation of polypropylene and polyethylene", *Journal of Analytical and Applied Pyrolysis*, 48(2) (1999) 93-109.

[81] Johannes, I., Tamvelius, H. and Tiikma, L., "A step-by-step model for pyrolysis kinetics of polyethylene in an autoclave under non-linear increase of temperature", *Journal of Analytical and Applied Pyrolysis*, 72(1) (2004) 113-119.

[82] Chan, J.H. and Balke, S.T., "The thermal degradation kinetics of polypropylene: Part I. Molecular weight distribution", *Polymer Degradation and Stability*, 57(2) (1997) 113-125.

[83] Chan, J.H. and Balke, S.T., "The thermal degradation kinetics of polypropylene: Part II. Time-temperature superposition", *Polymer Degradation and Stability*, 57(2) (1997) 127-134.

[84] Faravelli, T., Pinciroli, M., Pisano, F., Bozzano, G., Dente, M. and Ranzi, E., "Thermal degradation of polystyrene", *Journal of Analytical and Applied Pyrolysis*, 60 (1) (2001) 103-121.

[85] Ranzi, E., Dente, M., Faravelli, T., Bozzano, G., Fabini, S., Nava, R., Cozzani, V. and Tognotti, L., "Kinetic Modeling of Polyethylene and Polypropylene Thermal Degradation", *Journal of Analytical and Applied Pyrolysis*, 40-41 (1997) 305-319.

[86] Poutsma, M.L., "Reexamination of the pyrolysis of polyethylene: Data needs, free-radical mechanistic considerations, and thermochemical kinetic simulation of initial product-forming pathways", *Macromolecules*, 36(24) (2003) 8931-8957.

[87] Marongiu, A., Faravelli, T. and Ranzi, E., "Detailed kinetic modeling of the thermal degradation of vinyl polymers", *Journal of Analytical and Applied Pyrolysis*, 78(2) (2007) 343-362.

[88] Mehta, K. and Madras, G., "Dynamics of molecular weight distributions for polymer scission", *AIChE Journal*, 47(11) (2001) 2539-2547.

[89] Sterling, W.J. and McCoy, B.J., "Distribution kinetics of thermolytic macromolecular reactions", *AICHE Journal*, 47(10) (2001) 2289-2303.

[90] Kumar, G.S., Kumar, V.R. and Madras, G., "Continuous distribution kinetics for the thermal degradation of LDPE in solution", *Journal of Applied Polymer Science*, 84(4) (2002) 681-690.

[91] Fake, D.M., Nigam, A. and Klein, M.T., "Mechanism based lumping of pyrolysis reactions: Lumping by reactive intermediates", *Applied catalysis A: General*, 160(1) (1997) 191-221.

[92] Ranzi, E., Dente, M., Goldaniga, A., Bozzano, G. and Faravelli, T., "Lumping procedures in detailed kinetic modeling of gasification, pyrolysis, partial oxidation and combustion of hydrocarbon mixtures", *Progress in Energy and Combustion Science*, 27(1) (2001) 99-139.

[93] Lin, Y.-H., Hwu, W.-H., Ger, M.-D., Yeh, T.-F. and Dwyer, J., "A combined kinetic and mechanistic modeling of the catalytic degradation of polymers", *Journal of Molecular Catalysis A-Chemical*, 171(1-2) (2001) 143-151.

[94] Cardona, S.C. and Corma, A., "Kinetic study of the catalytic cracking of polypropylene in a semibatch stirred reactor", *Catalysis Today*, 75(1-4) (2002) 239-246.

[95] Buekens, A., "Introduction of feedstock recycling of plastics", In. Scheirs, J. and Kaminsky, W., (Eds.), *Feedstock Recycling and Pyrolysis of Waste Plastics*, John Wiley & Sons Ltd, West Sussex, 2006.

[96] Lattimer, R.P., "Pyrolysis field ionization mass spectrometry of polyolefins", *Journal of Analytical and Applied Pyrolysis*, 31 (1995) 203-225.

[97] Holland, B.J. and Hay, J.N., "The thermal degradation of PET and analogous polyesters measured by thermal analysis–Fourier transform infrared spectroscopy", *Polymer*, 43(6) (2002) 1835-1847.

[98] Montaudo G., Puglisi C. and Samperi F., "Primary thermal degradation mechanisms of PET and PBT', *Polymer Degradation and Stability*, 42 (1) (1993) 13-28.

[99] Buxbaum, L. H., "The Degradation of Poly(ethylene terephthalate)", *Angewandte Chemie International Edition*, 7(3) (1968) 182-190.

[100] Zimmermann, H., "Degradation and Stabilization of polyesters", In. Grassie, N., (Ed.), *Developments in Polymer Degradation*, Elsevier Applied Science Publishers Ltd., Volume 5, London, 1984.

[101] McNeill, I. C. and Bounekhel, M., "Thermal degradation studies of terephthalate polyesters: 1. Poly(alkylene terephthalates)", *Polymer Degradation and Stability*, 34(1-3) (1991) 187-204.

[102] Frenklach, M., Clary, D., Gardiner, W.C. and Stein, S.E., "Detailed kinetic modeling of soot formation in shock-tube pyrolysis of acetylene", In: *Twentieth International Symposium on Combustion,* The Combustion Institute, Pittsburgh, (1984) 887–901.

[103] Mukherjee, J., Sarofim, A.F. and Longwell, J.P., "Polycyclic Aromatic Hydrocarbons from the High-Temperature Pyrolysis of Pyrene", *Combustion and Flame*, 96(3) (1994) 191-200.

[104] Lee, K-H. and Shin, D-H., "Characteristics of liquid product from the pyrolysis of waste plastics mixture at low and high temperatures: Influence of lapse time of reaction", *Waste Management*, 27(2) (2007) 168-176.

[105] Walendziewski, J. and Steininger, M., "Thermal and catalytic conversion of waste polyolefines", *Catalysis Today*, 65(2-4) (2001) 323-330.

[106] Mastral, J.F., Berrueco, C. and Ceamanos, J., "Modelling of the pyrolysis of high density polyethylene: Product distribution in a fluidized bed reactor", *Journal of Analytical and Applied Pyrolysis*, 79(1-2) (2007) 313-322.

[107] Faravelli, T., Bozzano, G., Scassa, C., Perego, M., Fabini, S., Ranzi, E. and Dente, M., "Gas product distribution from polyethylene pyrolysis", *Journal of Analytical and Applied Pyrolysis*, 52(1) (1999) 87-103.

[108] Williams P.T. and Williams E.A., "Recycling plastic waste by pyrolysis", *Journal of the Institute of Energy*, 71 (1998), 81-93.

[109] Kaminsky, W. and Sinn, H., "Petrochemical Processes for Recycling Plastics", In Brandrup, H.J., Bittner, M., Michaeli, W. and Menges, G., (Eds.), *Recycling and Recovery of Plastics*, Hanser 1996, München, 434-443.

[110] Samperi F., Puglisi C., Alicata, R. and Montaudo G., "Thermal degradation of poly(ethylene terephthalate) at the processing temperature", *Polymer Degradation and Stability*, 83(1) (2004) 3-10.

[111] Kaminsky, W., Schlesselmann, B. and Simon, C.M., "Thermal degradation of mixed plastic waste to aromatics and gas" *Polymer Degradation and Stability*, 53(2) (1996) 189-197.

[112] Conesa, J.A., Font, R., Marcilla, A. and Caballero, J.A., "Kinetic model for the continuous pyroiysis of two types of polyethylene in a fluidized bed reactor", *Journal of Analytical and Applied Pyrolysis*, 40-41 (1997) 419-431.

[113] Williams, E.A. and Williams, P.T., "The pyrolysis of individual plastics and a plastic mixture in a fixed bed reactor", *Journal of Chemical Technology and Biotechnology*, 70 (1) (1997) 9–20.

[114] Bhaskar T., Uddin, M.A., Murai, K., Kaneko, J., Hamano, K., Kusaba, T., Muto, A. and Sakata, Y., "Comparison of thermal degradation products from real municipal waste plastic and model mixed plastics", *Journal of Analytical and Applied Pyrolysis*, 70(2) (2003) 579-587.

[115] Ortega, D., Noreña, L., Aguilar, J., Hernández, I. and Ramírez, V., "Recycling of plastic materials employing zeolite amd MCM-41 materials", *Revista Mexicana de Ingenería Química*, 5(3) (2006) 189-195.

[116] Achilias, D.S., Roupakias, C., Megalokonomos, P., Lappas, A.A. and Antonakou, E.V., "Chemical recycling of plastic wastes made from polyethylene (LDPE and HDPE) and polypropylene (PP)", *Journal of Hazardous Materials*, 149(3) (2007) 536-542.

[117] Miranda, R., Pakde,l H., Roy, C. and Vasile, C., "Vacuum pyrolysis of commingled plastics containing PVC II. Product analysis", *Polymer Degradation and Stability*, 73(1) (2001) 47-67.

[118] Seo, Y-H., Lee, K-H. and Shin, D-H., "Investigation of catalytic degradation of high-density polyethylene by hydrocarbon group type analysis", *Journal of Analytical and Applied Pyrolysis*, 70(2) (2003) 383-398.

[119] Predel, M. and Kaminsky, W., "Pyrolysis of mixed polyolefins in a fluidized-bed reactor and on a pyro-GC/MS to yield aliphatic waxes", *Polymer Degradation and Stability*, 70(3) (2000) 373-385.

[120] Williams, P.T. and Slaney, E., "Analysis of products from the pyrolysis and liquefaction of single plastics and waste plastic mixtures", *Resources, Conservation and Recycling*, 51(4) (2007) 754-769.

[121] Kaminsky, W., Predel, M. and Sadiki, A., "Feedstock recycling of polymers by pyrolysis in a fluidised bed", *Polymer Degradation and Stability*, 85(3) (2004) 1045-1050.

[122] Yoshioka, T., Grause, G., Eger, C., Kaminsky, W. and Okuwaki, A., "Pyrolysis of poly(ethylene terephthalate) in a fluidized bed plant", *Polymer Degradation and Stability*, 86(3) (2004) 499-504.

[123] Zadgaonkar, A., "Process and Equipment for Conversions of Waste Plastics into Fuels", In Scheirs, J. and Kaminsky, W., (Eds.), *Feedstock Recycling and Pyrolysis of Waste Plastics*, John Wiley & Sons Ltd, West Sussex 2006.

[124] Prausnitz, J.M., Lichtenthaler, R.N. and De Azevedo, E.G., "*Molecular Thermodynamics of Fluid-phase Equilibria*", 3rd Ed., Prentice Hall India, New Delhi, 1999.

[125] Case, F.H. and Honeycutt, J.D., "Will my polymers mix? Methods for studying polymer miscibility", *Trends in Polymer Science*, 2(8) (1994) 259-266.

[126] Utracki, L.A., (Ed.), "*Polymer Blends Handbook*", Kluwer-Academic Publishers, Netherlands, 2002.

[127] Teraoka, I., "*Polymer Solutions: An Introduction to Physical Properties*", John Wiley & Sons Inc., New York, 2002.

[128] Van Krevelen, D.L., "*Properties of Polymers*", Elsevier, Amsterdam, 1990.

[129] Hujuri, U., Ghoshal, A.K. and Gumma S., "Modeling pyrolysis kinetics of plastic mixtures", *Polymer Degradation and Stability*, 93(10) (2008) 1832-1837.

[130] Scott, R.P.W., "*Gas Chromatography*", Chrom-Ed Book Series, Library4Science, LLC, 2003. Available at: http://www.library4science.com

[131] Hujuri, U., Ghoshal, A. K. and Gumma, S., "Temperature-dependent pyrolytic product evolution profile for low-density polyethylene from gas chromatographic study", *Waste Management*, 30(5) (2010) 814-820.

[132] Hujuri, U., Ghoshal, A.K. and Gumma, S., "Temperature-dependent pyrolytic product evolution profile for polypropylene", *Journal of Applied Polymer Science*, 119(4) (2011) 2318-2325.

[133] Billmeyer, F.W., "*Textbook of Polymer Science*", 2nd Ed., Wiley-Interscience, New York, 1971.

[134] Wampler, T.P., (Ed.) "*Applied Pyrolysis Handbook*", 2nd Ed., Taylor & Francis Group, Florida, 2007.

[135] Marongiu, A., Faravelli, T., Bozzano, G., Dente, M. and Ranzi, E., "Thermal degradation of poly(vinylchloride)", *Journal of Analytical and Applied Pyrolysis*, 70(2) (2003) 519–553.

[136] Kiran, E. and Gillham, J.K., "Pyrolysis-molecular weight chromatography: A new on-line system for analysis of polymers. II. Thermal decomposition of polyolefins: Polyethylene, polypropylene, polyisobutylene", *Journal of Applied Polymer Science*, 20(8) (1976) 2045–2068.

[137] Cheremisinoff, N. P., (Ed.), "*Handbook of Engineering Polymeric Materials*", Marcel Dekker, New York, 1997.

[138] Blazso, M., In "*Feedstock Recycling and Pyrolysis of Waste Plastics*", 1st Ed., Scheirs, J. and Kaminsky, W., (Eds.), John Wiley & Sons, West Sussex, 2006.

[139] De Amorim, M.T.S.P., Comel, C. and Vermande, P., "Pyrolysis of polypropylene: I. Identification of compounds and degradation reactions", *Journal of Analytical and Applied Pyrolysis*, 4(1) (1982) 73-81.

[140] Montaudo, G. and Puglisi, C., In. "Direct pyrolysis of polymers into the ion source of a mass spectrometer (DP-MS)", *Mass spectrometry of polymers*, 1st Ed., Montaudo, G. and Lattimer, R.P., (Eds.), CRC Press, Florida, 2001.

[141] McNeill, I. C. and Bounekhel, M., "Thermal degradation studies of terephthalate polyesters: 1. Poly(alkylene terephthalates)", *Polymer Degradation and Stability*, 34(1-3) (1991) 187-204.

[142] Fairgrieve, S., "*Degradation and stabilization of aromatic polyesters*", Smithers Rapra, Shawbury, 2009.

[143] Kalontarov, I.Y., Niyazi, F.F. and Chajko, Y.V., "Photooxidative Destruction and Stabilization of Polycaproamide by Bis-Aroilenbenzimidazole Derivatives", *International Journal of Polymeric Materials*, 13(1-4) (1990) 53-61.

[144] Niyazi, F.F., Kasymova, E.I., Kalontarov, I.Y. and Abdullaev, K.A., "Photostabilizing Thermostable Dyes for Polycaproamide and Polyethylenterephthalate", *International Journal of Polymeric Materials*, 19(3-4) (1993) 231-238.

[145] Pasquale, G. D., Pollicino, A., Recca, A., Bottino, F.A. and Sandri, M., "Leucopur EGM influence on the surface photooxidation of poly(ethylene terephthalate) and poly(vinyl chloride)", *Polymer*, 37(4) (1996) 703-705.

[146] Krestinin, A.V., Kislov, M.B., Raevskii, A.V., Kolesova, O.I. and Stesik, L.N., "On the mechanism of soot particle formation", *Kinetics and Catalysis*, 41(1) (2000) 90-98.

[147] Lam, F.W., "The formation of aromatic polycyclic aromatic hydrocarbons and soot in a jet-stirred plug-flow reactor", *PhD Thesis*, Massachusetts Institute of Technology, 1988.

[148] Ciliz, N.K., Ekinci, E. and Snape, C.E., "Pyrolysis of virgin and waste polypropylene and its mixtures with waste polyethylene and polystyrene", *Waste Management*, 24(2) (2004) 173-181.

APPENDIX 1

GC Calibration Details

A1.1 Calculations for ASTM D3710

Volume of sample injected = 0.5μl

Weight of *i*-pentane	$= \rho \times V \times vol.\%$ $= 0.8646 \times 0.5 \times 10^{-3} \times {}^{12.3}/_{100}$ $= 5.317 \times 10^{-5} g$	$\rho =$ Density (g/cc) $V =$ Volume (cc)
Weight of *n*-pentane	$= \rho \times V \times vol.\%$ $= 0.7341 \times 0.5 \times 10^{-3} \times {}^{9.39}/_{100}$ $= 3.447 \times 10^{-5} g$	
Weight of C5 hydrocarbon	= weight of (*i*-pentane + *n*-pentane)	$= 8.764 \times 10^{-5} g$

Weight of 2-methylpentane	$= \rho \times V \times vol.\%$ $= 0.7526 \times 0.5 \times 10^{-3} \times {}^{6.45}/_{100}$ $= 2.427 \times 10^{-5} g$	
Weight of *n*-hexane	$= \rho \times V \times vol.\%$ $= 0.6882 \times 0.5 \times 10^{-3} \times {}^{6.39}/_{100}$ $= 2.199 \times 10^{-5} g$	
Weight of C6 hydrocarbon	= weight of (2-methylpentane + *n*-hexane)	$= 4.626 \times 10^{-5} g$

Weight of 2,4-Dimethylpentane	$= \rho \times V \times vol.\%$ $= 0.664 \times 0.5 \times 10^{-3} \times {}^{6.27}/_{100}$ $= 2.082 \times 10^{-5} g$	
Weight of *n*-heptane	$= \rho \times V \times vol.\%$ $= 0.7068 \times 0.5 \times 10^{-3} \times {}^{11.17}/_{100}$ $= 3.948 \times 10^{-5} g$	
Weight of toluene	$= \rho \times V \times vol.\%$ $= 0.7721 \times 0.5 \times 10^{-3} \times {}^{9.74}/_{100}$ $= 3.76 \times 10^{-5} g$	
Weight of C7 hydrocarbon	= weight of (2,4 Dimethylpentane + *n*-heptane + toluene)	$= 9.789 \times 10^{-5} g$

Weight of *n*-octane	$= \rho \times V \times vol.\%$ $= 0.6312 \times 0.5 \times 10^{-3} \times {}^{6.01}/_{100}$ $= 1.897 \times 10^{-5}\, g$	$\rho =$ Density () $V =$ Volume ()
Weight of *p*-xylene	$= \rho \times V \times vol.\%$ $= 0.8666 \times 0.5 \times 10^{-3} \times {}^{11.84}/_{100}$ $= 5.1303 \times 10^{-5}\, g$	
Weight of C8 hydrocarbon	= weight of (*n*-octane + *p*-xylene)	$= 7.027 \times 10^{-5}\, g$
Weight of *n*-propylbenzene	$= \rho \times V \times vol.\%$ $= 0.7667 \times 0.5 \times 10^{-3} \times {}^{3.97}/_{100}$ $= 1.522 \times 10^{-5}\, g$	
Weight of C9 hydrocarbon	= weight of *n*-propylbenzene	$= 1.522 \times 10^{-5}\, g$
Weight of *n*-decane	$= \rho \times V \times vol.\%$ $= 0.7601 \times 0.5 \times 10^{-3} \times {}^{3.49}/_{100}$ $= 1.3264 \times 10^{-5}\, g$	
Weight of *n*-butylbenzene	$= \rho \times V \times vol.\%$ $= 0.8657 \times 0.5 \times 10^{-3} \times {}^{2.96}/_{100}$ $= 1.2812 \times 10^{-5}\, g$	
Weight of C10 hydrocarbon	= weight of (*n*-decane + *n*-butylbenzene)	$= 2.608 \times 10^{-5}\, g$
Weight of *n*-dodecane	$= \rho \times V \times vol.\%$ $= 0.8719 \times 0.5 \times 10^{-3} \times {}^{3.40}/_{100}$ $= 1.482 \times 10^{-5}\, g$	
Weight of C12 hydrocarbon	= weight of *n*-dodecane	$= 1.482 \times 10^{-5}\, g$
Weight of *n*-tridecane	$= \rho \times V \times vol.\%$ $= 0.6248 \times 0.5 \times 10^{-3} \times {}^{2.21}/_{100}$ $= 6.904 \times 10^{-6}\, g$	
Weight of C13 hydrocarbon	= weight of *n*-tridecane	$= 6.904 \times 10^{-6}\, g$
Weight of *n*-tetradecane	$= \rho \times V \times vol.\%$ $= 0.6579 \times 0.5 \times 10^{-3} \times {}^{2.23}/_{100}$ $= 7.336 \times 10^{-6}\, g$	
Weight of C14 hydrocarbon	= weight of *n*-tetradecane	$= 7.336 \times 10^{-6}\, g$

Weight of *n*-pentadecane	$= \rho \times V \times vol.\%$ $= 0.6772 \times 0.5 \times 10^{-3} \times {}^{2.18}/_{100}$ $= 7.382 \times 10^{-6} g$	
Weight of C15 hydrocarbon	= weight of *n*-pentadecane	$= 7.382 \times 10^{-6} g$

A1.2 Calculations for ASTM D5442

Amount of solid standard in $0.5ml$ of hexane = $48mg$

Volume of sample injected = $1\mu l$

Weight of standard in injected volume $(W_{std}) = {}^{48}/_{0.5} \times 10^{3} \times 10^{-6} mg = 0.096mg$

Weight of C16 hydrocarbon	$= W_{std} \times wt.\%$ $= 0.096 \times {}^{8.295}/_{100} = 7.963 \times 10^{-6} g$
Weight of C18 hydrocarbon	$= W_{std} \times wt.\%$ $= 0.096 \times {}^{8.307}/_{100} = 7.975 \times 10^{-6} g$
Weight of C20 hydrocarbon	$= W_{std} \times wt.\%$ $= 0.096 \times {}^{8.303}/_{100} = 7.971 \times 10^{-6} g$
Weight of C22 hydrocarbon	$= W_{std} \times wt.\%$ $= 0.096 \times {}^{8.361}/_{100} = 8.027 \times 10^{-6} g$
Weight of C24 hydrocarbon	$= W_{std} \times wt.\%$ $= 0.096 \times {}^{8.296}/_{100} = 7.964 \times 10^{-6} g$
Weight of C26 hydrocarbon	$= W_{std} \times wt.\%$ $= 0.096 \times {}^{8.314}/_{100} = 7.981 \times 10^{-6} g$
Weight of C28 hydrocarbon	$= W_{std} \times wt.\%$ $= 0.096 \times {}^{8.373}/_{100} = 8.038 \times 10^{-6} g$

Weight of C30 hydrocarbon	$= W_{std} \times wt.\%$ $= 0.096 \times {}^{8.298}/_{100} = 7.966 \times 10^{-6}\, g$

Weight of C32 hydrocarbon	$= W_{std} \times wt.\%$ $= 0.096 \times {}^{8.467}/_{100} = 8.128 \times 10^{-6}\, g$

Weight of C36 hydrocarbon	$= W_{std} \times wt.\%$ $= 0.096 \times {}^{8.291}/_{100} = 7.959 \times 10^{-6}\, g$

Weight of C40 hydrocarbon	$= W_{std} \times wt.\%$ $= 0.096 \times {}^{8.30}/_{100} = 7.968 \times 10^{-6}\, g$

Weight of C44 hydrocarbon	$= W_{std} \times wt.\%$ $= 0.096 \times {}^{8.397}/_{100} = 8.061 \times 10^{-6}\, g$

A1.3 Calibration procedure

1. *Calculation of area% and mole% values of the standard hydrocarbons*: Tables A1.1 and A1.2 show the calculation of area% values for the standard hydrocarbons present in the ASTM D3710 and ASTM D5442 respectively. The calculations for determination of the amount of different hydrocarbons (in terms of carbon number) in injected volume of the sample are shown in previous sections (*Section A1.1 and A1.2).*

Table A1.1 Mol% of the standard hydrocarbons (C5-C15) present in ASTM D3710 mix standard

Carbon no.	RT_i^* (min)	RT_f^* (min)	Area (counts)	Area %	Amt. in injected volume (g)	Mol. wt.	moles	mol%
C5-C7	1.64	6.43	6.21E+08	63.91	2.29E-04	84	2.72E-06	70.62
C8	8.85	10.82	1.39E+08	14.32	7.03E-05	112	6.27E-07	16.27
C9	14.98	17.23	7.86E+07	8.09	1.52E-05	126	1.21E-07	3.13
C10	26.79	29.24	3.49E+07	3.59	2.61E-05	140	1.86E-07	4.83
C12	40.08	41.85	3.29E+07	3.38	1.48E-05	168	8.82E-08	2.29
C13	44.46	45.07	2.18E+07	2.25	6.90E-06	182	3.79E-08	0.98
C14	46.48	46.98	2.19E+07	2.25	7.34E-06	196	3.74E-08	0.97
C15	47.95	48.44	2.14E+07	2.20	7.38E-06	210	3.52E-08	0.91

*- RT_i – retention time at start of peak, RT_f – retention time at end of peak

Table A1.2 Mol% of the standard hydrocarbons (C16-C44) present in ASTM D5442 mix standard

Carbon no.	RT_i	RT_f	Area (counts)	Area %	Wt. %	Amt. in injected volume (g)	Mol. Wt.	moles	mol %
C16	49.13	49.25	7.57E+05	12.79	8.29	1.39E-06	224	6.18E-09	13.27
C18	51.25	51.35	6.92E+05	11.69	8.31	1.39E-06	252	5.51E-09	11.82
C20	53.09	53.20	6.24E+05	10.54	8.30	1.39E-06	280	4.95E-09	10.63
C22	54.76	54.87	5.36E+05	9.05	8.36	1.40E-06	308	4.53E-09	9.73
C24	56.30	56.40	4.66E+05	7.87	8.29	1.39E-06	336	4.12E-09	8.85
C26	57.71	57.82	4.45E+05	7.51	8.31	1.39E-06	364	3.81E-09	8.19
C28	59.02	59.20	4.12E+05	6.96	8.37	1.40E-06	392	3.57E-09	7.66
C30	60.27	60.36	4.11E+05	6.94	8.29	1.39E-06	420	3.30E-09	7.08
C32	61.42	61.51	4.25E+05	7.17	8.48	1.41E-06	448	3.16E-09	6.77
C36-C44	62.14	63.59	1.15E+06	19.49	24.99	4.17E-06	560	7.45E-09	16.00

Quantification was not done for the PAH standard. They are used to have a qualitative idea about the retention times for the PAHs. Table A1.3 shows the retention times of the standard hydrocarbons present in the PAH mix. The boiling temperature for PAH ranges from 218^{o}C (for naphthalene, a C10 compound) to 536^{o}C (for indeno(1,2,3-cd)pyrene, a C22 compound), which corresponds to their aliphatic counterparts having carbon number C12 (boiling temperature 216^{o}C) and C40 (boiling temperature 527^{o}C). Thus, retention times corresponding to C12 and C40 aliphatic hydrocarbons should be comparable to their C10 and C22 aromatic counterparts respectively. The same has been confirmed from RT studies using PAH standard, wherein C10 starts eluting at about 44 minutes, and C22 at about 64 minutes (Table A1.3). Notably the aliphatic hydrocarbons with carbon number C12 start eluting at about 42 minutes and C44 at about 64 minutes (Tables A1.1 and A1.2).

Table A1.3 Retention times of the standard hydrocarbons present in PAH standard

Carbon No.	Retention Time (min)	
	RT_i	RT_f
C10	44.20	44.60
C12	49.40	50.80
C13	53.20	53.40
C14	55.80	56.40
C16	58.85	59.10
C18	61.10	61.40
C20	61.80	62.00
C22	63.80	64.20

The chromatograms for the C5-C15 and C16-C44 standard aliphatic hydrocarbon mixtures as obtained from VARIAN 3800 GC are shown in Figures A1.1 and A1.2 respectively. Figure A1.3 shows the chromatogram for PAH (C10-C22) standard hydrocarbon mixture as obtained from VARIAN 450 GC. The chromatograms for the C5-C15 and C16-C44 standard aliphatic hydrocarbon mixtures as obtained from VARIAN 450 GC are shown in Figure A1.4 and A1.5 respectively. It can be seen from these figures that retention time of the standard hydrocarbons obtained from Varian 450 GC are similar to those obtained from Varian 3800 GC.

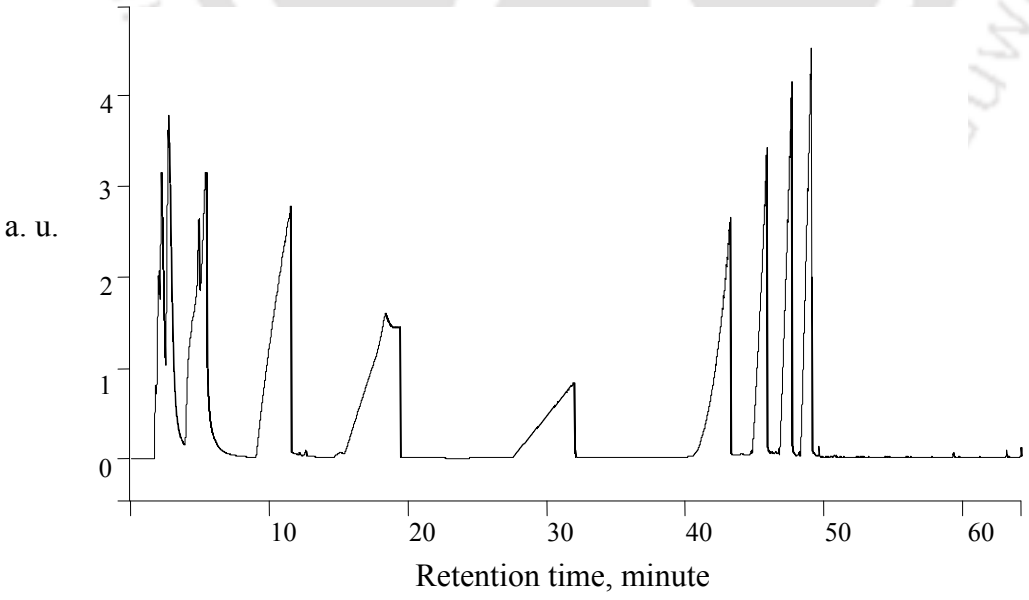

Figure A1.1 Chromatogram for C5-C15 standard hydrocarbons present in ASTM D3710 standard mix from Varian 3800 GC

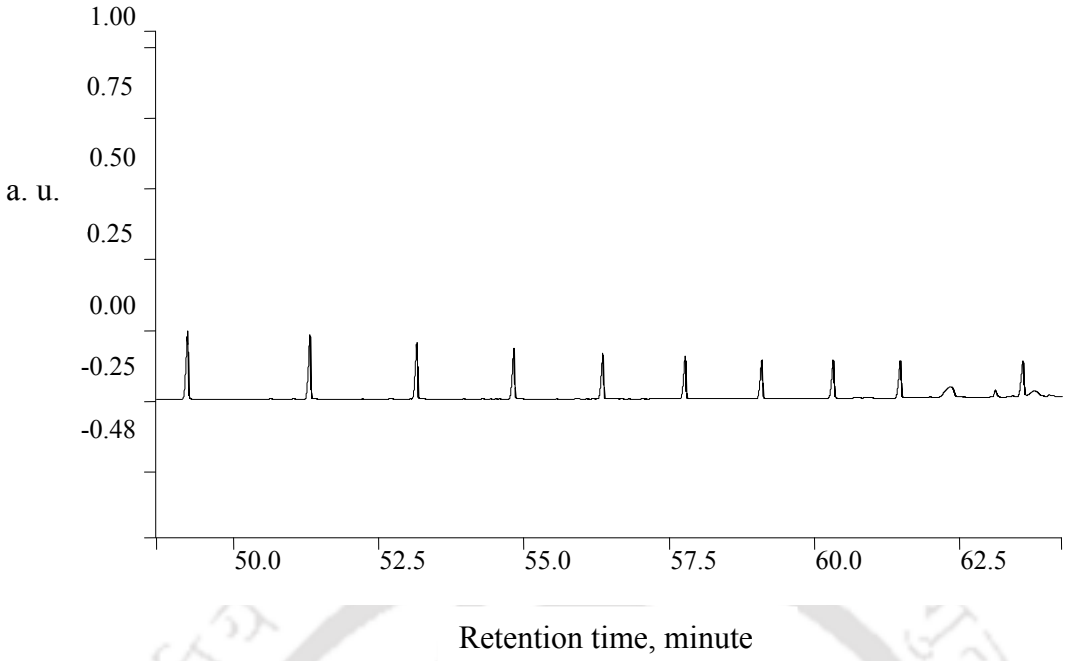

Figure A1.2 Chromatogram for C16-C44 standard hydrocarbons present in ASTM D 5442 standard mix from Varian 3800 GC

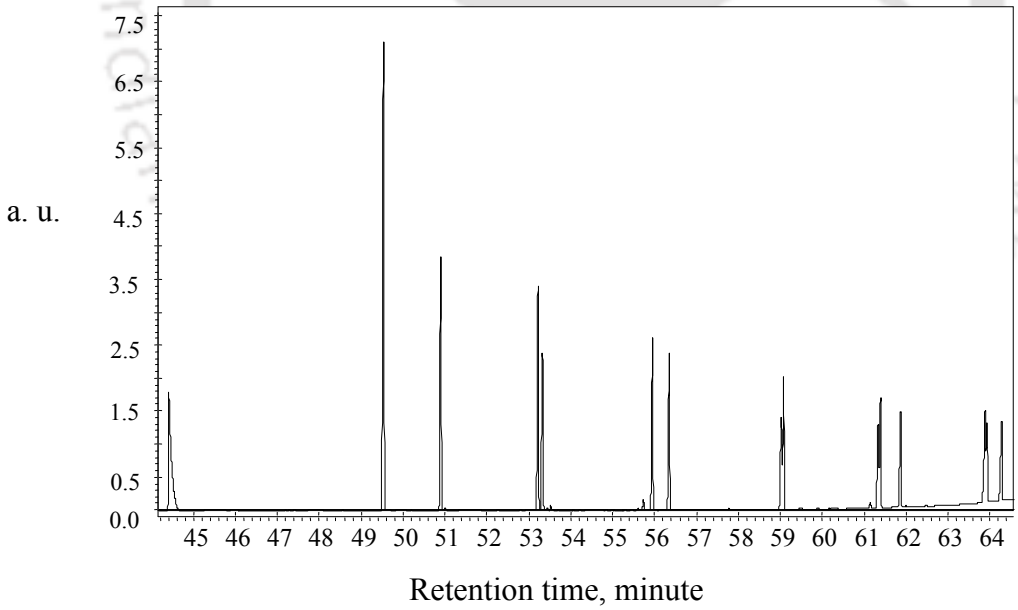

Figure A1.3 Chromatogram for C10-C22 standard hydrocarbons present in PAH standard mix from Varian 450 GC

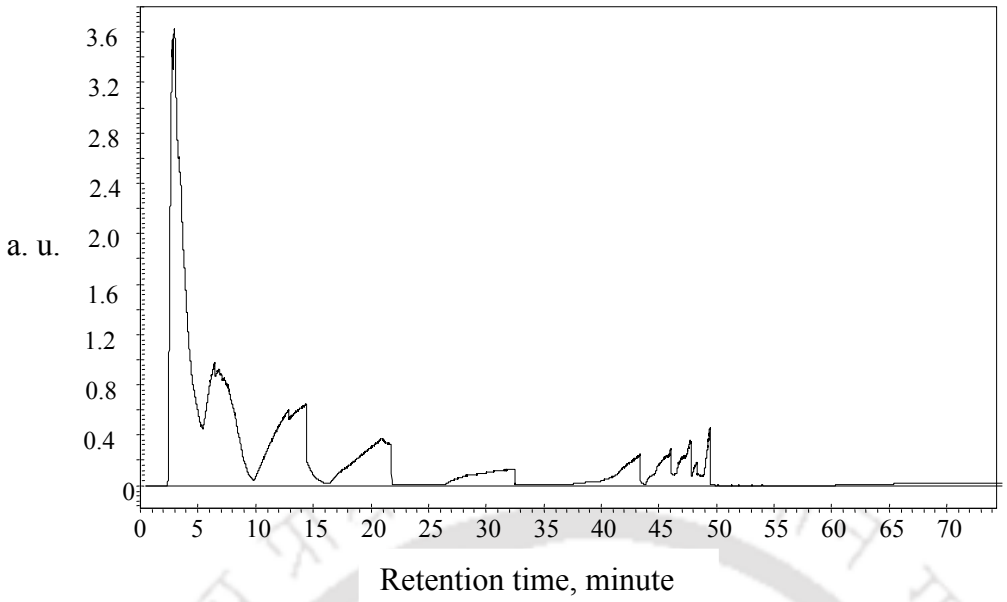

Figure A1.4 Chromatogram for C5-C15 standard hydrocarbons present in ASTM D3710 standard mix from Varian 450 GC

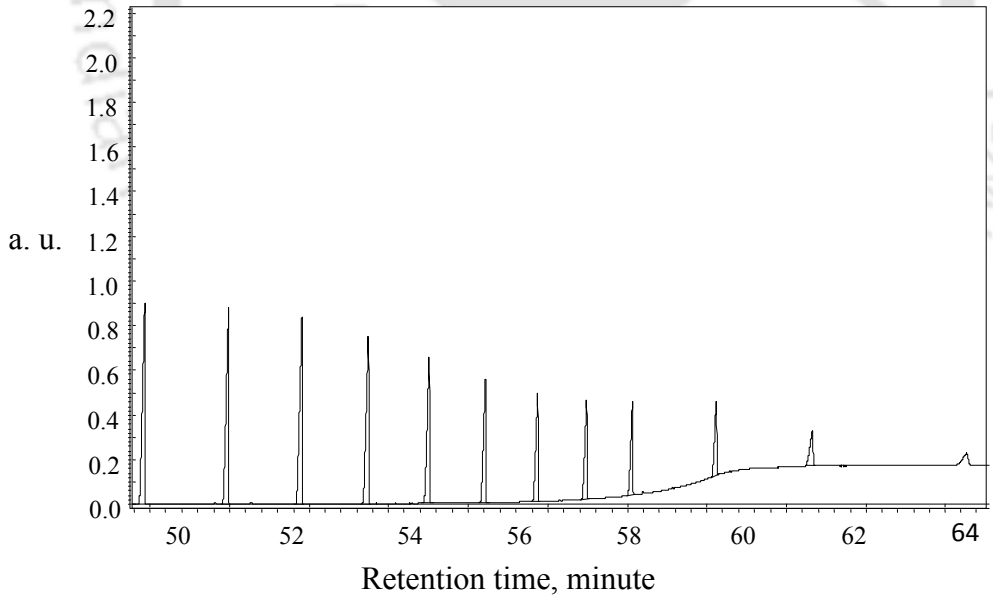

Figure A1.5 Chromatogram for C16-C44 standard hydrocarbons present in ASTM D5442 standard mix from Varian 450 GC

2. *Calculation of mol% from area%:* Area% values of the standard hydrocarbons are plotted against the corresponding mol% values of the hydrocarbons. The plots for both the lighter (C5-C15) and heavier hydrocarbon (C16-C44) groups are presented in Figures 4.8 and 4.9 respectively. A linear regression of these values for the C5-C15 hydrocarbons (ASTM D3710 mix standard) yields a straight line as depicted in *equation (4.1)*:

$$y=1.103\,x \qquad (4.1)$$

where, y denotes area% and x denotes mol%.

Linear regression of the area% vs. mol% values for C16-C44 hydrocarbons (ASTM D5442 standard) yields another straight line as shown in *equation (4.2)*:

$$y=1.039\,x \qquad (4.2)$$

where, y and x have the same meaning as in *equation (4.1)*

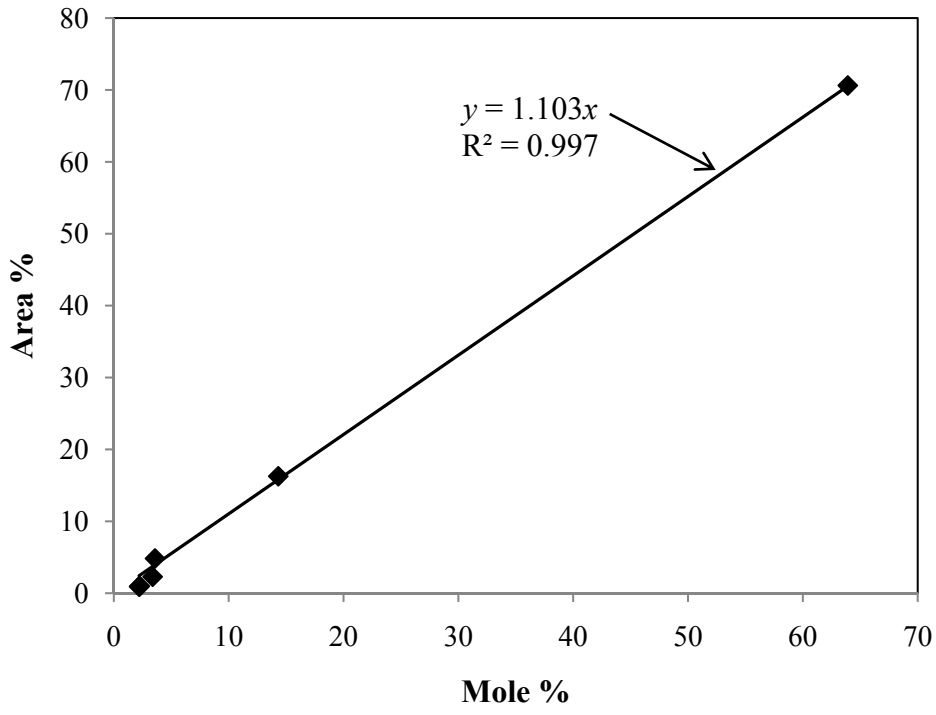

Figure A1.6 Area% vs. Mole% plot for C5-C15 hydrocarbons

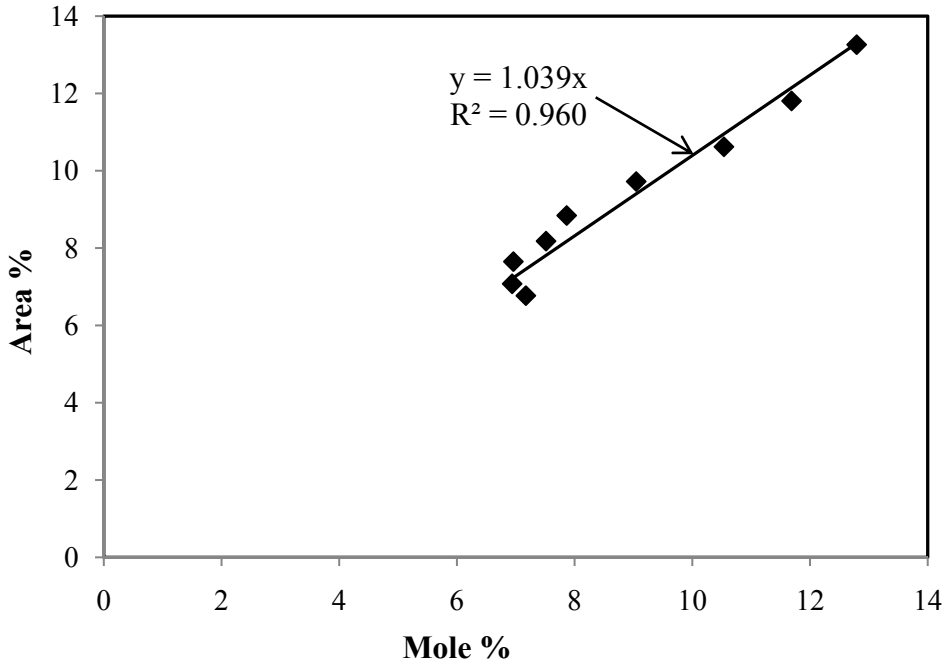

Figure A1.7 Area% vs. Mole% plot for C16-C44 hydrocarbons

Thermogravimetric Curves for Pyrolysis Kinetics Study

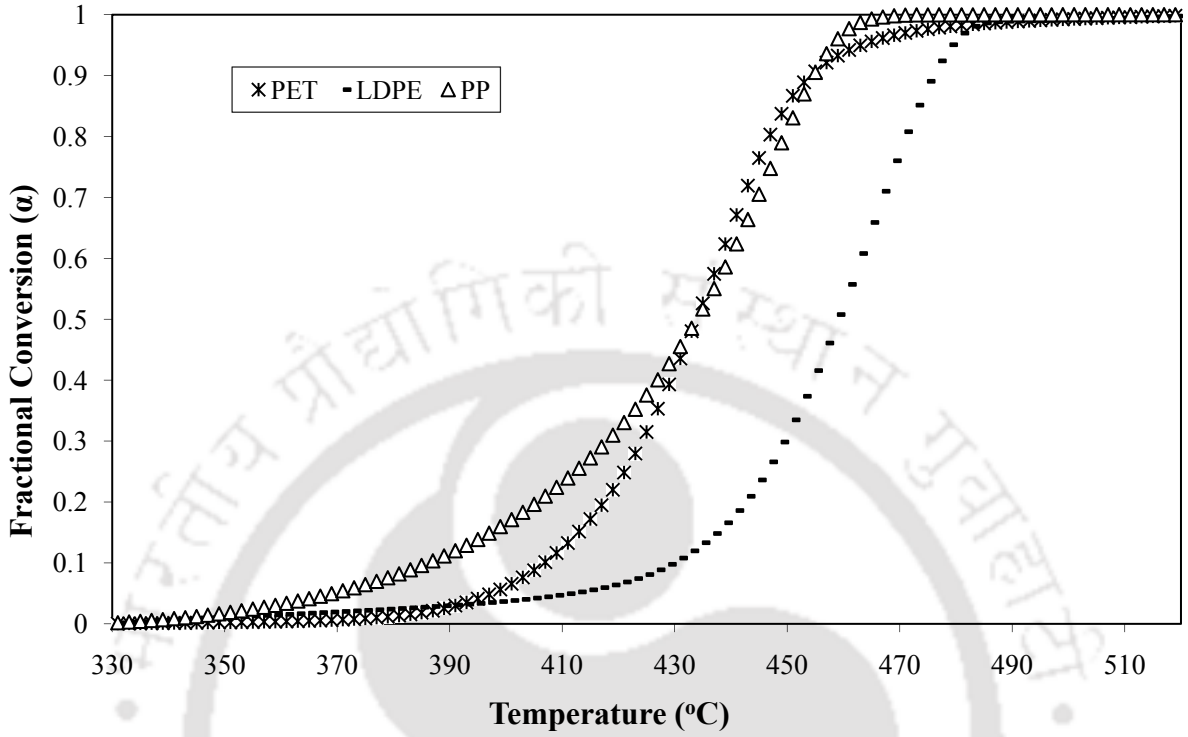

Figure A2.1 Thermogravimetry (TG) curves for single plastics PET, LDPE and PP

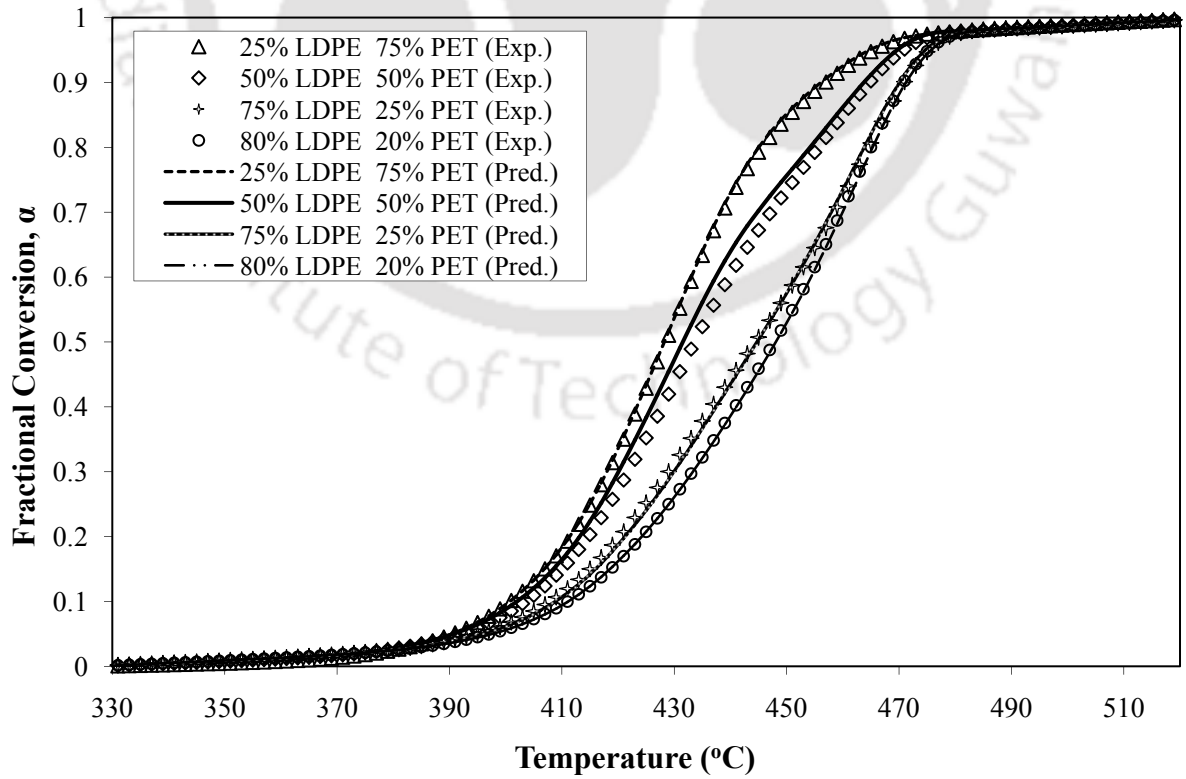

Figure A2.2 Thermogravimetry (TG) curves for LDPE-PET mixture

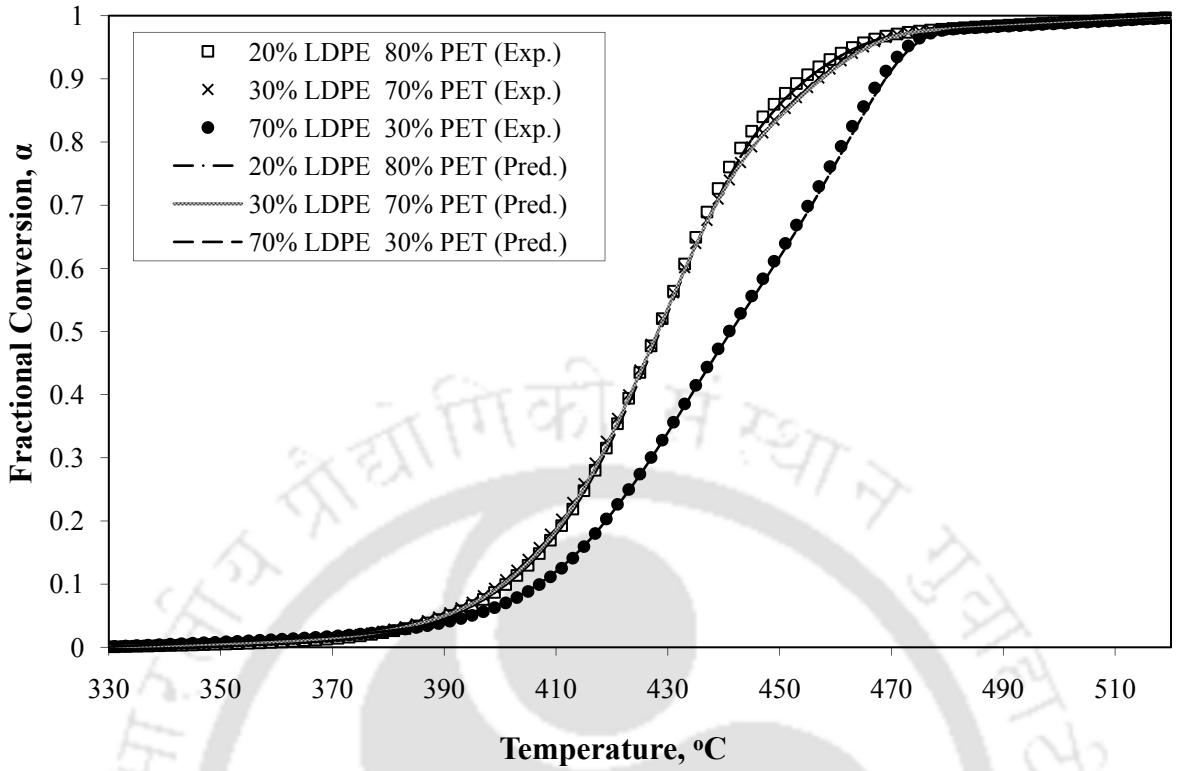

Figure A2.3 Thermogravimetry (TG) curves for LDPE-PET mixture

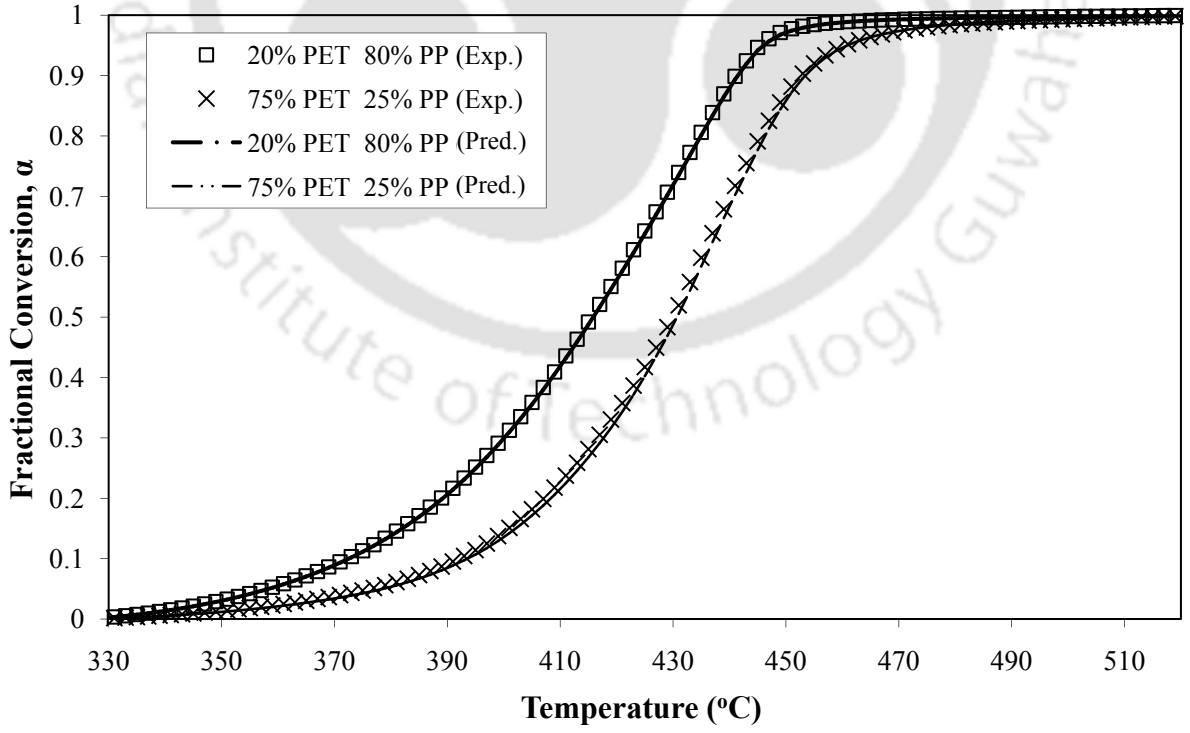

Figure A2.4 Thermogravimetry (TG) curves for PP-PET mixture

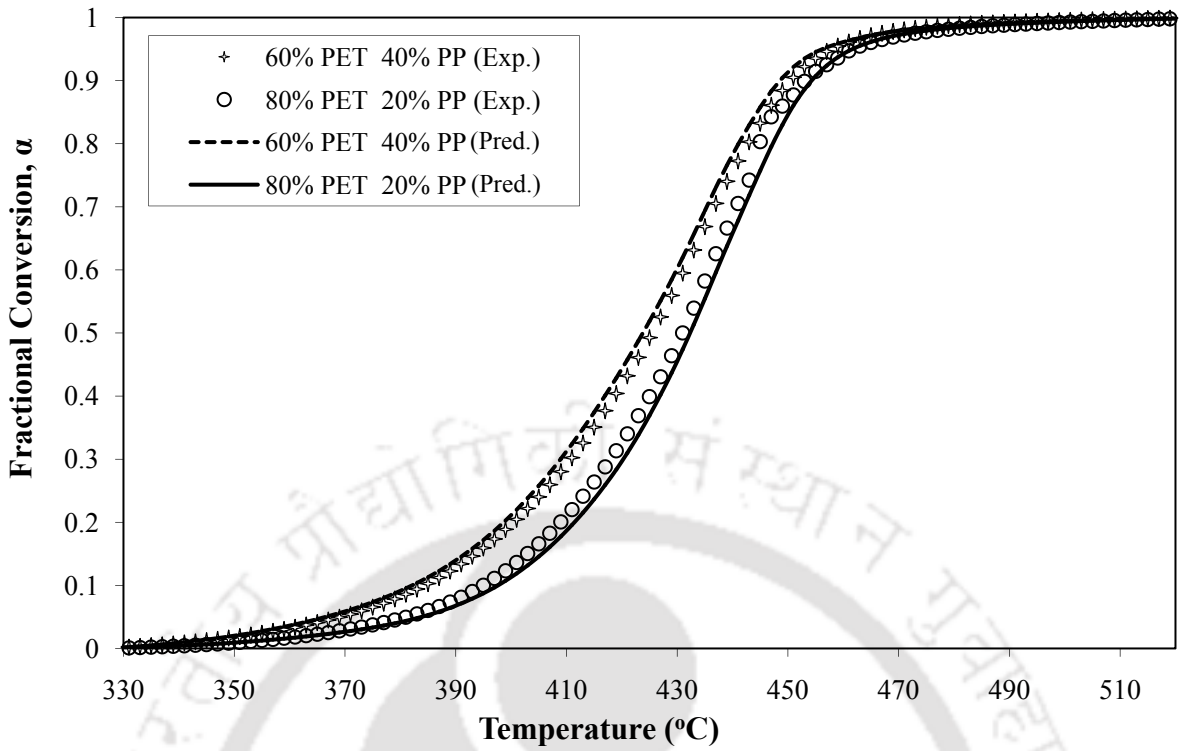

Figure A2.5 Thermogravimetry (TG) curves for PP-PET mixture

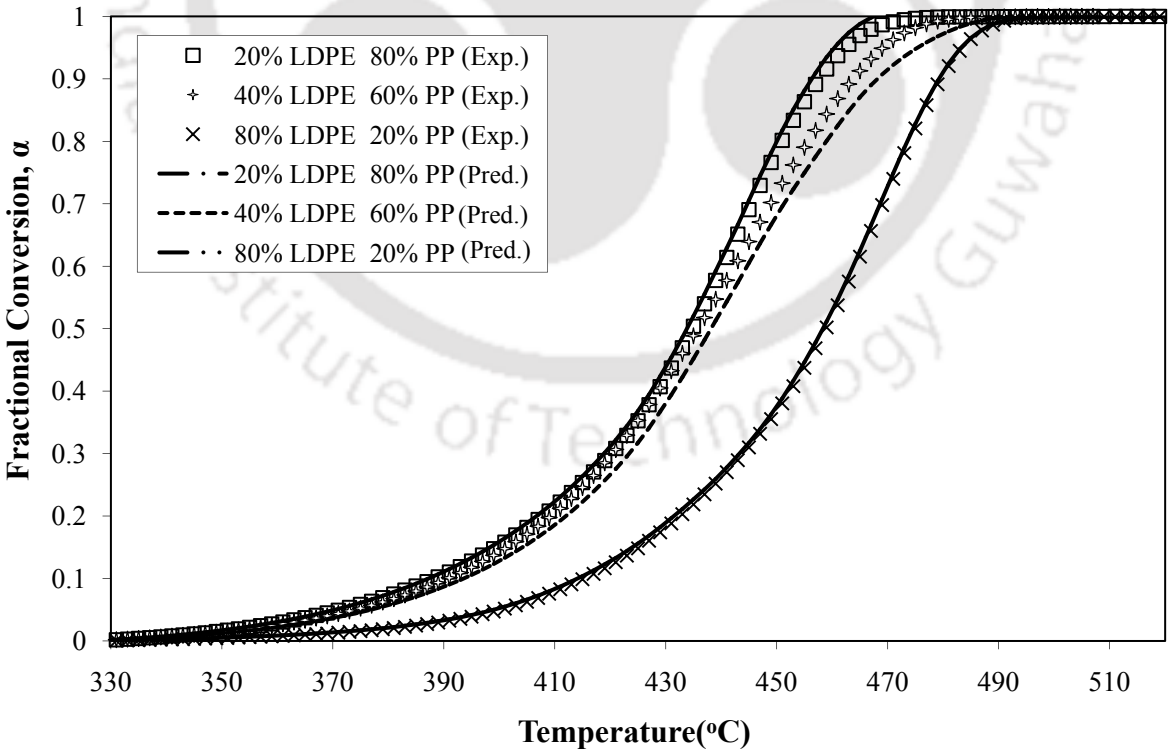

Figure A2.6 Thermogravimetry (TG) curves for LDPE-PP mixture

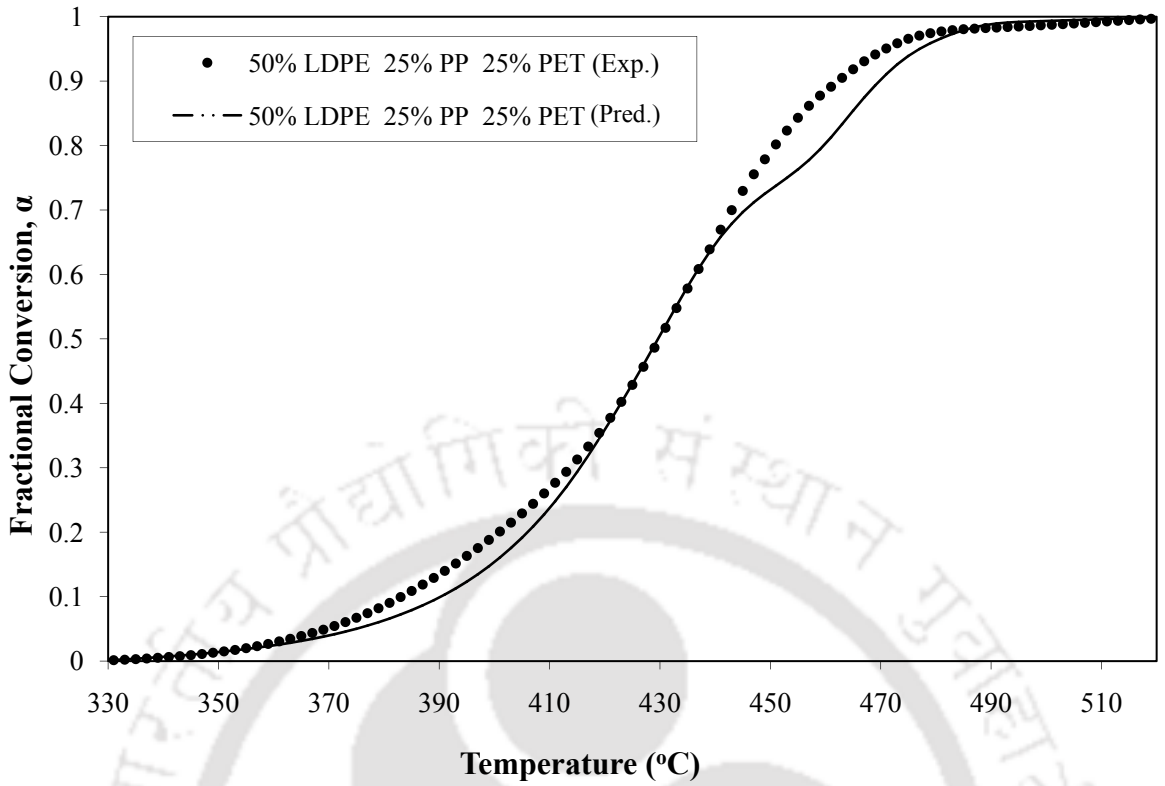

Figure A2.7 Thermogravimetry (TG) curves for LDPE-PP-PET mixture

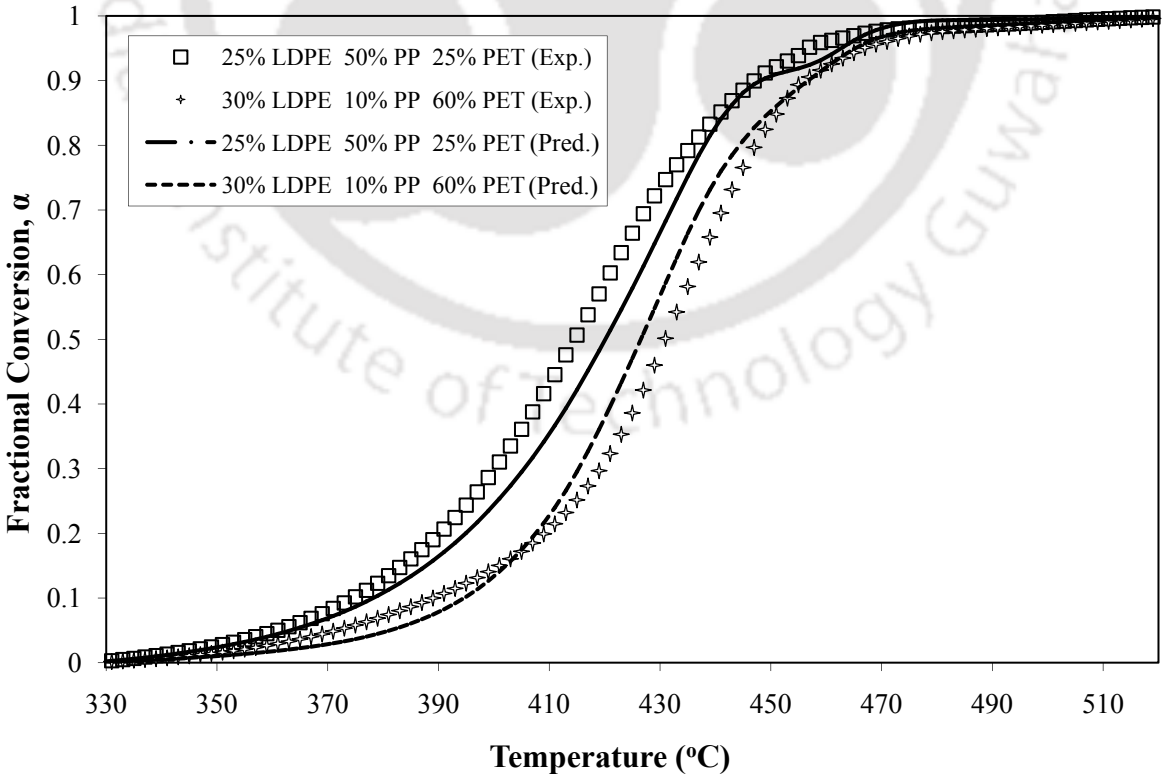

Figure A2.8 Thermogravimetry (TG) curves for LDPE-PP-PET mixture

APPENDIX 3

Pyrograms

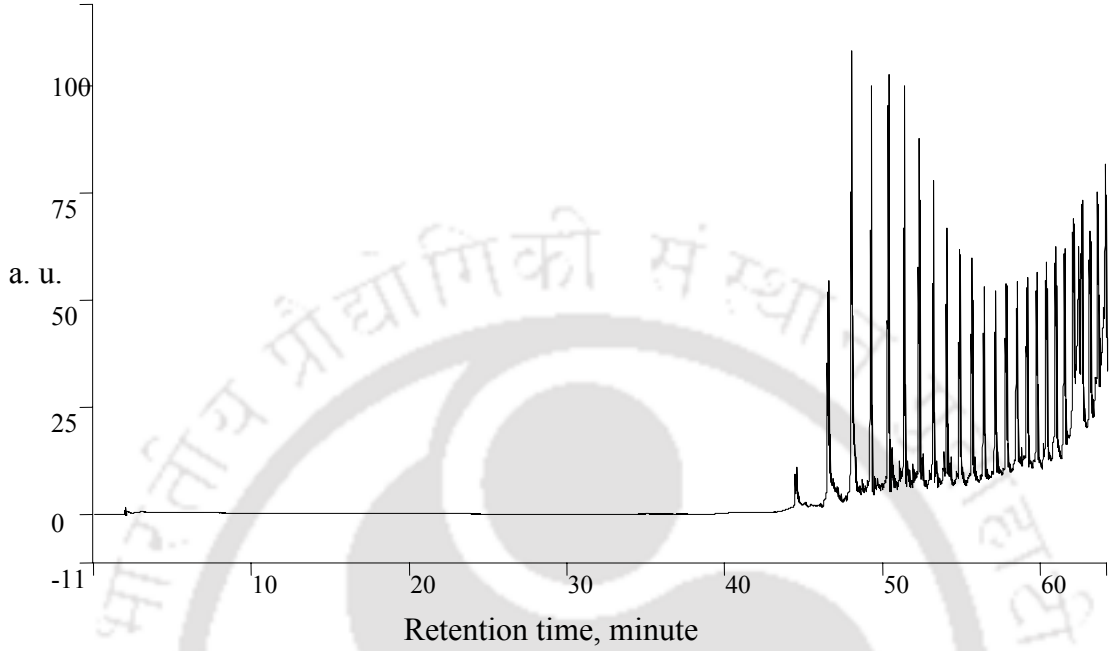

Figure A3.1 Pyrogram of LDPE at 200°C

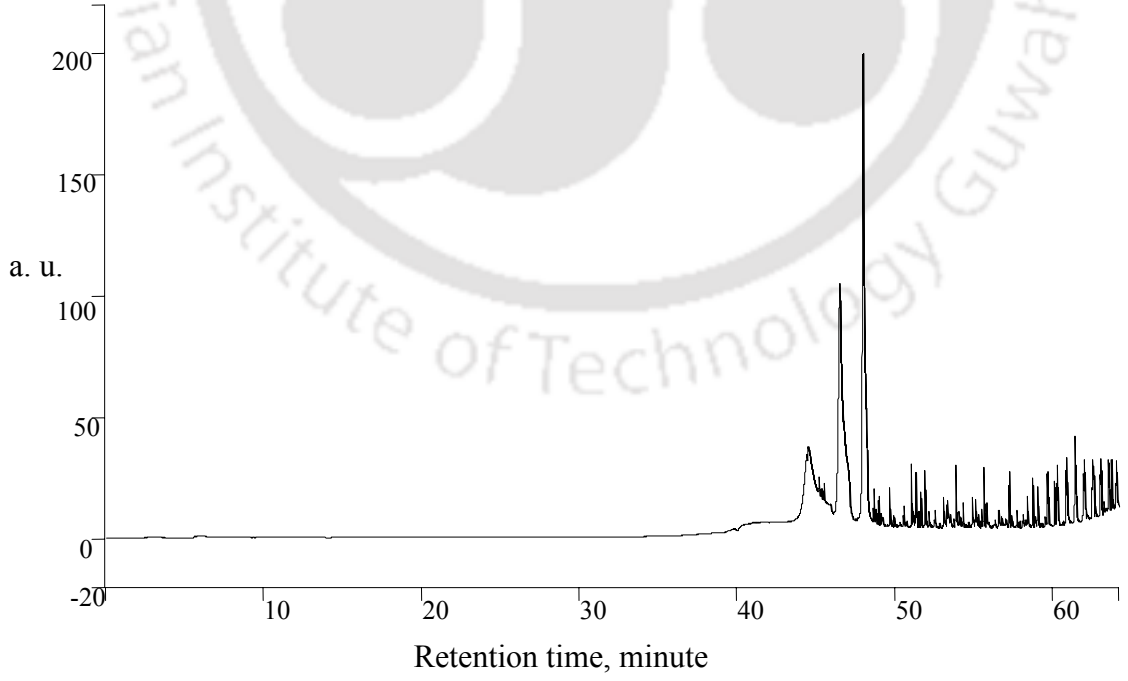

Figure A3.2 Pyrogram of LDPE at 250°C

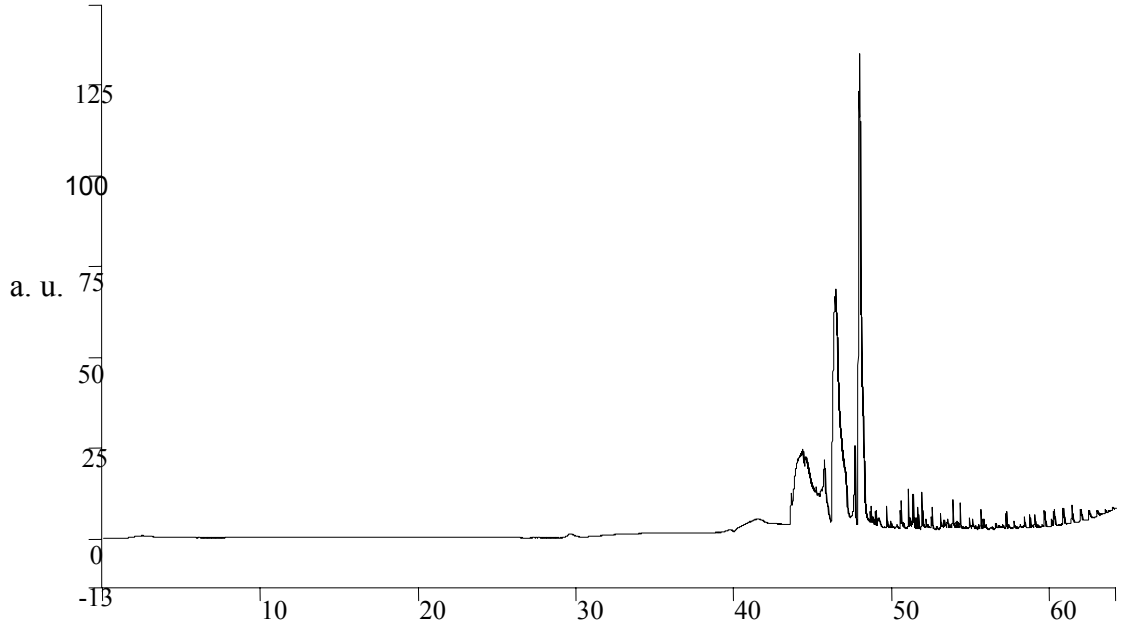

Figure A3.3 Pyrogram of LDPE at 300°C

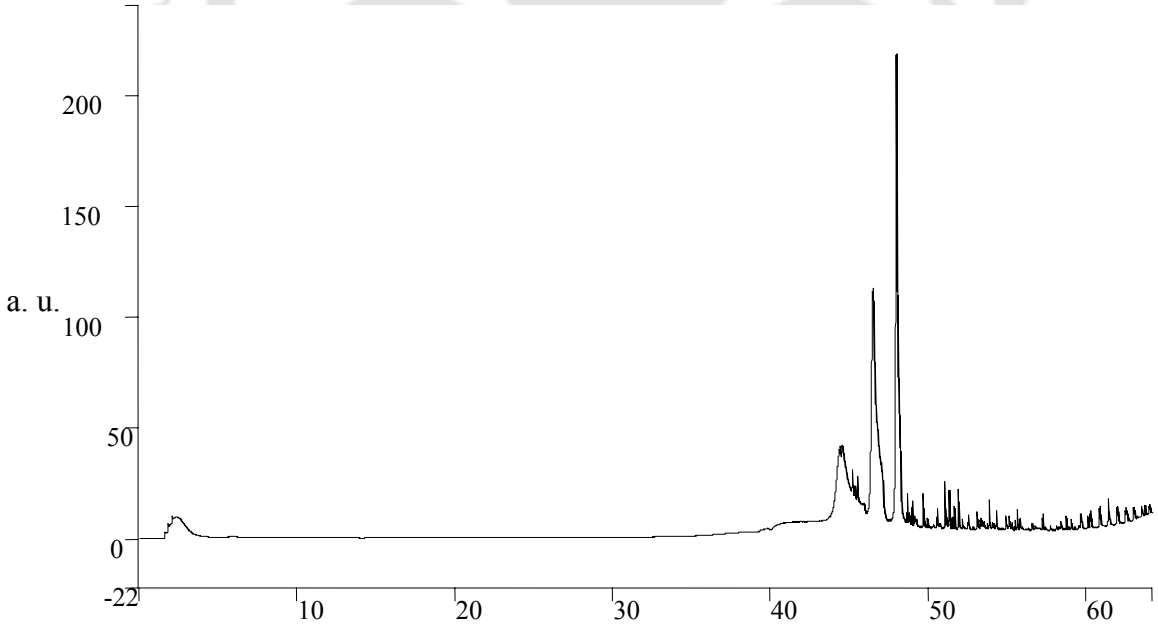

Figure A3.4 Pyrogram of LDPE at 350°C

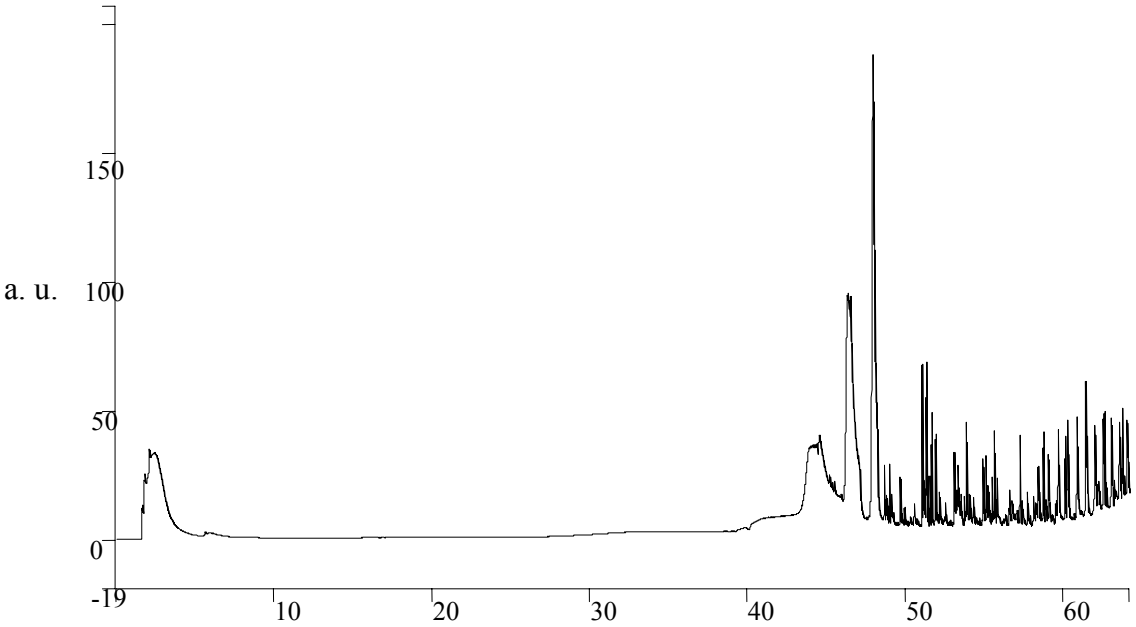

Figure A3.5 Pyrogram of LDPE at 400°C

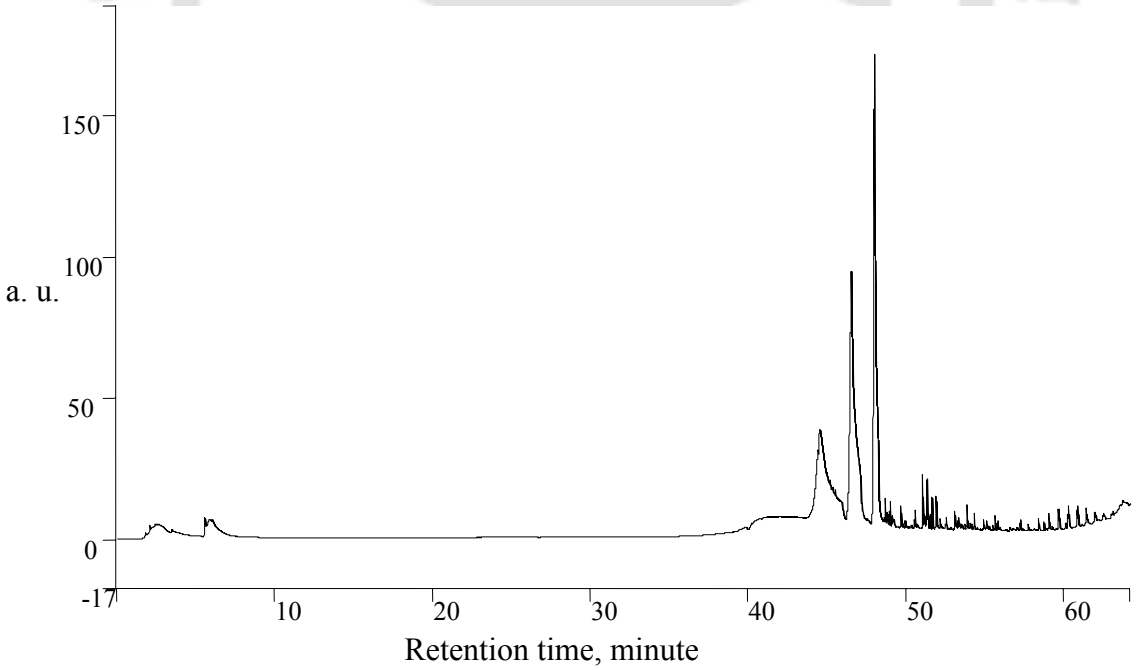

Figure A3.6 Pyrogram of LDPE at 500°C

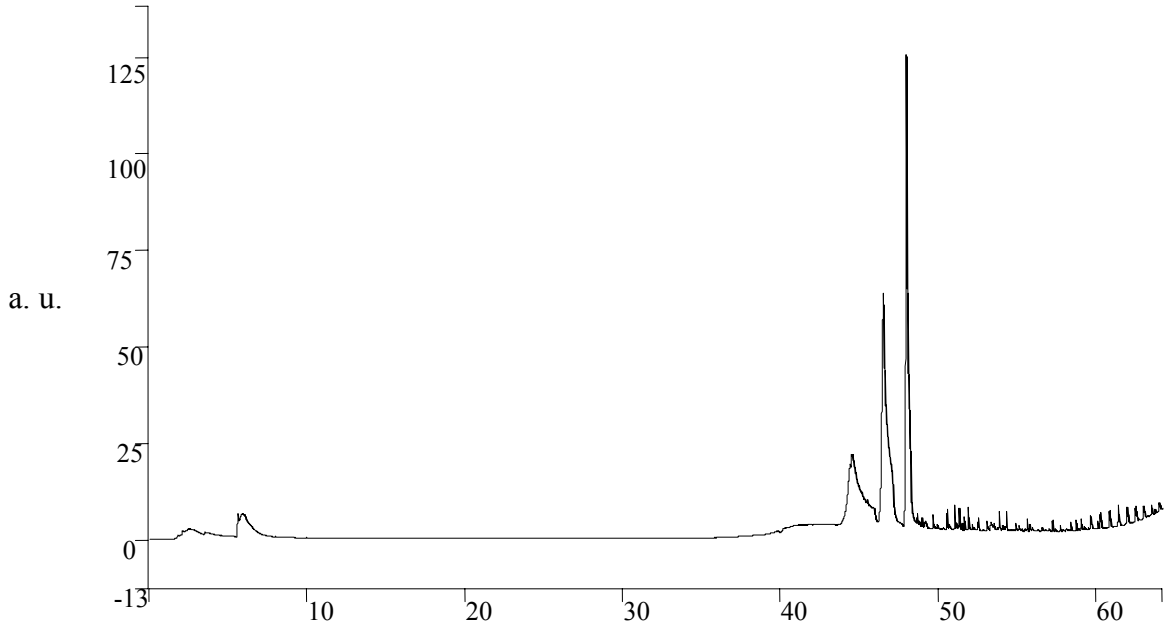

Figure A3.7 Pyrogram of LDPE at 550°C

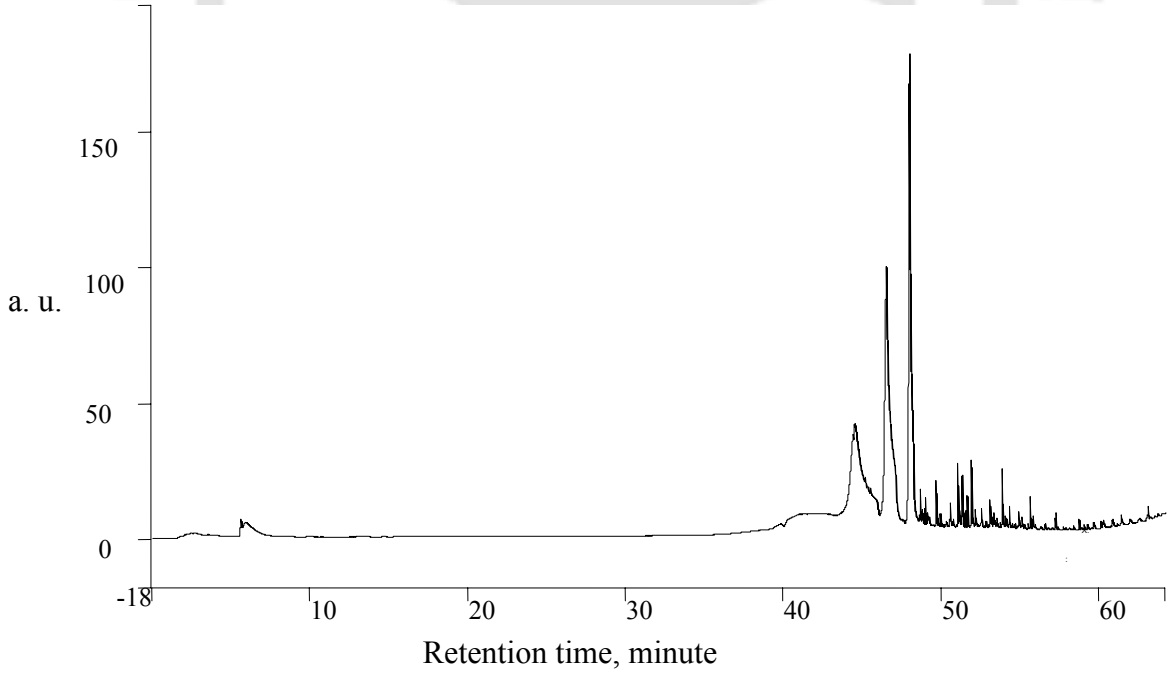

Figure A3.8 Pyrogram of LDPE at 600°C

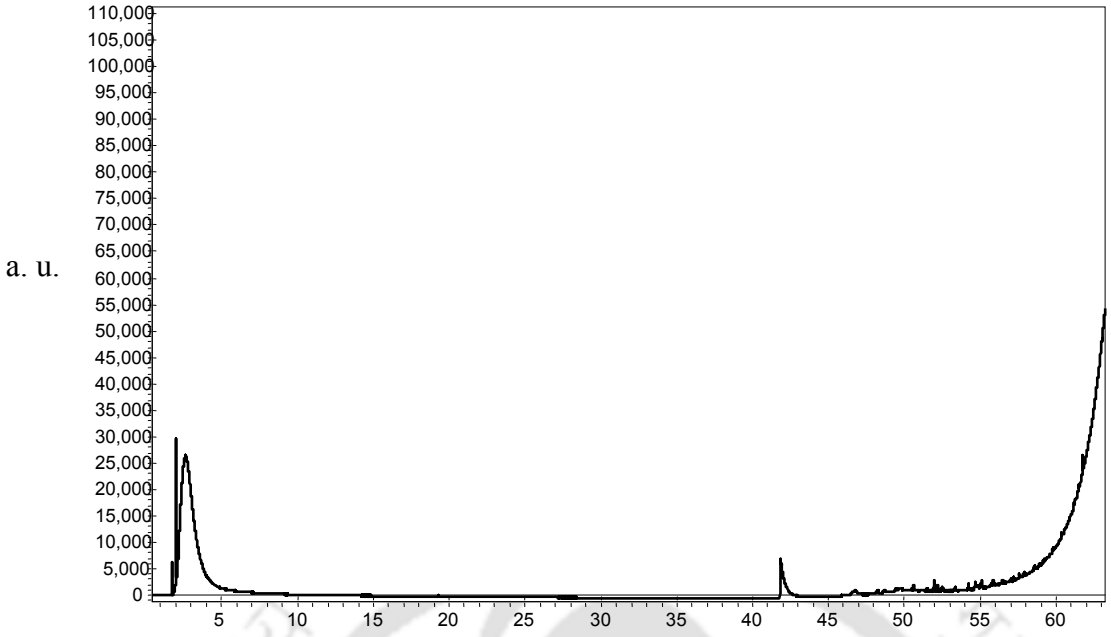

Figure A3.9 Pyrogram of PET at 400^{o}C

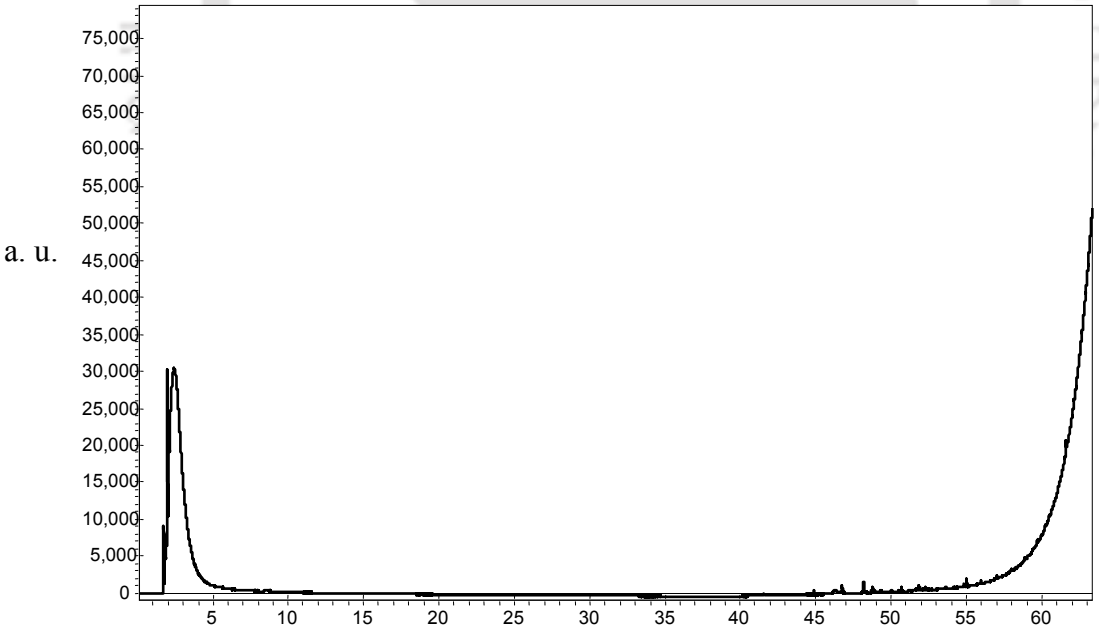

Figure A3.10 Pyrogram of pure PET at 500^{o}C

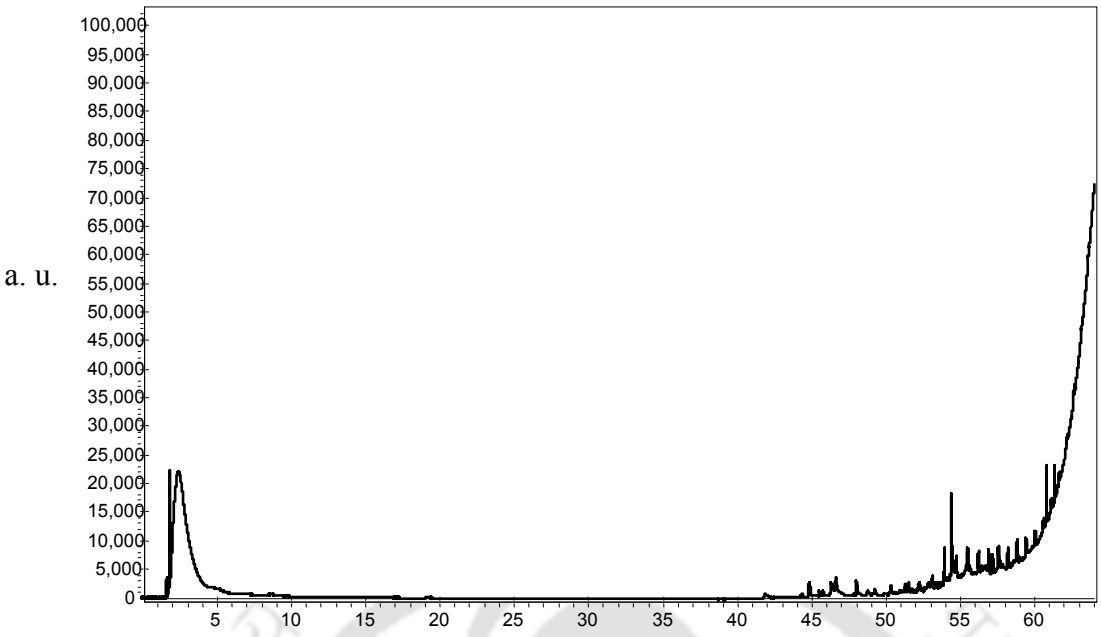

Figure A.3.11 Pyrogram of 20% LDPE and 80% PET mixture at 400^{o} C

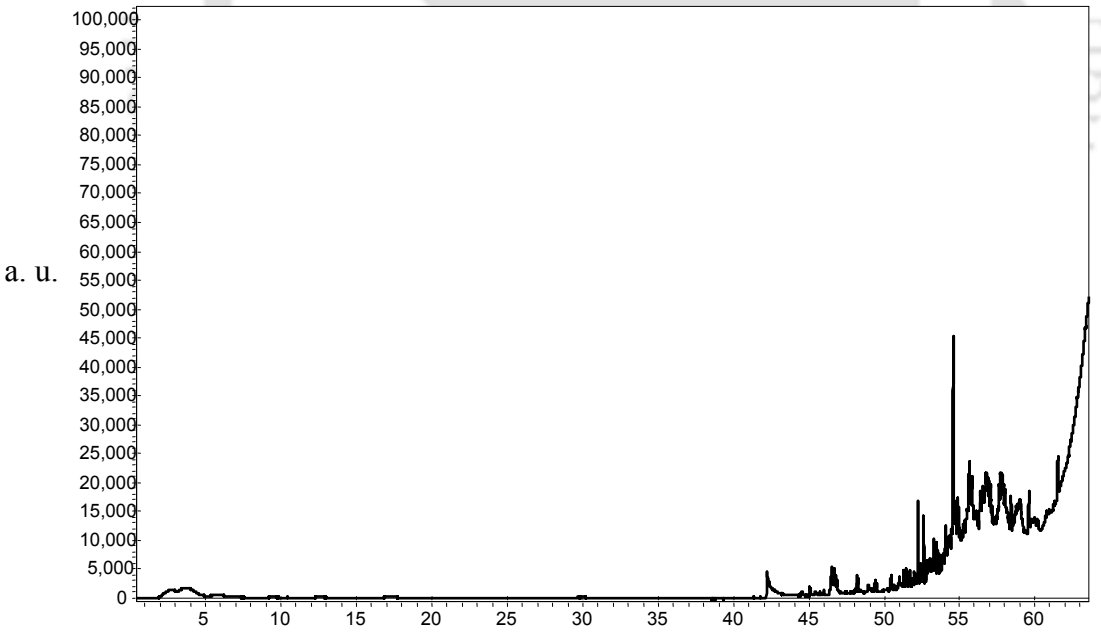

Figure A3.12 Pyrogram of 20% LDPE and 80% PET mixture at 500^{o} C

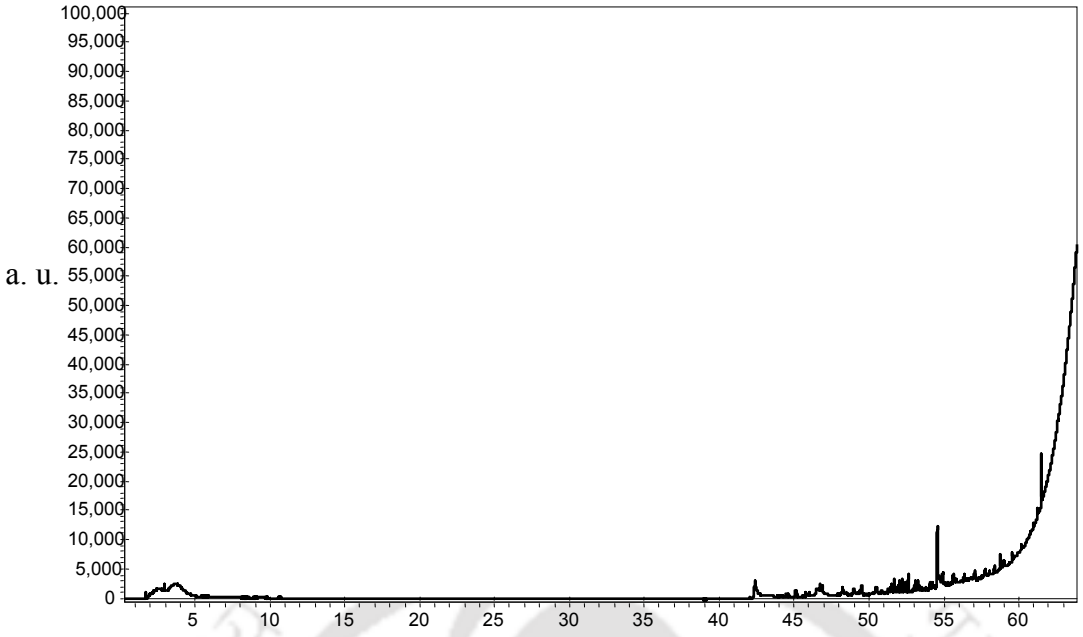

Figure A3.13 Pyrogram of 20% LDPE and 80% PET mixture at 600^{o} C

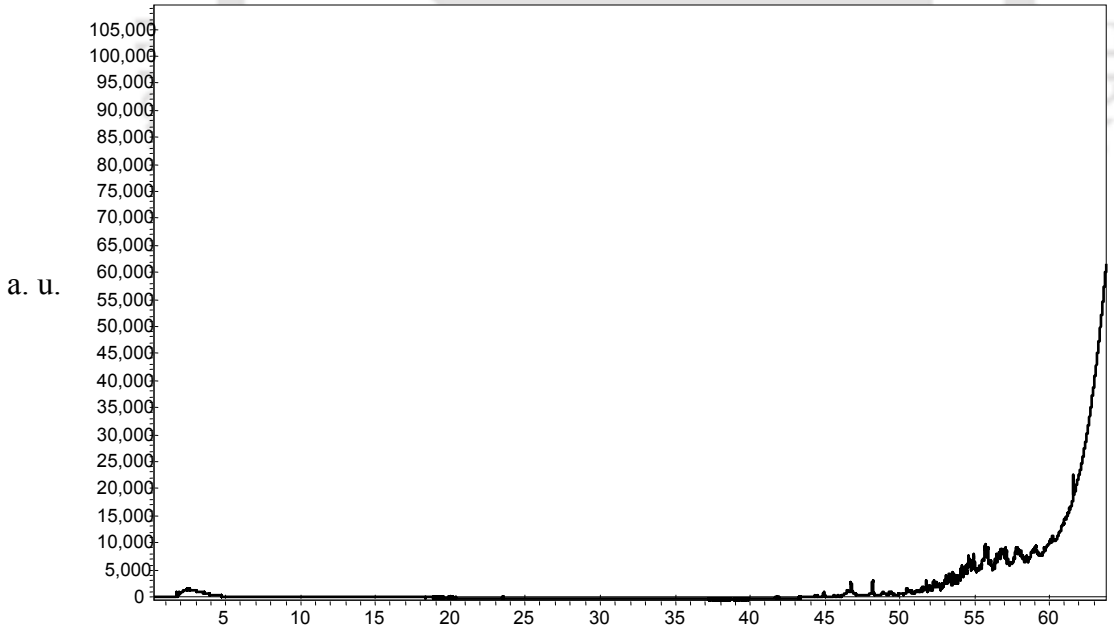

Figure A3.14 Pyrogram of 50% LDPE and 50% PET mixture at 300^{o} C

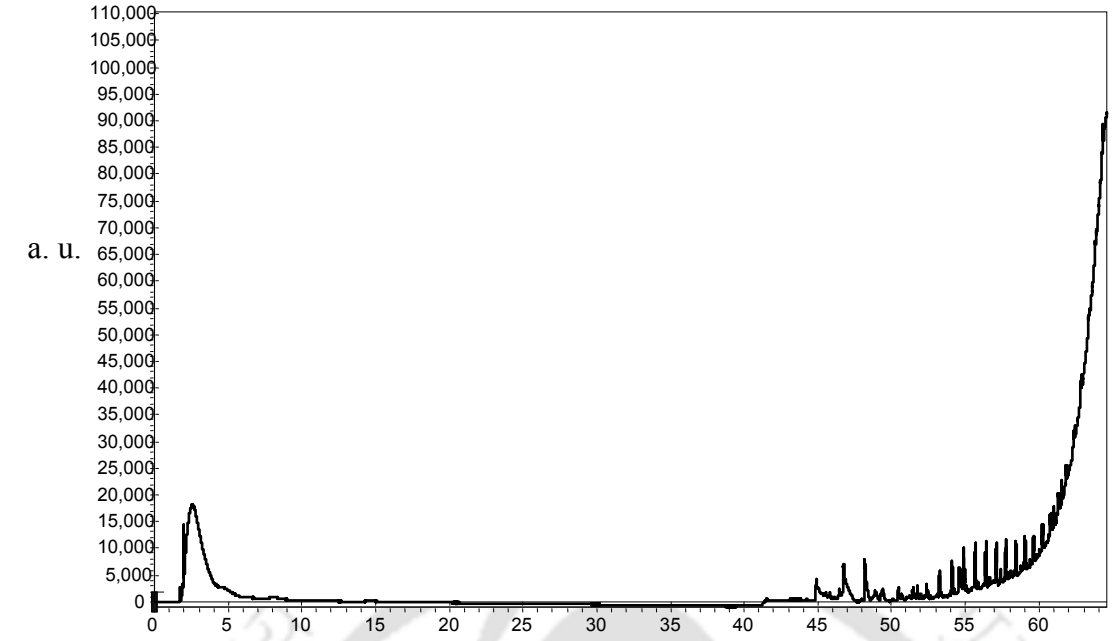

Figure A3.15 Pyrogram of 50% LDPE and 50% PET mixture at 400^{o} C

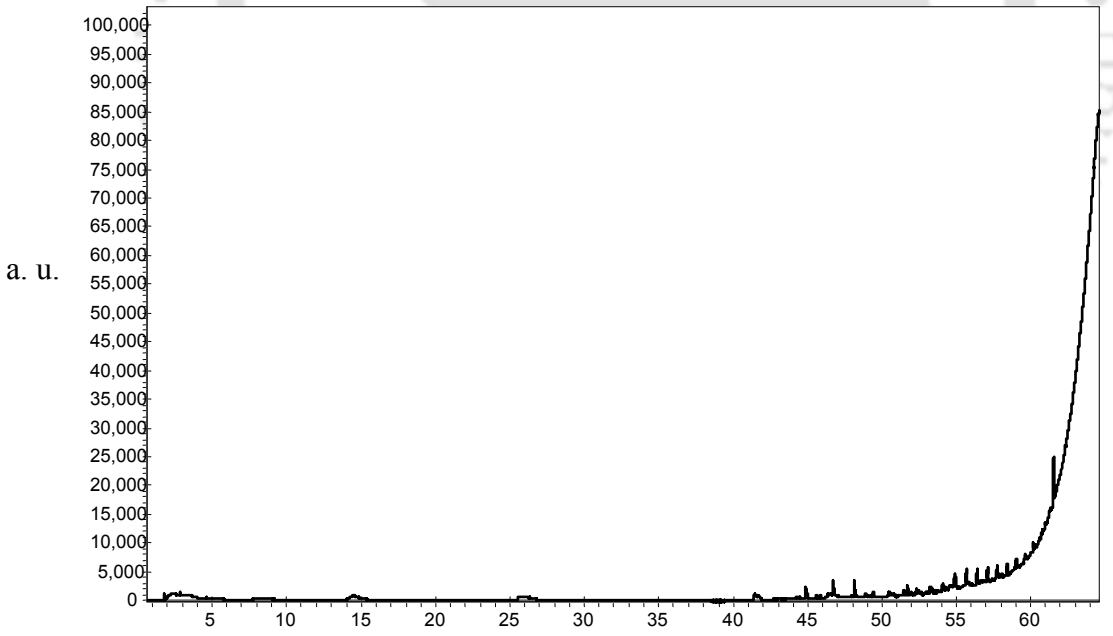

Figure A3.16 Pyrogram of 50% LDPE and 50% PET mixture at 500^{o} C

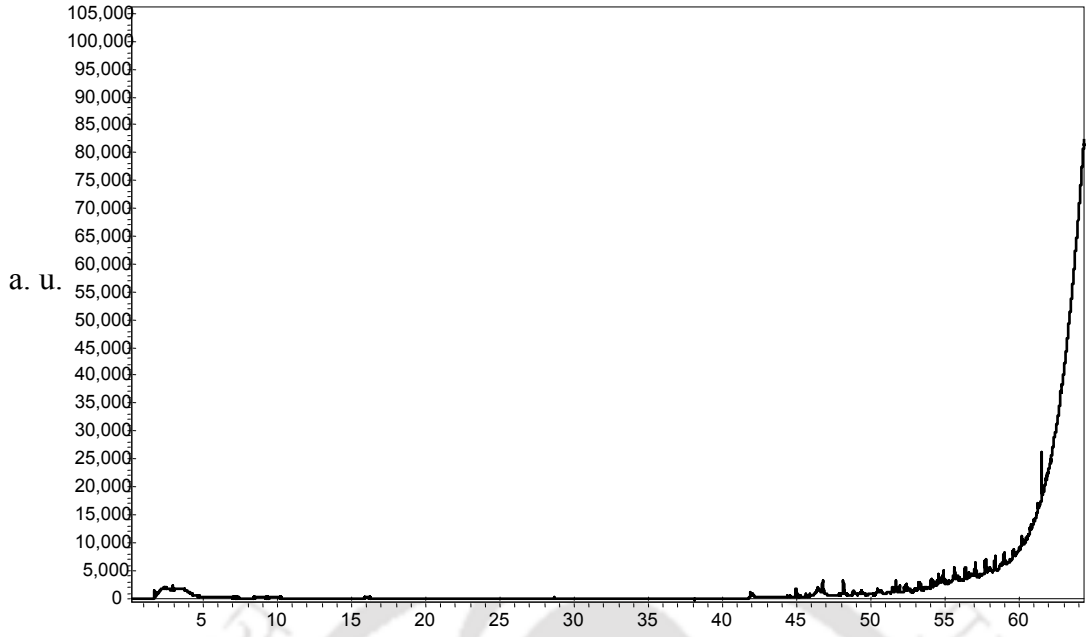

Figure A3.17 Pyrogram of 50% LDPE and 50% PET mixture at 600^{o} C

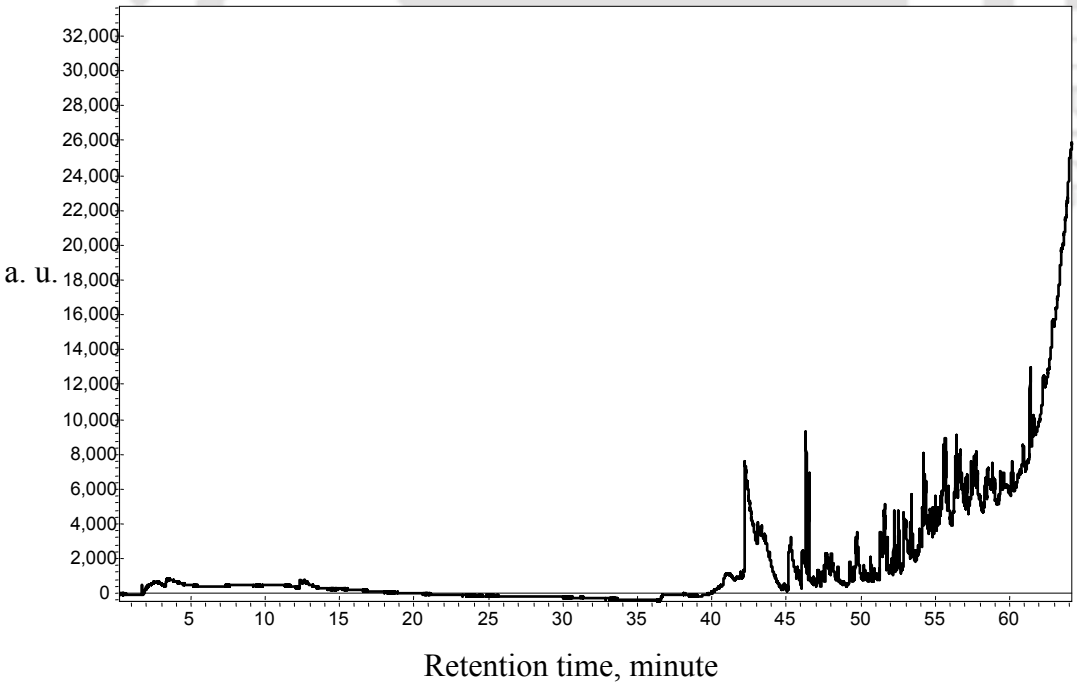

Figure A3.18 Pyrogram of 80% LDPE and 20% PET mixture at 300^{o} C

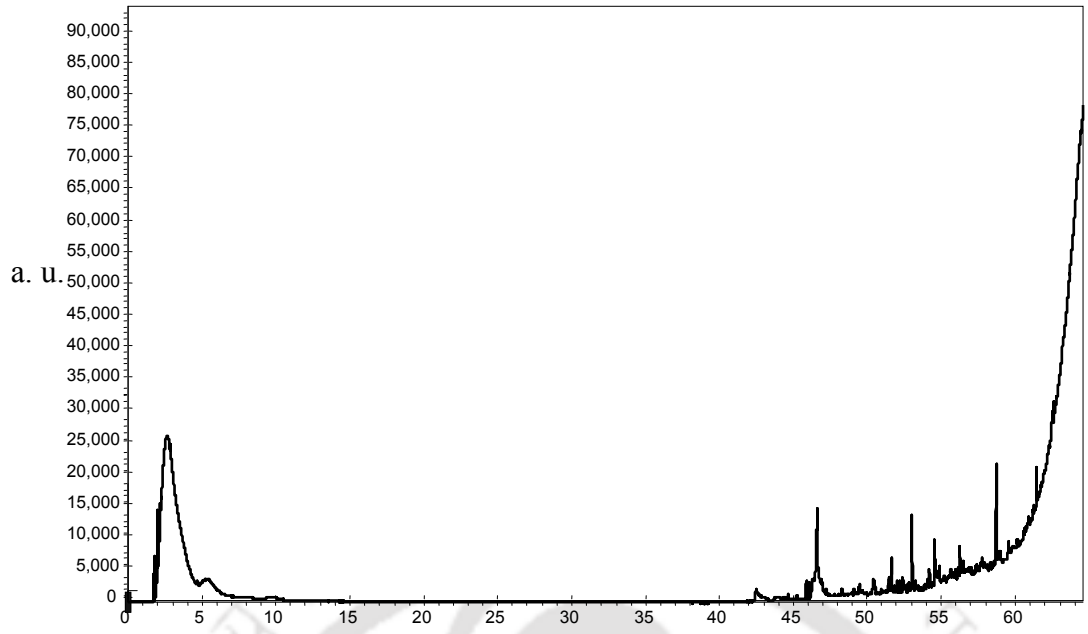

Figure A3.19 Pyrogram of 80% LDPE and 20% PET mixture at 400^{o} C

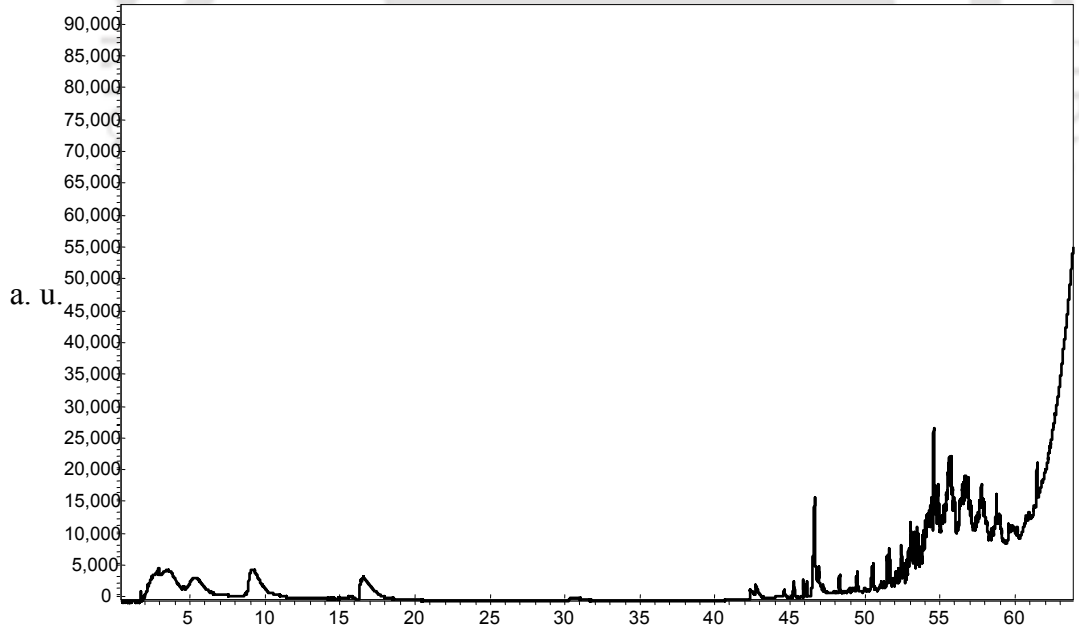

Figure A3.20 Pyrogram of 80% LDPE and 20% PET mixture at 500^{o} C

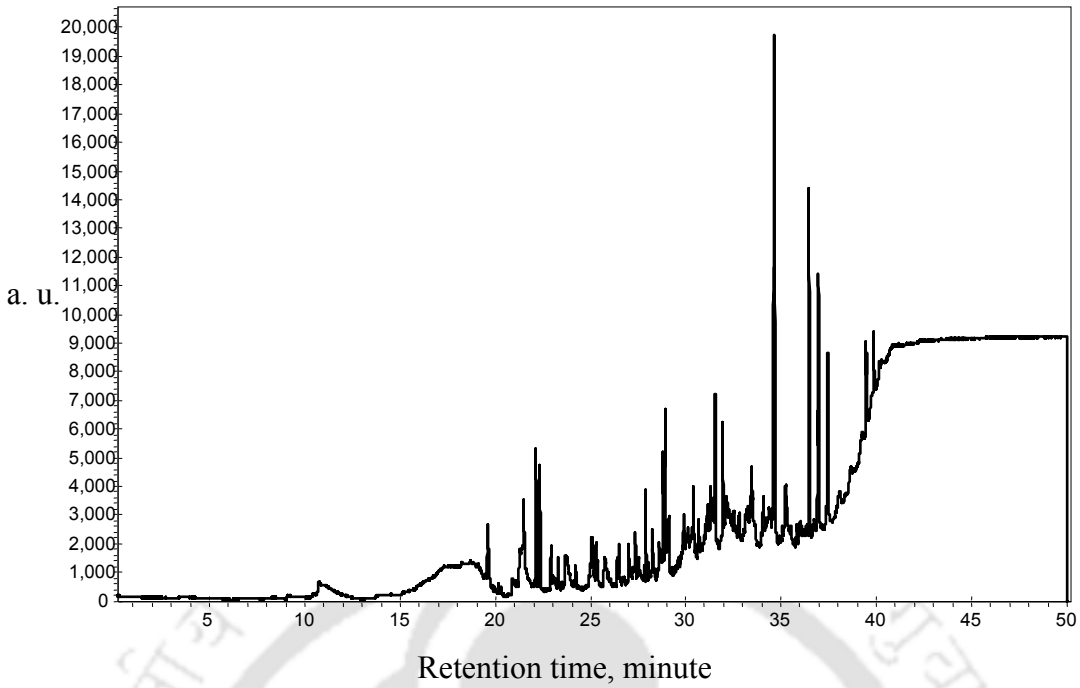

Figure A3.21 Pyrogram of 80% LDPE and 20% PET mixture at 600^{o} C

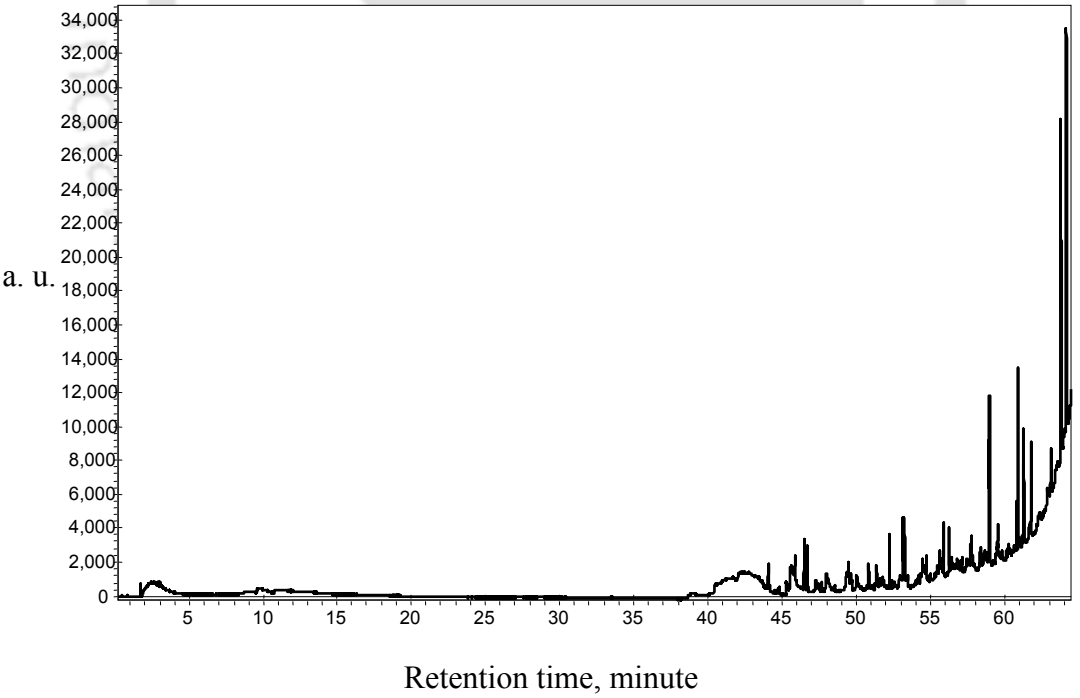

Figure A3.22 Pyrogram of 20% PP and 80% PET mixture at 300^{o} C

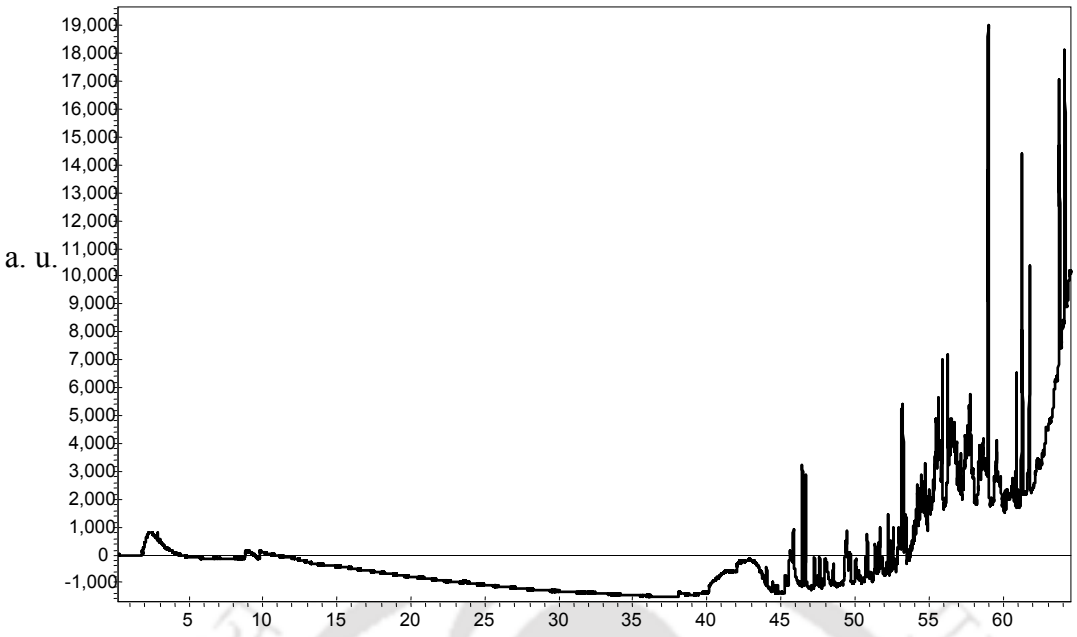

Figure A3.23 Pyrogram of 20% PP and 80% PET mixture at 400^{o} C

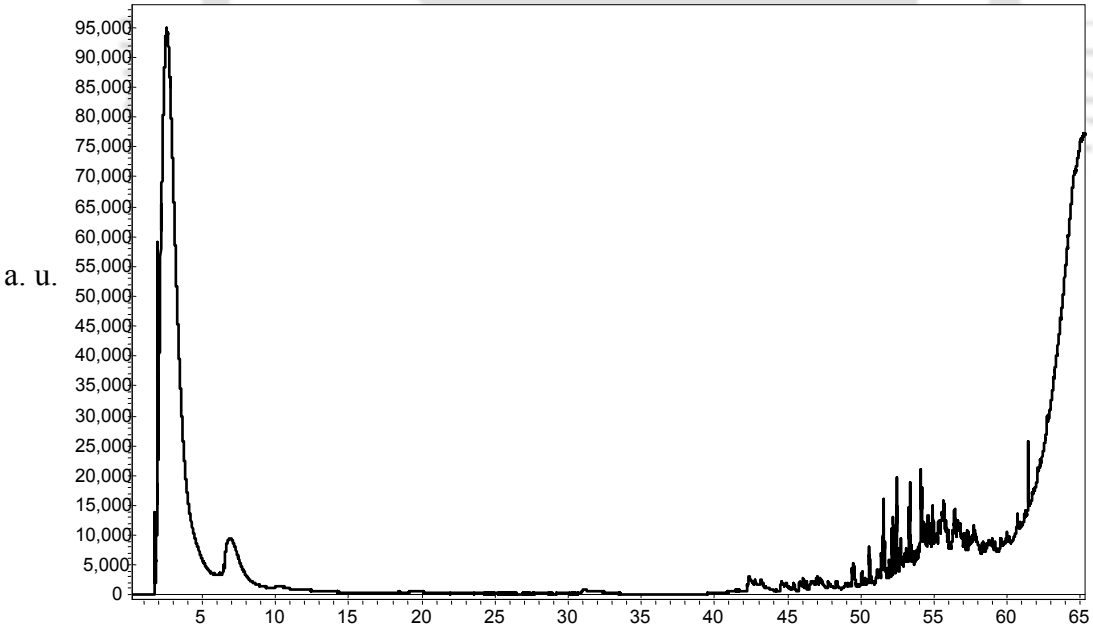

Figure A3.24 Pyrogram of 20% PP and 80% PET mixture at 500^{o} C

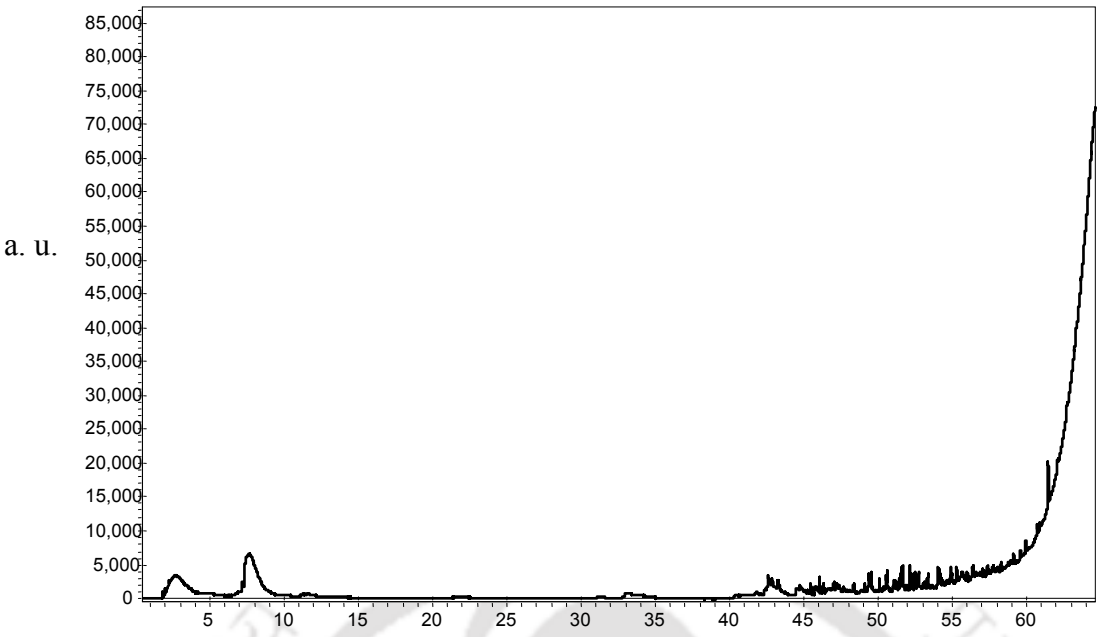

Figure A3.25 Pyrogram of 50% PP and 50% PET mixture at 300^{o} C

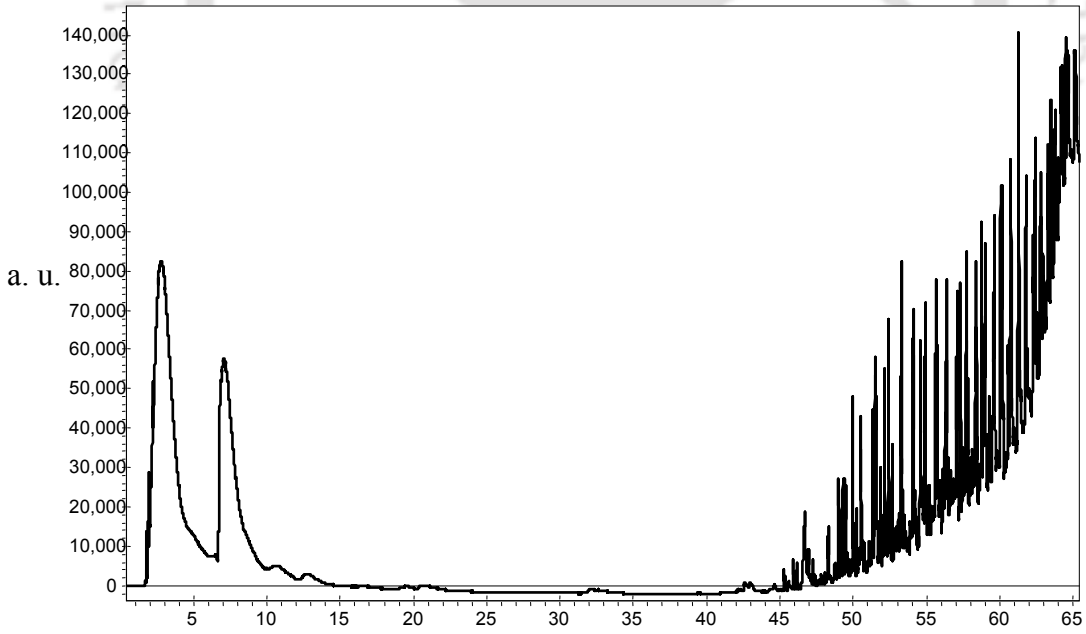

Figure A3.26 Pyrogram of 50% PP and 50% PET mixture at 400^{o} C

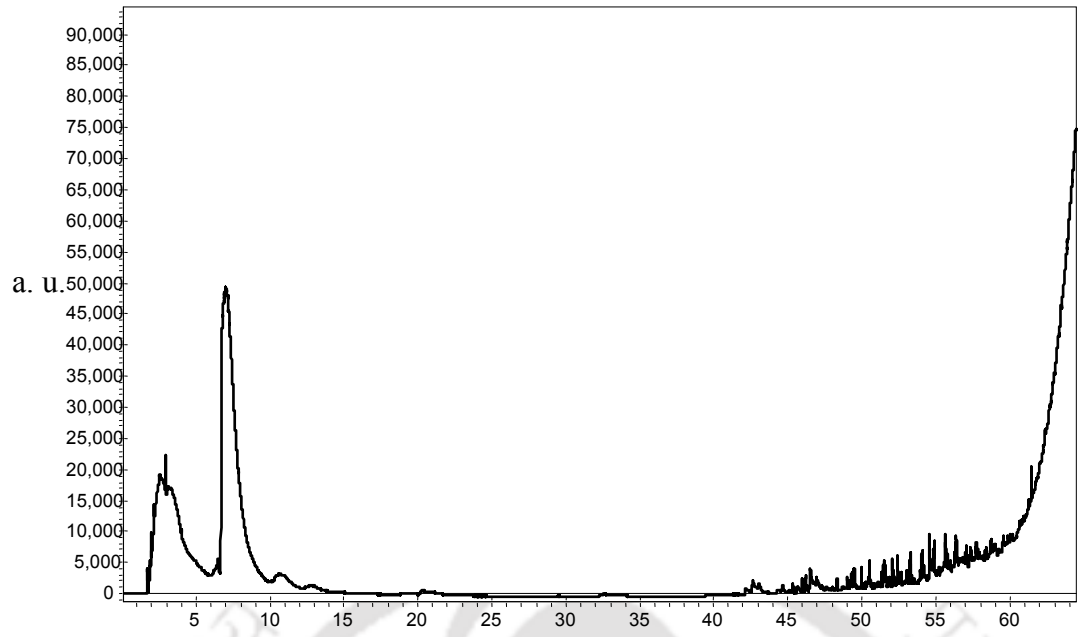

Figure A3.27 Pyrogram of 50% PP and 50% PET mixture at 500^{o} C

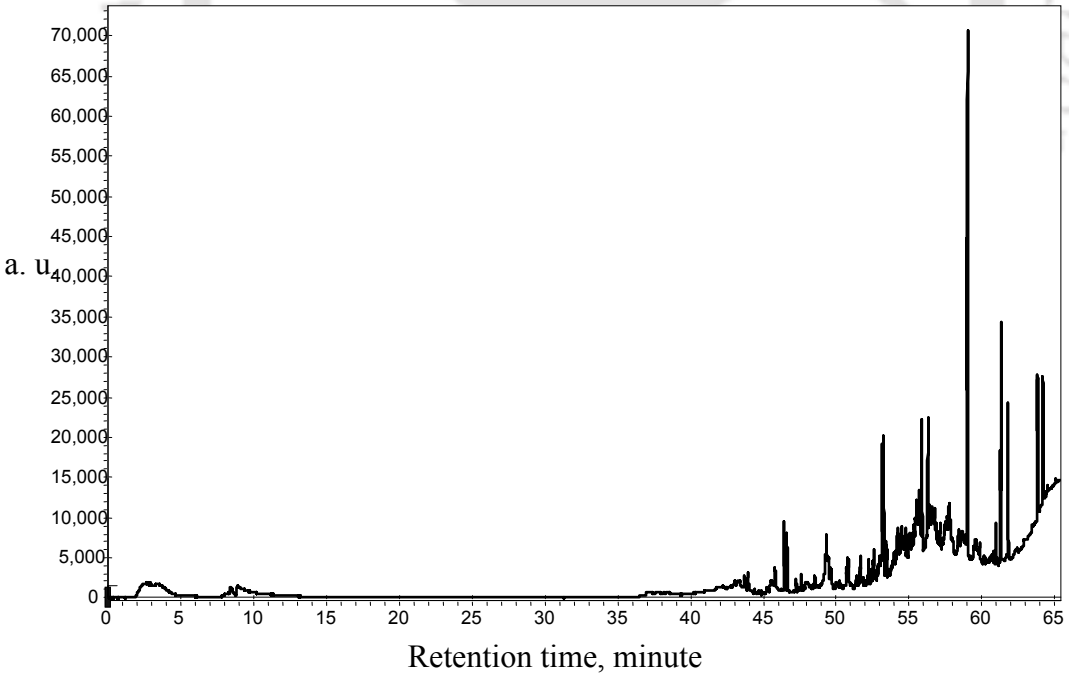

Figure A3.28 Pyrogram of 50% PP and 50% PET mixture at 600^{o} C

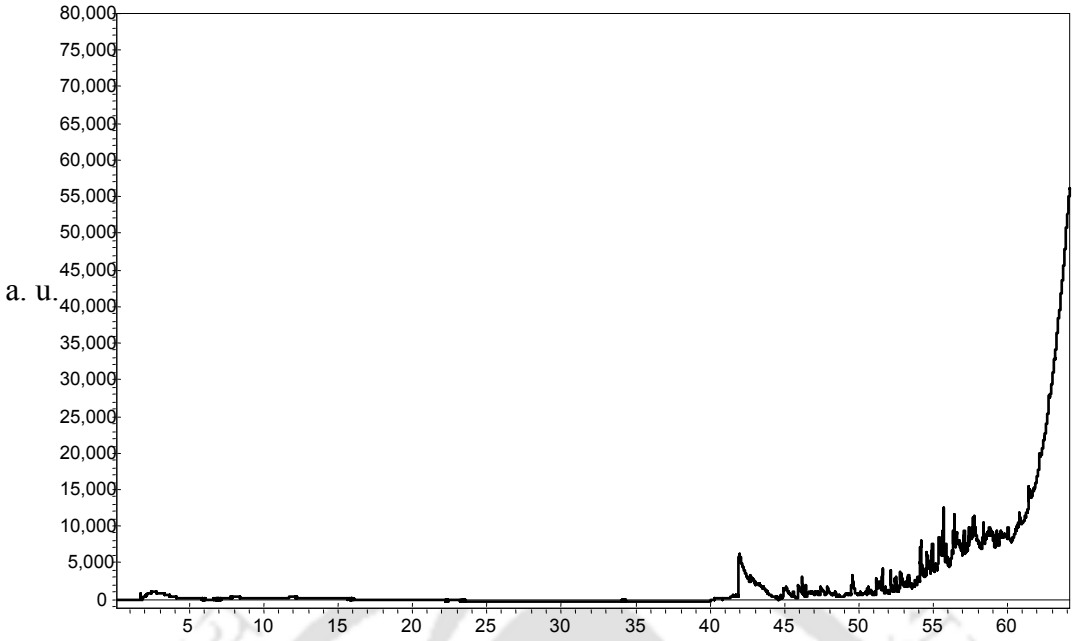

Figure A3.29 Pyrogram of 80% PP and 20% PET mixture at 300^{o} C

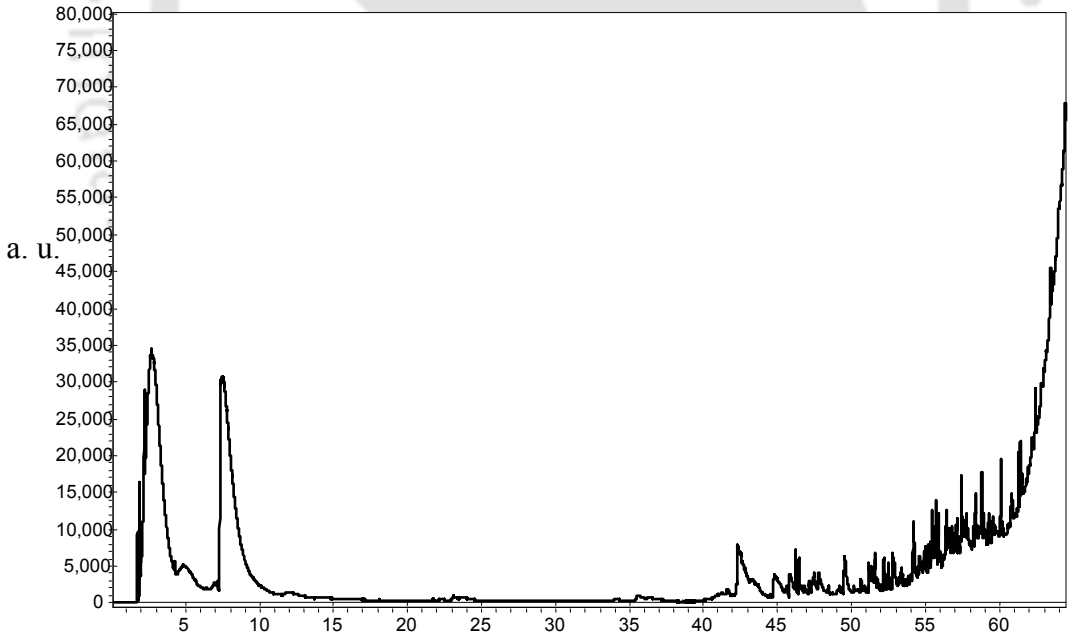

Figure A3.30 Pyrogram of 80% PP and 20% PET mixture at 400^{o} C

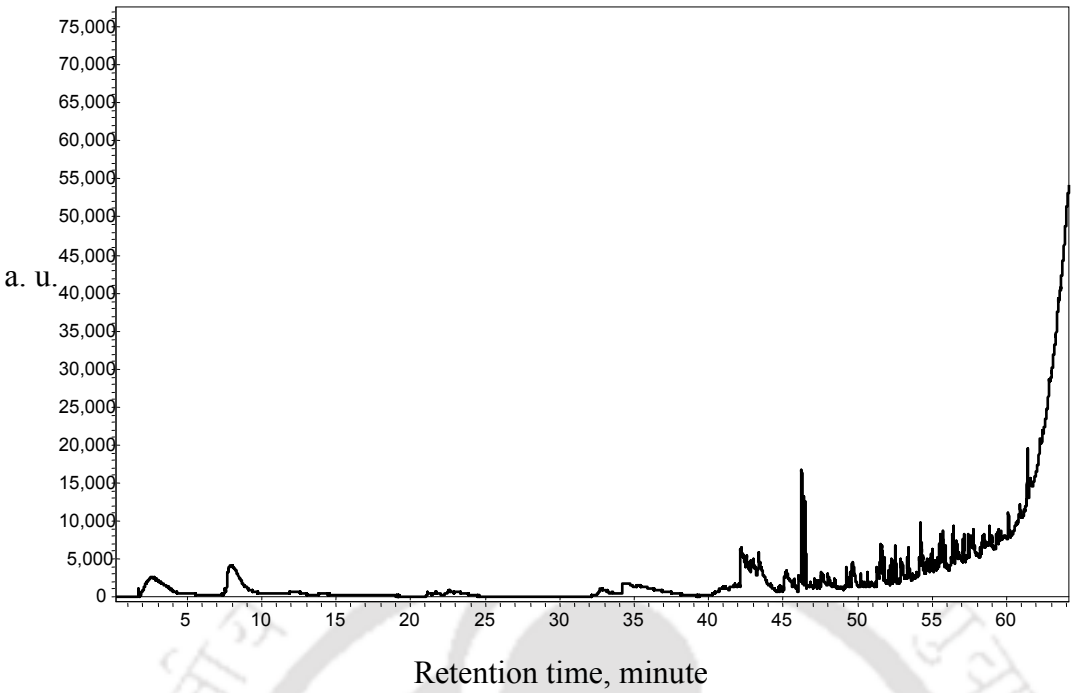

Figure A3.31 Pyrogram of 80% PP and 20% PET mixture at 500^{o} C

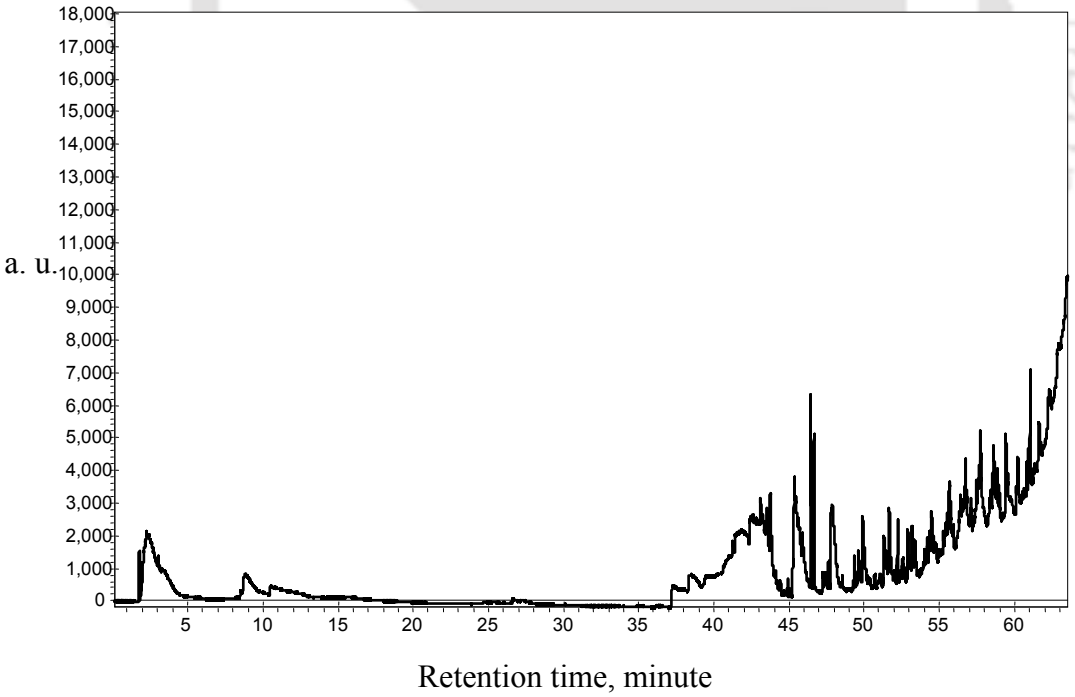

Figure A3.32 Pyrogram of 80% PP and 20% PET mixture at 600^{o} C

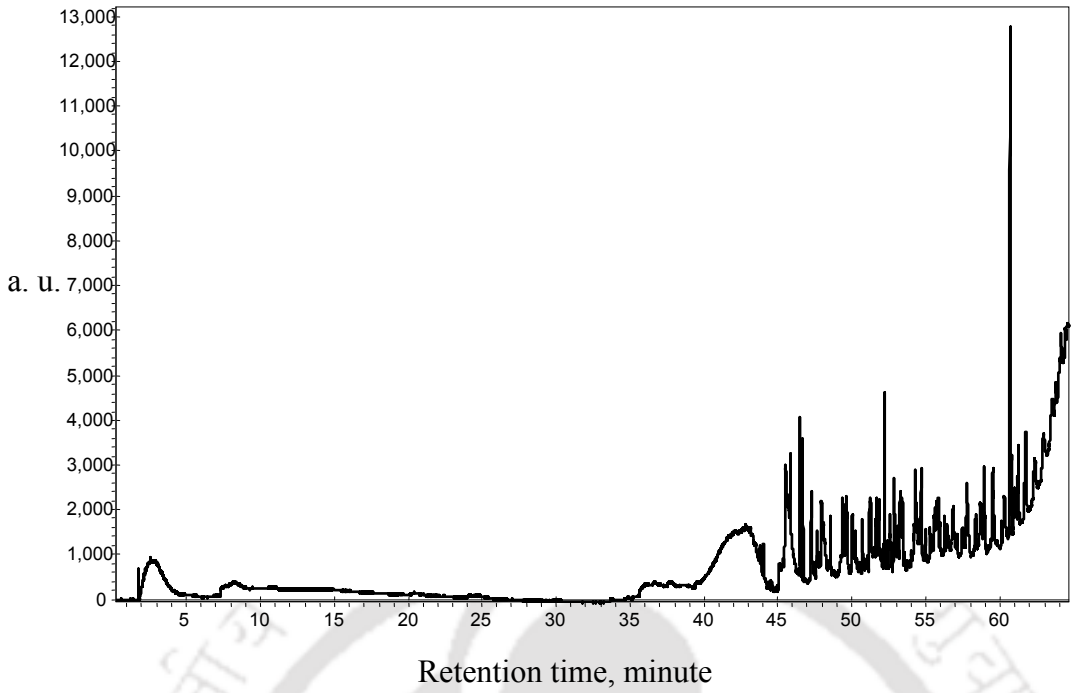

Figure A3.33 Pyrogram of 25% LDPE, 25% PP and 50% PET mixture at 300^{o} C

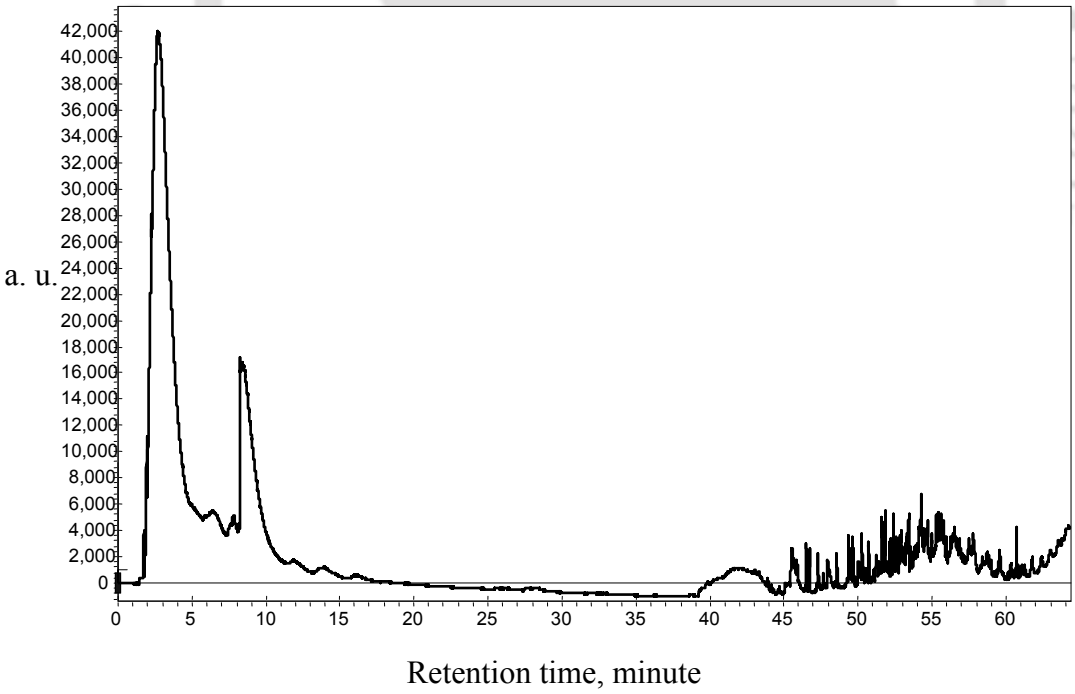

Figure A3.34 Pyrogram of 25% LDPE, 25% PP and 50% PET mixture at 400^{o} C

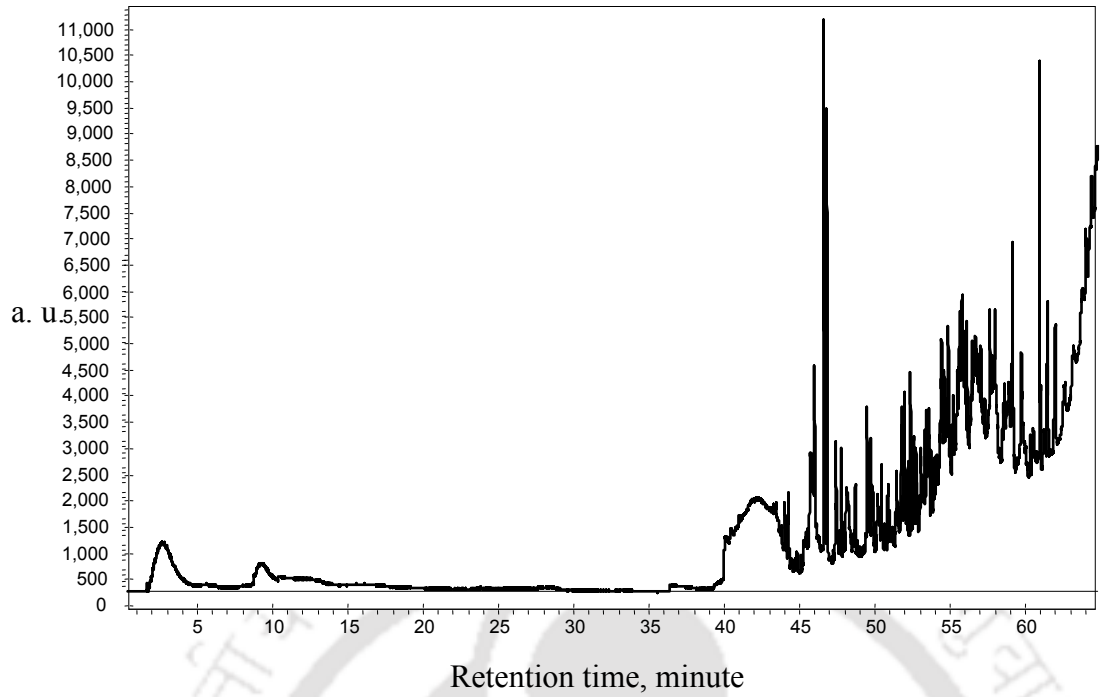

Figure A3.35 Pyrogram of 25% LDPE, 50% PP and 25% PET mixture at 300^{o} C

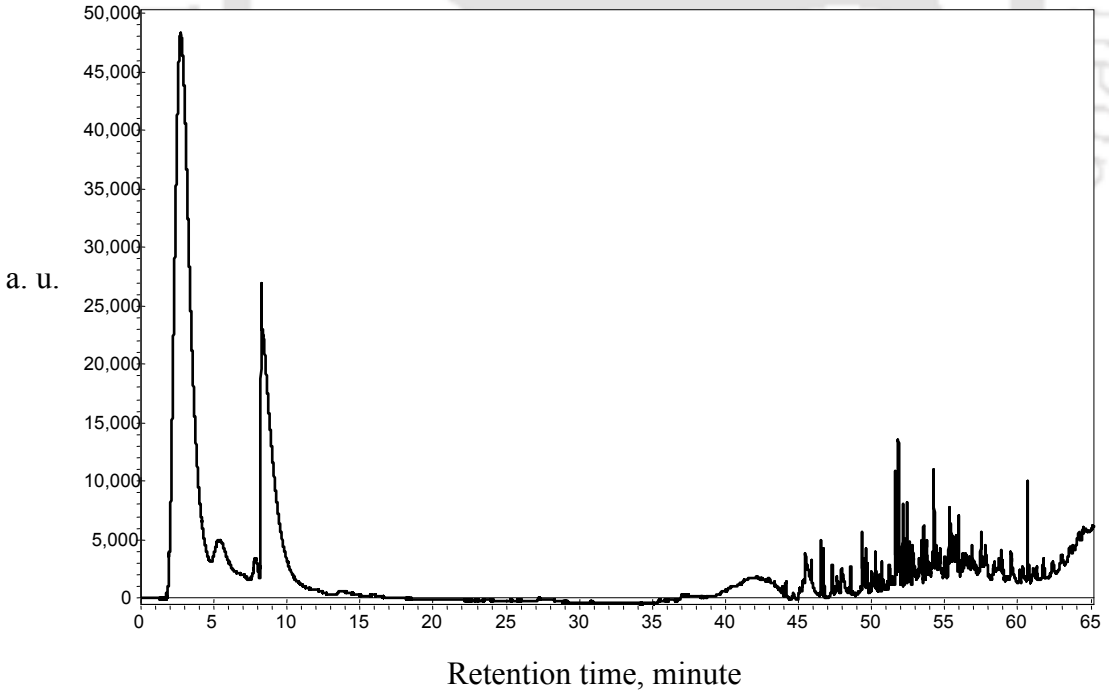

Figure A3.36 Pyrogram of 25% LDPE, 50% PP and 25% PET mixture at 400^{o} C

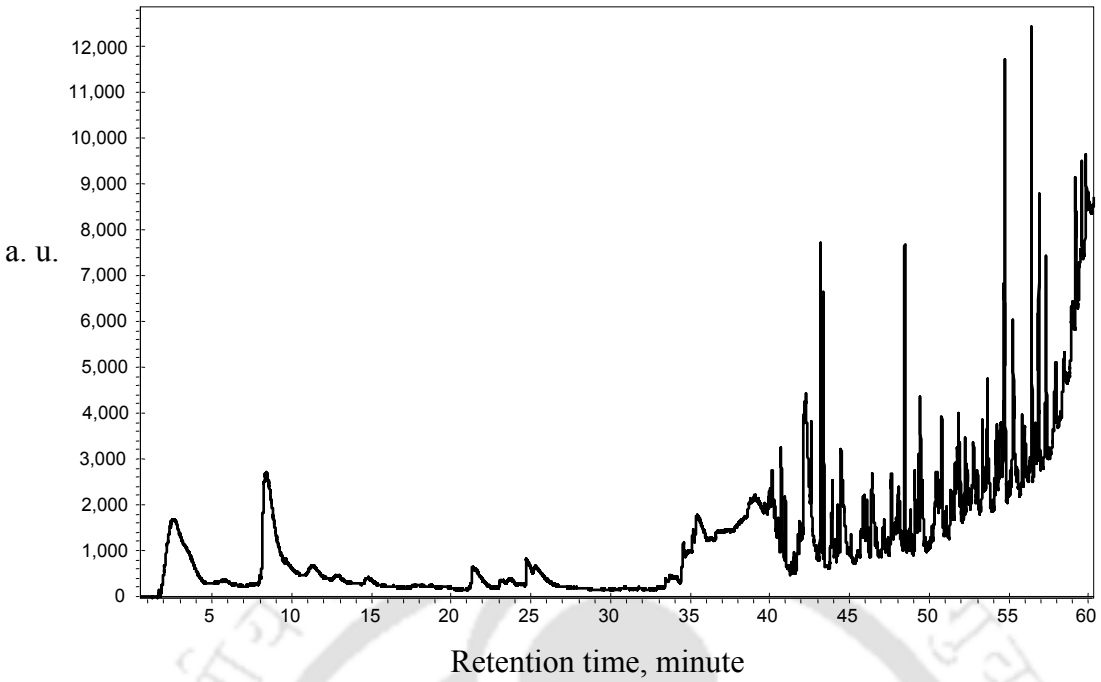

Figure A3.37 Pyrogram of 25% LDPE, 50% PP and 25% PET mixture at 500^{o} C

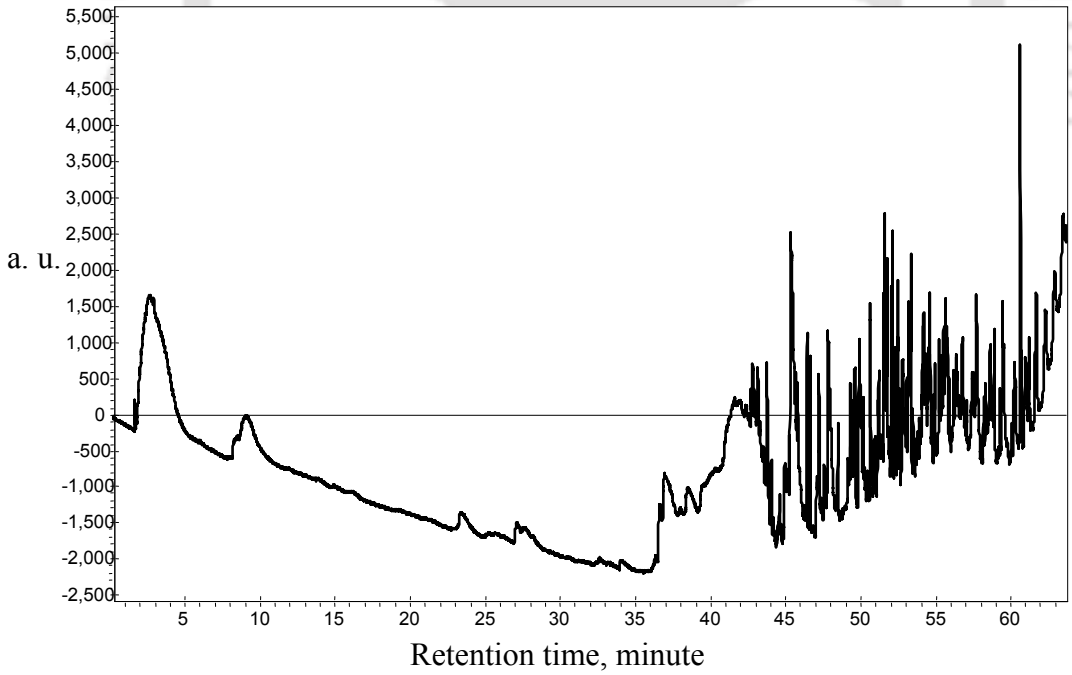

Figure A3.38 Pyrogram of 25% LDPE, 50% PP and 25% PET mixture at 600^{o} C

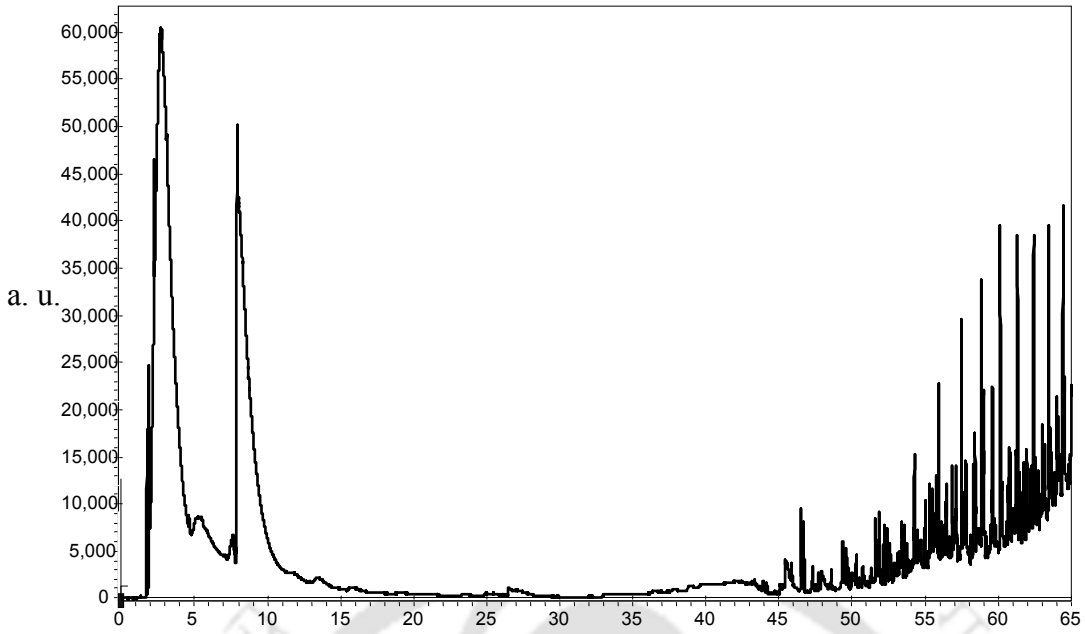

Figure A3.39 Pyrogram of 25% LDPE, 50% PP and 25% PET mixture at 429^{o} C (maximum decomposition temperature,T_{max})

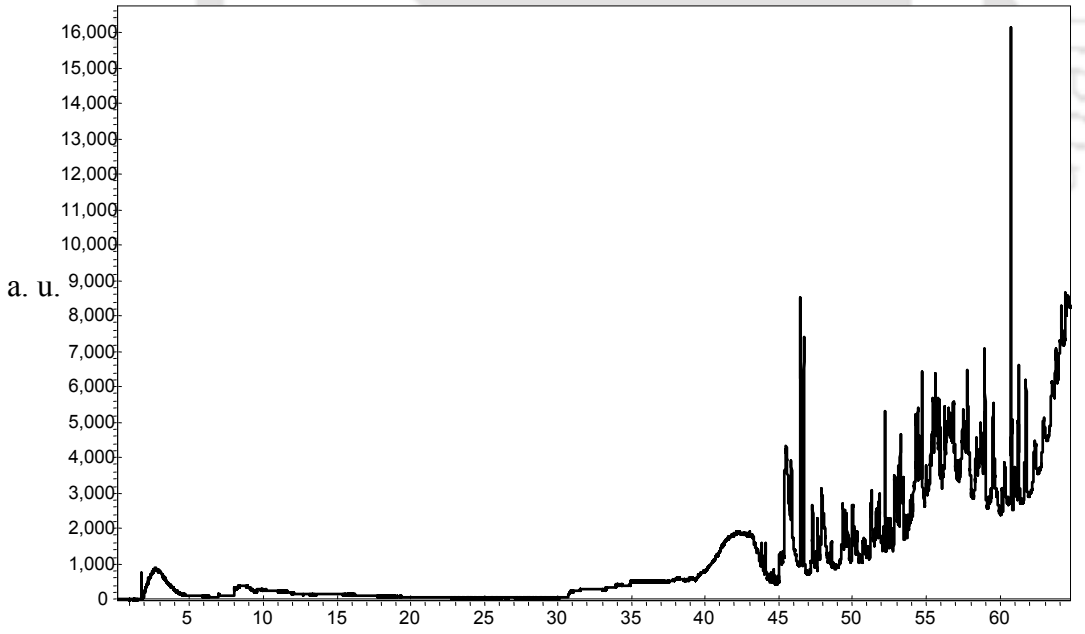

Figure A3.40 Pyrogram of 50% LDPE, 25% PP and 25% PET mixture at 300^{o} C

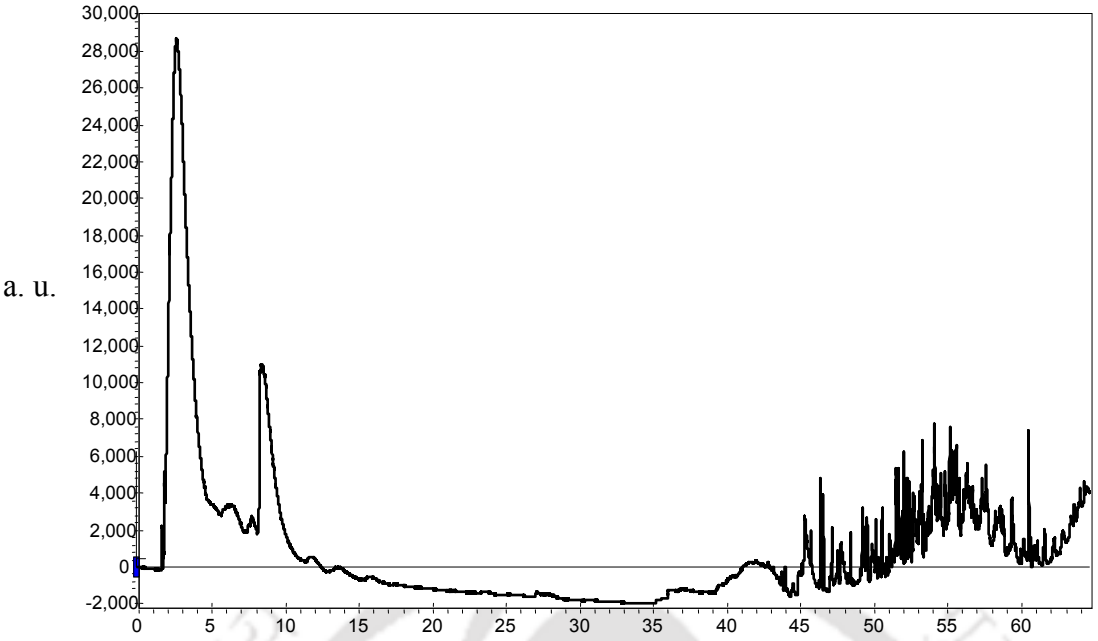

Figure A3.41 Pyrogram of 50% LDPE, 25% PP and 25% PET mixture at 400^{o} C

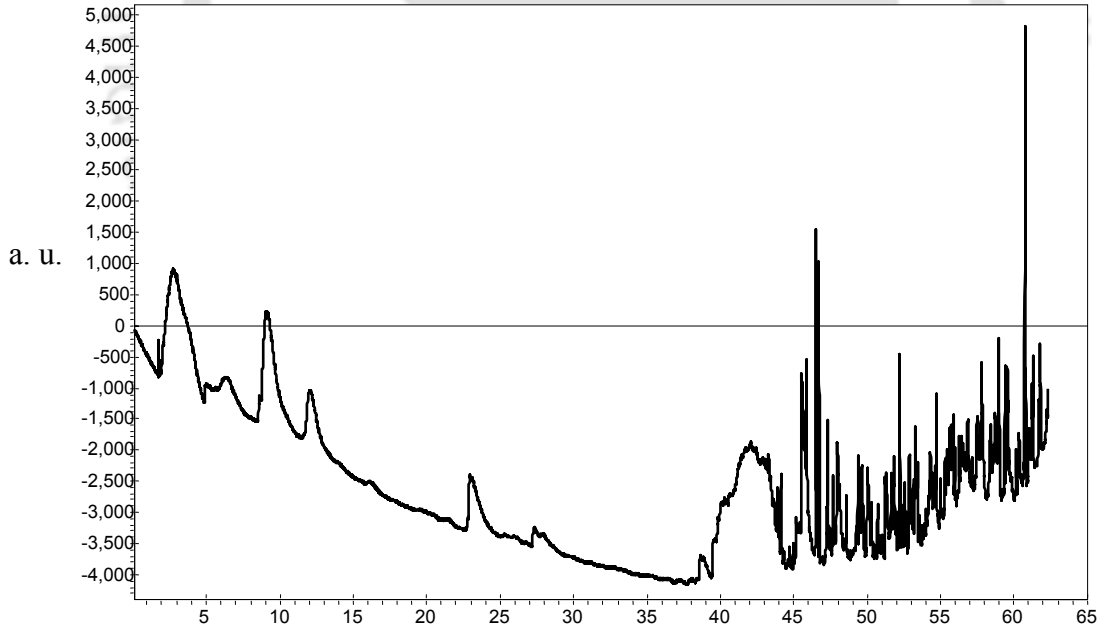

Figure A3.42 Pyrogram of 50% LDPE, 25% PP and 25% PET mixture at 500^{o} C

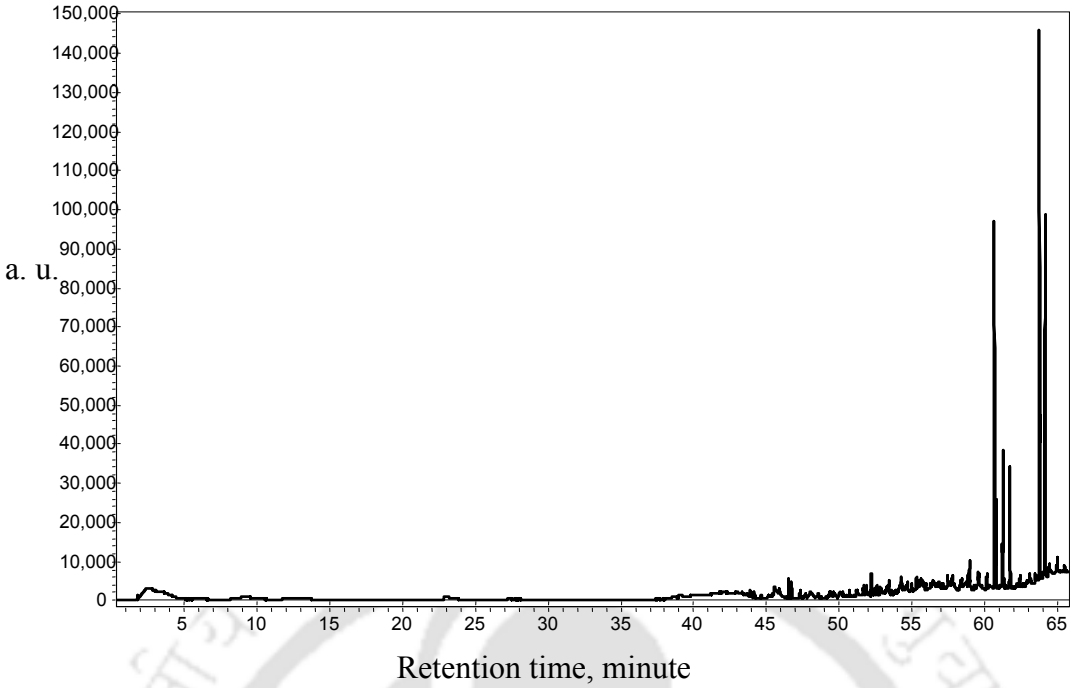

Figure A3.43 Pyrogram of 50% LDPE, 25% PP and 25% PET mixture at 600^{o} C

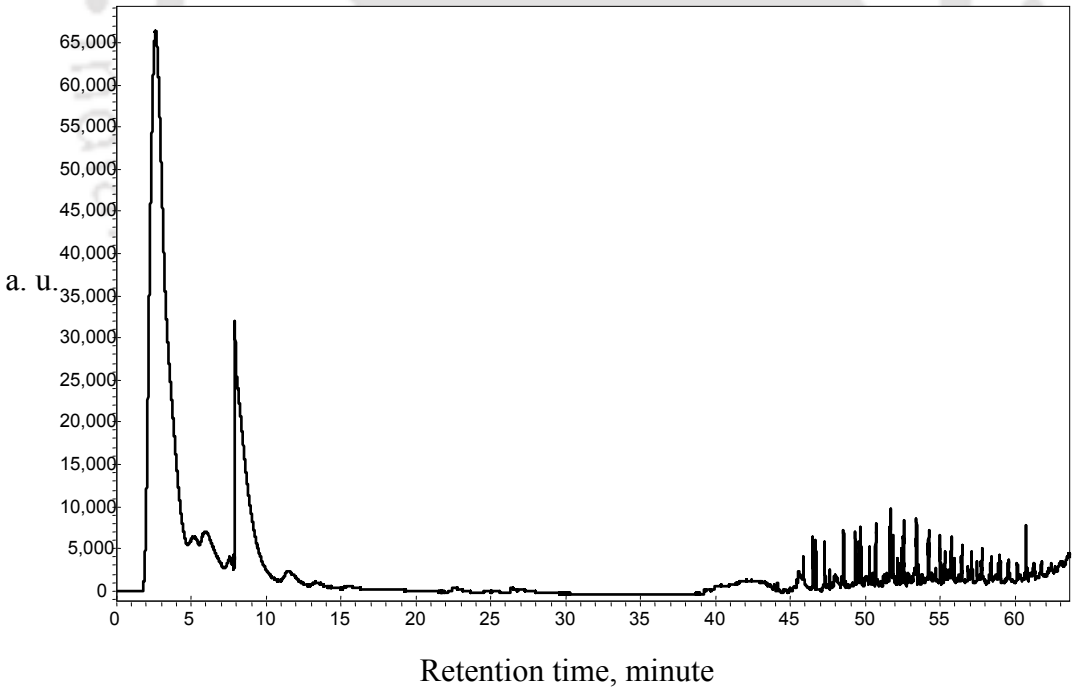

Figure A3.44 Pyrogram of 50% LDPE, 25% PP and 25% PET mixture at 436^{o} C (maximum decomposition temperature T_{max})

APPENDIX 4

Mole fractions of hydrocarbon fractions (C5-C44) in the pyrolyzates

A4.1 Calculations for LDPE

Table A4.1 Mole fraction of products in LDPE pyrolyzate at different temperatures

Temperature (^oC)	Carbon No.	RT_i (min)	RT_f (min)	area%	mole%	mole fraction(corrected)
200	C5-C10	1.64	29.24	0.46	0.51	0.51
	C12-C15	40.08	48.44	7.41	8.17	8.23
	C16-C22	49.13	54.87	69.19	90.57	91.25
	C24-C30	56.30	60.36	0.00	0.00	0.00
	C32-C44	61.42	63.59	0.00	0.00	0.00
300	C5-C10	1.64	29.24	2.42	2.67	2.72
	C12-C15	40.08	48.44	15.00	16.55	16.84
	C16-C22	49.13	54.87	76.04	79.01	80.44
	C24-C30	56.30	60.36	0.00	0.00	0.00
	C32-C44	61.42	63.59	0.00	0.00	0.00
400	C5-C10	1.64	29.24	13.93	15.36	16.39
	C12-C15	40.08	48.44	12.43	13.71	14.63
	C16-C22	49.13	54.87	62.21	64.63	68.98
	C24-C30	56.30	60.36	2.84	2.95	3.15
	C32-C44	61.42	63.59	4.49	4.66	4.98
470 (T_{max})	C5-C10	1.64	29.24	9.08	10.02	10.70
	C12-C15	40.08	48.44	13.01	14.35	15.33
	C16-C22	49.13	54.87	39.72	41.27	44.09
	C24-C30	56.30	60.36	15.44	16.04	17.14
	C32-C44	61.42	63.59	11.48	11.93	12.74
500	C5-C10	1.64	29.24	40.10	44.23	42.31
	C12-C15	40.08	48.44	50.62	55.83	53.40
	C16-C22	49.13	54.87	4.32	4.48	4.29
	C24-C30	56.30	60.36	2.15	2.23	2.13
	C32-C44	61.42	63.59	0.08	0.08	0.08
600	C5-C10	1.64	29.24	4.31	4.75	4.48
	C12-C15	40.08	48.44	4.47	4.93	4.65
	C16-C22	49.13	54.87	61.93	64.34	60.68
	C24-C30	56.30	60.36	30.19	31.37	29.58
	C32-C44	61.42	63.59	0.62	0.64	0.60

A4.2 Calculations for PP

Table A4.2 Mole fraction of products in PP pyrolyzate at different temperatures

Temperature (^{o}C)	Carbon No.	RT_i (min)	RT_f (min)	area%	mole%	mole fraction(corrected)
200	C5-C10	1.64	29.24	3.71	4.09	3.78
	C12-C15	40.08	48.44	80.94	89.28	82.58
	C16-C22	49.13	54.87	14.19	14.74	13.64
	C24-C30	56.30	60.36	0.00	0.00	0.00
	C32-C44	61.42	63.59	0.00	0.00	0.00
300	C5-C10	1.64	29.24	7.30	8.05	7.43
	C12-C15	40.08	48.44	68.51	75.57	69.73
	C16-C22	49.13	54.87	23.83	24.76	22.85
	C24-C30	56.30	60.36	0.00	0.00	0.00
	C32-C44	61.42	63.59	0.00	0.00	0.00
400	C5-C10	1.64	29.24	52.77	58.20	56.01
	C12-C15	40.08	48.44	7.26	8.01	7.71
	C16-C22	49.13	54.87	13.72	14.26	13.72
	C24-C30	56.30	60.36	9.35	9.72	9.35
	C32-C44	61.42	63.59	13.21	13.73	13.21
446 (T_{max})	C5-C10	1.64	29.24	42.57	46.96	48.02
	C12-C15	40.08	48.44	4.85	5.35	5.47
	C16-C22	49.13	54.87	19.54	20.30	20.76
	C24-C30	56.30	60.36	14.07	14.61	14.95
	C32-C44	61.42	63.59	10.16	10.56	10.79
500	C5-C10	1.64	29.24	43.24	47.70	46.04
	C12-C15	40.08	48.44	14.35	15.82	15.27
	C16-C22	49.13	54.87	11.51	11.96	11.55
	C24-C30	56.30	60.36	11.96	12.42	11.99
	C32-C44	61.42	63.59	15.10	15.69	15.15
600	C5-C10	1.64	29.24	33.44	36.88	37.94
	C12-C15	40.08	48.44	10.61	11.70	12.04
	C16-C22	49.13	54.87	10.56	11.65	11.98
	C24-C30	56.30	60.36	11.18	12.33	12.68
	C32-C44	61.42	63.59	22.36	24.66	25.36

A4.3 Calculations for PET

Table A4.3 Mole fraction of products in PET pyrolyzate at different temperatures

Temperature (^oC)	Carbon No.	RT_i (min)	RT_f (min)	area%	mole%	mole fraction(corrected)
200	C5-C10	1.85	29.00	2.31	2.55	2.42
	C12-C15	41.00	48.50	16.75	18.47	17.53
	C16-C22	49.40	55.10	39.18	40.71	38.64
	C24-C30	56.80	61.00	24.92	25.89	24.58
	C32-C44	62.00	64.00	17.06	17.73	16.83
300	C5-C10	1.85	29.00	5.31	5.86	4.33
	C12-C15	41.00	48.50	21.39	23.59	17.42
	C16-C22	49.40	55.10	40.98	42.58	31.45
	C24-C30	56.80	61.00	28.57	29.68	21.92
	C32-C44	62.00	64.00	32.42	33.69	24.88
400	C5-C10	1.85	29.00	85.79	94.63	86.11
	C12-C15	41.00	48.50	7.48	8.26	7.51
	C16-C22	49.40	55.10	3.53	3.66	3.33
	C24-C30	56.80	61.00	2.53	2.62	2.39
	C32-C44	62.00	64.00	0.69	0.72	0.65
435 (T_{max})	C5-C10	1.85	29.00	76.09	83.93	76.94
	C12-C15	41.00	48.50	4.51	4.98	4.56
	C16-C22	49.40	55.10	10.89	11.32	10.37
	C24-C30	56.80	61.00	7.11	7.39	6.77
	C32-C44	62.00	64.00	1.42	1.47	1.35
500	C5-C10	1.85	29.00	96.54	106.48	96.65
	C12-C15	41.00	48.50	1.06	1.17	1.06
	C16-C22	49.40	55.10	1.65	1.72	1.56
	C24-C30	56.80	61.00	0.52	0.54	0.49
	C32-C44	62.00	64.00	0.25	0.26	0.24
600	C5-C10	1.85	29.00	22.65	24.99	23.34
	C12-C15	41.00	48.50	24.78	27.33	25.54
	C16-C22	49.40	55.10	23.06	23.96	22.38
	C24-C30	56.80	61.00	25.07	26.05	24.34
	C32-C44	62.00	64.00	4.53	4.71	4.40

A4.4 Calculations for 20% LDPE, 80% PP binary mixture

Table A4.4 Mole fraction of products in 20% LDPE, 80% PP pyrolyzate at different temperatures

Temperature (^oC)	Carbon No.	RT_i (min)	RT_f (min)	area%	mole%	mole fraction(corrected)
200	C5-C10	1.64	29.24	0.00	0.00	0.00
	C12-C15	40.08	48.44	4.06	4.48	4.47
	C16-C22	49.13	54.87	71.18	73.96	73.75
	C24-C30	56.30	60.36	20.33	21.12	21.06
	C32-C44	61.42	63.59	0.70	0.73	0.73
300	C5-C10	1.64	29.24	5.62	6.20	6.01
	C12-C15	40.08	48.44	8.39	9.25	8.98
	C16-C22	49.13	54.87	84.31	87.60	85.01
	C24-C30	56.30	60.36	0.45	0.47	0.46
	C32-C44	61.42	63.59	0.58	0.60	0.59
400	C5-C10	1.64	29.24	42.73	47.14	46.16
	C12-C15	40.08	48.44	4.02	4.44	4.34
	C16-C22	49.13	54.87	42.14	43.78	42.88
	C24-C30	56.30	60.36	3.77	3.92	3.84
	C32-C44	61.42	63.59	2.74	2.84	2.79
435 (T_{max})	C5-C10	1.64	29.24	43.06	47.50	47.94
	C12-C15	40.08	48.44	6.45	7.12	7.18
	C16-C22	49.13	54.87	17.01	17.67	17.83
	C24-C30	56.30	60.36	12.35	12.83	12.95
	C32-C44	61.42	63.59	13.44	13.97	14.10
500	C5-C10	1.64	29.24	21.89	24.15	23.79
	C12-C15	40.08	48.44	7.21	7.95	7.83
	C16-C22	49.13	54.87	66.82	69.42	68.39
	C24-C30	56.30	60.36	2.11	2.20	2.16
	C32-C44	61.42	63.59	1.09	1.13	1.11
600	C5-C10	1.64	29.24	33.65	37.12	36.75
	C12-C15	40.08	48.44	17.48	19.28	19.09
	C16-C22	49.13	54.87	29.06	30.20	29.90
	C24-C30	56.30	60.36	10.63	11.05	10.94
	C32-C44	61.42	63.59	3.22	3.34	3.31

A4.5 Calculations for 50% LDPE, 50% PP binary mixture

Table A4.5 Mole fraction of products in 50% LDPE, 50% PP pyrolyzate at different temperatures

Temperature (^oC)	Carbon No.	RT_i (min)	RT_f (min)	area%	mole%	mole fraction(corrected)
200	C5-C10	1.64	29.24	0.93	1.02	1.02
	C12-C15	40.08	48.44	6.89	7.60	7.58
	C16-C22	49.13	54.87	88.25	91.69	91.40
	C24-C30	56.30	60.36	0.00	0.00	0.00
	C32-C44	61.42	63.59	0.00	0.00	0.00
300	C5-C10	1.64	29.24	0.94	1.04	1.03
	C12-C15	40.08	48.44	9.69	10.69	10.67
	C16-C22	49.13	54.87	85.15	88.48	88.30
	C24-C30	56.30	60.36	0.00	0.00	0.00
	C32-C44	61.42	63.59	0.00	0.00	0.00
400	C5-C10	1.64	29.24	74.03	81.65	75.82
	C12-C15	40.08	48.44	3.49	3.85	3.57
	C16-C22	49.13	54.87	21.36	22.19	20.61
	C24-C30	56.30	60.36	0.00	0.00	0.00
	C32-C44	61.42	63.59	0.00	0.00	0.00
450 (T_{max})	C5-C10	1.64	29.24	70.35	77.60	78.39
	C12-C15	40.08	48.44	5.96	6.58	6.64
	C16-C22	49.13	54.87	14.26	14.82	14.97
	C24-C30	56.30	60.36	4.93	5.12	5.17
	C32-C44	61.42	63.59	2.54	2.64	2.67
500	C5-C10	1.64	29.24	23.80	26.25	25.62
	C12-C15	40.08	48.44	9.76	10.77	10.51
	C16-C22	49.13	54.87	62.97	65.43	63.87
	C24-C30	56.30	60.36	0.00	0.00	0.00
	C32-C44	61.42	63.59	0.00	0.00	0.00
600	C5-C10	1.64	29.24	4.87	5.37	5.15
	C12-C15	40.08	48.44	14.54	16.04	15.37
	C16-C22	49.13	54.87	79.88	82.99	79.49
	C24-C30	56.30	60.36	0.08	0.08	0.08
	C32-C44	61.42	63.59	0.00	0.00	0.00

A4.6 Calculations for 80% LDPE, 20% PP binary mixture

Table A4.6 Mole fraction of products in 80% LDPE, 20% PP pyrolyzate at different temperatures

Temperature (^oC)	Carbon No.	RT_i (min)	RT_f (min)	area%	mole%	mole fraction(corrected)
200	C5-C10	1.64	29.24	0.00	0.00	0.00
	C12-C15	40.08	48.44	6.17	6.80	6.76
	C16-C22	49.13	54.87	90.29	93.81	93.24
	C24-C30	56.30	60.36	0.00	0.00	0.00
	C32-C44	61.42	63.59	0.00	0.00	0.00
300	C5-C10	1.64	29.24	0.00	0.00	0.00
	C12-C15	40.08	48.44	7.59	8.37	8.33
	C16-C22	49.13	54.87	88.75	92.21	91.67
	C24-C30	56.30	60.36	0.00	0.00	0.00
	C32-C44	61.42	63.59	0.00	0.00	0.00
400	C5-C10	1.64	29.24	66.51	73.36	67.96
	C12-C15	40.08	48.44	2.86	3.15	2.92
	C16-C22	49.13	54.87	30.26	31.44	29.12
	C24-C30	56.30	60.36	0.00	0.00	0.00
	C32-C44	61.42	63.59	0.00	0.00	0.00
463 (T_{max})	C5-C10	1.64	29.24	20.06	22.12	21.05
	C12-C15	40.08	48.44	17.87	19.71	18.75
	C16-C22	49.13	54.87	31.50	32.73	31.14
	C24-C30	56.30	60.36	14.74	15.32	14.57
	C32-C44	61.42	63.59	14.67	15.24	14.50
500	C5-C10	1.64	29.24	43.29	47.75	45.24
	C12-C15	40.08	48.44	5.53	6.10	5.78
	C16-C22	49.13	54.87	49.76	51.70	48.98
	C24-C30	56.30	60.36	0.00	0.00	0.00
	C32-C44	61.42	63.59	0.00	0.00	0.00
600	C5-C10	1.64	29.24	2.44	2.69	2.67
	C12-C15	40.08	48.44	6.68	7.37	7.33
	C16-C22	49.13	54.87	85.11	88.43	87.99
	C24-C30	56.30	60.36	1.45	1.51	1.50
	C32-C44	61.42	63.59	0.49	0.51	0.50

A4.7 Calculations for 20% LDPE, 80% PET binary mixture

Table A4.7 Mole fraction of products in 20% LDPE, 80% PET pyrolyzate at different temperatures

Temperature (^oC)	Carbon No.	RT_i (min)	RT_f (min)	area%	mole%	mole fraction(corrected)
300	C5-C10	1.85	29.00	2.45	2.70	3.39
	C12-C15	41.00	48.50	17.22	18.99	23.87
	C16-C22	49.40	55.10	21.81	22.66	28.48
	C24-C30	56.80	61.00	30.32	31.50	39.59
	C32-C44	62.00	64.00	3.57	3.71	4.66
400	C5-C10	1.85	29.00	25.23	27.83	31.97
	C12-C15	41.00	48.50	17.36	19.15	22.00
	C16-C22	49.40	55.10	16.80	17.45	20.05
	C24-C30	56.80	61.00	18.96	19.70	22.63
	C32-C44	62.00	64.00	2.81	2.92	3.35
434 (T_{max})	C5-C10	1.85	29.00	27.26	30.07	35.14
	C12-C15	41.00	48.50	9.60	10.59	12.37
	C16-C22	49.40	55.10	14.51	15.07	17.62
	C24-C30	56.80	61.00	22.38	23.25	27.17
	C32-C44	62.00	64.00	6.34	6.59	7.70
500	C5-C10	1.85	29.00	2.00	2.21	5.00
	C12-C15	41.00	48.50	2.82	3.11	7.05
	C16-C22	49.40	55.10	11.28	11.72	26.54
	C24-C30	56.80	61.00	25.77	26.78	60.65
	C32-C44	62.00	64.00	0.32	0.33	0.76
600	C5-C10	1.85	29.00	0.55	0.61	11.04
	C12-C15	41.00	48.50	1.09	1.20	21.90
	C16-C22	49.40	55.10	2.05	2.13	38.73
	C24-C30	56.80	61.00	1.28	1.33	24.11
	C32-C44	62.00	64.00	0.22	0.23	4.21

A4.8 Calculations for 50% LDPE, 50% PET binary mixture

Table A4.8 Mole fraction of products in 50% LDPE, 50% PET pyrolyzate at different temperatures

Temperature (^oC)	Carbon No.	RT_i (min)	RT_f (min)	area%	mole%	mole fraction(corrected)
300	C5-C10	1.85	29.00	0.22	0.24	4.21
	C12-C15	41.00	48.50	0.35	0.38	6.67
	C16-C22	49.40	55.10	1.83	1.90	33.03
	C24-C30	56.80	61.00	3.02	3.14	54.51
	C32-C44	62.00	64.00	0.09	0.09	1.58
400	C5-C10	1.85	29.00	3.74	4.13	22.96
	C12-C15	41.00	48.50	1.35	1.49	8.29
	C16-C22	49.40	55.10	4.52	4.70	26.12
	C24-C30	56.80	61.00	5.97	6.21	34.51
	C32-C44	62.00	64.00	1.40	1.46	8.12
439 (T_{max})	C5-C10	1.85	29.00	26.93	29.70	37.36
	C12-C15	41.00	48.50	3.20	3.53	4.44
	C16-C22	49.40	55.10	14.12	14.67	18.45
	C24-C30	56.80	61.00	16.33	16.97	21.35
	C32-C44	62.00	64.00	14.07	14.62	18.39
500	C5-C10	1.85	29.00	3.24	3.58	14.82
	C12-C15	41.00	48.50	3.53	3.89	16.14
	C16-C22	49.40	55.10	6.21	6.45	26.74
	C24-C30	56.80	61.00	8.37	8.70	36.05
	C32-C44	62.00	64.00	1.45	1.51	6.24
600	C5-C10	1.85	29.00	0.11	0.12	2.47
	C12-C15	41.00	48.50	0.85	0.94	18.61
	C16-C22	49.40	55.10	1.45	1.50	29.83
	C24-C30	56.80	61.00	1.67	1.73	34.38
	C32-C44	62.00	64.00	0.71	0.74	14.71

A4.9 Calculations for 80% LDPE, 20% PET binary mixture

Table A4.9 Mole fraction of products in 80% LDPE, 20% PET pyrolyzate at different temperatures

Temperature (^oC)	Carbon No.	RT_i (min)	RT_f (min)	area%	mole%	mole fraction(corrected)
400	C5-C10	1.85	29.00	25.23	27.83	31.97
	C12-C15	41.00	48.50	17.36	19.15	22.00
	C16-C22	49.40	55.10	16.79	17.44	20.04
	C24-C30	56.80	61.00	18.96	19.70	22.64
	C32-C44	62.00	64.00	2.81	2.92	3.35
459 (T_{max})	C5-C10	1.85	29.00	3.42	3.77	12.82
	C12-C15	41.00	48.50	3.56	3.92	13.33
	C16-C22	49.40	55.10	6.48	6.74	22.88
	C24-C30	56.80	61.00	5.22	5.42	18.42
	C32-C44	62.00	64.00	9.22	9.58	32.55
500	C5-C10	1.85	29.00	21.12	23.30	26.08
	C12-C15	41.00	48.50	8.40	9.26	10.37
	C16-C22	49.40	55.10	23.34	24.25	27.15
	C24-C30	56.80	61.00	30.61	31.81	35.61
	C32-C44	62.00	64.00	0.68	0.71	0.79
600	C5-C10	1.85	29.00	5.48	6.04	6.69
	C12-C15	41.00	48.50	9.29	10.25	11.35
	C16-C22	49.40	55.10	39.16	40.69	45.08
	C24-C30	56.80	61.00	19.93	20.70	22.94
	C32-C44	62.00	64.00	12.11	12.58	13.94

A4.10 Calculations for 20% PP, 80% PET binary mixture

Table A4.10 Mole fraction of products in 20% PP, 80% PET pyrolyzate at different temperatures

Temperature (^oC)	Carbon No.	RT_i (min)	RT_f (min)	area%	mole%	mole fraction(corrected)
300	C5-C10	1.85	29.00	1.22	1.34	1.88
	C12-C15	41.00	48.50	25.26	27.86	39.17
	C16-C22	49.40	55.10	12.49	12.98	18.24
	C24-C30	56.80	61.00	18.07	18.77	26.38
	C32-C44	62.00	64.00	9.80	10.19	14.32
400	C5-C10	1.85	29.00	2.80	3.09	4.57
	C12-C15	41.00	48.50	6.41	7.07	10.48
	C16-C22	49.40	55.10	11.02	11.45	16.95
	C24-C30	56.80	61.00	33.90	35.22	52.16
	C32-C44	62.00	64.00	10.29	10.70	15.84
432 (T_{max})	C5-C10	1.85	29.00	8.95	9.87	21.31
	C12-C15	41.00	48.50	11.24	12.40	26.77
	C16-C22	49.40	55.10	6.84	7.11	15.35
	C24-C30	56.80	61.00	12.66	13.15	28.40
	C32-C44	62.00	64.00	3.65	3.79	8.18
500	C5-C10	1.85	29.00	34.87	38.46	44.30
	C12-C15	41.00	48.50	6.90	7.62	8.77
	C16-C22	49.40	55.10	19.27	20.03	23.06
	C24-C30	56.80	61.00	18.76	19.49	22.45
	C32-C44	62.00	64.00	1.18	1.23	1.42
600	C5-C10	1.85	29.00	13.60	15.01	14.95
	C12-C15	41.00	48.50	39.83	43.93	43.75
	C16-C22	49.40	55.10	15.68	16.29	16.22
	C24-C30	56.80	61.00	21.27	22.10	22.01
	C32-C44	62.00	64.00	2.96	3.08	3.07

A4.11 Calculations for 50% PP, 50% PET binary mixture

Table A4.11 Mole fraction of products in 50% PP, 50% PET pyrolyzate at different temperatures

Temperature (^oC)	Carbon No.	RT_i (min)	RT_f (min)	area%	mole%	mole fraction(corrected)
300	C5-C10	1.85	29.00	30.24	33.35	38.30
	C12-C15	41.00	48.50	21.06	23.23	26.68
	C16-C22	49.40	55.10	16.51	17.15	19.70
	C24-C30	56.80	61.00	10.98	11.40	13.10
	C32-C44	62.00	64.00	1.87	1.94	2.23
400	C5-C10	1.85	29.00	22.12	24.40	28.26
	C12-C15	41.00	48.50	2.71	2.99	3.46
	C16-C22	49.40	55.10	16.47	17.11	19.82
	C24-C30	56.80	61.00	23.62	24.55	28.43
	C32-C44	62.00	64.00	16.63	17.28	20.02
434 (T_{max})	C5-C10	1.85	29.00	82.48	90.98	87.84
	C12-C15	41.00	48.50	3.75	4.14	4.00
	C16-C22	49.40	55.10	4.77	4.96	4.79
	C24-C30	56.80	61.00	2.94	3.05	2.95
	C32-C44	62.00	64.00	0.42	0.44	0.43
500	C5-C10	1.85	29.00	23.35	25.76	59.41
	C12-C15	41.00	48.50	1.41	1.55	3.58
	C16-C22	49.40	55.10	1.96	2.04	4.70
	C24-C30	56.80	61.00	1.67	1.73	3.99
	C32-C44	62.00	64.00	11.82	12.28	28.32
600	C5-C10	1.85	29.00	2.64	2.91	3.08
	C12-C15	41.00	48.50	8.40	9.27	9.81
	C16-C22	49.40	55.10	22.78	23.67	25.07
	C24-C30	56.80	61.00	49.95	51.90	54.97
	C32-C44	62.00	64.00	6.42	6.67	7.07

A4.12 Calculations for 80% PP, 20% PET binary mixture

Table A4.12 Mole fraction of products in 80% PP, 20% PET pyrolyzate at different temperatures

Temperature (^oC)	Carbon No.	RT_i (min)	RT_f (min)	area%	mole%	mole fraction(corrected)
300	C5-C10	1.85	29.00	1.05	1.16	2.23
	C12-C15	41.00	48.50	14.85	16.38	31.54
	C16-C22	49.40	55.10	9.77	10.15	19.55
	C24-C30	56.80	61.00	22.33	23.20	44.66
	C32-C44	62.00	64.00	1.01	1.05	2.03
400	C5-C10	1.85	29.00	12.32	13.58	45.09
	C12-C15	41.00	48.50	1.80	1.99	6.60
	C16-C22	49.40	55.10	2.29	2.38	7.90
	C24-C30	56.80	61.00	3.68	3.83	12.70
	C32-C44	62.00	64.00	8.03	8.35	27.71
440 (T_{max})	C5-C10	1.85	29.00	8.53	9.41	21.16
	C12-C15	41.00	48.50	9.83	10.84	24.38
	C16-C22	49.40	55.10	5.29	5.50	12.37
	C24-C30	56.80	61.00	6.74	7.00	15.75
	C32-C44	62.00	64.00	11.27	11.71	26.34
500	C5-C10	1.85	29.00	2.50	2.75	14.29
	C12-C15	41.00	48.50	4.97	5.48	28.46
	C16-C22	49.40	55.10	3.28	3.41	17.68
	C24-C30	56.80	61.00	3.92	4.08	21.16
	C32-C44	62.00	64.00	3.42	3.55	18.41
600	C5-C10	1.85	29.00	5.89	6.50	9.57
	C12-C15	41.00	48.50	22.18	24.47	36.05
	C16-C22	49.40	55.10	10.96	11.39	16.78
	C24-C30	56.80	61.00	19.75	20.52	30.23
	C32-C44	62.00	64.00	4.81	5.00	7.37

A4.13 Calculations for 25% LDPE, 25% PP, 50% PET ternary mixture

Table A4.13 Mole fraction of products in 25% LDPE, 25% PP, 50% PET pyrolyzate at different temperatures

Temperature (^{o}C)	Carbon No.	RT_i (min)	RT_f (min)	area%	mole%	mole fraction(corrected)
300	C5-C10	1.85	29.00	1.79	1.98	2.26
	C12-C15	41.00	48.50	33.09	36.49	41.76
	C16-C22	49.40	55.10	20.59	21.39	24.48
	C24-C30	56.80	61.00	15.81	16.42	18.79
	C32-C44	62.00	64.00	10.68	11.10	12.70
400	C5-C10	1.85	29.00	72.80	80.30	74.41
	C12-C15	41.00	48.50	10.29	11.34	10.51
	C16-C22	49.40	55.10	9.09	9.44	8.75
	C24-C30	56.80	61.00	5.36	5.56	5.16
	C32-C44	62.00	64.00	1.22	1.26	1.17
500	C5-C10	1.85	29.00	18.72	20.65	23.88
	C12-C15	41.00	48.50	26.45	29.17	33.75
	C16-C22	49.40	55.10	18.27	18.98	21.95
	C24-C30	56.80	61.00	10.22	10.62	12.28
	C32-C44	62.00	64.00	6.77	7.03	8.13
600	C5-C10	1.85	29.00	23.15	25.53	25.34
	C12-C15	41.00	48.50	41.31	45.57	45.22
	C16-C22	49.40	55.10	14.26	14.81	14.70
	C24-C30	56.80	61.00	10.63	11.04	10.96
	C32-C44	62.00	64.00	3.68	3.82	3.79

A4.14 Calculations for 25% LDPE, 50% PP, 25% PET ternary mixture

Table A4.14 Mole fraction of products in 25% LDPE, 50% PP, 25% PET pyrolyzate at different temperatures

Temperature (^oC)	Carbon No.	RT_i (min)	RT_f (min)	area%	mole%	mole fraction(corrected)
300	C5-C10	1.85	29.00	2.76	3.05	3.26
	C12-C15	41.00	48.50	38.32	42.27	45.23
	C16-C22	49.40	55.10	18.46	19.18	20.52
	C24-C30	56.80	61.00	24.36	25.31	27.08
	C32-C44	62.00	64.00	3.51	3.65	3.91
400	C5-C10	1.85	29.00	78.57	86.66	80.53
	C12-C15	41.00	48.50	6.18	6.82	6.34
	C16-C22	49.40	55.10	7.74	8.04	7.47
	C24-C30	56.80	61.00	4.73	4.91	4.56
	C32-C44	62.00	64.00	1.14	1.18	1.10
429 (T_{max})	C5-C10	1.85	29.00	51.62	56.94	61.07
	C12-C15	41.00	48.50	4.10	4.53	4.85
	C16-C22	49.40	55.10	7.11	7.39	7.92
	C24-C30	56.80	61.00	14.11	14.66	15.73
	C32-C44	62.00	64.00	9.35	9.72	10.42
500	C5-C10	1.85	29.00	22.84	25.19	28.51
	C12-C15	41.00	48.50	28.77	31.74	35.92
	C16-C22	49.40	55.10	10.75	11.17	12.64
	C24-C30	56.80	61.00	11.38	11.82	13.38
	C32-C44	62.00	64.00	8.11	8.43	9.54
600	C5-C10	1.85	29.00	8.07	8.90	8.98
	C12-C15	41.00	48.50	27.75	30.61	30.90
	C16-C22	49.40	55.10	27.68	28.76	29.03
	C24-C30	56.80	61.00	22.12	22.98	23.20
	C32-C44	62.00	64.00	7.53	7.83	7.90

A4.15 Calculations for 50% LDPE, 25% PP, 25% PET ternary mixture

Table A4.15 Mole fraction of products in 50% LDPE, 25% PP, 25% PET pyrolyzate at different temperatures

Temperature (^oC)	Carbon No.	RT_i (min)	RT_f (min)	area%	mole%	mole fraction(corrected)
300	C5-C10	1.85	29.00	1.25	1.38	1.46
	C12-C15	41.00	48.50	35.33	38.96	41.33
	C16-C22	49.40	55.10	20.11	20.89	22.16
	C24-C30	56.80	61.00	25.20	26.19	27.78
	C32-C44	62.00	64.00	6.59	6.85	7.26
400	C5-C10	1.85	29.00	54.59	60.22	57.08
	C12-C15	41.00	48.50	6.45	7.12	6.75
	C16-C22	49.40	55.10	17.07	17.73	16.81
	C24-C30	56.80	61.00	18.13	18.83	17.85
	C32-C44	62.00	64.00	1.53	1.59	1.51
436 (T_{max})	C5-C10	1.85	29.00	82.42	90.91	85.82
	C12-C15	41.00	48.50	3.44	3.79	3.58
	C16-C22	49.40	55.10	7.14	7.42	7.01
	C24-C30	56.80	61.00	2.19	2.27	2.15
	C32-C44	62.00	64.00	1.48	1.53	1.45
500	C5-C10	1.85	29.00	23.89	26.35	30.78
	C12-C15	41.00	48.50	16.30	17.97	21.00
	C16-C22	49.40	55.10	13.30	13.82	16.14
	C24-C30	56.80	61.00	18.98	19.72	23.04
	C32-C44	62.00	64.00	7.45	7.74	9.04
600	C5-C10	1.85	29.00	2.30	2.54	2.88
	C12-C15	41.00	48.50	11.25	12.40	14.05
	C16-C22	49.40	55.10	13.32	13.83	15.67
	C24-C30	56.80	61.00	25.86	26.87	30.44
	C32-C44	62.00	64.00	31.41	32.63	36.96

RESEARCH PUBLICATIONS

International Journals

1. Hujuri, U., Ghoshal, A.K. and Gumma, S., "Modeling pyrolysis kinetics of plastic mixtures", *Polymer Degradation and Stability*, 93(10) (2008) 1832-1837.

2. Hujuri, U., Ghoshal, A. K. and Gumma, S., "Temperature-dependent pyrolytic product evolution profile for low-density polyethylene from gas chromatographic study", *Waste Management*, 30(5) (2010) 814-820.

3. Hujuri, U., Ghoshal, A.K. and Gumma, S., "Temperature-dependent pyrolytic product evolution profile for polypropylene", *Journal of Applied Polymer Science*, 119 (2011) 2318-2325.

Conference Proceedings

1. Hujuri U., Gumma, S. and Ghoshal, A.K., "Study of Product Distribution and Mechanistic Aspects of Pyrolytic Decomposition of Polyethylene and Polypropylene mixture", *International Conference on Recycling and Reduce of Materials*, Kottayam, Kerala, 2009.

2. Hujuri U., Gumma, S. and Ghoshal, A.K., "Binary Interaction between Polyethylene and Polypropylene: Effects on Thermal Degradation and Product Distribution", *AIChE Annual Meeting 2010*, Salt Lake City, USA.